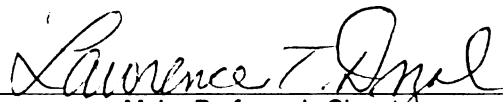This is to certify that the
thesis entitled

LIFE CYCLE ASSESSMENT AND BIODEGRADABILITY OF
BIOBASED COMPOSITES

presented by

Salil Arora

has been accepted towards fulfillment
of the requirements for the

M.S. degree in Chemical Engineering and
Materials Science

Laurence T. Drzal
Major Professor's Signature

12/15/2006

Date

PLACE IN RETURN BOX to remove this checkout from your record.
TO AVOID FINES return on or before date due.
MAY BE RECALLED with earlier due date if requested.

DATE DUE	DATE DUE	DATE DUE
		NOV 0 1 2008

LIFE CYCLE ASSESSMENT AND BIODEGRADABILITY OF BIOBASED COMPOSITES

By

Salil Arora

A THESIS

Submitted to
Michigan State University
in partial fulfillment of the requirements
for the degree of

MASTER OF SCIENCE

Department of Chemical Engineering and Materials Science

2007

ABSTRACT

LIFE CYCLE ASSESSMENT AND BIODEGRADABILITY OF BIOBASED COMPOSITES

By

Salil Arora

The current research analyzes the sustainability of novel biobased composites developed at the Composite Materials and Structures Center (CMSC) as an alternative to petroleum-based composites for automotive applications. A Comparative cradle-to-pellet life cycle assessment (LCA) of Polyhydroxybutyrate (PHB)-Kenaf and Polypropylene (PP)-Glass composites was carried out based on ISO 14040 series of standards. Inventory analysis for both the composites included resource consumption and emissions, and for a better understanding of this data, CML impact assessment methods were used to classify inventory flows based on their environmental impacts. Impact assessment results present qualified improvement in the environment profile of biobased composites, with significant reduction in energy consumption and global warming potential, and increased eutrophication and acidification potential for PHB-Kenaf composites. Finally, the sensitivity of the LCA results due to use of different allocation and impact assessment method was analyzed. In the second part of the research, the biodegradability of these composites under controlled composting environment was assessed based on ASTM D5338 standard. The study, carried out for more than two months, revealed that biobased composites degraded substantially, evident from the quantitative evaluation of carbon dioxide emissions, as well as from the visual inspection of the composite samples. LCA results in combination with biodegradability assessment, confirmed the sustainability of the biobased composites analyzed.

TABLE OF CONTENTS

LIST OF TABLES

LIST OF FIGURES

Images in this thesis are presented in color.

Chapter 1: Introduction

The concept of sustainable development was highlighted when the World Commission on Environment and Development chaired by Dr. Brundtland, published its report Our Common Future in April 1987. The commission aptly defined sustainability as meeting the needs of current generation without affecting the ability of future generations to meet their own needs. The recommendations by the commission led to the Earth Summit-the United Nations Conference on Environment and Development (UNCED) in Rio de Janeiro in 1992, which endorsed the Rio declaration on environment and development and adopted Agenda 21, a 300-page plan for achieving sustainable development in the 21st century. It was followed up by the World Summit on Sustainable Development (WSSD) in Johannesburg, 2002.

There are various indicators available to highlight the importance of sustainable development, one of the most important being: available non-renewable energy reserves. Based on the World energy outlook-2004[1], there are 36 to 44 years of crude oil and natural gas reserves remaining as per the year 2003 consumption levels. In such a scenario the need for application of resolution such as Agenda 21 cannot be more critical and immediate.

Since the 1992 Earth Summit, many countries (especially developed countries) have adopted the principles of sustainable development. However, that application has been to regulation of environmental stresses, to a lesser extent to sustainable production, and rarely to sustainable consumption. Phenomena such as globalisation have catalysed the economic growth in

developing countries such as China, India, etc; thus increasing the demand for already depleting world resources[i]. Therefore, the current priorities are to develop technologies for sustainable production and improve the existing consumption patterns.

In United States several initiatives are being taken by industries, government, and other organizations in order to aid sustainable production and encourage sustainable consumption. One of the recent developments is the approval by federal government of section 9002 of the Farm Security and Rural Investment Act of 2002 (FSRIA) in 2005[2]. This is a significant development, since this statute requires all the federal agencies to purchase biobased products based on the regulations defined to implement the final rule, for all biobased products within selected items costing over $10,000 or when the quantities of equivalent items purchased in last fiscal year totalled $10,000 or more. This regulation provides an incentive for new biobased products for whom the market has yet not matured and also provides financial support for testing biobased products in order to establish the biobased content and performance in comparison to available products.

In my thesis research work, I have worked in the team of Michigan State University (MSU) researchers to develop Green composites from natural fibers and bioplastics. This research was funded by National Science Foundation (NSF) under Product Realization and Environmental Manufacturing Innovative Systems of Eco-Efficiency (PREMISE) program[3]. The objectives of this project were to

---

[i] An example being, China becoming the 2nd largest consumer of crude oil, overtaking Japan consumption levels in 2004.

design and engineer, eco-friendly biobased composites for automotive applications. Polyhydroxybutyrate (PHB) was selected as the biopolymer for this study because it is a semi-crystalline polymer and hydrophobic. However, their are issues with the properties and sustainability of PHB, which have prevented its widespread use in the industry.

The main drawbacks of PHB are its brittleness, very limited processing window, and thermal instability. In the current research project, graft copolymerisation, maleation in particular was used to improve the physico-chemical properties. In addition, maleated-PHB acts as a compatibilizer and has been proved to improve biopolymer matrix-natural fibers adhesion[4]. Therefore, in this project effect of compatibilizer to improve mechanical properties of the biocomposites was studied.

Selection of natural fibers for the project was based on the type of fiber and the improvements related to its use. Incorporation of bast fibers is known to improve the stiffness, while leaf fibers increase the toughness of the biocomposites. Thus, two bast fibers, kenaf and hemp; and two leaf fibers, henequen and pineapple leaf fiber were used in this research and the improvement in mechanical properties due to these different fibers was studied.

To develop biocomposites, "Cascade Engineering" processing approach was used in order to avoid multiple steps for processing of biocomposites. In this approach PHB pellets with or without maleated-PHB (functionalised before through reactive extrusion) and chopped natural fibers were extruded in a twin-screw extruder ZSK 30 (Werner Pfleiderer). The extruded composite strands

were pelletized before injection molding the pellets as standard tensile coupons for mechanical property evaluation. Details about the processing of biopolymer and biocomposites and the optimised results have been discussed in the Section-2.a (literature review of biocomposites).

As discussed above, their are existing concerns about the sustainability of PHB[5,6,7] and therefore PHB-based composites. However, these sustainability evaluation studies lack the detail, which is needed to reach a reasonable conclusion. Therefore in the present NSF project, I developed the cradle to pellet life cycle profile for PHB based on recently published data by Akiyama et al.[8] In addition life cycle data for kenaf cultivation and processing was also collected in order to fully evaluate the sustainability of biobased composites. The overall scope of the LCA study was cradle to pellet, i.e. evaluating from the point raw materials were obtained to the production of finished composite.

One of the other issues with using conventional composites such as PP-Glass, is there non-biodegradability; thus rendering disposal options of landfilling and composting useless. Moreover, disposal by incineration is energy intensive and known to leave toxic residues and emissions. Therefore, every disposal option for conventional composites increases environmental burdens.

For biocomposites, both the biopolymers as well as natural fibers are degradable in nature, but it is important to determine the rate of degradation of composites under chosen disposal conditions and determine the effects of disposal end products on the environment. Therefore, in the present research biodegradability of biocomposites was determined under controlled composting

4

environment and the effect of disposal end product i.e. compost, on growth of plants was determined. The overall scope of the NSF-PREMISE project is described in Figure 1.1, with sustainability evaluation being my Master's thesis research work.
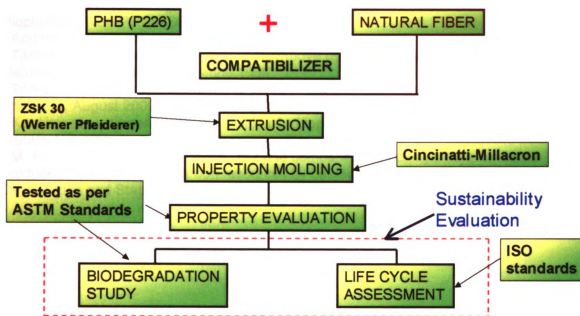
Figure 1.1 Scope of NSF-Premise Project

References:

[1] IEA (2004), World Energy Outlook 2004, OECD/IEA, Paris

[2] Guidelines for Designating Biobased Products for Federal Procurement, Section 9002, Farm Security and Rural Investment Act of 2002 (FSRIA), 7 U.S.C. 8102. Accessed through internet at http://www.biobased.oce.usda.gov

[3] "Design and Engineering of Green Composites from Bio-Fibers and Bacterial Bioplastics", NSF-PREMISE 2002 award# 0225925

[4] Add the missing reference.

[5] Tillman U. Gerngross, Can biotechnology move us toward a sustainable society? Nature Biotechnology, Vol 17, June 1999.

[6] Tillman U. Gerngross and Steven C. Slater, How green are green plastics? Scientific American, August 2000.

[7] Kurdikar et al., Greenhouse gas profile of a biopolymer, Journal of Industrial Ecology, 4 (2000), 107-122.

[8] M. Akiyama et al., Environmental life cycle comparison of polyhydroxyalkanoates produced from renewable carbon resources by bacterial fermentation. Polymer Degradation and Stability, 80 (2003), 183-194.

Chapter 2: Literature Review

In this chapter, the properties of relevant natural fibers, biopolymers, and biobased composites are reviewed. The results of previous life cycle assessment studies of natural fibers, biopolymers and biobased composites are also reviewed. Finally, ASTM standards used for determining the biodegradability of biobased composites under controlled composting conditions are reviewed.

2.1 Biobased Composites

The concept of using fibers as reinforcement for polymeric materials originated in early 20th century, with the use of cellulose fibers in phenolics and fiber reinforced polymeric composites were commercialized in 1940s, with glass fibers being used as reinforcement in unsaturated polyesters[12]. Around the same time in 1940, Ford Motor Company experimented with using glass fiber reinforced soy-protein plastic composites for car panels[1]. However, the use of soy protein plastic based composites did not commercialize because of abundance and low prices of petroleum. All of these previous examples attempted to produce partial biobased composites, where either the polymer matrix or fiber is non-biodegradable.

In 1989, DLR (German Aerospace Center) – Institute of Structural Mechanics began a project to develop biobased composites from renewable resources[2], by using natural fibers and biodegradable polymers, so as to reduce the reliance on non-renewable resources and alleviate the disposal problems arising due to conventional polymeric composites, which are non-biodegradable and difficult to recycle. Since then several review publications[3,12,9,2] have

covered the research progress on processing natural fibers and biopolymers to obtain biobased composites with comparable performance properties to conventional polymeric composites. However, majority of the industrial applications originating from this research area are partial biobased composites (i.e. containing less than 80% renewable content). DiamlerChrysler has worked since 1992 on developing a natural fiber reinforced components for interior and exterior automotive applications and beginning in late 1990s, has used flax reinforced polypropylene (PP) composites as underbody components and flax, sisal reinforced composites as interior door panels[5]. In 2004, it announced using abaca (banana fiber) reinforced PP composites for another exterior application, as a covering for the spare wheel recess. Similar to Ford's earlier attempts to commercialize biocomposites in 1940s, the Affordable Composites from Renewable Resources (ACRES) research group at University of Delaware in collaboration with John Deere & Co. has developed soy-based fiberglass composites, which are used as tractor panels and hay balers[1]. Natural fibers are ductile and have superior impact resistance in comparison to glass fibers, and thus have replaced glass fibers in components requiring better energy absorption. For e.g. since 1998, Ford Motor Co. has used PP-Kenaf composites in interior door panel and trunk liner applications[1]. Similarly, Saab (1999 Saab 9S) and General Motors (2003 small passenger cars) have used LoPreFin PP/PET/natural-fiber composites as full door panels[4].

As evident from these industrial applications, renewable materials are increasingly being used in composites on a partial basis, though there are few

examples of completely biobased composite applications, such as Environ® composite board developed by Phenix Biocomposites using wastepaper and soy-flour, and is currently marketed for home & office, and architectural non-structural applications[9]. Their are several reasons to non-applicability of fully biobased composites in industrial applications. First of all, higher costs of biopolymers such as PHB, PLA in comparison to conventional commodity polymers such as PP, LDPE, HDPE, and PVC have restricted the use of biopolymers in commercial applications[9]. Regarding use of natural fibers in composite applications, there are justifiable concerns related to large variation in physical and chemical properties of natural fibers, and the resulting biocomposites. This issue, as demonstrated by researchers at DiamlerChrysler for Green Flax, can be resolved by obtaining fibers from a single source, limiting weather related variation by reducing the fiber retting from 3 weeks to a maximum of 2-3 days, and standardizing the harvesting process. Additionally, natural fibers are hydrophilic, which reduces their compatibility with generally hydrophobic polymers and moisture absorption/desorption can significantly reduce the mechanical properties of these composites. Surface-chemical modification and/or coating of natural fibers are known to improve polymer-fiber interfacial adhesion and hydrophobicity of natural fibers and these methods are briefly reviewed in Section 2.1.1.2 of Natural Fibers.

As discussed in the Introduction chapter of the thesis, current research work under NSF-PREMISE program focused on developing completely biobased composites using PHB biopolymer and various natural fibers and thus

addressing the issues highlighted above for limited commercialization of completely biobased composites. The physical, chemical, and mechanical properties of natural fibers relevant to the current research work are briefly reviewed in one of the subsections below. PHB biopolymer is classified as a polyester; and the current manufacturing process and industrial applications of the commercially important polyesters are also reviewed below. Additionally in the current research work, maleated-PHB was processed and used as compatabilizer for these composites, in order to improve the fiber-matrix interfacial adhesion. Finally, mechanical properties and morphology of these composites was studied, so as to determine the optimal natural fiber reinforcement and effectiveness of the compatibilizer. These results are briefly reviewed in the subsection on PHB-Natural fiber composites.

2.1.1 Natural fibers

Natural fibers have been used since ancient times, with early applications as textiles, ropes and more recently to produce automotive door panels, underbody panels and dashboards, acoustic ceiling tiles, wall panels, load-bearing composites. These fibers can be classified based on the source of origin, as either animal or plant derived. Examples of plant-derived fibers are kenaf, sisal, cotton; while fibers such as wool and silk are animal-derived fibers. Animal and plant fibers can also be classified based on the difference in chemical structure; where animal fibers are protein (polypeptide) based, and plant fibers have cellulose as the main chemical structure. In composites industry, majority of

the natural fibers used are plant based, therefore only plant-derived fibers are reviewed further.

Classification of plant-derived natural fibers is done based on the part of the plant from which they are derived, and classified into following five categories: 1) Bast fibers: obtained from plant stem, such as kenaf, flax, hemp, jute, ramie; 2) Leaf fibers: examples are sisal, pineapple leaf fiber (PALF), henequen; 3) Seed/Fruit fibers: such as cotton (from seed hair), coir (from coconut husk); 4) Straw/Grass fibers: include wild grasses such as switchgrass, indian grass and straw fibers from corn, wheat, and rice farming, which are otherwise considered a waste product; 5) Wood fibers: obtained from soft and hard woods, usually a waste from sawmills, furniture manufacture, packaging pallets.

2.1.1.1 Chemical composition

Along with cellulose, hemicellulose and lignin are major polymeric components for plant-based fibers, with small amounts of pectin and wax present for some of these fibers. Cellulose acts as a reinforcing material in plant cell walls, with microfibrils of highly crystalline cellulose used as reinforcement in the matrix of hemicelluloses and lignin. Chemical structure of cellulose consists of a linear, crystalline polymer composed of 1,4-β-D-glucopyranose units.

Hemicelluloses are copolymers of sugars such as glucose, mannose, xylose, galactose, and arabinose. They cover the surface of cellulosic microfibrils by hydrogen bonding to the surface cellulose chains. Pectins are an important matrix component of cell walls for non-wood fibers. They are classified as

polysaccharides, which can have complex structures and can be branched. Hemicelluloses and pectins are hydrophilic in nature, and are largely responsible for the hydrophilic nature of plant-based natural fibers.

During cell development, lignin polymer is the last component to be incorporated in the plant cell wall, binding hemicelluloses and cellulose microfibrils components and thus imparting rigidity, hydrophobicity and decay resistance to the cell walls. The chemical structure of lignin consists of a disordered, polyaromatic, cross-linked polymer, which is obtained from the free-radical polymerization of two or three monomers structurally related to phenyl propane. The chemical composition of various natural fibers is presented below in Table 2.1.

Table 2.1 Chemical Composition of Natural Fibers

Fiber	Cellulose (wt%)	Hemicellulose (wt%)	Pectin (wt%)	Lignin (wt%)
Flax	71	18.6 – 20.6	2.3	2.2
Hemp	70.2 – 74.4	17.9 – 22.4	0.9	3.7 – 5.7
Kenaf	31 – 39	21.5	–	15 – 19
Sisal	67 – 78	10.0 – 14.2	10.0	8.0 – 11.0
PALF	70 – 82	–	–	5 – 12
Henequen	77.6	4 – 8	–	13.1
Cotton	82.7	5.7	–	–
Coir	36 – 43	0.15 – 0.25	3 – 4	41 – 45
Softwood	40 – 45	–	0 – 1	26 – 34
Hardwood	40 – 50	–	0 – 1	20 – 30

As discussed above, natural fibers are composed of cellulose, hemicelluloses, lignin, and pectin in varying quantities (Table 2.1). Out of these components, crystalline-cellulose mainly contributes towards the strength of natural fibers. The natural fibers can degrade by biological action

(biodegradation), temperature increase (thermal degradation), and UV radiation (ultraviolet degradation). Biological degradation of fiber components is closely related to there moisture absorption capacity and decreases in the following order: hemicellulose > accessible crystalline cellulose > non-crystalline cellulose > crystalline cellulose > lignin. In case of exposure to ultraviolet radiation, degradation primarily happens in the lignin and to a much lesser scale in the cellulose component. The thermal degradation of natural fiber components is in contrast to the ultraviolet degradation, where hemicellulose and cellulose components degrade much earlier compared to lignin.

2.1.1.2 Physical and Mechanical properties

Natural fibers show a large deviation in most characteristics (diameter, length, chemical composition, crystallinity, surface properties), thus causing a variation in mechanical properties. The deviation in fiber properties can be attributed to the variation in quality of fibers arising due to factors such as climate variation (during fiber cultivation), fiber maturity (at the time of harvesting), harvesting, retting[5] (water retting, dew retting or minimal retting-example is "green" flax) and processing methods.

The strength of natural fibers has a direct dependence on crystallinity, molecular chain orientation and is inversely proportional to the defects, cracks, imperfections and degree of polymerization. The modulus (stiffness) of natural fibers decreases with increase in fiber diameter. Increase in relative humidity reduces the fiber modulus, and this effect becomes more pronounced for fibers with higher amorphous content.

In addition to strength and modulus of natural fibers, fiber-matrix adhesion is an important factor towards improving composite mechanical properties. Since natural fibers are hydrophilic in nature and have high moisture absorption, there compatibility with hydrophobic polymer matrixes is poor, thus causing weak interfacial adhesion. Mohanty et al.[6] have reported improvements in fiber-matrix adhesion and composite mechanical properties by various surface-chemical modifications of natural fibers, such as alkali treatment, etherification, acetylation, isocyanate treatment, dewaxing, etc.

The physical and mechanical properties of various natural and synthetic fibers have been compared previously, and are presented below for reference in Table 2.2.

Table 2.2 Comparison of Physical and Mechanical properties for Natural and Synthetic Fibers

Fiber	Density (g/cm^3)	Diameter (µm)	Tensile strength (MPa)	Young's modulus (GPa)
Flax[7]	1.4 – 1.5	19	500 – 900	50 – 70
Hemp[7]	1.48	25	300 – 800	30 – 60
Kenaf[8]	1.25	–	79.2 – 513.3	8.6 – 32.7
Sisal[12]	1.45	50 – 200	468 – 640	9.4 – 22.0
PALF[12]	–	20 – 80	413 – 1627	34.5 – 82.5
Cotton[7]	1.5	20	300 – 600	6 – 10
Coir[12]	1.15	100 – 450	131 – 175	4 – 6
Softwood[7]	1.4	33	100 – 170	10 – 50
Hardwood[7]	1.4	20	90 – 180	10 – 70
Glass[7]	2.54	10 – 20	3530	72
Aramid[7]	1.44	12	3600	58
Carbon[7]	1.75	7	3530	235

2.1.1.3 Comparison with synthetic fibers

There are several reasons for greater use of natural fibers in materials industry, especially at the level of commodity materials, where high performance materials are usually not required, as is the case for defense and aerospace industry. Most of the natural fibers are renewable on annual basis, thus ensuring an abundant and continuous supply. The degradable nature of these fibers makes it possible to process composites, which are completely degradable (by combining with biopolymer matrix). In contrast, composites processed from synthetic polymers (PP, PE, PS, PVC) and fibers (glass, carbon) are non-degradable and contribute towards ever worsening situation of properly disposing non-degradable materials at the end of there use phase.

Based on the comparison in Table 2.2, use of natural fibers instead of synthetic fibers in materials industry offers several advantages. These fibers in comparison to synthetic fibers are relatively inexpensive, have low density thus a potential for weight reduction, and better noise and thermal insulation[9] (because of there hollow tubular structure). In terms of mechanical properties, they have comparable specific strength and high modulus. Additionally, processing natural fiber reinforced composites poses no significant EHS (environment, health and safety) risks (in contrast glass fiber processing can cause skin rashes and respiratory diseases such as silicosis), and causes reduced tool wear because of there non-abrasiveness.

Though the degradability of natural fibers is considered an advantage, it is an undesirable attribute for many composite applications, where standard

outdoor performance is expected from the components during its use phase (in years). Another drawback associated with natural fibers is their hydrophilic nature, which reduces the compatibility with hydrophobic polymers. Both of these issues can be resolved by surface-chemical modification and/or coating of these fibers, as discussed before in Section 2.1.1.2. Additionally, rapid degradation of natural fibers due to temperatures in excess of 200°C, limits the choice of polymer matrix. Therefore, low melting polymers such as polypropylene and PHB are selected for processing natural fiber-reinforced composites.

2.1.2 Biopolymers from polyesters

Biopolymers include the polymers, which are biodegradable and not necessarily derived from renewable resources. Thus, biopolymers are classified as: renewable resource based, fossil fuel based, and partial renewable resource based polymers. Recently, biopolymers directly derived from renewable resources or coupled with fossil fuel derived polymers have received increased attention from scientific and industrial community, in order to reduce the reliance on fossil fuel resources. In last 10 – 15 years, biopolymers have been comprehensively reviewed in several journal publications[10,11,12,13,14] and books[15,16,17,18]; the properties and industrial applications of these polymers are briefly reviewed in following subsections below.

Biodegradability of polymers depends not only on the source of origin but also on the chemical structure of the polymers[18]. In case of polyesters, aliphatic polyesters are biodegradable, irrespective of the source from which they are derived. Examples of aliphatic polyesters are PLA and PHAs, which are derived

from renewable resources; and PCL, PBS, which are petroleum based biodegradable polyesters. In contrast to aliphatic polyesters, aromatic polyesters like poly(ethylene terephthalate) (PET) are non-biodegradable. However, some of the commercially developed aliphatic-aromatic copolyesters such as Eastman's Eastar Bio® and BASF's Ecoflex® retain the biodegradability of aliphatic polyesters, and have higher strength because of substitution of aliphatic diacid monomers with more rigid aromatic diacids. The chemical structures of these polyesters are presented below:

Poly(lactic acid)

Poly(β-hydroxybutyrate)

Poly(caprolactone)

Poly(butylene succinate)
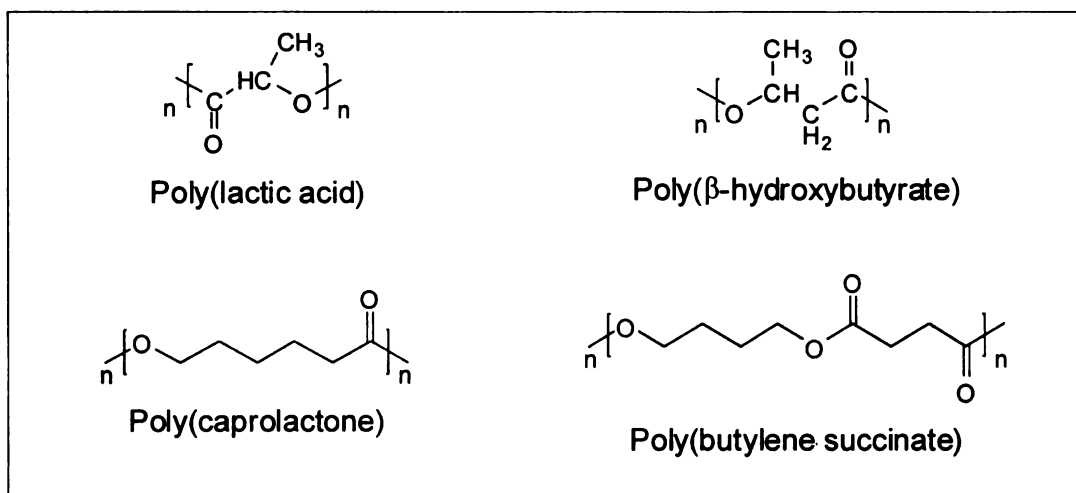
2.1.2.1 Polyhydroxyalkanoates

Polyhydroxyalkanoates (PHAs) are biodegradable polyesters, which are commercially produced by bacterial fermentation of plant-derived sugars and oils, and ongoing research aims to directly extract these polyesters from genetically modified plants such as switchgrass[19,20]. Initial discovery and chemical identification of PHAs was done in 1920s by a French microbiologist, Maurice Lemoigne[21], who characterized poly-3-hydroxybutyrate (PHB), a reserve polymer

found in several types of bacteria. However, significant development work on PHAs did not begin until 1960s, because the bacteria which could produce these polyesters was unknown to polymer chemists and majority of biochemistry and microbiologists before 1958, when it was simultaneously rediscovered by microbiologists in United States and England. ICI Zeneca started the commercial production of PHAs in late 1980s under the trade name of Biopol®, which is a copolyester of HB (hydroxybutyrate) and HV (hydroxyvalerate) units. This copolyester has been used to manufacture blow molded shampoo bottles by Wella AG and potential uses as motor oil containers, films, paper coating material have been previously reviewed[15]. However, greater commercialization of Biopol did not happen because of its higher costs compared to conventional polymers such as PE. In 1995, Monsanto bought the process and patents associated with production of PHAs from ICI Zeneca, and focused on PHA production from genetically modified plants. Out of available options of corn, sugarcane, and switchgrass, Monsanto researchers selected corn plant for genetic modification because of its well-characterized genome. Corn plant is genetically modified in such a way that excess PHA is expressed in the non-edible part of the plant, i.e. corn stover (leaves and stems) and extracted using organic solvents. Based on the sustainability assessment studies[22,23,20] of PHA production by Monsanto researchers, energy and resource consumption as well as greenhouse gas emissions were higher for cradle-to-pellet life cycle of PHA compared to conventional polymers such as PE. Additionally, PHA polymers were still not cost competitive to conventional polymers. Therefore, Monsanto

abandoned further development work on PHAs in 1998 and Metabolix[24] (Cambridge, MA) purchased its technology in 2001. As per the latest Metabolix brochure[25], "it has demonstrated economic production of PHAs by fermentation of plant-derived sugars and oils, and is in the process of making PHAs directly in crop plants." In March 2006, Metabolix announced its plans in partnership with Archer Daniels Midland Company (ADM), for annual production of 50,000 tons of PHA natural plastics from corn starch in Clinton, Iowa adjacent to ADM's wet corn mill. Another company, Biomer[26] (Germany) is currently pursuing commercial scale production of PHB by bacterial fermentation using sugar (sucrose) as a feedstock, and several grades[27] of its Biomer® resin (P226, P209, P240) are commercially available.

2.1.2.2 Polylactic acid

Polylactic acid (PLA) is a rigid thermoplastic polymer, manufactured either by direct condensation of lactic acid or by ring-opening polymerization of the cyclic lactide dimer. Carothers[28] investigated production of PLA from lactic acid in 1932, with further development work by DuPont and Ethicon. PLA production by direct condensation process limits the ultimate molecular weight achievable for PLA and requires costly, environment unfriendly solvents for removal of water, in order to obtain high molecular weight polymer. Mitsui Chemicals has developed an improved process[29], which yields high molecular weight PLA from direct polycondensation of L-lactic acid, without using any organic solvent. In contrast to direct condensation process, ring-opening polymerization utilizes tin catalyst to obtain high molecular weight PLA from cyclic lactide dimer, thus eliminating the

need for any solvent. This production technology is used by Cargill Dow LLC, which started full-scale production of its NatureWorks™ PLA in 2001. The degradation of PLA after disposal takes place in high temperature and high humidity conditions, primarily by hydrolysis, followed by microbial action[13,18]. Because of this unique degradation characteristics, PLA based objects are stable for years under normal conditions. Additionally, PLA is easily melt spinnable and crystallizes upon drawing. Therefore, PLA is currently used for apparel, non-wovens, household and industrial fabrics, carpets, fiberfill, and food packaging applications[29,18].

2.1.2.3 Polycaprolactone

Poly(ε-caprolactone), PCL is a thermoplastic biodegradable polyester, obtained from crude oil by chemical synthesis, and followed by ring opening polymerization using tin catalyst. PCL biopolymer has good water, oil, solvent, and chlorine resistance, low melting point, and good mechanical properties. The low melting point of 60°C, limits the applications where it can be used. Therefore, it is frequently blended with other biopolymers e.g. starch, in order to improve their properties. Some of the common applications of PCL have been as blown films for compost bags, as matrix in the materials ensuring controlled release of pesticides, herbicides, and fertilizers[17]. Additionally, PCL is used in biomedical products[14] for e.g. as stiffeners for orthopedic splints, sutures, and as matrix for bone repair.

2.1.2.4 Poly(alkylene dicarboxylate)

Poly(alkylene dicarboxylate) type of aliphatic polyesters are manufactured by Showa Highpolymer, and marketed under the trade name Bionolle™, which include following grades: polybutylene succinate (PBS), poly(butylene succinate-co-butylene adipate) (PBSA), and poly(ethylene succinate)[18]. These polymers are produced by polycondensation reactions of glycols (e.g. ethylene glycol, 1,4-butanediol) and aliphatic dicarboxylic acids (e.g. succinic acid, adipic acid) and have properties (physical and mechanical) similar to those of commodity polymers such as LDPE. Bionolle polymers have excellent processability, and therefore can be converted into various products such as fibers, films, bottles using a combination of injection, extrusion and blow molding[12]. Unlike commodity polymers, Bionolle polymers biodegrade in soil, compost, activated sludge, freshwater and marine environments[13].

2.1.3 PHB-Natural fiber Composites

In the previous studies on PHB based biocomposites, various natural fibers such as wood[30], jute[31,32], wheat straw[33], and flax[34] have been used as reinforcements; while determining mechanical, thermal, morphological, and degradation properties of these composites. Additionally, some publications have studied the effect of natural fiber reinforcement on PHB crystallinity[30], and the effect of surface/chemical modification[31,32] of natural fibers on properties of PHB based biocomposites.

The current research work under NSF-PREMISE program was comprised of following three parts:

- Functionalization of Polyhydroxyalkanoates (PHAs)

- Processing and property evaluation of PHB-Natural fiber composites

- Life cycle assessment and biodegradability evaluation of PHB-Natural fiber composites

In the first part of the research work, solvent free functionalization of PHAs was achieved by successfully grafting maleic anhydride (MA), octadecenyl succinic anhydride (ODSA) on Poly(3-hydroxybutyrate) and Poly(3-hydroxybutyrate-co-3-hydroxyvalerate) using a DSM Micro 15, twin-screw mini extruder. The grafting of MA and ODSA was confirmed by using NMR, FTIR, DSC, and TGA analytical techniques. The grafted PHAs were utilized as compatibilizer in the second step of the research work, in order to improve the fiber-matrix interfacial adhesion.

The third part of this research project involved sustainability evaluation of PHB-Natural fiber composites based on a LCA and biodegradation study. This part of the research work is covered in the main chapters of my thesis.

In second part of the research project, PHB-Natural fiber composites were processed using ZSK 30 (Werner Pfleiderer) twin-screw extruder and injection molded into tensile coupons using 85-ton Cincinatti-Millacron press. The main objectives of this part of the research work were: to study the effect of different natural fibers, PHB-g-MA compatibilizer, different extruder screw configurations on the mechanical properties of the biobased composites and explore ways to commercialize the biobased composites for automotive and packaging applications. Natural fibers selection as reinforcement was based on the

expected property improvement by its use, which is stiffness in case of BAST fibers and toughness for leaf fibers. Two BAST fibers, hemp and kenaf; and two leaf fibers, henequen and pineapple leaf fibers were used in this research. Use of two different screw configurations was related to the goal of commercializing processing of biobased composites. The first screw configuration had two kneading zones (aids in polymer/fiber mixing) and three conveying zones (for polymer transport in extruder), and processing composites in this configuration involved manual fiber addition. In order to commercialize the processing of biobased composites, automation of the process is very important, which in this case was achieved by automatic fiber addition through ZSB 25 side feeder (Coperion Corporation). For effective polymer/fiber mixing during automatic fiber addition, extruder screw configuration was modified, and contained three kneading zones and four conveying zones; thus enabling better mixing and longer residence times for the polymer in the extruder. These two screw configurations and ZSK 30 extruder set up with side feeder are presented below in Figure 2.1 (a-c).

Injection molded tensile coupons were used to evaluate tensile, flexural, and impact properties of PHB-Natural fiber composites. Tensile and flexural properties were determined based on ASTM D 638 and D 790 standards using United Calibration Corp SFM 20 machine. Impact testing of these composites was done using Testing Machines Inc. (TMI) 43-OA-01 machine, based on ASTM D 256 standard.
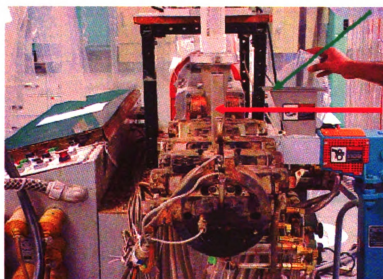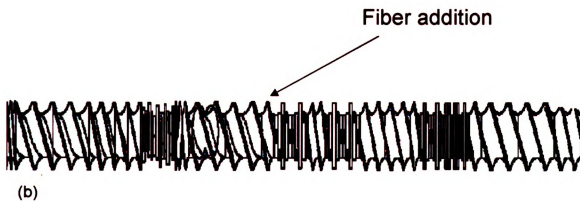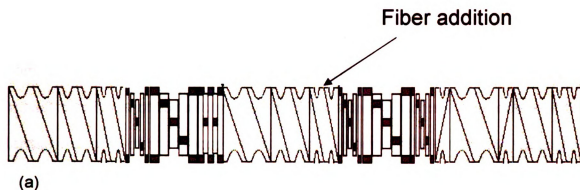
Figure 2.1(a) Screw configuration during manual fiber addition; 2.1(b) Screw configuration during automatic fiber addition; 2.1 (c) ZSK 30 twin-screw extruder with ZSB 25 side feeder

Comparison of mechanical properties using screw configuration for manual and automatic fiber addition was done by processing 30 wt% Henequen fiber composites with both screw configurations and evaluating tensile, flexural, and impact properties of these composites. Their was significant improvement in the tensile modulus of the biocomposites using automatic fiber addition, which can be attributed to better dispersion and greater mixing of fiber with polymer matrix during extrusion process. No significant difference in other mechanical properties: tensile strength, flexural and impact properties was noticed. A comparison of tensile properties for PHB-Henequen fiber composites, using both screw configurations is presented below in Figure 2.2.
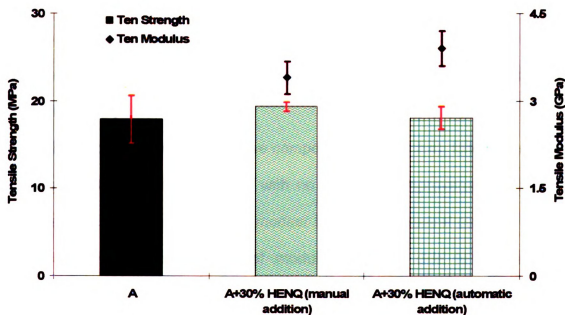
Figure 2.2 Tensile strength and modulus comparison of 30-wt% henequen fiber composites (A= PHB (P-226); HENQ: henequen). (processed in screw configuration-I (manual addition) and screw configuration-II (automatic addition)

The effect of different natural fiber reinforcements and compatibilizer on mechanical properties of PHB based composites was also evaluated. The tensile properties of PHB-(30wt%) Natural fiber composites are compared below in Figure 2.3. The use of compatibilizer slightly increases the tensile strength of hemp, kenaf, and PALF fiber composites, while the strength of henequen fiber composites remains the same. No significant increase in tensile modulus values was recorded by the addition of compatibilizer. Among natural fibers, in comparison to neat PHB samples, moderate increase in tensile strength was recorded for all the natural fibers, with greatest increase in compatibilized hemp and PALF fiber composite samples. The tensile modulus values increased significantly due to natural fiber reinforcement as compared to neat PHB samples, with greatest increase in kenaf fiber reinforced composites, whose modulus values were also significantly higher (roughly double) compared to other natural fiber composites.

The flexural properties of these composites (Figure 2.4), follows the same trend as that for tensile properties, with no significant improvement in flexural properties by use of compatibilizer, modest increase in flexural strength values, and significant increase in flexural modulus values due to natural fiber reinforcement. Additionally, kenaf fiber composites had significantly higher flexural modulus values compared to other natural fiber reinforced composites.

Comparison of impact strength values of these composites is presented below in Figure 2.5. Moderate increase in impact strength values was recorded for hemp, PALF, and kenaf reinforced composites; while impact strength values

of henequen reinforced composites is significantly higher compared to neat PHB as well as other fiber reinforced composites. The higher impact value for henequen fiber composites was expected, since henequen is a leaf fiber and leaf fibers are generally tougher compared to BAST fibers such as hemp and kenaf. Use of compatibilizer had insignificant effect on impact strength of these composites.

In addition to mechanical property evaluation, interface studies were conducted to study the effect of compatibilizer addition on composite properties, by investigating fiber pull-out and fiber-matrix adhesion using ESEM.

ESEM micrographs for PHB+30%Hemp and PHB+5%PHB-g-MA+30%Hemp composites are presented below in Figures 2.6 and 2.7. The fracture surface of 30 wt% hemp fiber composites shows single fiber pullouts, indicating poor fiber-matrix adhesion. In comparison compatibilized hemp fiber composites had lesser single fiber pullouts, thus better fiber-matrix adhesion compared to non-compatibilized hemp fiber composites. These results corroborate the mechanical property results for hemp fiber composites, where use of compatibilizer leads to moderate increase in tensile and flexural strength.

Similar interface studies were conducted for PHB+30%Kenaf and PHB+5%PHB-g-MA+30%Kenaf composites, with ESEM micrographs presented below in Figures 2.8 and 2.9. For kenaf fiber composites, addition of compatibilizer did not improve the fiber-matrix adhesion, since fractured surfaces had similar amount of fiber pullouts, before and after the addition of compatibilizer. This observation is in agreement with mechanical property results,

since relatively small increases (compared to hemp, PALF) in tensile and flexural strength were recorded in kenaf fiber composites due to addition of compatibilizer.
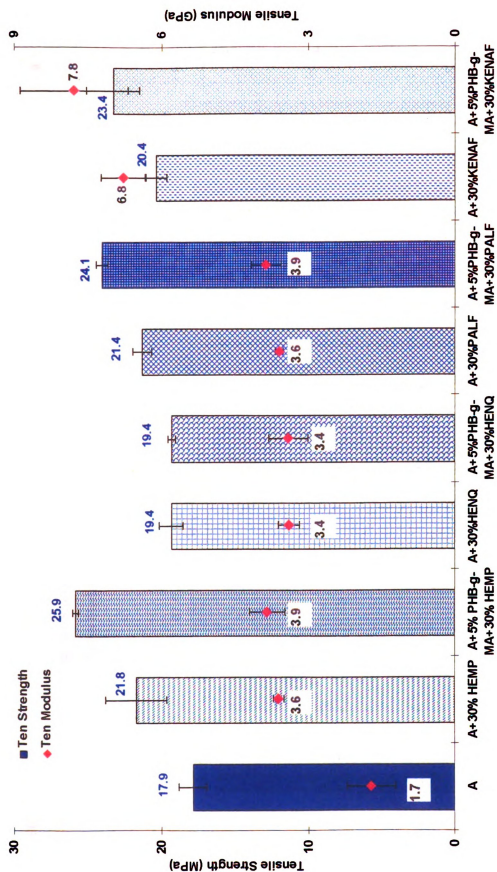
Figure 2.3 Tensile strength comparison of 30-wt% natural fiber composites (A= PHB (P-226); HENQ: henequen; PALF: pine apple leaf fiber) (processed in screw configuration-II)
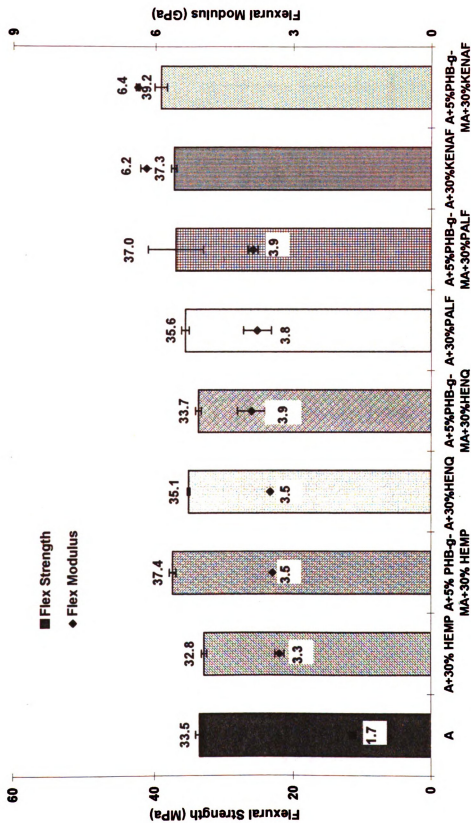
Figure 2.4 Flexural strength comparison of 30-wt% natural fiber composites (A= PHB (P-226); HENQ: henequen; PALF: Pineapple leaf fiber). (Processed in screw configuration-II)
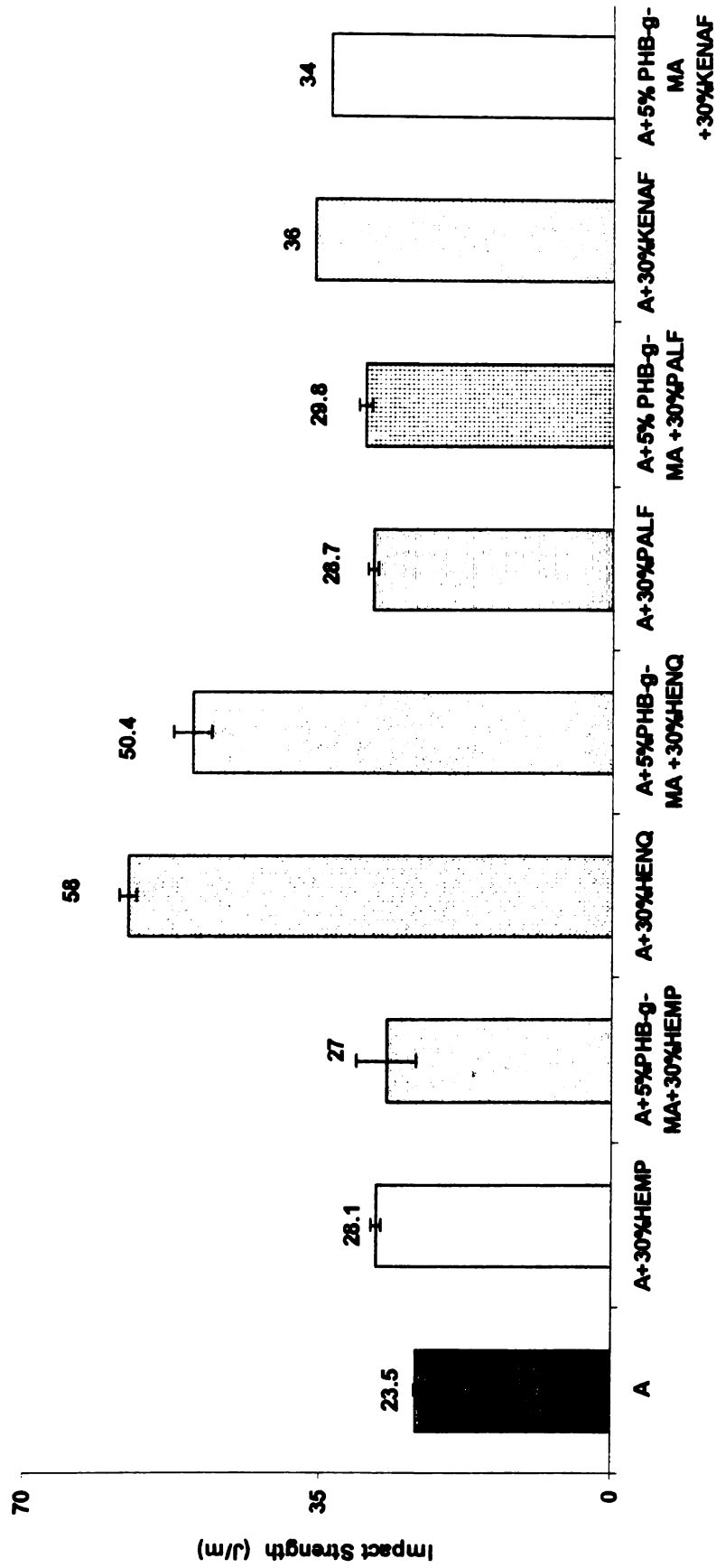
Figure 2.5 Impact strength comparison of 30-wt% natural fiber composites (A= PHB (P-226); HENQ: henequen; PALF: pineapple leaf fiber). (Processed in screw configuration-II)

31
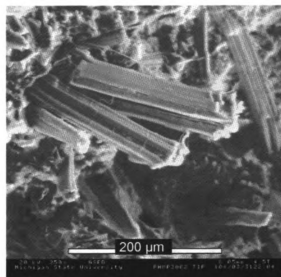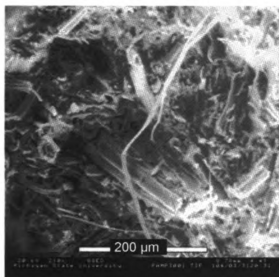
Figure 2.6 ESEM micrographs of PHB+30wt% hemp fiber composites with screw configuration-II
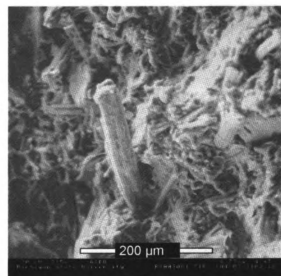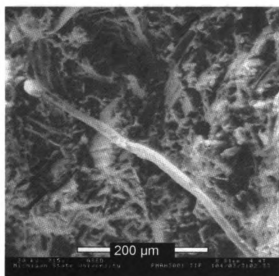
Figure 2.7 ESEM micrographs of PHB+5wt%PHB-g-MA+30wt% hemp fiber composites with screw configuration-II
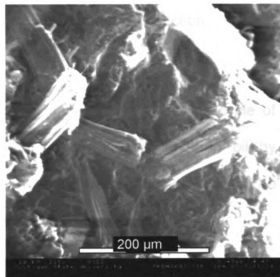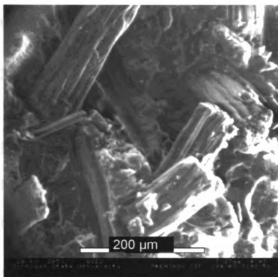
Figure 2.8 ESEM micrographs of PHB+30wt% kenaf fiber composites in screw configuration-II
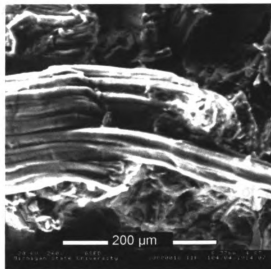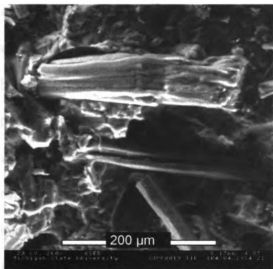
Figure 2.9 ESEM Images of PHB+5wt%PHB-g-MA+30wt% kenaf fiber composites in screw configuration-II

2.2 Previous Life Cycle Assessment Studies

LCA studies of natural fibers, biopolymers, and biobased composites relevant to the current research work are briefly reviewed in this section.

2.2.1 Polyhyroxyalkanoate LCA studies

Several academic and industrial studies have analyzed the life cycle of PHA production from biomass such as corn, corn stover, soybean oil by fermentation process or direct production in genetically modified plant. The results and conclusions of these studies are summarized below.

2.2.1.1 Gerngross, 1999

In this study, Gerngross[22] has compared cradle to pellet production of PHA with PS (polystyrene) production to obtain polymer resin. PHA is assumed to be produced by fermentation of glucose, where glucose is obtained by corn wet milling process. Energy and raw material requirements for corn cultivation, wet milling and PHA production process are calculated for production in US. Based on these calculations, Gerngross has estimated that PHA fermentation process consumes 22% more steam, 19 times more electricity, and 7 times more water compared to conventional PS production process. Therefore, energy requirements in terms of FFE[1] (fossil fuel equivalents) for production of a kilogram of polymer is greater for PHA (2.39 kg FFE) compared to PS (2.26 kg FFE), and thus PHA production has greater net greenhouse gas emissions compared to PS production. The difference between energy requirements for

---

[1] Amount of fossil fuel (kg) consumed to produce a unit of electricity (kWh) and steam (kg)

PHA and PS is not that large; however, the fact that all the energy requirement for PHA is used as process energy, and only 1 kg of 2.26 kg is used as process energy for PS, makes the PHA production process less sustainable.

The conclusions obtained from this study are contrary to popular perception that biobased, biodegradable polymers are environment friendly and sustainable. However, there are some shortcomings/limitations in the calculations, which can significantly modify the final conclusions for this study. First of all, fossil fuel requirements for PS production does not consider energy required to produce/extract those fossil fuels from crude oil or natural gas, thus lacking a true cradle to pellet scope used for other parts of this study. Secondly, greenhouse gas emission calculations in this study does not include carbon sequestered during corn cultivation, which significantly lowers the CO_2 emissions during PHA production process.

2.2.1.2 Gerngross and Slater, Kurdikar et al., 2000

These two studies are a follow-up of the 1999 study by Gerngross and focus on the cradle to pellet production of PHA obtained from a genetically modified corn plant. Both the publications have a greater industrial focus compared to the previous study by Gerngross and lists industry researchers as co-authors.

In the first study, Gerngross and Slater[23] have computed energy requirements for PHA production from genetically modified corn plant and compared it with PHA production from bacterial fermentation, PLA production by bacterial fermentation, and production of PE, PET, nylon polymers derived from

fossil fuel resources. The comparative results in terms of process energy and feedstock energy are presented below in Table 2.3. In addition, technical challenges associated with PHA extraction from corn plant are also discussed. The research work related to genetic modification of corn plant has been carried out at Monsanto Company since 1995, when it bought the process and patents from ICI Zeneca (see Section 2.1.2.1 for more details) and it has focused on PHA production in corn stover, which is non-harvestable portion of corn plant. One of the problems associated with PHA production in plants is inhibition of photosynthesis due to high plastic content in leaves, and thus reducing grain yields. Additionally, theoretical scale-up of the PHA extraction and collection process concludes that the process requires large amount of solvent and infrastructure comparable to that required for petrochemical based polymers, and thus rightly questioning the sustainability of PHA biopolymer obtained from corn plant. The comparison of energy requirements as shown below in Table 2.3, further questions the "greenness" of PHA biopolymer, with process energy required for a kilogram of PHA (from corn plant) 300 percent more than 29 MJ required for petroleum based PE polymer. However, authors do argue that process technologies for PHA and PLA are in the nascent stage and thus offer a lot of scope for process improvement and energy reduction, while conventional polymers have benefited from almost 100 years of development and innovation in petrochemical industry. Finally, based on the energy comparisons in this study, authors recommend using waste plant material (corn stover in current scenario) as a source of energy during PHA production, thus replacing non-renewable

energy source with plant-based renewable energy source and improving the sustainability of PHA biopolymers. The environmental impacts of this switch to renewable energy source are discussed in their follow-up publication by Kurdikar et al.[20]

Table 2.3 Comparison of process and feedstock energy requirements for some biobased and fossil fuel based polymers (Gerngross and Slater[23])

Polymer type	Process Energy (MJ/kg polymer)	Feedstock Energy (MJ/kg polymer)
PHA (from corn plant)	90	–
PHA (bacterial fermentation)	81	–
PLA	56	–
PE	29	52
PET	37	39
Nylon	93	49

In the follow-up study to Gerngross and Slater[23], Kurdikar et al.[20], have compared the Global Warming Potential (GWP) for cradle to pellet production of PHA from genetically modified corn plant with polyethylene (PE) production. The authors have studied four different scenarios for PHA production with different energy sources (biomass, natural gas, coal, oil) used during extraction and compounding of PHA biopolymer. The default allocation approach, system allocation for PHA production, allocates all the impacts for production of

genetically modified corn to harvested stover, while subtracting impacts for producing same amounts of traditional corn grain. Since, corn grain yield from genetically modified plant is less compared to traditional corn crop, this allocation approach attributes the yield loss to harvested corn stover of the genetically modified corn plant. In order to check the sensitivity of the results, an alternative allocation approach, mass partitioning is used, which allocates impacts based on the mass of harvested co-products, i.e. corn grains and stover in the current study. The mass based comparison of GWP for different scenarios using system allocation approach (Figure 2.10) presents a significantly lower and negative GWP for PHA production in biomass scenario compared to fossil fuel energy usage scenarios as well as production of different grades of PE. The lower GWP for biomass scenario is due to carbon sequestered during corn cultivation and CO_2 credit obtained from excess energy produced by burning of corn stover, which is not utilized during PHA processing. In fossil fuel scenarios, even though carbon sequestered during corn cultivation is considered, CO_2 credit from burning biomass is converted into CO_2 emissions from fossil fuel use in PHA processing and stover decomposition. Since, LDPE and HDPE have lower densities (0.93 and 0.95) compared to PHA (1.2), volumetric comparison presents lower GWP for PE polymer grades, though it is still higher than GWP for PHA production in biomass scenario. Sensitivity analysis using mass partitioning approach allocates eight times the impact for farming step to harvested stover, compared to system allocation approach, and therefore GWP for all PHA scenarios is 20% higher in comparison to scenarios obtained using system

allocation approach. Despite higher CO_2 allocation for the farming step, biomass scenario has negative and lower GWP compared to GWPs for different grades of PE (Figure 2.11). Based on the results of sensitivity analysis, it is an accurate assertion that actual GWP for PHA production lie between those calculated by system allocation and mass partitioning approach. Therefore, PHA production using corn stover as energy source is the only scenario with lower GWP compared to PE production, which depends on switching from fossil fuels to corn stover for energy requirements during processing and compounding of PHA biopolymer. However, in their conclusions, authors have expressed doubts regarding feasibility of such a switch, since most of the corn farming states in US use electrical energy derived from fossil fuels.
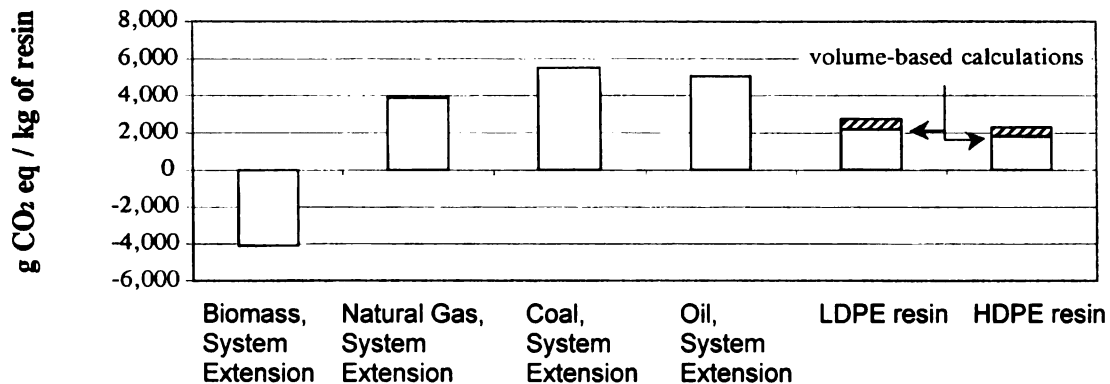
Figure 2.10 Global Warming Potential for PHA production in biomass and fossil fuel scenarios and comparison with different grades of PE(reproduced from Kurdikar et al., 2000)
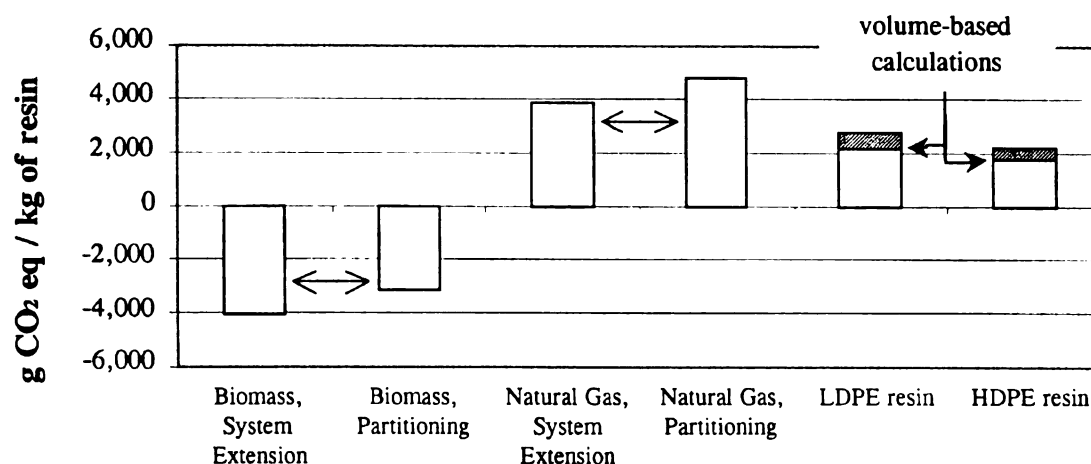
Figure 2.11 Comparison of Global Warming Potential for PHA production process using System allocation and Mass partitioning approach and PE prodution (reproduced from Kurdikar et al., 2000)

2.2.1.3 Akiyama et al., 2003

In this study, Akiyama et al.[35] have conducted a cradle to pellet life cycle inventory (LCI) analysis for PHA production using soybean oil and glucose as carbon source and compared it with production of conventional polymers such as LDPE, HDPE, PP, PS, PET on the basis of energy usage and CO_2 emissions metrics. The scope of this study is more comprehensive compared to other PHA LCA studies reviewed in previous subsections. LCI data for agriculture and milling of corn and soybean to obtain glucose and soybean oil respectively has been obtained from USDA for US based farming operations. The PHA fermentation and processing LCI data is based on a full scale simulation of PHA production and therefore this data is more comprehensive compared to previous studies. In the laboratory studies, authors have obtained relatively higher yields of 0.76 g-P(3HB)/g-soybean oil compared to known high yields of 0.3 to 0.4 g-P(3HB)/g-glucose. Therefore, in this study they have mainly focused on the PHA

production using soybean oil as a carbon source. In addition to energy and CO_2 calculations, cost estimates for PHA production are also computed. Comparison of energy consumption and CO_2 emissions for the median cost case of PHA production using soybean oil as carbon source with PHA produced using glucose, and petroleum based polymers is presented below in Table 2.4, and clearly shows a lower energy consumption and CO_2 emissions for PHA production using soybean oil compared to PHA produced from glucose and petroleum based polymers.

Table 2.4 Comparison of energy consumption and CO_2 emissions for fermentative production of PHA using different carbon sources with production of petroleum based polymers (Akiyama et al.[35])

Polymer type	Energy consumption (MJ/kg polymer)	CO_2 emissions (kg/kg polymer)
PHA (soybean as C source)	50	0.26
PHA (glucose as C source)	59	0.45
LDPE	81	1.9
HDPE	80	1.7
PP	77	1.9
PS	87	2.6
PET	79	3.1

For the current study, LCI of PHA production was based on the median cost scenario for PHA produced using soybean oil, because of the favorable environmental profile and comprehensiveness of this study compared to the previous studies by Gerngross and Slater[22,23], and Kurdikar et al.[20]. The results of this study and its application in the current LCA study are discussed in detail in Section 4.3.5.

2.2.2 Biobased composites LCA studies

A couple of LCA studies have compared the sustainability profile of biobased composites to conventional composites, considering replacement of glass fibers with hemp or china reed fibers. However, none of these studies have reviewed the LCA of completely biobased composites, i.e. obtained from biopolymers such as PHB, PLA, etc. and natural fibers. The results and conclusions from these studies are presented below.

2.2.2.1 Wotzel et al., 1999

This study[36] computes cradle to pellet inventory, impacts, and valuation of these impacts for the production of side panel for AUDI A3 car by injection molding of ABS copolymer resin and comparing the results with an alternative hemp fiber (66 vol%)-epoxy resin biocomposites. The cultivation, harvesting, and processing of hemp fibers as well as production of reinforced side panels have been modeled to be produced in South-West Germany. Inventory data for production of ABS copolymer and Epoxy resin is based on the data published by APME (Association of Plastics Manufacturers in Europe). Impact assessment of the inventory results follows UBA methods (ecological protection agency of

Germany), while Eco-indicator 95 method developed by Pre' Consultants is used to calculate Eco-indicator value from impact assessment results.

The emissions, which contribute towards majority of impacts, as well as total energy usage for both the systems are compared below in Table 2.5. Total energy consumption for hemp fiber-epoxy composites is 59 MJ lower compared to ABS copolymer side panel, mainly due to low energy consumption of 5% (of total energy used for hemp-epoxy composites) for hemp cultivation and processing. ABS copolymer side panel has higher global warming, acidification, winter smog, and summer smog impacts compared to hemp fiber -epoxy side panels, primarily due to higher CO_2, CH_4, SO_2 emissions from greater fossil fuel consumption. Eutrophication and ozone depletion impacts are higher for hemp fiber-epoxy composites because of fertilizer consumption for hemp cultivation and fluorohydrocarbon emissions from epoxy resin production. The cumulative impacts computed using Eco-indicator 95 valuation method are 8% lower for hemp fiber-epoxy side panels, with majority contribution from acidification impacts (47% for ABS copolymer and 45% for hemp-epoxy side panels).

The inventory analysis, impact assessment, and valuation results clearly shows a superior environmental profile for production of hemp fiber-epoxy side panels. Since the study does not consider use-phase and disposal phase of side panels, authors have partially addressed this issue in the scenario analysis by computing energy benefits from use phase of 200,000 km (14 yrs) and disposal by incineration. Even though, energy benefit from incineration of ABS copolymer is higher compared to hemp fiber-epoxy side panel (because of higher

hydrocarbon content for ABS copolymer), this benefit is offset by fuel savings from using lower weight hemp fiber-epoxy side panel and presents significantly lower overall energy consumption for hemp fiber-epoxy side panel, compared to ABS copolymer side panel.

Table 2.5 Inventory data for cradle to pellet production of automotive side panel using Hemp fiber-Epoxy and ABS copolymer composites (Wotzel et al.[36])

Inventory results[2]	Hemp fiber-Epoxy composites	ABS copolymer
Weight of side panel (g)	820	1125
Total energy usage (MJ)	73	132
(a) CO_2 (kg)	4.19	4.97
(a) CH_4 (g)	16.96	17.43
(a) NO_x (g)	18.64	14.14
(a) SO_2 (g)	10.70	17.54
(a) Dust (g)	6.96	4.25
(w) NO_3^- (g)	12.05	0.08×10^{-3}

2.2.2.2 Schmidt and Beyer, 1998

The main goal of this LCA study[37] is to determine environmental benefits of substituting glass fibers with hemp fibers as reinforcement in an insulation component for a Ford automobile. Authors have carried out a simplified LCA with cradle to grave scope for production of PP-EPDM (ethylene propylene diene copolymer)-glass fiber (43 wt%) and PP-EPDM-hemp fiber (30 wt%) composites,

[2] Prefix (a) denotes air emissions, and (w) denotes water emissions

assuming a use-phase of 100,000 km and equal amounts of disposal by landfilling and incineration. For inventory analysis, data for different components of the system are obtained from various public databases; APME for PP and EPDM data, Pre' and ETH databases for glass fiber data, IDEA, ETH, and BUWAL databases for utility and other chemical datasets, and from a hemp fiber supplier, Hemcore Limited for data regarding production of hemp. Since the study has been conducted for internal reporting in Ford, no explicit data has been reported, instead selected inputs and outputs are reported in terms of net benefits from the substitution of glass fiber with hemp fiber in the insulation component, and presenting net benefits of: 88. 90 MJ for total energy consumption, 2.12 kg oil equivalents, 8.18 kg CO_2 equivalents, 0.056 kg SO_2 equivalents, 0.018 kg NO_3^- equivalents. In addition to inventory analysis and impact assessment, interpretation of the results using scenario and sensitivity analysis is conducted, which further affirms the environmental benefits of substituting glass fibers with hemp fibers in the insulation component.

2.2.2.3 Corbiere-Nicollier et al., 2001

Similar to the scope of the previous LCA studies of biobased composites, this study[38] compares the environmental performance of PP-China reed fiber (CR) and PP-Glass fiber (GF) composites. A transport pallet with same tensile modulus or stiffness for both materials is selected as a functional unit; while scope of the study is cradle to grave, which includes cultivation, harvesting, and processing of CR fibers, PP and glass fiber production, use as a transport pallet for 5 years (with transport of 1000 km per year), and disposal by incineration or

bioactive discharge. The inventory analysis and comparison of the systems shows lower non-renewable energy consumption, and in general lower air and water emissions for CR pallets. CR pallets have higher soil emissions of heavy metals, N_2O and NH_3 air emissions, and phosphate and nitrate water emissions, all attributed to CR fiber cultivation and fertilizer use. A detailed analysis of these results has been done using CST95 (Critical Surface-Time) impact assessment method, and compared with impact assessment results from CML 92, Ecopoints, and Eco-Indicator 95 methods. Comparison of important inventory and impact assessment data for CR and GF pallets is presented below in Table 2.6. The impact assessment results computed using CST95 method are comparable to those obtained using other methods, except eutrophication and CR pallets have lower impacts than GF pallets. In case of eutrophication, other methods include NO_x emissions as a contributor to eutrophication, while CST95 assumes phosphate emissions as the only contributor to eutrophication (because of the fact that European lakes are generally P-limited), and therefore CST95 eutrophication impacts are higher for CR pallets compared to GF pallets. A scenario analysis of the end of life disposal options recommends incineration over bioactive discharge, even though incineration of PP component of the pallet leads to heavy metal air emissions, the energy credit obtained from incineration and water emissions from bioactive discharge makes incineration a better disposal solution. Finally, authors have determined the sensitivity of LCA results due to variation in pallet's use-phase life time, fiber composition, and use-phase transport distances. The results of the sensitivity analysis concludes that CR

pallets have superior environmental profile and lower energy use, as long as the pallets are used for a minimum of 3 years. Since the use of china reed fibers reduce the pallet weight, whereas glass fibers increase the pallet weight (density of glass fibers is three times the PP), the environmental benefits from china reed fiber use become more significant due to increased fiber content in pallets and greater transport distances during use-phase of the pallets.

Table 2.6 Inventory and Impact Assessment data for production of PP-China Reed fiber and PP-Glass fiber pallet (Corbiere-Nicollier et al.[38])

Inventory results	PP-CR pallets	PP-GF pallets
Energy consumption (MJ)	717	1400
(a) CO_2 (kg)	42	73.1
(a) N_2O (g)	2.2	1.96
(a) NH_3 (g)	11.3	0.12
(a) NO_x (g)	349	513
(w) Nitrate (g)	153	1.72
(w) Phosphate (g)	1.67	0.59
CML-Human Toxicity (kg 1,4- DCB^3 eq.)	9.04	21.2
CML-Terrestrial Ecotoxicity (kg 1,4- DCB eq.)	4480	5250
CML-Aquatic Ecotoxicity (kg 1,4- DCB eq.)	0.67	1.09
CML-Greenhouse effect (kg CO_2 eq.)	40.4	75.3
CML-Ozone formation (kg ethylene eq.)	0.13	0.21
CML-Acidification (kg SO_2 eq.)	0.43	0.65
CML-Eutrophication (kg PO_4^{3-} eq.)	0.063	0.068
CST95-Eutrophication (kg PO_4^{3-} eq.)	1.81×10^{-3}	8.23×10^{-4}

[3] DCB = dichlorobenzene

2.3 Biodegradation

The standards relevant to the current biodegradation study are reviewed briefly in the following subsection below.

2.3.1 ASTM standards

Various national and international bodies such as The American Society for Testing and Materials (ASTM), European Committee for Standardization (CEN), Deutsches Institut für Normung (DIN), Japanese Industrial Standards (JIS), and International Standards Organization (ISO) have established standards to quantify and evaluate the biodegradability of polymers in different environments such as compost, soil, marine-waters, wastewater treatment facilities, and aerobic digesters.

ASTM has published a series of standards for determining the compostability of plastics, the latest being D 6400 (ASTM, 1999) "Standard specification for compostable plastics". This standard lays down the detailed requirements for labeling a plastic as compostable. The other standards in this series are as follows:

1. D 5338 (ASTM, 1998): "Standard test method for determining aerobic biodegradation of plastic materials under controlled composting conditions".

2. D 6002 (ASTM, 1996): "Standard guide for assessing the compostability of environmentally degradable plastics".

ASTM D 6400 and D 6002 have no equivalent ISO standards; however, D 5338 has an equivalent ISO standard: ISO 14855, "Determination of the ultimate

aerobic biodegradability and disintegration of plastic materials under controlled composting conditions – Method by analysis of evolved carbon dioxide".

The requirements based on D 6400 for labeling a product as compostable can be summarized as follows:

1. Disintegration during composting – At the end of a composting study the residual plastic material should be indistinguishable from the other organic material in the final product. On sieving the final product, no more than 10% of the plastic material should remain on a 2.0-mm sieve.

2. Inherent Biodegradation – A plastic material must demonstrate one of the following rates of biodegradation (ratio of conversion of organic carbon to carbon dioxide):

   a. For a product containing a single polymer (homopolymers or random copolymers), the biodegradation rate must be 60% as compared to a known reference material.

   b. If a product contains more than one polymer (block copolymers, segmented copolymers, blends, or low molecular weight additives), 90% of the material should degrade in comparison to a known reference material.

   c. Products containing more than one polymer, any of which exceeds 1% concentration, must achieve the 60% rate of biodegradation.

The standard D 6400 recommends a test period of no more than 180 days for materials that are not radiolabeled and a test period of 365 days for

radiolabeled materials. Materials are radiolabeled with the (radioactive isotope) carbon-14 if the material biodegradation rate is slow.

3. No adverse impacts on ability of compost to support plant growth – the materials tested should not have harmful impacts on the ability of compost to support plant growth in comparison to compost using cellulose as a control, when the finished compost is introduced in soil. In addition, the composted materials should not release unacceptable levels of heavy metals and other toxic substances into the environment. The tests and guidelines to fulfill these requirements are:

   a. The composted material should have heavy metal concentrations less than 50% of those recommended in 40 CFR part 503.13; the individual pollutant concentrations recommended are provided in Table 2.7 (from 40 CFR part 503.13).

Table 2.7 Pollutant Concentrations (from 40 CFR part 503.13)

Pollutant	Monthly average concentration (mg/kg)[4]
Arsenic	41
Cadmium	39
Copper	1500
Lead	300
Mercury	17
Nickel	420
Selenium	100
Zinc	2800

   b. The composted material should fulfill the requirements for plant germination and plant growth using the cress seed test and the plant

---

[4] Dry weight basis

50

growth test respectively, following OECD (Organization for Economic

Development) Guideline 208.

References:

[1] Valigra L. 2000 January 20. Tough as Soybeans. The Christian Science Monitor.

[2] Nickel J, Riedel U. 2003. Activities in biocomposites. Materials Today 6(4):44-48.

[3] Saheb DN, Jog JP. 1999. Natural fiber polymer composites: A review. Advances in Polymer Technology 18(4):351-363.

[4] Sherman LM. 1999 October. Natural Fibers: The New Fashion In Automotive Plastics. Plastics Technology:62-68.

[5] DaimlerChrysler HighTech Report, 1999. Grown to Fit the Part. 82–85.

[6] Mohanty AK, Misra M, Drzal LT. 2001. Surface modifications of natural fibers and performance of the resulting biocomposites: An overview. Composite Interfaces 8(5):313-343.

[7] Lilholt H, Mark Lawther J. 2000. Natural Organic Fibers. In: Chou T-W, editor. Comprehensive composite materials. 1st ed. Amsterdam ; New York: Elsevier. p 303-325.

[8] Arora S. 2003. Single fiber testing of Kenaf fibers. Unpublished work, Composite Materials and Structures Center, Michigan State University.

[9] Netravali A N, Chabba S. 2003. Composites get greener. Materials Today (April 2003) 22-29.

[10] Albertsson AC, Karlsson S. 1995. Degradable Polymers for the Future. Acta Polymerica 46(2):114-123.

[11] Amass W, Amass A, Tighe B. 1998. A review of biodegradable polymers: Uses, current developments in the synthesis and characterization of biodegradable polyesters, blends of biodegradable polymers and recent advances in biodegradation studies. Polymer International 47(2):89-144.

[12] Mohanty AK, Misra M, Hinrichsen G. 2000. Biofibres, biodegradable polymers and biocomposites: An overview. Macromolecular Materials and Engineering 276(3-4):1-24.

[13] Gross RA, Kalra B. 2002. Biodegradable polymers for the environment. Science 297(5582):803-807.

[14] Flieger M, Kantorova M, Prell A, Rezanka T, Votruba J. 2003. Biodegradable plastics from renewable sources. Folia Microbiologica 48(1):27-44.

[15] Griffin GJL, editor. 1994. Chemistry and technology of biodegradable polymers. 1st ed. London ; New York: Blackie Academic & Professional. xiii, 154 p.

[16] Kaplan D, editor. 1998. Biopolymers from renewable resources. Berlin ; New York: Springer. xviii, 417 p.

[17] Stevens ES. 2003. Environmentally Degradable Plastics. In: Kroschwitz JI, editor. Encyclopedia of polymer science and technology. 3rd ed. Hoboken, N.J.: John Wiley. p 135-162.

[18] Mohanty AK, Misra M, Drzal LT, editors. 2005. Natural fibers, biopolymers, and biocomposites. Boca Raton, FL: Taylor & Francis/CRC Press. 875 p.

[19] Biodegradable Performance Polymers from Switchgrass – Fact Sheet, Office of Industrial Technologies Industries of the Future--Agriculture Program, 2002. Downloaded from: http://devafdc.nrel.gov/pdfs/8444.pdf

[20] Kurdikar et al., Greenhouse gas profile of a biopolymer, Journal of Industrial Ecology, 4 (2000), 107-122.

[21] Lenz RW, Marchessault RH. 2005. Bacterial polyesters: Biosynthesis, biodegradable plastics and biotechnology. Biomacromolecules 6(1):1-8.

[22] Gerngross TU. 1999. Can biotechnology move us toward a sustainable society? Nature Biotechnology 17(6):541-544.

[23] Gerngross TU, Slater SC. 2000. How green are green plastics? Scientific American 283(2):36-41.

[24] Boswell C. 2001 August 20 - 27. Bioplastics Aren't the Stretch They Once Seemed. Chemical Market Reporter.

[25] http://www.metabolix.com/, Metabolix Brochure, accessed May 2006.

[26] http://www.biomer.de/, Production of PHB, accessed May 2006.

[27] http://www.biomer.de/MechDatE.html

[28] Carothers W.H., Dorough, G.L., van Natta, F.J. 1932. Studies of Polymerization and Ring Formation. X. The Reversible Polymerization of Six-Membered Cyclic Esters. Journal of the American Chemical Society 54(2):761 - 772.

[29] Vink ETH, Rabago KR, Glassner DA, Gruber PR. 2003. Applications of life cycle assessment to NatureWorks (TM) polylactide (PLA) production. Polymer Degradation and Stability 80(3):403-419.

[30] Veronika E. Reinsch SSK. 1997. Crystallization of poly(hydroxybutrate-co-hydroxyvalerate) in wood fiber-reinforced composites. J Appl Polym Sci 64(9):1785-1796.

[31] Mohanty AK, Khan MA, Hinrichsen G. 2000. Surface modification of jute and its influence on performance of biodegradable jute-fabric/Biopol composites. Composites Science and Technology 60(7):1115-1124.

[32] Mohanty AK, Khan MA, Sahoo S, Hinrichsen G. 2000. Effect of chemical modification on the performance of biodegradable jute yarn-Biopol composites. Journal of Materials Science 35(10):2589-2595.

[33] Avella M, Rota GL, Martuscelli E, Raimo M, Sadocco P, Elegir G, Riva R. 2000. Poly(3-hydroxybutyrate-co-3-hydroxyvalerate) and wheat straw fibre composites: thermal, mechanical properties and biodegradation behaviour. Journal of Materials Science 35(4):829-836.

[34] Wong S, Shanks R, Hodzic A. 2002. Properties of poly(3-hydroxybutyric acid) composites with flax fibres modified by plasticiser absorption. Macromolecular Materials and Engineering 287(10):647-655.

[35] Akiyama M, Tsuge T, Doi Y. 2003. Environmental life cycle comparison of polyhydroxyalkanoates produced from renewable carbon resources by bacterial fermentation. Polymer Degradation and Stability 80(1):183-194.

[36] Wotzel K, Wirth R, Flake M. 1999. Life cycle studies on hemp fibre reinforced components and ABS for automotive parts. Angewandte Makromolekulare Chemie 272:121-127.

[37] Schmidt WP, Beyer HM. 1998. Life cycle study on a natural fiber reinforced component. SAE Total Life-cycle Conference. Graz, Austria: SAE.

[38] Corbiere-Nicollier T, Gfeller-Laban B, Lundquist L, Leterrier Y, Manson JAE, Jolliet O. 2001. Life cycle assessment of biofibres replacing glass fibres as reinforcement in plastics. Resources Conservation and Recycling 33(4):267-287.

Chapter 3: Project Definition

The current project is part of a research funded by National Science Foundation (NSF) under Product Realization and Environmental Manufacturing Innovative Systems of Eco-Efficiency (PREMISE) program. The overall objectives of the NSF-PREMISE project were to design and engineer eco-friendly biobased composites for automotive applications. These composites were processed using polyhydroxybutyrate (PHB) biopolymer reinforced with one of the BAST fibers, kenaf and hemp; or leaf fibers, henequen and pineapple leaf fiber.

The objective of the current research was to evaluate the sustainability of these biocomposites compared to conventional PP-Glass composites. This evaluation was done by conducting a life cycle assessment (LCA) study and by determining the biodegradation of these composites under controlled composting conditions. The LCA study considered cradle to pellet production of equal volumes of PHB-(30wt%)Kenaf and PP-(30wt%)Glass composites, and compares energy consumption and environmental impacts for the complete life cycle of these composites, as defined by ISO 14040 series of standards. The biodegradation of these composites was tested under controlled composting conditions, as specified by ASTM D 5338 standard, and compares percentage biodegradation as well as the effect of disposal end-products on growth of plants.

Chapter 4: Comparative Life Cycle Assessment of Biobased Composites and Conventional Composites

4.1 Introduction

The United Nations Bruntland Commission defined sustainability as meeting the needs of the present without comprising the ability of future generations to meet their own needs[1]. Life Cycle Assessment (LCA) is one of the quantitative methods available to evaluate the sustainability of a process/product.

ISO 14040(1997) defines life cycle assessment as compilation and evaluation of the inputs, outputs and the potential environmental impacts of a product system throughout its life cycle. Figure 4.1 highlights the different phases of an LCA, as defined by ISO 14043.
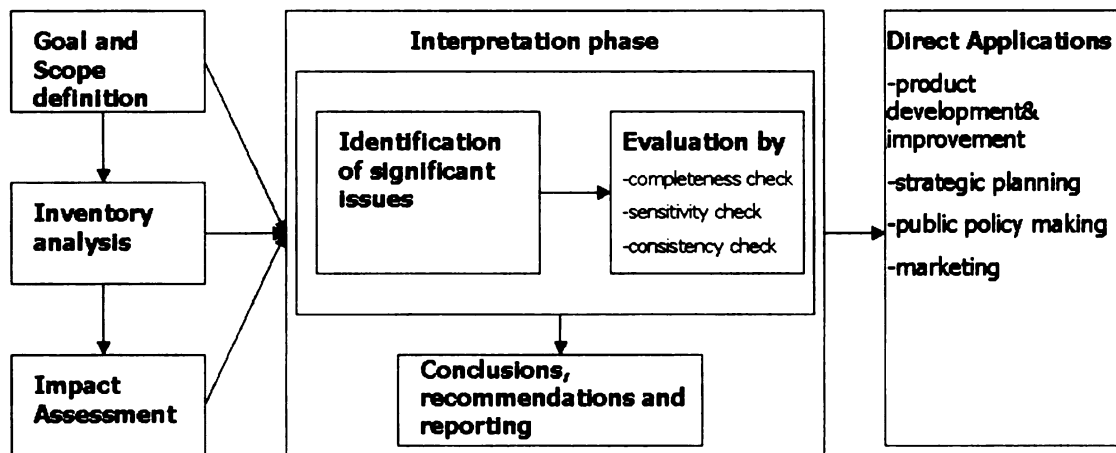
(ISO 14043, 2000)

Figure 4.1 Phases of an LCA

Inventory analysis (as defined by ISO 14040) involves data collection and calculation procedures to quantify relevant inputs and outputs of a product system (Figure 4.2).

Product Life Cycle

M, E   material and energy inputs for process and distribution
W   waste(gaseous, liquid, solid) output from product, process and distribution
⟶   material flow of product component
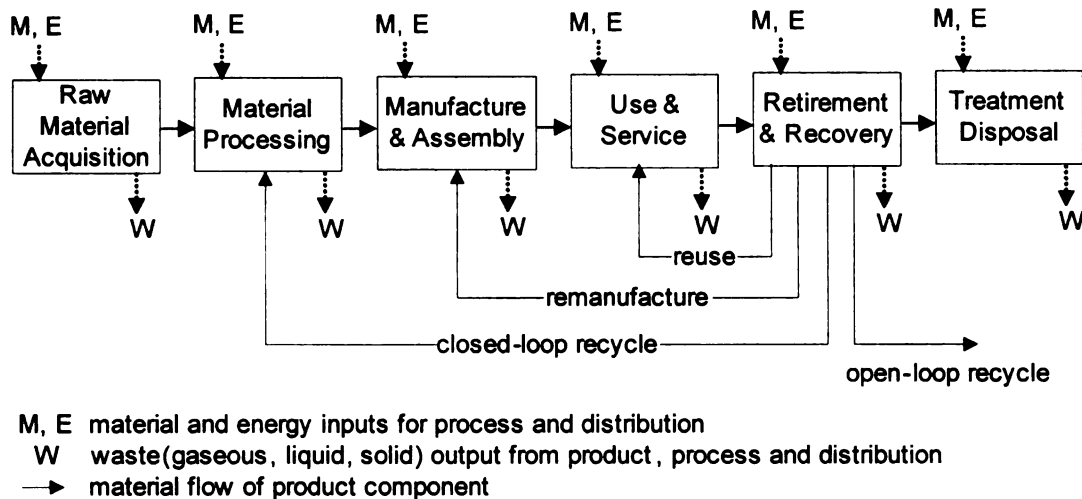
Figure 4.2: Life cycle assessment stages and boundaries (ref: css.snre.umich.edu)

Fiber reinforced polymer composites have been used in various industries for structural applications, with initial use in aerospace industry; currently they are being used for automotive parts, building materials, sporting goods, electronic components, etc[2,3]. Traditionally composites have been manufactured using unsaturated polyesters, polyurethanes, phenolic, or epoxy resins reinforced with glass, carbon or aramid fibers. However, the production of these conventional polymers and fibers is energy and resource intensive as highlighted by previous LCA studies done by the Association of Plastics Manufacturers in Europe (APME)[4], and the Department of Energy (DOE)[9] and uses significant amount of

petroleum based materials (both as feedstock and fuel) in the production process. Moreover, conventional composites are usually made using nondegradable matrices and fibers, which pose significant issues in the disposal phase because of the limited landfill capacity and also because incineration is energy intensive and known to result in toxic residues and emissions.

Therefore, the substitution of conventional polymers with biobased polymers and conventional fibers with natural fibers offers an instinctive solution to the issues of reducing the dependence on petroleum feedstocks and nondegradable composites. However, such a solution cannot be justified without quantifying the material and energy requirements over the entire life cycle of biocomposites, and thus addressing the following questions regarding the net-environmental benefits associated with biocomposites:

- What is the total energy consumption associated with the entire life cycle of biocomposites and conventional composites? How much of this energy is used as feedstock and fuel energy? Is there a net reduction in energy usage for biocomposites?

- What are the environmental emissions associated with the life cycle of biocomposites and conventional composites?

- How do biocomposites compare with conventional composites in important impact categories such as global warming, eutrophication, acidification, etc? If biocomposites have higher impacts in some categories, what are the steps in biocomposites life cycle which contribute the most to those categories?

4.2 Goal and Scope definition

4.2.1 Goal of the study

The ultimate goal of the present LCA study was to carry out a "cradle-to-grave" analysis for Polyhydroxybutyrate (PHB)-Kenaf fiber and Polypropylene (PP)-Glass fiber composites, which includes mass & energy flows related to extraction of raw materials, intermediate products manufacturing, transportation, use-phase and end-of-life or disposal phase. However, the actual analysis was limited to "cradle-to-factory-gate" study, with the reasons to limit the study, mentioned below in following sections.

4.2.2 Scope of the study

As specified in ISO 14040[5] standard, to clearly define the scope of the study, the following items were considered:

- Functional unit for the products

- System boundaries of the products being analyzed

- Allocation method

- Data quality requirements

- Impact assessment and Interpretation methods used

4.2.2.1 Functional unit

To compare the LCA of different products or systems, a reference is required so as to normalize the results. Therefore, such a functional unit is selected which is a measure of the performance of the output of the product or system being studied. For composites, mechanical properties are the most important performance characteristics and based on a feedback[6] from a major

automaker, the modulus is the most important property considered while selecting composites for structural applications. As discussed in the Introduction chapter of this thesis, under the present NSF-Premise project, processing and mechanical property evaluation of PHB-based composites was done and a comparison of the tensile properties for PP (polypropylene)-Glass, PHB-Kenaf composites is presented in Figure 4.3.
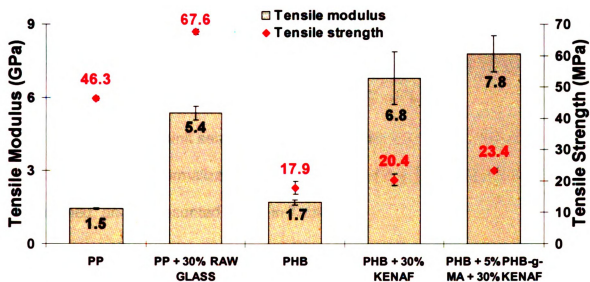
Figure 4.3 Comparison of tensile properties for PHB - (30wt%)Kenaf and PP-(30wt%)Glass composites

The tensile property evaluations above clearly indicate comparable tensile modulus for PHB-(30wt%)Kenaf and PP-(30wt%)Glass composites, and therefore the tensile modulus was selected as the performance criterion to compare these composites. Processing of these composites was done by extruding polymer matrix and fibers to obtain composite strands, which were pelletized and injection molded to obtain standard tensile coupons/dogbone samples for mechanical property evaluations. Since reliable industry data regarding processing of biocomposites to produce automotive components was

unavailable, data from composites processed in CMSC (Composite Materials Structures Center) was used to estimate the processing energy requirements. Therefore, tensile coupons (Figure 4.4) were selected as a functional unit, in order to accurately describe the system boundaries for the current LCA study.
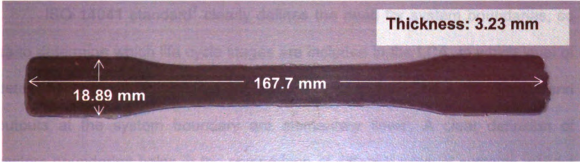
Figure 4.4 Standard tensile coupon for PHB-Kenaf composite

The functional unit selected for the study was a multiple of tensile coupon; and to get relevant normalized LCA data, the weight of the tensile coupons was determined, and is presented below in Table 4.1:

Table 4.1 Average weight of tensile coupons

Component	Average weight (grams)
PHB – (30wt%)Kenaf	10.8058 ± 0.0093
PP – (30wt%)Glass	9.8050 ± 0.0358

The slightly higher weight of the tensile coupons of PHB-Kenaf composites as compared to PP-Glass composites was expected. Even though Kenaf fiber has lower density (1.25 g/cc) as compared to Glass fiber (2.5 g/cc); it is more than offset by higher density of PHB (1.25 g/cc) as compared to PP (0.9 g/cc). To accentuate the differences between the LCA of PHB-Kenaf and PP-Glass composites, a multiple of 1000 was used for the functional unit. Therefore,

all the LCA results were normalized to the production of 1000 tensile coupons for PHB-(30wt%)Kenaf composites (weight = 10.81 kg) and PP-(30wt%)Glass composites (weight = 9.81 kg).

4.2.2.2 System boundaries

ISO 14041 standard[7] clearly defines the need for system boundaries, so as to determine which life cycle stages are included in the LCA, to which level of detail the environmental flows are tracked, and to make sure that inputs and outputs at the system boundary are elementary flows[i]. A clear definition of system boundaries helps in the comparison of different product systems without any ambiguity.

Process flow charts along with the system boundaries for the products being studied are described below in following subsections.

4.2.2.2.1 PP-Glass composite system boundaries

Polypropylene is one of the olefin polymers which is classified as commodity polymer because large volumes of the polymer are produced annually. It is obtained by *free radical polymerization*[8] of the propylene monomer, which is obtained by refining and subsequent cracking of crude oil. Therefore, significant amount of crude oil is used as feedstock energy in the production of polypropylene.

Glass fiber manufacturing[9] consists of four major processing steps: batch preparation, melting and refining, glass forming, and post forming operations.

---

[i] As defined in ISO 14040, "material or energy entering/leaving the system being studied, which has been drawn/discarded from/into the environment without previous/subsequent human transformation"

61

Details of these processing steps will be discussed in the LCI (life cycle inventory) results part of this chapter.

The outputs from the production steps above, PP pellets and chopped fiberglass strands are transported to the composites processing facility, where composite parts are obtained by extrusion and injection molding. As an example of use-phase, these composites are used as structural components in an automobile. Since both the components of these composites are nondegradable, at the end of use-phase these composites are either landfilled or incinerated and the ash component after incineration is landfilled. The process flow chart with the complete life cycle of PP-Glass composites is presented below in Figure 4.5.

4.2.2.2.2 PHB-Kenaf composite system boundaries

Polyhydroxybutyrate (PHB) is the most widely studied among the polyhydroxyalkanoates (PHA) family of biopolymers and belongs to the polyester class of polymers. PHB is currently being produced at pilot scale by a couple of companies: 1) As per the latest Metabolix brochure[10], "it has demonstrated economic production of PHAs by fermentation of plant-derived sugars and oils, and are in the process of making PHAs directly in crop plants." 2) Biomer[11] produces PHB by bacterial fermentation using sugar (sucrose) as a feedstock.

The current LCA study is based on the LCI study of PHB published by Akiyama et al.[12], in which they have compared the fermentative production processes for PHB using soybean oil and glucose as carbon source. The best scenario highlighted in their publication is the use of soybean oil as carbon sources and thus this scenario has been selected for the current analysis.

However, the soybean cultivation and soybean oil milling data was modified to improve accuracy, and fertilizer use and run-off data was added to account for important missing flows. The details of these improvements are mentioned in LCI section of this chapter.

Kenaf is a warm season annual fiber crop which is successfully cultivated in the southern states of the United States. For composites processing, long fibers are preferred, thus only BAST fibers, which are obtained from the bark of the kenaf stalk are used in the composites processing. Details of the kenaf cultivation and processing are presented in LCI section of this chapter.

Transportation of polymer and fiber, composites processing, and use-phase steps for PHB-Kenaf are same as those defined for PP-Glass composites. However, end-of-life step for PHB-Kenaf is different from PP-Glass composites. Since both the PHB polymer and the kenaf fibers are degradable, composting was considered as the most practical way of disposing the PHB-Kenaf composites. The process flowchart for the complete life cycle of PHB-Kenaf composites is presented below in Figure 4.6.

For the current LCA study, the system boundary included processes from extraction of raw materials till the processing of composites. The use phase for the composites was excluded because of the current ambiguity regarding the exact amount of composites used as structural composites in automobiles. The end-of-life comparison for PHB-Kenaf and PP-Glass composites was not done because of the data unavailability for use-phase and different viable disposal processes involved for PHB-Kenaf (Figure 4.6) and PP-Glass (Figure 4.5)

composites[SA7]. However, biodegradability evaluation under controlled composting conditions was done and the results are discussed in Chapter 5 of the thesis.

4.2.2.3 Allocation method

Allocation methods are necessary in order to accurately distribute the energy and material inputs and outputs in a process where multiple products are produced. Such scenarios are common in any industry, thus the ISO 14041 standard requires a relevant allocation procedure to be used in the LCA study. This standard recommends that allocation procedures should be avoided if possible, by collecting additional information about the sub-processes involved for individual products. If avoiding allocation is not possible, then partitioning of flows can be done based on the physical relationships between co-products of the system or economic value of these co-products. Additionally, this standard recommends another useful approach for avoiding allocation, called system expansion. In this approach, for a system with co-products allocation procedures are avoided by assuming that product systems with an equivalent function have the same environmental impacts[SA9]. This approach has been effectively used by Kim et al.[13,14] for LCA studies of Ethanol production system and PHA production from corn, where they have replaced co-products corn oil with soybean oil, and corn gluten meal, corn gluten feed with a sum of corn cultivation and nitrogen in urea.

For the current LCA study, mass based allocation was adopted because of the data limitations due to which system expansion approach is not used,

complexity of the system involving polymer and fiber LCIs, and use of mass based allocation for the PP production LCI obtained from DEAM database.

4.2.2.4 Data quality

<u>Time related coverage</u>: to ensure collected data were not outdated, only the most recent studies were referred[SA11].

<u>Geographical coverage</u>: wherever possible data pertinent to US production was used and if relevant data were unavailable, modifications to the available data were done so as to make them relevant to US industry.

<u>Technology coverage</u>: technology mix for the data provided has been mentioned; instances where data was relevant to a specific site or derived from a case study have been documented.
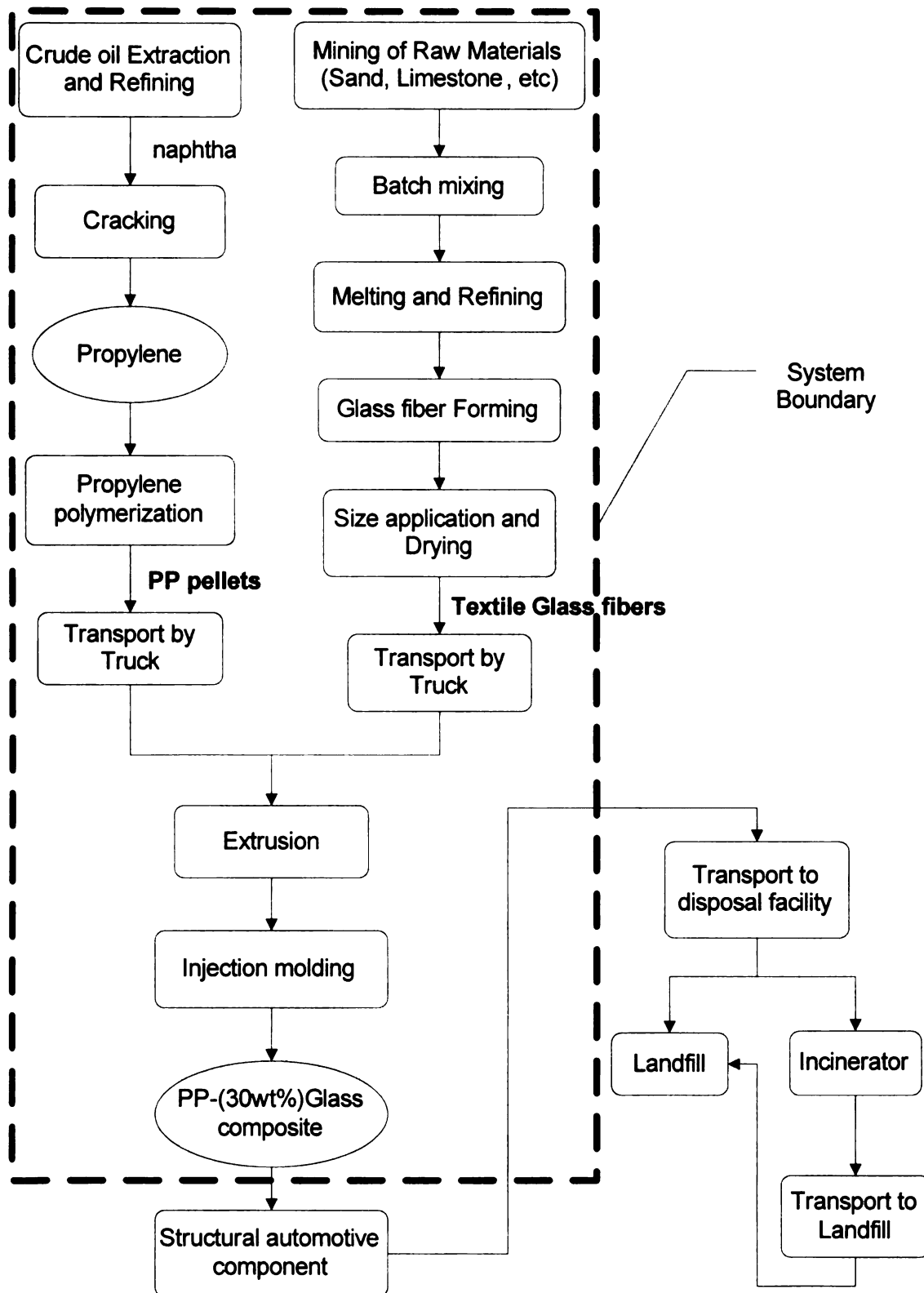
Figure 4.5 PP-Glass composites process flow chart and system boundary
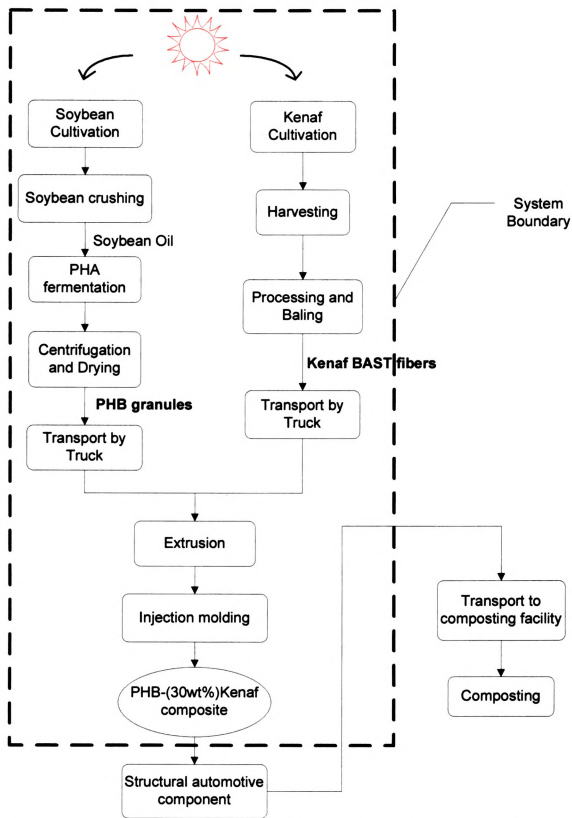
Figure 4.6 PHB-Kenaf composites process flow chart and system boundary

4.2.2.5 Impact assessment and Interpretation methods used

For further understanding of the life cycle inventory (LCI) results, emissions data are classified according to specific environmental impacts in order to determine the significance of these impacts for LCI results[5]. International Standards Organization (ISO) has laid out the requirements for reporting Life cycle impact assessment (LCIA) results in ISO 14042 standard[15]. [SA14]

In the current study, midpoint impact methods were used because of their comprehensive coverage of inventory flows as compared to endpoint categories and more international consensus for midpoint models compared to endpoint models[16]. To compute endpoint categories greater amount of detail is required compared to midpoint categories, thus computing endpoint indicators might exclude some inventory flows, which lack such detail.

Initially, for this study TRACI impact assessment methods[17], developed by the U.S. Environmental Protection Agency and adopted in BEES model[18], were used. These impact assessment methods are currently under revision, thus the final impact assessment results were calculated using CML methods[19] published by Centre of Environmental Science (CML) at Leiden University. The impact assessment methods selected are presented below in Table 4.2.

Table 4.2 Selected impact assessment categories

CML Impact Category	Units
Acidification	g SO_2 equivalent
Freshwater-Aquatic EcoToxicity	g 1,4-dichlorobenzene equivalent
Depletion of abiotic resources	kg antimony (Sb) equivalent
Depletion of the stratospheric ozone	g CFC-11 equivalent
Eutrophication	g PO_4^{3-} equivalent
Climate change (100 years)	g CO_2 equivalent
Human Toxicity	g 1,4-dichlorobenzene equivalent
Photo-oxidant formation	g ethylene equivalent
Terrestrial EcoToxicity	g 1,4-dichlorobenzene equivalent

All the impact categories noted above are midpoint categories. Every emission in the inventory analysis has associated effects, for e.g. SO_2 emissions from the system lead to smog formation, acid rain and thus causing respiratory diseases and effecting crops, forests respectively. In this example, respiratory diseases, effects on crops and forests are endpoint categories while photo-oxidant formation and acidification are midpoint categories respectively. Thus, midpoint categories are located somewhere in between the emissions (cause) – endpoint (effects) link and this connection is described below in Figure 4.7[20].
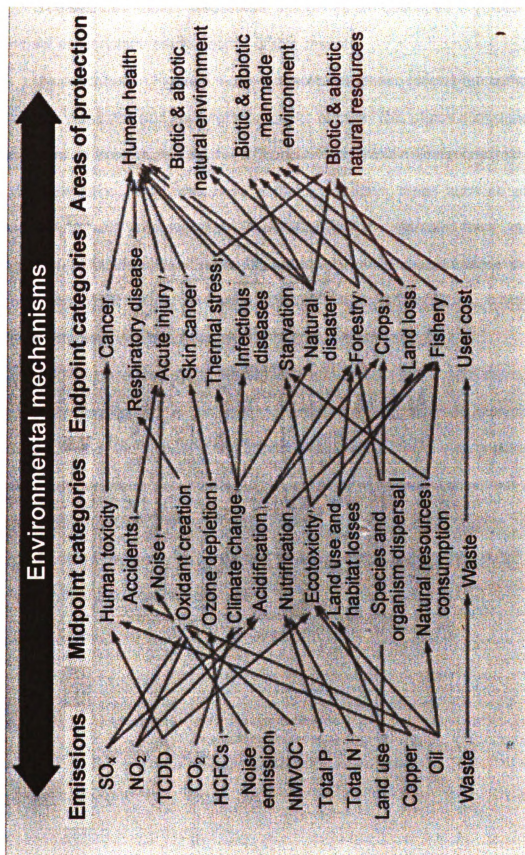
Figure 4.7 Connection between emissions, midpoint and endpoint categories

The selected impact assessment categories are described in greater detail in impact assessment results section of this chapter.

As described in Figure 4.1, the interpretation phase follows the completion of inventory analysis and interpretation phase of LCA. This phase allows the LCA practitioner to analyze results, reach conclusions, explain limitations and make recommendations, which can have a direct impact in areas such as product development and improvement. The ISO 14043[21] standard lays out the requirements for life cycle interpretation, and this phase should include steps to identify significant issues and evaluation of the results by steps, which may include completeness check, sensitivity check, consistency check, etc.

For the current study, significant issues in the LCI and impact assessment results were highlighted by contribution, dominance, and influence analysis. The completeness of the inventory and impact assessment results was checked and gaps in the data were documented. The sensitivity of impact assessment results (computed using CML characterization factors) was determined by using different nutrient-outflow allocation method for soybean cultivation and TRACI[22] (beta version 2.0) eutrophication potentials.

4.3 Life Cycle Inventory (LCI) Analysis

LCI is the phase of LCA, which is carried out once the goal and scope of the project have been defined. However, this sequence of analysis is not required to be rigid and ISO 14041 standard recommends that recursive process should be followed in order to refine the system boundaries of the systems being studied. This process was also adopted for the current study, first to modify the functional unit from being mass-based (production of 1 kg of composites) to volume-based (production of 1000 tensile coupons of composites), and second to include runoff emissions from cultivation of soybeans for PHB production.

4.3.1 Data categories

The current inventory analysis was modeled using TEAM™ software. Thus, the data category classification defined by this software was used for the LCI analysis, and these data categories are classified as follows: a) inputs, which include raw material, energy, and additional inputs; b) outputs, which include products, emissions to air, water, land, and recovered matter, waste categories; c) reminders[SA15], which include energy indicators such as total primary energy and intermediate flows (usually not visible) presented for greater understanding of the LCI results.

The data categories as defined above use prefixes to differentiate flows, with (r) representing non-extracted natural resources, (a) for air emissions, (w) for water emissions, (s) for emissions to land, (ar) for radioactive air emissions, (wr) for radioactive water emissions, and E for energy indicators. The energy indicators included in the reminders data category are: Total Primary Energy,

Non-Renewable Energy, Renewable Energy, Feedstock Energy, and Fuel Energy. These indicators are defined below.

Total Primary Energy: the sum of all energy derived from natural resources, either burned as fuel (Fuel Energy) or used as raw material in a product (Feedstock Energy[SA16]);.

Non-Renewable Energy: the fraction of total primary energy which is obtained from non-renewable resources (e.g. gasoline, diesel, natural gas, LPG);

Renewable Energy: the fraction of total primary energy obtained from renewable resources (e.g. wood, wind energy, geothermal, solar energy);

Feedstock Energy: the fraction of the total primary energy which is used as raw material in the products (e.g. naphtha is used as raw material for production of propylene, Figure 4.5);

Fuel Energy: the fraction of the total primary energy used as fuel for various unit processes in the system (e.g. gasoline & diesel used for transportation, natural gas for production of steam).

As per the definitions above, the following relationship among energy indicators was confirmed for the LCI results:

Total Primary Energy = Non-Renewable Energy + Renewable Energy = Fuel Energy + Feedstock Energy

The results from the inventory analysis contained as many as 350 flows, and not all of them contribute significantly to the selected impact assessment categories. Therefore, significant flows were selected by contribution[SA19] analysis of impact assessment results for PHB-Kenaf and PP-Glass composites

and the data for only these significant flows along with few additional flows[ii][SA21] are presented as LCI results[iii]. The flows selected by contribution analysis are presented below in Table 4.3. The percent contribution of individual flows to the impact categories in the table below should not be compared across the systems, for e.g. (a) NH₃ contribution of 47% to acidification impact for PHB-Kenaf system cannot be compared with 0.03% contribution for PP-Glass system. If the percent contribution from one of the LCI systems is missing for a flow, this means that the specific flow did not have significant contribution to the impact category, but included in the LCI results for comparison across the systems.

Table 4.3 Significant flows for PHB-Kenaf and PP-Glass composites (selected by Contribution Analysis)

Flows	PHB-Kenaf LCI Impact Contribution (%)	PP-Glass LCI Impact Contribution (%)
CML2000-Acidification		
(a) Ammonia (NH3)	47%	0.03%
(a) Nitrogen Oxides (NOx as NO2)	18%	27%
(a) Sulphur Dioxide (SO2)	0.32%	
(a) Sulphur Oxides (SOx as SO2)	34%	73%
CML2000-Aquatic Toxicity		
(a) Arsenic (As)	1%	1%
(a) Beryllium (Be)	44%	50%
(a) Hydrogen Fluoride (HF)	9%	10%
(a) Nickel (Ni)	19%	21%
(a) Selenium (Se)	9%	10%
(a) Vanadium (V)	4%	
(w) Barium (Ba++)	3%	
(w) Phenol (C6H5OH)	4%	
CML2000-Depletion of abiotic resources		
(r) Coal (in ground)	62%	23%
(r) Natural Gas (in ground)	32%	23%
(r) Oil (in ground)	6%	54%

[ii] These additional flows were selected based on their contribution as raw materials; and emissions, which currently cannot be quantified by available impact assessment methods, for e.g. (w) Acids (H⁺), (w) Water: chemically polluted, Waste (hazardous).
[iii] Impact assessment and interpretation phase calculations uses all inventory data; however, because of large number of flows (350), contribution analysis is used to limit the display of results to flows with significant contribution

74

Flows	PHB-Kenaf LCI Impact Contribution (%)	PP-Glass LCI Impact Contribution (%)
CML2000-Depletion of the stratospheric ozone		
(a) Halon 1301 (CF3Br)	13%	
(a) Methyl Bromide (CH3Br)	72%	82%
(a) Methyl Chloride (CH3Cl)	13%	15%
(a) Trichloroethane (1,1,1-CH3CCl3)	3%	3%
CML2000-Eutrophication		
(a) Ammonia (NH3)	30%	0.1%
(a) Nitrogen Oxides (NOx as NO2)	13%	99%
(w) Nitrate (NO3-)	0%	0.1%
(w) Nitrogenous Matter (unspecified, as N)	48%	0.2%
(w) Phosphorus (P)	9%	
CML2000-Greenhouse effect (direct, 100 years)		
(a) Carbon Dioxide (CO2, biomass)	-83%	
(a) Carbon Dioxide (CO2, fossil)	183%	100%
(a) Methane (CH4)	0%	
CML2000-Human Toxicity		
(a) Arsenic (As)	41%	36%
(a) Benzene (C6H6)	11%	20%
(a) Beryllium (Be)	3%	3%
(a) Dioxins (unspecified)	2%	2%
(a) Hydrogen Fluoride (HF)	29%	26%
(a) Nickel (Ni)	6%	5%
(a) Nitrogen Oxides (NOx as NO2)	2%	4%
(a) Selenium (Se)	4%	4%
CML2000-Photo-oxidant formation		
(a) Benzene (C6H6)	4%	12%
(a) Carbon Monoxide (CO)	24%	50%
(a) Ethylene (C2H4)	50%	
(a) Methane (CH4)	15%	30%
(a) Sulphur Dioxide (SO2)	2%	
CML2000-Terrestrial Toxicity		
(a) Arsenic (As)	39%	42%
(a) Beryllium (Be)	5%	5%
(a) Mercury (Hg)	44%	46%
(a) Nickel (Ni)	4%	4%
(a) Selenium (Se)	1%	1%
(a) Vanadium (V)	2%	
(s) Zinc (Zn)	3%	
Additional emission flows		
(w) Acids (H+) (w) Suspended Matter (unspecified) (w) Water: Chemically Polluted Waste (hazardous) Waste (total)	**NA**	**NA**

4.3.2 Glass fibers LCI

The glass fiber LCI analysis was conducted using data mainly from a 2002 study[9] published by the Office of Industrial Technologies, U.S. Department of Energy (DOE). This study presents energy and emissions data for the production of various types of glass using current technology mix for production in United States.

As mentioned in section 4.2.2.2.2, glass fiber manufacturing consists of four main processing steps, and these processing steps until end of melting and refining are the same for all types of glass (flat, container, blown, fiber glass). Forming and post-forming processes for fiber glass vary significantly from other glass types. A detailed fiber glass production process is presented in Figure 4.8 (reproduced from the Energy and environmental profile of the U.S. glass industry document[23],[24],[25]).

The first step in glass fiber production is batch preparation, involving mixing of raw materials for glass in the desired composition, which varies for different types of glass. The composition for E-glass (also known as textile fibers, glass fibers) is listed below in Table 4.4.

Table 4.4 Fiber Glass Composition (weight percent)[9]

Glass type	SiO_2	Na_2O	CaO	B_2O_3	Al_2O_3
Aluminoborosilicate: low-alkali (E-Glass)	54.5	0.5	22	8.5	14.5
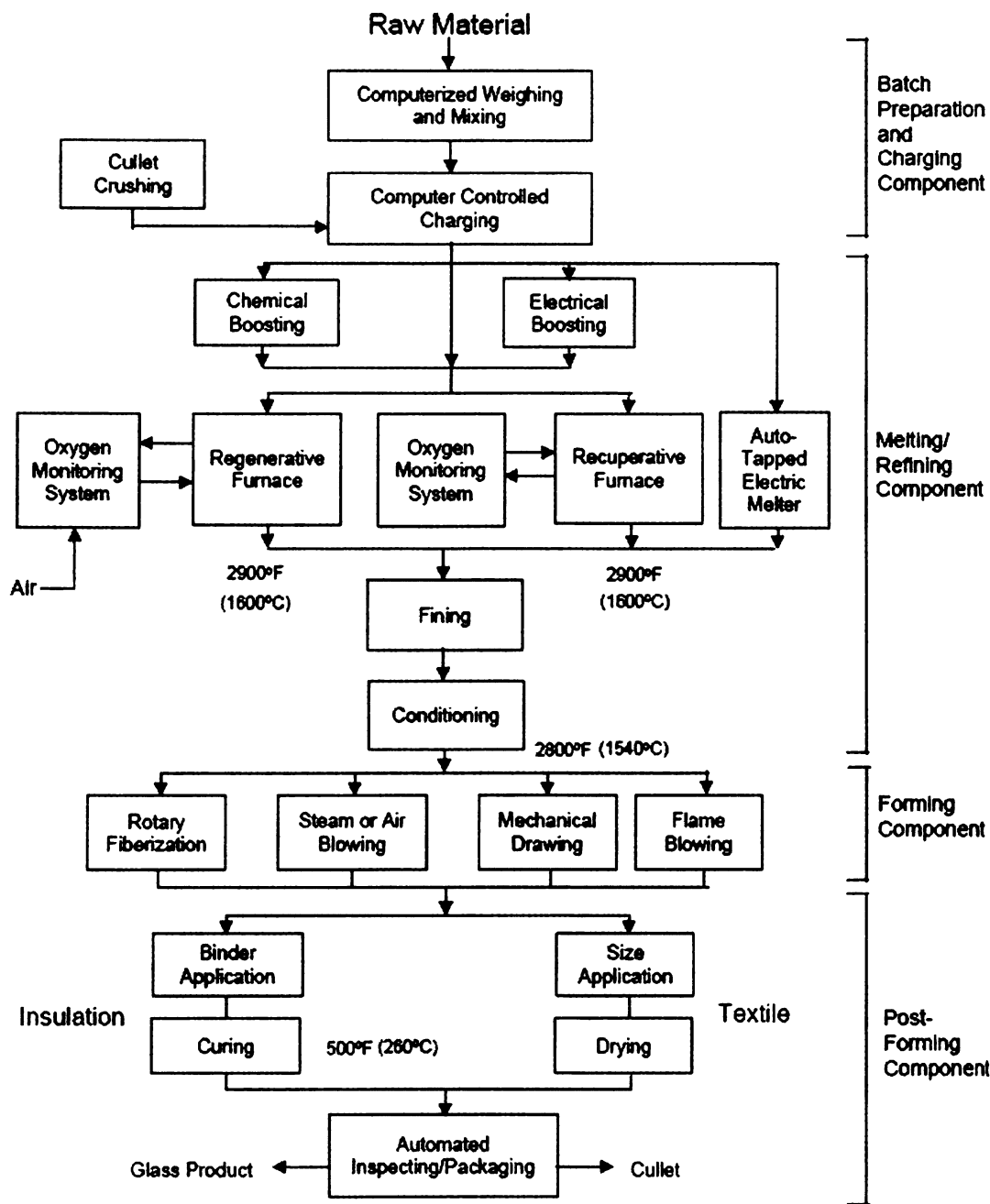
Figure 4.8 Fiber glass production [Brown 1996, EPA 1995, EPRI 1988]

In general, glass batch contains formers, fluxes, stabilizers and optional colorants. Formers are the basic ingredients for glass, with Silica (SiO_2), Feldspar

(as a source of alumina), and Boric acid (B_2O_3) used as formers for E-glass. Glass products can be produced using only silica. Since the melting point of silica is very high (1723°C), fluxes are added to lower the melting point of the batch. For E-glass, soda ash (Na_2CO_3 or Na_2O) is used as alkali flux. To make glass more chemically and physically stable, stabilizers are added, with limestone (source of $CaCO_3$ / CaO) used as stabilizer for E-glass.

Electricity use is the main source of energy consumption for E-glass batch preparation. Blending or batch mixing of raw materials account for the majority of the electricity use in this step. The energy use for crushing, grinding, and sieving of raw materials, before being shipped to the production site is not considered in the DOE study. Particulate emissions are the major emissions from the batch preparation process, and the following steps contribute to these emissions: unloading and conveying, storage bins, mixing and weighing.

Melting and refining is the second step, after the addition of batch mix to the melting furnace. This mix of raw materials is heated in the furnace to temperatures ranging from 2600°F to 3100°F. Because of such extreme temperature conditions, melting and refining is the most energy-intensive part of E-glass production process. Such a high temperature is required to facilitate a series of physical and chemical reactions including melting, dissolution, volatilization, and redox reactions. Melting of raw materials is complete when glass is free of crystalline materials.

The refining process (also referred as fining) follows the completion of melting, and involves removal of gas bubbles from the batch and molten glass,

homogenizing, and thermal conditioning of the glass melt. E-glass is produced using recuperative furnaces and oxy-fuel fired furnaces, both furnaces use natural gas as an energy source, the difference being the higher oxygen content of air used in oxy-fuel furnaces, which improves the energy efficiency of these furnaces since less amount of nitrogen is used in combustion (nitrogen absorbs large amount of heat, and this heat is lost through nitrogen oxide emissions). Additionally, oxy-fuel furnaces have significantly reduced nitrogen oxides emissions when 100 percent oxygen is used for fuel combustion.

The majority of the E-glass production emissions are from the melting and refining step, in the form of particulates, nitrogen oxides (NO_x), sulfur oxides (SO_x), carbon monoxide (CO), and fluorides.

The third step in E-glass production is forming, in which molten glass is converted into the final product. Continuous filaments of textile glass fibers are formed by forcing molten glass through very small holes and collecting glass filaments over a roller, and applying a coating of water-soluble sizing and/or coupling agents. These coated fibers are then sent to post-forming and finishing operations. The main energy requirement in the forming operations is electricity consumption for running machine operations, fans, blowers, compressors, conveyors, and additional equipment. Particulate matter emissions are the only emissions reported for forming operations of textile glass fibers in the DOE study.

The final step for textile glass fibers involves post-forming and finishing operations. Textile fibers coated with sizing and/or coupling agents are passed through drying oven to remove moisture, and are subsequently sent to curing

oven to cure the coatings. Finally, the cured glass fibers are chopped to obtain glass fibers used for making composites. The natural gas used in the ovens is the only energy requirement for post-forming and finishing step. Combustion products including particulate matter, NO_x, CO from dryers and ovens are the main emissions.

The total energy requirements and emissions (normalized to 1 kg of textile glass fiber production), including the individual steps energy requirements, are summarized below in Table 4.5 and 4.6 respectively.

Table 4.5 Total Energy requirements for 1 kg of Textile glass fiber production

Processing steps	Electricity consumption (MJ electricity/kg glass fiber)	Natural Gas consumption (MJ/kg glass fiber)
Batch preparation	1.34	NA
Melting and Refining	NA	11.98
Glass forming	8.37	NA
Post forming and Finishing	NA	3.81
Total	**9.71**	**15.79**

The data obtained from the DOE study only reported energy and environmental numbers for the production step of glass fibers, and thus cannot be considered as a complete LCI analysis. Based on the computed raw material requirements (Table 4.4), energy requirements (Table 4.5) and emissions from

the production step (Table 4.6), the cradle to pellet LCI for production of textile glass fibers was modeled using TEAM™ 4.0 LCA software[iv], with missing data inserted from the associated DEAM™ LCI database.

Table 4.6 Emissions from 1 kg of Textile glass fiber production

Processing steps	Emissions (kg/kg glass fiber)				
	Particulates	SO_x	NO_x	CO	Fluorides
Batch preparation	1.90E-03	←	NA		→
Melting and Refining	8.00E-03	1.50E-02	1.00E-02	5.00E-04	1.00E-03
Glass forming	5.00E-04	←	NA		→
Post forming and Finishing	6.00E-04	NA	1.30E-03	7.50E-04	NA
Total	**1.10E-02**	**1.50E-02**	**1.13E-02**	**1.25E-03**	**1.00E-03**

Modeling was carried out in two steps: first to develop LCI for mining of raw materials and there transportation, and second for LCI of textile glass fiber production. Mining of raw materials model was developed based on the raw material requirements (Table 4.4) for 1 kg of raw material mix for glass fiber production. This model is described below in Figure 4.9. Datasets for sand quarrying, feldspar quarrying, limestone quarrying, and sodium carbonate production were included from the DEAM™ database. Data for boric acid (B_2O_3)

[iv] TEAM™ acronym refers to Tools for Environmental Analysis and Management, software developed by Ecobilan, PricewaterhouseCoopers.

production were unavailable in the DEAM™ database or other sources and[SA23] hence not included in the inventory calculations. Transport by rail for 100 km was assumed for all the raw materials shipped to the glass fiber production site and associated energy use and emissions data obtained from DEAM database.

The Glass fiber production process was modeled based on the energy and emission numbers computed for the DOE study and is described below in Figure 4.10. DEAM™ datasets for Electricity, Natural Gas, Diesel production, Natural Gas combustion, and Road transport by truck were included in the modeling of textile-glass fiber production. Finished textile-glass fibers were assumed to be transported 100 km in a 40-ton truck to composites processing plant. Information regarding the source, year, and geographical coverage of the datasets is mentioned below in Table 4.7.
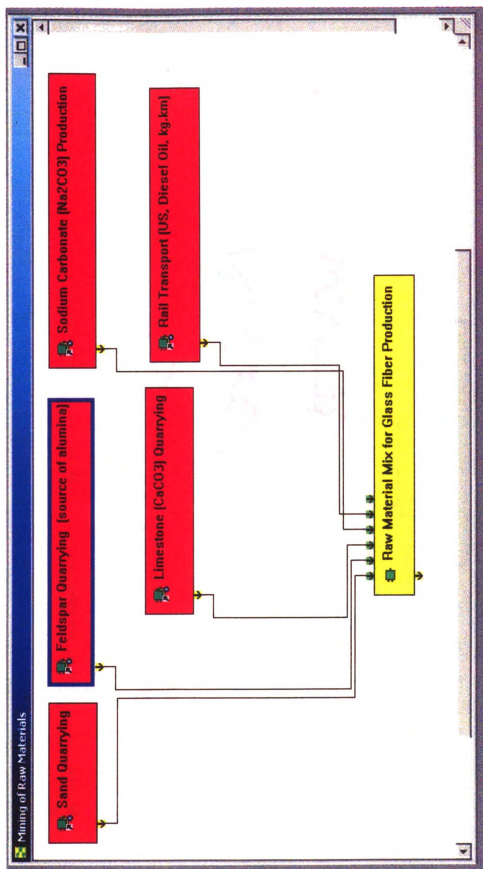
Figure 4.9 Model for Glass fiber raw material mix
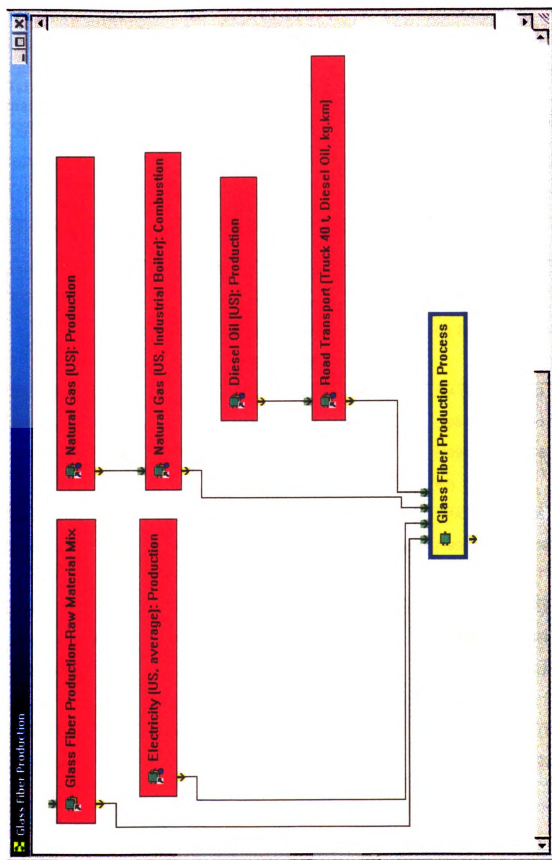
Figure 4.10 Model for Glass fiber production process

Table 4.8 shows the LCI data for the production of 1 kg of Glass fibers,

based on the model described in Figure 4.10.

Table 4.7 DEAM datasets used for modeling of Glass fiber-mining of raw materials and production process

DEAM™ datasets	Data characterization	Sources
Sand Quarrying	Energy production included (US Data)	BUWAL Environmental Series No. 132. 1991
Feldspar Quarrying	Energy Production included (US Data)	Ibid.
Limestone Quarrying	Energy production included (US Data)	Ibid.
Sodium Carbonate	One US site data for all inputs (source (1)). One US site data for emissions and wastes (source (2)). Energy Production (US data)	(1) OCI Wyoming (2) Tg Soda Ash, Inc.
Electricity (US, average) Production	Coal (56.6%), Natural Gas (8.6%), Heavy Fuel Oil (2.2%), Nuclear (22%), Hydroelectricity (10.6%)	EIA (1996, 95, 94), DOE (1988, 83), DeLuchi (1993), EPA (1996, 94, 85)
Natural Gas (US) Production	Processes include recovery, glycol dehydration, gas sweetening, pipeline transport of natural gas.	EPA, AP-42 (1996). GRI (1995, 96). EIA (1996). DeLuchi (1987)
Natural Gas (US, Industrial Boiler): Combustion	No waste or water effluents considered. Heating value: 52 MJ/kg	EPA AP-42 (1998), EIA (1994), GRI (1995), Argonne National Labs (1993)
Diesel (US) Production	Includes:- domestic and foreign crude oil production. US refinery operations only.	EIA (1994), EPA (1993, 85), DOE (1988, 83)

DEAM™ datasets	Data characterization	Sources
Road Transport (Truck 40 t, Diesel Oil, kg.km)	Data from diesel truck fuel consumption and emissions (max and average load: 40 000kg). Actual load of truck: 24 000 kg & empty return accounted. Diesel consumption with max load: 39 liter per 100 km.	ETH 1996. Anhang B: Strassengutertransport
Rail Transport (Diesel Oil, kg.km)	European Average data (1993-1994) for Diesel oil consumption: 0.0056 liter/km.metric ton (shipped). Diesel Oil Production: US data	Laboratorium fur Energiesysteme ETH, Zurïch, 1996

Table 4.8 LCI of Glass Fiber (cradle to pellet): Production of 1 kg of Glass Fibers

Flow	Units	Glass Fiber Production (total)	Electricity Production	Natural Gas Production	Natural Gas Combustion	Diesel Oil Production	Road Transport (Diesel Truck 40 t)	Raw Material Mix	Glass Fiber Production Process
Inputs:									
Boric Acid (B2O3)	kg	**0.085**	0	0	0	0	0	0.085	0
(r) Coal (in ground)	kg	**0.818**	0.807	0.003	0	8.70E-05	0	0.008	0
(r) Feldspar (ore)	kg	**0.145**	0	0	0	0	0	0.145	0
(r) Limestone (CaCO3, in ground)	kg	**0.285**	0.064	2.02E-04	0	6.90E-06	0	0.221	0
(r) Natural Gas (in ground)	kg	**0.384**	0.006	0.374	0	2.81E-04	0	0.004	0
(r) Oil (in ground)	kg	**1.28E-02**	5.27E-03	9.22E-04	0	2.56E-03	0	4.06E-03	0
(r) Sand (in ground)	kg	**0.545**	2.02E-07	6.05E-08	0	1.58E-07	0	0.545	0
(r) Sodium Carbonate (Na2CO3, in ground)	kg	**0.005**	0	0	0	0	0	0.005	0
(r) Sodium Chloride (NaCl, in ground or in sea)	kg	**3.05E-07**	9.28E-08	2.78E-08	0	7.25E-08	0	1.12E-07	0
(r) Uranium (U, ore)	kg	**1.34E-06**	1.17E-06	4.38E-08	0	1.46E-09	0	1.31E-07	0
Water Used (total)	liter	**0.528**	0.086	0.023	0	0.061	0	0.358	0
Water: Unspecified Origin	liter	**0.528**	0.086	0.023	0	0.061	0	0.358	0
Outputs:									
(a) Ammonia (NH3)	g	**1.50E-02**	5.84E-04	1.72E-02	0	1.33E-05	0	2.19E-04	0
(a) Arsenic (As)	g	**7.18E-04**	7.07E-04	2.32E-06	1.26E-06	9.06E-08	0	6.88E-06	0
(a) Benzene (C6H6)	g	**0.143**	0.003	0.139	1.32E-05	8.81E-05	2.40E-06	0.001	0
(a) Beryllium (Be)	g	**8.36E-05**	8.12E-05	3.07E-07	1.26E-06	9.08E-09	0	7.96E-07	0
(a) Carbon Dioxide (CO2, biomass)	g	**2.09E-02**	2.08E-02	1.23E-05	0	4.32E-07	0	3.94E-05	0

Flow	Units	Glass Fiber Production (total)	Electricity Production	Natural Gas Production	Natural Gas Combustion	Diesel Oil Production	Road Transport (Diesel Truck 40 t)	Raw Material Mix	Glass Fiber Production Process
(a) Carbon Dioxide (CO_2, fossil)	g	2967.840	2017.410	145.323	755.865	0.925	7.560	40.761	0
(a) Carbon Monoxide (CO)	g	2.772	0.415	0.560	0.497	0.003	0.019	0.029	1.25
(a) Dioxins (unspecified)	g	6.60E-09	6.52E-09	2.06E-11	0	7.03E-13	0	6.29E-11	0
(a) Ethylene (C_2H_4)	g	0	0	0	0	0	0	0	0
(a) Halon 1301 (CF_3Br)	g	1.24E-11	3.77E-12	1.13E-12	0	2.94E-12	0	4.55E-12	0
(a) Hydrogen Fluoride (HF)	g	6.12E-02	6.04E-02	1.91E-04	0	6.51E-06	0	5.83E-04	0
(a) Mercury (Hg)	g	4.62E-05	4.39E-05	2.07E-07	1.64E-06	5.62E-09	0	4.44E-07	0
(a) Methane (CH_4)	g	9.238	3.611	5.513	0.014	0.005	2.88E-04	0.094	0
(a) Methyl Bromide (CH_3Br)	g	6.53E-05	6.44E-05	2.04E-07	0	6.94E-09	0	6.22E-07	0
(a) Methyl Chloride (CH_3Cl)	g	2.16E-04	2.13E-04	6.76E-07	0	2.30E-08	0	2.06E-06	0
(a) Nickel (Ni)	g	9.71E-04	9.40E-04	5.67E-06	1.32E-05	8.19E-07	0	1.18E-05	0
(a) Nitrogen Oxides (NOx as NO_2)	g	19.789	6.441	1.025	0.796	0.004	0.098	0.125	11.3
(a) Selenium (Se)	g	5.30E-04	5.24E-04	1.68E-06	1.51E-07	6.07E-08	0	5.07E-06	0
(a) Sulphur Dioxide (SO_2)	g	0	0	0	0	0	0	0	0
(a) Sulfur Oxides (SOx as SO_2)	g	22.324	7.182	0.030	0.004	0.005	0.006	0.097	15
(a) Trichloroethane (1,1,1-CH_3CCl_3)	g	8.16E-06	8.05E-06	2.55E-08	0	8.68E-10	0	7.77E-08	0
(a) Vanadium (V)	g	2.47E-05	2.94E-06	1.93E-06	1.45E-05	1.80E-06	0	3.54E-06	0
(s) Zinc (Zn)	g	0	0	0	0	0	0	0	0
(w) Acids (H+)	g	9.35E-07	1.38E-08	9.12E-07	0	5.73E-10	0	9.44E-09	0
(w) Barium (Ba++)	g	6.84E-09	2.08E-09	6.22E-10	0	1.62E-09	0	2.51E-09	0

88

Flow	Units	Glass Fiber Production (total)	Electricity Production	Natural Gas Production	Natural Gas Combustion	Diesel Oil Production	Road Transport (Diesel Truck 40 t)	Raw Material Mix	Glass Fiber Production Process
(w) Nitrate (NO3-)	g	4.92E-05	4.20E-05	1.65E-06	0	3.57E-07	0	5.15E-06	0
(w) Nitrogenous Matter (unspecified, as N)	g	3.85E-10	1.17E-10	3.50E-11	0	9.14E-11	0	1.41E-10	0
(w) Phenol (C6H5OH)	g	8.81E-05	2.68E-05	8.06E-06	0	2.09E-05	0	3.23E-05	0
(w) Phosphorus (P)	g	0	0	0	0	0	0	0	0
(w) Suspended Matter (unspecified)	g	0.021	0.006	0.002	0	0.005	0	0.008	0
(w) Water. Chemically Polluted	liter	0.025	0.008	0.002	0	0.006	0	0.009	0
Glass Fiber	kg	1	0	0	0	0	0	0	1
Waste (hazardous)	kg	1.49E-05	4.54E-06	1.36E-06	0	3.54E-06	0	5.47E-06	0
Waste (total)	kg	0.493	0.361	0.013	0	4.66E-04	0	0.118	0
Reminders:									
Diesel Oil	kg	2.40E-03	0	0	0	0	2.40E-03	0	0
E Feedstock Energy	MJ	2.50	2.14	16.12	-15.79	0.11	-0.10	0.03	0
E Fuel Energy	MJ	48.13	28.12	3.45	15.79	0.02	0.10	0.65	0
E Non Renewable Energy	MJ	45.05	24.70	19.57	0	0.12	0	0.66	0
E Renewable Energy	MJ	5.57	5.55	0.00	0	1.18E-04	0	0.01	0
E Total Primary Energy	MJ	50.63	30.26	19.57	0	0.12	0	0.68	0
Electricity	MJ elec	9.71	0	0	0	0	0	0	9.71
Transport: Rail (kg.km)	kg.km	100	0	0	0	0	0	100	0
Transport: Road (diesel oil, kg.km)	kg.km	100	0	0	0	0	0	0	100

4.3.3 Polypropylene LCI

The system boundary for polypropylene (PP) manufacturing has already been defined under the goal and scope section of this chapter and was described before in Figure 4.5. For the current study, PP manufacturing data was directly obtained from DEAM™ database and is based on a cradle to pellet LCA of polypropylene published by the Association of Plastic Manufacturers in Europe (APME)[26]. PP pellets were assumed to be transported 100 km in a 40-ton truck to composites processing plant. DEAM™ datasets for Road transport by truck and Diesel production were used for the transportation step of PP-pellets, similar to textile-glass fibers. The assumptions for these datasets are described before in Table 4.7.

Since PP manufacturing data were directly obtained from DEAM™ database, the modeling of PP transportation step was combined with the modeling of PP-Glass composites, which is described in detail in following sub-sections.

4.3.4 Kenaf fiber LCI

Obtaining processed natural fibers for composites processing, generally involves 3 steps: 1) Cultivation and Harvesting 2) Transportation 3) Processing.

The material and energy requirements for cultivation and harvesting of kenaf were calculated from a resource use and cost estimation study done by the Dept. of Agricultural Economics at Mississippi State University in 1999[27] (see Appendix 4.3.4 for details). The estimates provided in the study are for growing kenaf in the state of Mississippi. Kenaf cultivation involves the following operating

steps: plowing (disk harrow & row conditioning), herbicide and fertilizer application, seed planting, cultivation, and irrigation. Fully grown kenaf plants are silage (forage) harvested, moved out of the field in a boll buggy, and finally compressed in a module builder (module builder is a stationary piece of equipment that compresses the harvested kenaf into a 32'x8' module or block). The compressed kenaf module is then transported to the fiber processing facility. Transportation by 16-ton diesel truck for 50 km was assumed for shipping harvested kenaf from farm to processing facility.

The performance rate and diesel fuel consumption rate for the tractor used in each step are provided below in Table 4.9. The diesel fuel consumed was calculated as a product of performance rate and fuel consumption rate.

Table 4.9 Diesel consumption rates for Kenaf Cultivation and Harvesting

Operating steps	Tractor size (hp)	Performance rate (hr/acre)	Diesel consumption rate (gal/hr)	Diesel consumed (gal/kg BAST fiber)[v]
Disk harrow (2 times)	160	0.078	7.72	8.63E-05
Row conditioning	160	0.053	7.72	2.93E-05
Seed planting	160	0.070	7.72	3.87E-05
Cultivation (early)	160	0.095	7.72	5.25E-05
Silage harvester	100	0.600	5.40	2.32E-04
Boll buggy	160	0.220	7.72	1.22E-04
Module builder	160	0.220	7.72	1.22E-04

[v] Converted to kg/kg BAST fiber value, using Diesel calorific value = 150.84 MJ/gal, ρ_{Diesel} = 887.15 kg/m^3

The Mississippi State University cost estimation study provided useful information regarding the resources consumed by various farm operations. However, information regarding total kenaf yield/acre, BAST fiber percentage of the total yield, amount of fertilizers and herbicides used was not available in this study and thus obtained from other publications. In a 1993 study, Webber[28] has presented kenaf yield and fertilizer use data for 5 kenaf cultivars. Out of these cultivars, yield data for Everglades 41 was selected because of its greater percent stalk production (78.5%) than leaf production and kenaf stalks having mid-range bark to core ratio (0.52, bark content is 34.2%). Herbicide application rates were calculated from a 1996 research report by Baldwin et al.[29] and Treflan™ (trifluralin as active ingredient) was selected as herbicide for kenaf production. Kenaf fiber yield, fertilizer and herbicide application rate data are presented below in Table 4.10.

Mass based allocation was used to distribute Kenaf fiber production data between BAST and core fibers, with no allocation to leaf production. Such a method of allocation is justified because of the economic value of the products obtained. BAST fibers are directly obtained from the bark of the kenaf plant and because of their long fiber length and superior mechanical properties compared to core fibers; they are used as reinforcement in composites and paper manufacture. Core fibers are obtained from the remaining portion of kenaf stalks and are used as fillers in composites, animal bedding, oil-absorbent material for spill cleanup[30,31]. The only use of kenaf leaves can be as livestock feed, thus justifying allocation of production data between BAST and core fibers.

Table 4.10 Kenaf fiber yield, fertilizer and herbicide application rates

Yield / Application rate	kg/acre	Allocating 34.2% to BAST fibers (kg/kg BAST fibers)
Kenaf Leaf yield	1092.66	NA
Kenaf Stalk yield	4775.31	NA
Ammonium Nitrate (NH_4NO_3, as N)	67.99	4.87E-03
Superphosphate (triple, as P_2O_5)	29.14	2.09E-03
Potassium Chloride (KCl, as K_2O)	56.25	4.03E-03
Treflan™	0.61	4.37E-05

Tractor emissions from kenaf cultivation and harvesting operating steps were calculated based on a 1999 Swedish study by Hansson et al[32]. This study reports variation in CO, NO_x, and HC (hydrocarbon) emissions for different farm operations, because of different load requirements for these operations. SO_2 and CO_2 emissions are assumed to be constant for all farming operations, with SO_2 emissions calculated based on the sulphur content in the diesel fuel. The emission factors obtained from this study are presented below in Table 4.11. These factors are measured from a standard 70 kW (94 hp) tractor used in Sweden. For kenaf cultivation and harvesting (Table 4.9), farm operations were performed using 160 or 100 hp tractor; the emission factors for these tractors were assumed to be same as the 94 hp tractor used in the study.

Table 4.11 Emission factors for various farming operations (in g/MJ diesel)

Operating steps	Emission factor (g/MJ diesel)				
	CO_2	SO_2	CO	NO_x	HC
Disk harrow (2 times)	74.6	0.094	0.042	0.897	0.016
Row conditioning	74.6	0.094	0.042	0.897	0.016
Seed planting	74.6	0.094	0.108	0.948	0.034
Cultivation (early)	74.6	0.094	0.076	0.747	0.030
Silage harvester	74.6	0.094	0.300	1.300	0.200
Boll buggy	74.6	0.094	0.300	1.300	0.200
Module builder	74.6	0.094	0.300	1.300	0.200

The emissions related to herbicide application were calculated based on the emission factors specified in EPA AP-42 document[33] for herbicide and pesticide application. Detailed calculations are described below:

Formulation of Treflan™ (from DowAgroSciences website[34])

Active Ingredient: Trifluralin = 43%

Inert Ingredient = 57%

Specific Gravity = 1.12

Vapor pressure of Trifluralin = 1.1×10^{-4} mm Hg @ 20-25°C

Application method: preplant soil incorporated treatment

Based on this information, the uncontrolled emission factor for active ingredient – Trifluralin is 52 kg/Mg (equivalent weight of active ingredients volatilized / unit weight of active ingredients applied), and the emission factor of

VOC from inert ingredients is 38% of the total inert ingredients applied. VOC emissions from active and inert ingredients were added; the calculated total Unspecified HC air emissions allocated to BAST fibers were: 1.043E-02 g/kg BAST fibers.

The LCI of Trifluralin was estimated based on the energy consumption values per kg of agrochemicals produced (obtained from a 1998 NREL study[35]), which are mentioned below in Table 4.12.

Table 4.12 Energy consumption values per kg of agrochemicals produced

Energy Inputs	kg / kg of agrochemicals
Natural Gas	0.64
Coke	0.045
Light Fuel	1.89
Steam	16.5
Electricity (MJ elec[SA25])	24.4

Trifluralin represents 26% of the agrochemicals-mix, for which the energy consumption values have been obtained from the NREL study. In the current inventory for trifluralin production, the same energy values (Table 4.12) were assumed to represent production of trifluralin alone. In absence of direct and comprehensive data available for trifluralin production, this assumption was useful in modeling trifluralin production in TEAM™ software, as described in Figure 4.11.
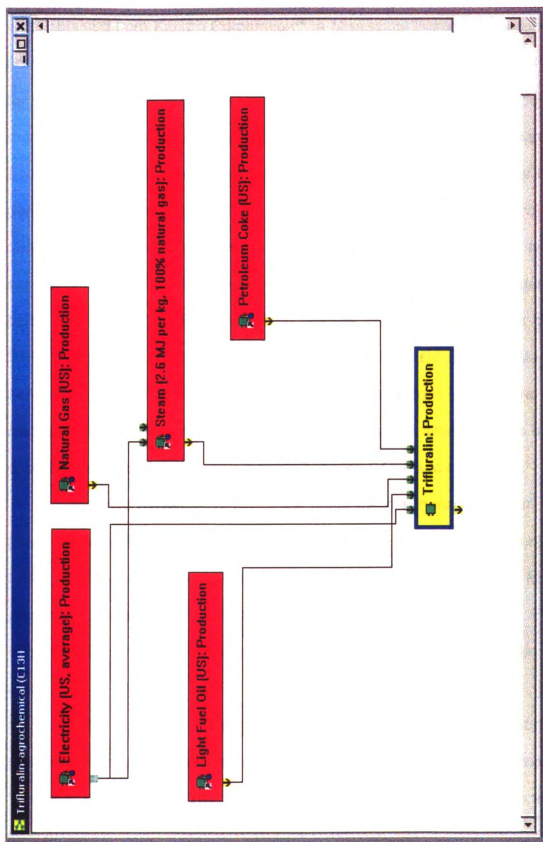
Figure 4.11 Model for Trifluralin production process

The energy requirements for processing and baling of raw kenaf fiber were obtained from Kengro Corporation[36], a Mississippi based kenaf-processing company. The average harvested kenaf fiber yield on there farms is 6 short-tons/acre (5443 kg/acre). Before harvesting the crop is left on the field for three months to facilitate dew retting, which aids in removal of unwanted bark material from the kenaf fiber strands in the bark. Separation of harvested kenaf fiber is done using equipment similar to stick machine, which is used for cleaning unginned cotton, as discussed in a 1999 patent by Stover[30]. The average separation capacity of this equipment is 9 short-tons/hr, with power requirement being 170 kW/hr. The fiber separation process produces a maximum of 32% BAST fibers, 62% core fibers, and the remaining is waste material. Maximum separation is obtained under dry atmospheric conditions, with more waste material produced under humid conditions. Mass-based allocation was used to split fiber separation power requirements between BAST and core fibers.

Separated Kenaf-BAST fibers are baled using a horizontal baler, with a baling capacity of 25 bales/hr (1 bale ≈ 300 lbs) and power requirement of 30 kW/hr. Particulate emissions are the only significant emissions arising from the processing operations for kenaf fibers, and are weather dependent. For the current study, this emission factor was not calculated because of the unavailable data.

Similar to Glass fiber LCI, Kenaf fiber cultivation, transport, and processing steps were modeled using TEAM™ software, to obtain inventory with "cradle to pellet" scope. The modeling was carried out in two steps. In the first

step, transportation of harvested-raw kenaf fibers for 50 km in a 16-ton truck was modeled. In the second, inputs and emissions from cultivation, transport, and processing steps were included (as specified in Table 4.9 through 4.11); the model is described in Figure 4.12 below. Datasets for Electricity, Diesel, Ammonium Nitrate, Potash, Superphosphate production and Transport by 40-ton truck were imported from DEAM™ database for this model. The assumptions for natural gas, electricity, diesel, and transport by 40-ton truck datasets have already been specified in Table 4.7. Table 4.13 provides details for rest of the datasets, associated with Trifluralin production, Raw kenaf transport, Kenaf cultivation and processing models.

The LCI data for the production of 1 kg of Kenaf fibers is presented below in Table 4.14, based on the model described in Figure 4.12.
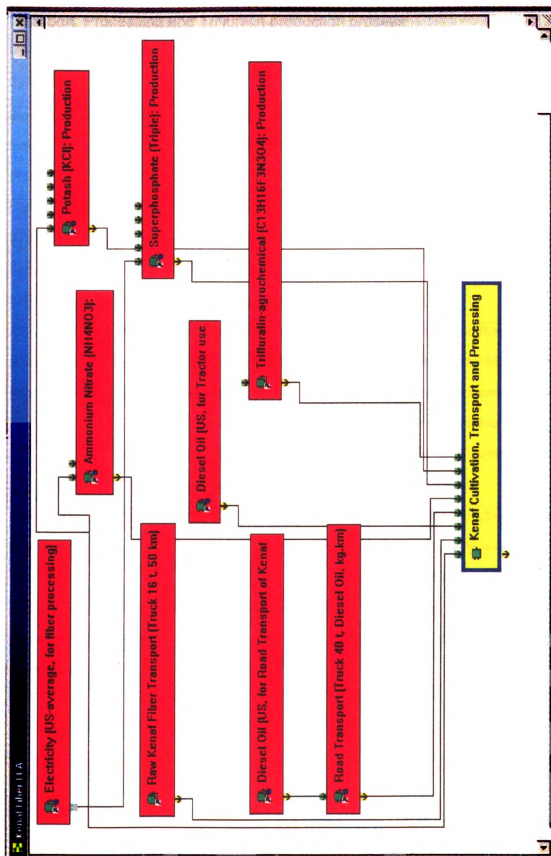
Figure 4.12 Model for Kenaf fiber Cultivation, Transport and Processing

Table 4.13 DEAM datasets used for modeling of Kenaf fiber Cultivation, Transport, Processing and Trifluralin production process

DEAM™ datasets	Data characterization	Sources
Steam (100% natural gas) Production	Production of steam with 100% natural gas, steam production model developed by Ecobilan	Ecobilan 2002
Light Fuel Oil (US) Production	Includes: - domestic and foreign crude oil production. US refinery operations only.	EIA (1994), EPA (1993, 85), DOE (1988, 83)
Petroleum Coke (US): Production	Includes: - domestic and foreign crude oil production. US refinery operations only.	Ibid.
Ammonium Nitrate (NH_4NO_3) Production	Production by neutralizing nitric acid (HNO_3) with ammonia (NH_3), unit processes are: neutralization, evaporation/concentration, prilling, cooling/drying. Water and solid waste emissions data not included.	The Fertilizer handbook for energy data (multiplied by 85% to account for process improvements) and based on the stoichiometric requirements; Air emissions data from EPA AP-42
Potash (KCl) Production	Production of Potash (KCl as K_2O)	The Fertilizer Handbook, values multiplied by 85% to account for efficiencies over time
Superphosphate (Triple) Production	Production of Superphosphate (triple as P_2O_5)	J.L. Vignes, G. André, F.Kapala. Union des Physiciens, Paris, 1994

DEAM™ datasets	Data characterization	Sources
Road Transport (Truck 16 t, Diesel Oil, kg.km)	Data from diesel truck fuel consumption and emissions (max and average load: 16 000 kg). Actual load of truck: 6000 kg & empty return accounted. Diesel consumption with max load: 29 liter per 100 km.	ETH 1996. Anhang B: Strassengutertransport

Table 4.14 LCI of Kenaf Fiber (cradle to pellet): Production of 1 kg of Kenaf Fibers

Flow	Units	Kenaf Fiber Production (total)	Diesel Oil Production (used for Road Transport)	Road Transport (Diesel Truck 40 t)	Diesel Oil Production (for Tractor use - cultivation & harvesting)	Raw Kenaf Fiber Transport (Diesel Truck 16 t)	Electricity Production (used for fiber processing)	Ammonium Nitrate Production	Potash Production	Superphosphate Production	Trifluralin Production	Kenaf Cultivation, Transport and Processing
Inputs:												
(r) Coal (in ground)	kg	7.27E-03	8.70E-05	0	8.30E-05	1.45E-04	6.69E-03	1.62E-04	4.94E-07	1.14E-05	9.53E-05	0
(r) Iron (Fe, ore)	kg	1.09E-05	0	0	0	0	0	8.93E-06	5.37E-07	1.10E-06	3.10E-07	0
(r) Limestone (CaCO3, in ground)	kg	5.69E-04	6.90E-06	0	6.58E-06	1.15E-05	5.28E-04	8.24E-06	2.25E-07	4.47E-07	7.63E-06	0
(r) Natural Gas (in ground)	kg	9.22E-03	2.81E-04	0	2.68E-04	4.69E-04	4.76E-05	6.73E-03	1.13E-04	1.20E-03	1.09E-04	0
(r) Oil (in ground)	kg	9.75E-03	2.56E-03	0	2.44E-03	4.26E-03	4.37E-05	2.54E-05	5.32E-05	2.81E-04	9.08E-05	0
(r) Phosphate Rock (in ground)	kg	0.016	0	0	0	0	0	0	0	0.016	0	0
(r) Potassium Chloride (KCl, as K2O, in ground)	kg	4.11E-03	0	0	0	0	0	0	4.11E-03	0	0	0
(r) Uranium (U, ore)	kg	3.12E-08	1.46E-09	0	1.40E-09	2.44E-09	9.66E-09	1.60E-08	1.04E-11	6.34E-11	1.94E-10	0
Water Used (total)	liter	0.306	0.061	0	0.058	0.101	7.16E-04	0.076	2.58E-04	0.007	0.002	0
Outputs:												
(a) Ammonia (NH3)	g	0.427	1.33E-05	0	1.27E-05	2.21E-05	4.84E-06	0.427	6.20E-09	1.10E-08	2.11E-06	0
(a) Arsenic (As)	g	6.30E-06	9.06E-08	0	8.64E-08	1.51E-07	5.86E-06	2.22E-09	1.13E-08	1.90E-08	8.39E-08	0
(a) Benzene (C6H6)	g	4.00E-04	8.81E-05	2.40E-06	8.41E-05	1.51E-04	2.18E-05	2.98E-05	2.21E-06	3.92E-06	1.71E-05	0
(a) Beryllium (Be)	g	7.15E-07	9.08E-09	0	8.67E-09	1.51E-08	6.73E-07	1.22E-11	7.59E-13	1.53E-12	9.58E-09	0
(a) Carbon Dioxide (CO2, biomass)	g	1.76E-04	4.32E-07	0	4.12E-07	7.20E-07	1.72E-04	0	0	0	2.38E-06	0
(a) Carbon Dioxide (CO2, fossil)	g	67.750	0.925	7.560	0.883	14.092	16.713	18.004	0.437	1.028	0.433	7.676
(a) Carbon Monoxide (CO)	g	0.099	0.003	0.019	0.002	0.045	0.003	0.002	4.76E-04	4.13E-04	2.39E-04	0.023
(a) Dioxins (unspecified)	g	5.74E-11	7.03E-13	0	6.70E-13	1.17E-12	5.40E-11	3.33E-14	2.01E-15	4.13E-15	7.69E-13	0
(a) Ethylene (C2H4)	g	1.10E-03	0	0	0	0	0	9.05E-04	5.49E-05	1.12E-04	3.16E-05	0
(a) Halon 1301 (CF3Br)	g	1.96E-08	2.94E-12	0	2.81E-12	4.91E-12	3.12E-14	2.01E-09	1.09E-08	6.61E-09	7.04E-11	0
(a) Hydrogen Fluoride (HF)	g	5.61E-04	6.51E-06	0	6.21E-06	1.08E-05	5.00E-04	2.67E-07	2.66E-08	2.98E-05	7.12E-06	0
(a) Mercury (Hg)	g	4.08E-07	5.62E-09	0	5.37E-09	9.37E-09	3.64E-07	1.46E-08	1.30E-09	2.43E-09	5.72E-09	0
(a) Methane (CH4)	g	0.169	0.005	2.88E-04	0.005	0.010	0.030	0.114	0.002	0.002	0.001	0
(a) Methyl Bromide (CH3Br)	g	5.67E-07	6.94E-09	0	6.62E-09	1.16E-08	5.34E-07	0	0	0	7.59E-09	0
(a) Methyl Chloride (CH3Cl)	g	1.88E-06	2.30E-08	0	2.19E-08	3.83E-08	1.77E-06	0	0	0	2.51E-08	0
(a) Nickel (Ni)	g	1.25E-05	8.19E-07	0	7.82E-07	1.37E-06	7.79E-06	7.56E-08	5.63E-07	9.45E-07	1.39E-07	0
(a) Nitrogen Oxides (NOx as NO2)	g	0.480	0.004	0.098	0.003	0.162	0.053	0.032	0.002	0.004	0.001	0.120
(a) Selenium (Se)	g	4.66E-06	6.07E-08	0	5.79E-08	1.01E-07	4.34E-06	2.63E-08	5.52E-09	9.26E-09	6.27E-08	0
(a) Sulphur Dioxide (SO2)	g	9.62E-03	0	0	0	0	0	0	0	0	0	9.62E-03
(a) Sulphur Oxides (SOx as SO2)	g	0.163	0.005	0.006	0.005	0.019	0.059	0.008	0.001	0.059	0.001	0
(a) Trichloroethane (1,1,1-CH3CCl3)	g	7.08E-08	8.68E-10	0	8.28E-10	1.45E-09	6.67E-08	0	0	0	9.48E-10	0

Flow	Units	Kenaf Fiber Production (total)	Diesel Oil Production (used for Road Transport)	Road Transport (Diesel Truck 40 t)	Diesel Oil Production (for Tractor use - cultivation & harvesting)	Raw Kenaf Fiber Transport (Diesel Truck 16 t)	Electricity Production (used for fiber processing)	Ammonium Nitrate Production	Potash Production	Superphosphate Production	Trifluralin Production	Kenaf Cultivation, Transport and Processing
(a) Vanadium (V)	g	1.08E-05	1.80E-06	0	1.71E-06	2.99E-06	2.43E-08	6.53E-08	1.56E-06	2.55E-06	6.60E-08	0
(s) Zinc (Zn)	g	7.05E-07	0	0	0	0	0	5.78E-07	3.50E-08	7.16E-08	2.02E-08	0
(w) Acids (H+)	g	0.168	5.73E-10	0	5.47E-10	9.55E-10	1.14E-10	4.14E-06	9.40E-10	0.168	1.05E-10	0
(w) Barium (Ba++)	g	2.42E-05	1.62E-09	0	1.55E-09	2.71E-09	1.72E-11	2.81E-06	1.32E-05	8.04E-06	9.83E-08	0
(w) Nitrate (NO3-)	g	8.20E-06	3.57E-07	0	3.40E-07	5.95E-07	3.48E-07	3.40E-07	5.55E-06	6.47E-07	2.92E-08	0
(w) Nitrogenous Matter (unspecified, as N)	g	7.26E-06	9.14E-11	0	8.72E-11	1.52E-10	9.69E-13	3.82E-06	1.70E-06	1.71E-06	2.12E-08	0
(w) Phenol (C6H5OH)	g	8.14E-05	2.09E-05	0	2.00E-05	3.49E-05	2.22E-07	3.65E-06	6.38E-07	4.30E-07	7.44E-07	0
(w) Phosphorus (P)	g	4.75E-08	0.00E+00	0	0.00E+00	0.00E+00	0.00E+00	1.07E-08	2.23E-08	1.41E-08	3.75E-10	0
(w) Suspended Matter (unspecified)	g	2.40E-02	4.94E-03	0	4.71E-03	8.23E-03	5.25E-03	2.37E-03	1.16E-04	3.39E-03	2.39E-04	0
(w) Water: Chemically Polluted	liter	2.17E-02	5.87E-03	0	5.60E-03	9.79E-03	6.37E-05	0.00E+00	7.25E-05	1.17E-04	2.07E-04	0
Processed-Kenaf BAST fiber	kg	1	0	0	0	0	0	0	0	0	0	1
Waste (hazardous)	kg	1.31E-05	3.54E-06	0	3.38E-06	5.90E-06	3.76E-08	3.23E-09	5.19E-08	3.06E-08	1.24E-07	0
Waste (total)	kg	0.021	4.66E-04	0	4.45E-04	7.77E-04	0.003	4.31E-05	0.004	0.012	5.86E-05	0
Reminders:												
Trifluralin (C13H16F3N3O4)	kg	4.37E-05	0	0	0	0	0	0	0	0	0	4.37E-05
Diesel Oil	kg	8.69E-03	0	2.40E-03	0	4.00E-03	0	0	0	0	0	2.29E-03
E Feedstock Energy	MJ	0.14	0.11	-0.10	0.10	0.01	0.02	1.78E-04	-8.86E-08	-7.07E-04	0.01	0
E Fuel Energy	MJ	0.96	0.02	0.10	0.02	0.20	0.23	0.32	0.01	0.06	0.01	0
E Non Renewable Energy	MJ	1.05	0.12	0.00	0.12	0.21	0.20	0.32	0.01	0.06	0.01	0
E Renewable Energy	MJ	0.05	1.18E-04	0	1.12E-04	1.96E-04	0.05	1.42E-04	8.02E-07	2.02E-06	6.36E-04	0
E Total Primary Energy	MJ	1.10	0.12	0	0.12	0.21	0.25	0.32	0.01	0.06	0.01	0
Electricity	MJ elec	0.089	0	0	0	0	0	0.023	0.004	0.004	0.001	0.057
Raw-Kenaf BAST fiber	kg	1	0	0	0	0	0	0	0	0	0	1
Transport: Road (diesel oil, kg.km)	kg.km	150	0	0	0	50	0	0	0	0	0	100

4.3.5 Polyhydroxybutyrate (PHB) LCI

LCA studies by Gerngross[37], Gerngross and Slater[38], Kurdikar et al.[39], have addressed the question of PHA's (polyhydroxyalkanoates) being sustainable; however these studies lack the detail, which is necessary in LCA studies to reach a reasonable conclusion.

For the current study, the inventory analysis for PHB production was based on the 2003 publication by Akiyama et al.[12], which provides a detailed life cycle comparison study of polyhydroxyalkanoates produced from soybean oil and glucose as well as petrochemical polymers such as LDPE, HDPE, PP, PS, and PET. The LCI comparison by Akiyama et al.[12] for poly(3-hydroxybutyrate-co-5mol% 3-hydroxyhexanoate) [P(3HB-co-5mol% 3HHx)] (see Figure 4.13) production using soybean oil as carbon source and poly(3-hydroxybutyrate) [P(3HB)] production using glucose as carbon source is based on a simulation of a full scale fermentative production using SuperPro Designer® simulation software[SA26]
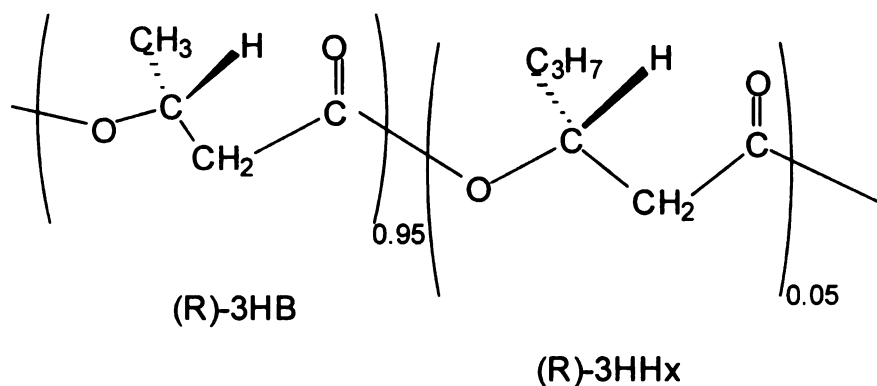
Figure 4.13 Structure of Poly(3-hydroxybutyrate-co-5mol% 3-hydroxyhexanoate) [P(3HB-co-5mol% 3HHx)]

Soybean oil is produced from soybeans in an oil mill, and glucose is produced in a similar way by wet milling using corn as a feedstock.

As per Akiyama et al.[12], for P(3HB) production, theoretical highest yields using glucose and linoleic acid ($C_{18}H_{32}O_2$, a main fatty acid component of soybean oil) are estimated at 0.48 g-P(3HB)/g-C source and 1.38 g-P(3HB) /g-C source respectively, as described in the stoichiometric equations below:

$$C_6H_{12}O_6 + 1.5\,O_2 \longrightarrow C_4H_6O_2 + 2\,CO_2 + 3\,H_2O$$
Glucose $\qquad\qquad\qquad$ PHB monomer

$$C_{18}H_{32}O_2 + 4.75\,O_2 \longrightarrow 4.5\,C_4H_6O_2 + 2.5\,H_2O$$
Linoleic acid $\qquad\qquad$ PHB monomer
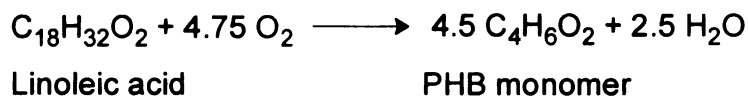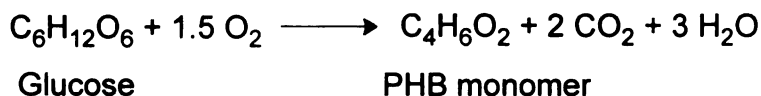
In their preliminary laboratory studies, they have obtained P(3HB) in the cultured *R. eutropha* bacteria, with relatively high yields of 0.76 g-P(3HB)/g-soybean-oil compared to experimental high yields of 0.3 to 0.4 g-P(3HB)/g-glucose. Therefore, in their study they have simulated large-scale fermentation of soybean oil in recombinant strain of *R. eutropha* bacteria culture to produce 5000 tonnes per year of P(3HB-co-5mol% 3HHx) copolymer, with yields varying from 0.7 to 0.8 g-P(3HB-co-5mol% 3HHx)/g-soybean-oil. The stoichiometric equation used in the simulation assumes the biomass formula as $C_{4.2}H_{7.4}O_2N_{0.79}$, and is described below:

$$0.81(C_{18}H_{31}O_2)_3C_3H_5 + 29.06\ O_2 + 0.79\ NH_3 \longrightarrow$$
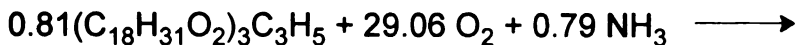
Tri-linoleyl glycerol
(soybean oil)

$$C_{4.2}H_{7.4}O_2N_{0.79} + 6.22\ C_4H_6O_2 + 0.33\ C_6H_{10}O_2 + 15.40\ CO_2 + 17.11\ H_2O$$

Cellular   PHB monomer 3HHx monomer
biomass

The fermentation process, including the downstream unit processes to obtain PHA granules is described below in Figure 4.14. As mentioned above, fermentation of soybean oil is done by the recombinant *R. eutropha* and mineral medium containing NH_3, Na_2HPO_4, KH_2PO_4, Na_3PO_4, $MgCl_2$, $(NH_4)_2SO_4$, and other minor components required for cell growth. Cellular growth takes place under nitrogen-limited environment till the nitrogen source is exhausted and is followed by PHA production from soybean oil. The fermentation medium is kept under constant conditions: aeration (aeration rate is 0.5 vvm[vi]), agitation (power requirement of 1.0 kW/m^3), compressor pressure of 2500 kPa (absolute), and a fermenter temperature of 34°C. The fermentation process is exothermic in nature, and a constant temperature is maintained by using cooling water. For comparison, glucose as carbon source replaces soybean oil, while keeping the same fermentation conditions. For both carbon sources, PHA granules are assumed to be recovered at 95 wt% from cells, and fermentation performance parameters (dry cell concentration, PHA content of cell-mass, PHA yield, and fermentation time) are variable.

[vi] Aeration rate vvm = gas volume flow per unit of liquid volume per minute (volume per volume per minute), where liquid volume = useful volume (or working volume).
Reference: BioDictionary, Bioengineering AG, www.bioengineering.ch

Once the fermentation is complete, PHA granules are extracted from the cells by using SDS (sodium dodecylsulfate) surfactant pretreatment, so as to dissociate cell membrane proteins from PHA. This step is followed by washing with NaOCl (sodium hypochlorite), a strong oxidizing agent used to digest cellular biomass. After each of these unit processes, PHA granules in the solution are concentrated by removal of cellular biomass using disk-stack centrifuges and finally dried by a spray dryer to obtain PHA granules.

In this simulation study, Akiyama et al.[12] have considered eight cases for PHA production using soybean oil and two cases using glucose as the carbon source and estimated the cost for production of PHA. These cases are generated by varying the fermentation performance variables. Both of the glucose cases have higher life cycle energy usage than all but one soybean oil cases. Akiyama et al.[12] have identified two factors responsible for the higher energy usage in the glucose-based PHAs than in soybean-based PHAs: higher energy required to extract glucose, and higher amount of glucose necessary for the production of 1 kg PHA. Based on the cost estimate for PHA production by soybean oil, authors have considered one of the median-cost case as the base case for LCI comparison with PHA production from glucose and conventional polymers including LDPE, HDPE, PP, PS, and PET. Performance variables for this median-case along with selected glucose case are mentioned below in Table 4.15.
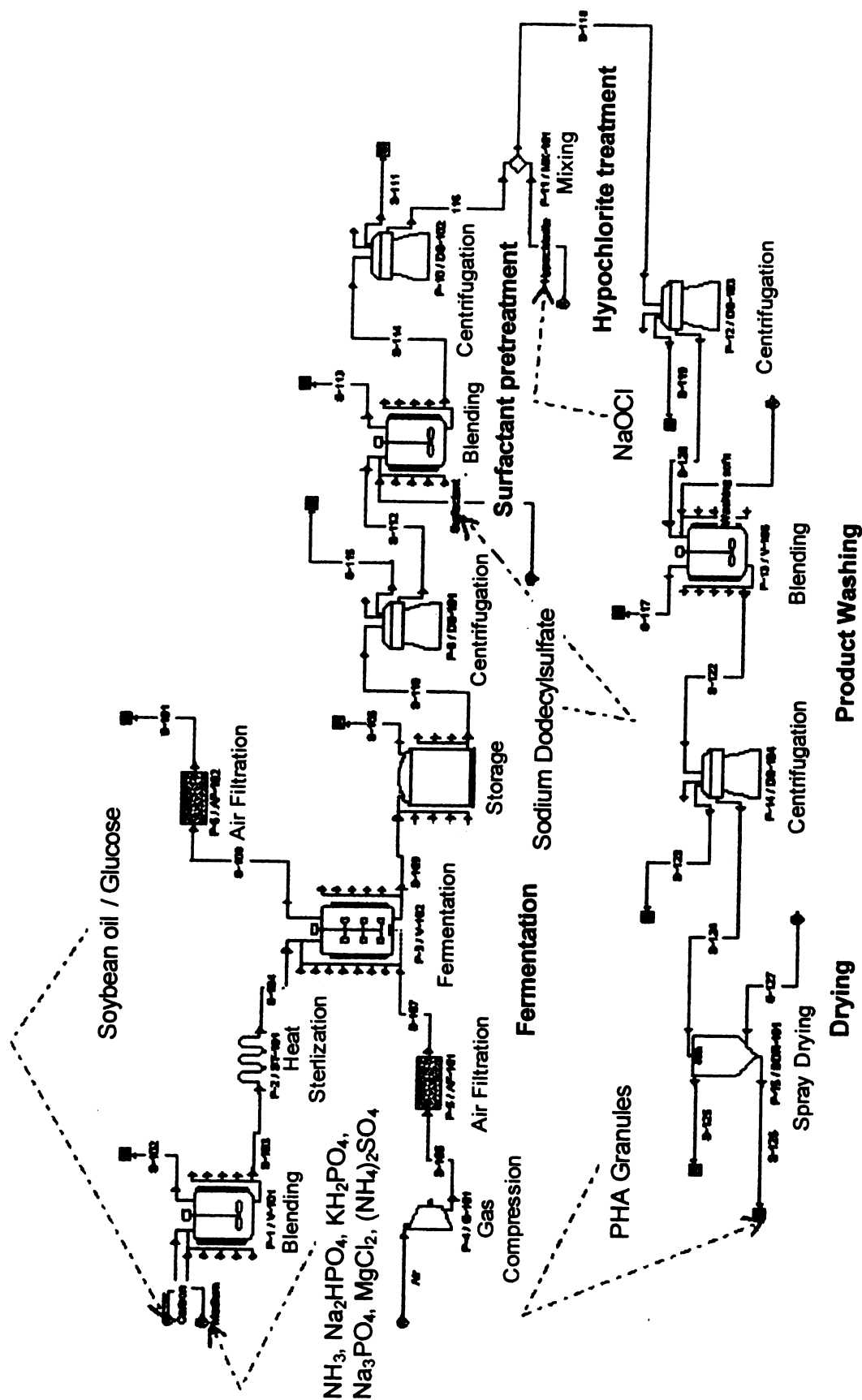
Figure 4.14 PHA production process (reference: Akiyama et al. 2003)

108

Table 4.15 Simulation conditions for Polyhydroxyalkanoates (PHA) production using soybean oil and glucose as carbon source (reference: Akiyama et al. 2003)

Raw material	Product	Production conditions				Operation conditions				PHA (tons/yr)
		Time (hr)	Cell conc. (g/l)	PHA conc. (%)	Yield (g/g)	Batches (run/yr)	Raw material (tons/run)	PHA (tons/run)	Fermenter size (m³)	
Soybean Oil	P(3HB-co-5mol% 3HHx)	40	100	85	0.80	152	43.4	34.7	600	5095
Glucose	P(3HB)	30	200	75	0.37	188	75.7	28.0	300	4978

Thus, the median-cost case or base case for PHA production from soybean oil was selected for current LCA study. Akiyama et al., in their LCI study have only reported stepwise/resource-wise total energy usage (MJ/kg-PHA), CO_2 emissions (kg/kg-PHA), and unit values (MJ/kg-resource, kg CO_2/kg-resource). This information was used to calculate the resource requirement per kg of PHA produced, and an example of such a calculation is described below:

$$\text{Electricity use (MJ)}_{\text{energy use}} = \left(\frac{21.99}{9.42}\right) \times 3.6 \ \frac{MJ}{kWh} = 8.40 \ \text{MJ-electricity}$$

$$\text{Electricity use (MJ)}_{CO_2 \ \text{emissions}} = \left(\frac{1.28}{0.55}\right) \times 3.6 \ \frac{MJ}{kWh} = 8.38 \ \text{MJ-electricity}$$

[SA29]

The electricity use for fermentation step has an energy requirement of 21.99 MJ/kg-PHA, and CO_2 emissions of 1.28 kg/kg-PHA. Energy use and CO_2 emissions per kWh of electricity are reported as 9.42 MJ/kWh, 0.55 kg/kWh respectively. Therefore, the electricity use (in MJ) for fermentation can be

calculated by dividing the energy requirement and CO_2 emissions by their respective unit values.

The calculations above clearly show a close agreement between the electricity use value calculated from energy use and CO_2 emissions. Similar calculations were done for every input use and, as a rule, the resource consumption value computed from energy use was used to calculate raw material use for the complete life cycle of PHA production, as described below in Table 4.16. Akiyama et al.[12], have not reported energy and emissions data for some of the fermentation inputs including Na_2HPO_4, KH_2PO_4, Na_3PO_4, $MgCl_2$, $(NH_4)_2SO_4$, and other minor components because of unavailability of data. Therefore, these inputs could not be included in the current LCI study.

Table 4.16 Raw material use per kg of PHB produced using Soybean Oil

Raw material use per kg of PHB	
Soybean Oil (kg)	1.296
Ammonia (kg)	0.024
Cooling Water (kg)	1475
Electricity (MJ-Electricity)	8.901
Process Water (kg)	7.895
Sodium Hypochlorite (kg)	0.491
Sodium Dodecylsulfate (kg)	0.222
Steam (kg)	3.024

4.3.5.1 Soybean Agriculture and Transport

Soybean cultivation data reported by Akiyama et al. are from a 1990 USDA-FCRS (Farm Costs and Returns Survey) study for soybean cultivation in nine major states in US. And soybean oil milling data has been obtained from 1994 oil milling operations reported by ERS/USDA. These calculations are shown below in Figure 4.15.

As shown in Figure 4.15, only energy use and CO_2 emissions data have been reported. For soybean agriculture there is significant ambiguity in the publication regarding inclusion of energy use and CO_2 emissions from the production of fertilizers and agrochemicals used in soybean cultivation. Also no fertilizer run-off emissions have been calculated, where such emissions can have significant eutrophication and human health impacts[40]. Excessive amount of N and P nutrients in waterways promote over-production of plant biomass (algae) and degradation of these biomass consumes oxygen, thus creating hypoxic conditions (low oxygen concentrations). This process of over-fertilization of waterways is also known as eutrophication, which effects local (lakes, rivers, etc) and regional (lakes, rivers, and sea) waterways. Fertilizer run-off from corn and soybean cultivation in US-Midwest is a major contributor to the increasing hypoxic zone in the Gulf of Mexico, which is currently the size of State of Massachusetts and considered ecologically dead during most summers, thus effecting the aquatic ecosystem in this area. Excess amount of N and P nutrients in drinking water can also affect human health by causing diseases such as Blue baby syndrome and Non-Hodgkin's lymphoma[40].
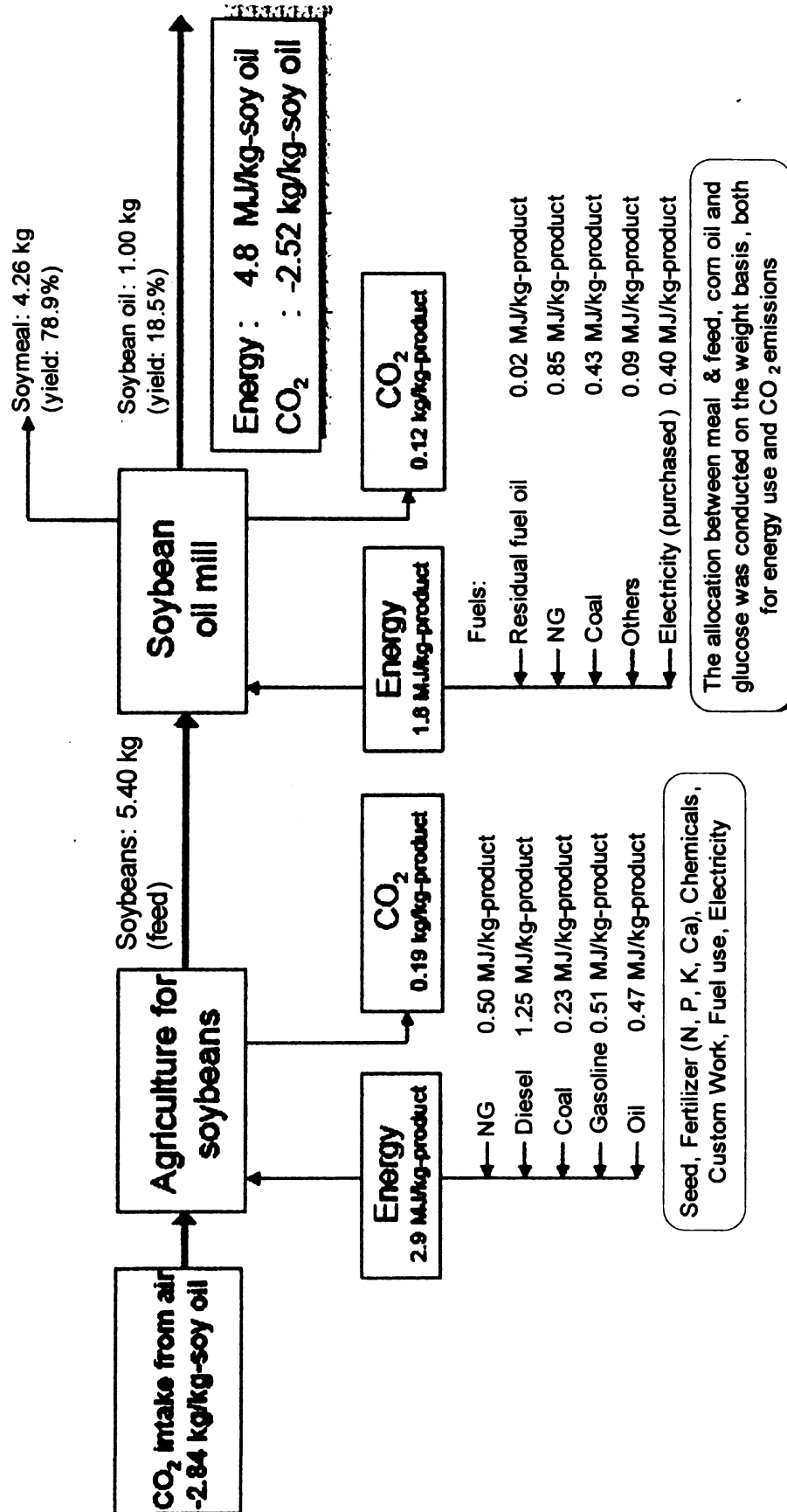
Figure 4.15 Soybean cultivation and oil milling data calculated by Akiyama et al.

112

In case of soybean oil milling, 1994 data have been used. However more recent and detailed data is available from other publications. Because of these inconsistencies and lack of detail in data reported by Akiyama et al.[12], soybean agriculture and oil milling data were substituted from other publications, with details mentioned below.

Inputs and emissions associated with soybean agriculture were obtained from a 2005 NREL-Technical Report[40], which primarily quantifies the eutrophication potential for corn-soybean rotational production in Eastern Iowa watershed region over a period of 13 years (1988-2000). This study focuses on agricultural production in the State of Iowa, so as to be consistent with the previous study regarding LCA of corn stover[41] production in the State of Iowa. However, a smaller subset region of Eastern Iowa counties with an approximate area of 50,000 km² is selected because of its high corn and soybean productivity; availability of agricultural production, resource consumption and erosion data; and being part of three major watersheds, which have several years of water quality data available. This data is utilized to develop and calibrate nutrient leaching models for corn and soybean cultivation. The region selected in this study is shown below in Figure 4.16.

Figure 4.16 Selected Iowa region for corn and soybean cultivation (reproduced from NREL/TP-510-37500)
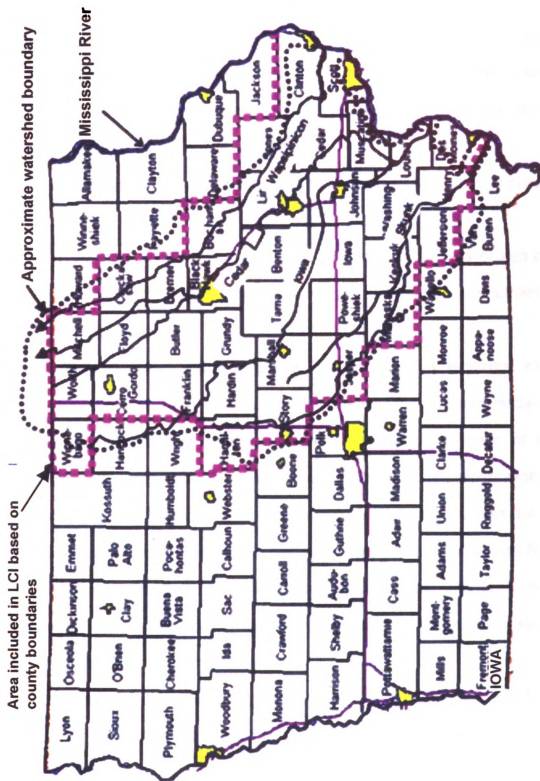
This study combines the analysis of fertilizer run-off emissions from corn and soybean cultivation, because of the interdependence of run-off emissions from corn and soybean cultivation. The study utilizes two different methods to allocate nutrient flows among corn and soybean crops. The first allocation approach is based on the study by Van Zeijts et al. (1999)[42] addressing allocation of fertilizer flows between various crops in the Netherlands. The assumptions for allocating nutrient flows are as follows:

- Nitrogen (N) flows are allocated to the crop to which it is applied in that particular year

- Phosphorus (P) and potassium (K) fertilizer flows are allocated over the entire crop rotation, proportionate to the fraction of these nutrients in the harvested crops

This allocation approach is relevant for P and K fertilizers, since the excess amount of these fertilizers is absorbed in the soil and leads to slow release of the nutrients over the entire crop rotation. In case of nitrogen allocation, this approach is termed simplistic because of two reasons: 1) N fixation by soybean crops, where fixed nitrogen becomes available during corn cultivation next year thus providing excess nitrogen and, 2) the excess N applied during corn cultivation is absorbed in soil and could become available during soybean cultivation next year. Therefore, a second approach, which specifically modifies the N fertilizer allocation is used.

The second allocation approach is based on the field data quantifying the actual leaching rates from corn and soybean cultivation (Weed and Kanwar[43],

1996; Bjorneberg et al.[44], 1996; Bakhsh et al.[45], 2002), and presents approximately equal nitrate leaching rates for corn and soybean crops, despite little or no N application during the soybean[vii] cultivation.

Based on the details provided above for allocating nutrient flows, the second allocation approach was selected for the current study, since it equally distributes the nitrogen flows to corn and soybean cultivation; while first approach exclusively allocates it for corn cultivation. The NREL study[40] acknowledges the large discrepancy between these two approaches, and assumes that the most probable accurate allocation lies somewhere in between these two methods. The study recommends that future research should focus on greater understanding of nitrogen flows between corn-soybean system. Therefore, the variation in LCI and impact assessment results by using first N-allocation approach was analyzed and presented in the interpretation phase of the current LCA study.

The NREL study quantifies the nutrient flows over a period of 13 years (1988-2000), which includes very wet (1993) and very dry (1988) years, and thus allowed the inclusion of variability of crop yield and nutrient flows as a function of rainfall in the nutrient flow model.

The nitrogen available in the agricultural system is transformed in various ways. Ammonia fertilizer in the soil is converted to nitrates within a few weeks by nitrification reaction, and taken up by plants, denitrified or leached into water. Denitrification process converts nitrate into N_2 and nitrous oxides (NO, N_2O) as intermediate products under anaerobic conditions, and in the presence of organic carbon. Products from denitrification process are released into atmosphere and

---

[vii] Soybeans are leguminous crops, i.e. there roots can capture/fix atmospheric nitrogen.

NO_x or NH_3 in the atmosphere is transformed quickly (within hours or days) by ammonification process, and returns nitrogen to the soil as HNO_3, NH_4NO_3, or $(NH_4)_2SO_4$. Additionally, some plants (such as soybean) fix atmospheric nitrogen and convert it into organic-N, which is part of soil. Soil erosion removes some of the fixed nitrogen and a fraction of this removed nitrogen is transferred to waterways. The chemical reactions involved and the N-transformation cycle (Figure 4.17) in the agricultural system are mentioned below.

Ammonification $\qquad NH_2.CO.NH_2 + H_2O \longrightarrow 2\,NH_3 + CO_2$

$NH_4^+ + 1.5\,O_2 \longrightarrow NO_2^- + 2\,H^+ + H_2O$

Nitrification

$NO_2^- + 0.5\,O_2 \longrightarrow NO_3^-$

Denitrification $\qquad 5\,(CH_2O) + 4\,NO_3^- + 4\,H^+ \longrightarrow 5\,CO_2 + 2\,N_2 + 7\,H_2O$
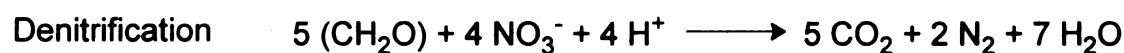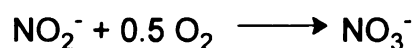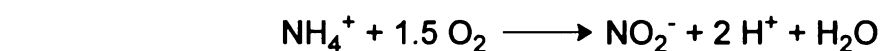
(intermediate steps involved are: $NO_3^- \longrightarrow NO_2^- \longrightarrow NO \longrightarrow N_2O \longrightarrow N_2$)
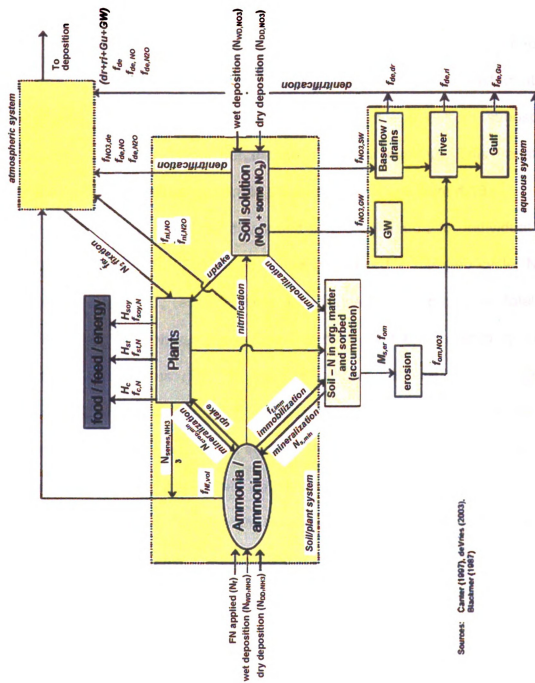
Figure 4.17 Nitrogen transformation cycle in a typical agricultural system (reproduced from NREL/TP-510-37500)

Phosphorus transformation in the agricultural system is less complex as compared to Nitrogen cycle. P-fertilizers are sparingly soluble in water (1-2%) and leaching of phosphorus is from this fraction in soluble form as orthophosphate (PO_4^{3-}), mainly to surface waters. The majority of P-fertilizers (70-95%) are absorbed by the soil and transferred to surface water bodies by soil erosion. Phosphorus acts as a limiting nutrient for crop production or algae growth. Hence, even a small P increase in the waterways can cause large increases in the algae biomass production. The phosphorus transformation cycle discussed in the NREL study ignores the contribution from atmospheric P, because of its very small percentage in the atmosphere. This transformation cycle for the agricultural system is presented below in Figure 4.18.

The NREL study has developed empirical models for individual N and P flows as described in Figures 4.17 and 4.18. For the nitrogen cycle, NH_3/NH_4^+, NO_3^-, N_2O and NO_x (as NO) flows are included in the model for total nitrogen (TN) flows. Phosphorus flows are modeled as total phosphorus (TP), with fertilizer phosphorus (FP) as only inflow and outflows as P removed with harvested crop and P leached to surface waters. Phosphorus absorbed in soil and transferred by erosion to surface water bodies is not considered because sorbed phosphorus is generally not accessible biologically. Potassium outflows to waterways are not considered because the NREL study assumes that no significant potassium inflows are distributed to air or water environments.
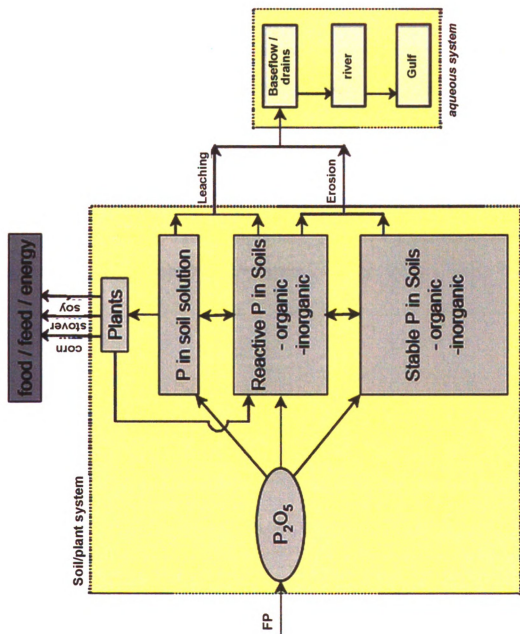
Figure 4.18 Phosphorus transformation cycle in a typical agricultural system (reproduced from NREL/TP-510-37500)

The empirical models developed are calibrated against the actual nutrient flow data for the Eastern Iowa watershed region from the USGS National Ambient Water Quality Assessment (NAWQA) and the NOAA/USGS Hypoxia in the Gulf of Mexico study. TN flows to the Mississippi River are calibrated against the actual flows from 1988-1998, and the calibrated model estimates cumulative TN flows (from 1988-1998) within 1% of the actual cumulative TN flows. The NREL study compares the calibrated model with actual flow data and estimates from GREET[46] model (which assumes a fixed fraction, 24% of fertilizer-nitrogen leaches to waterways), and calibrated model trends well with the actual flow data with a few exceptions related to dry years of 1988 and 1989. This comparison is presented below in Figure 4.19. Similar calibration of total phosphorus (TP) model is done against the actual flows from 1988-1998 and calibrated TP model has cumulative error (11 years) of +2.1%. The comparison of calibrated TP flows against the actual phosphorus flow data is presented below in Figure 4.20.
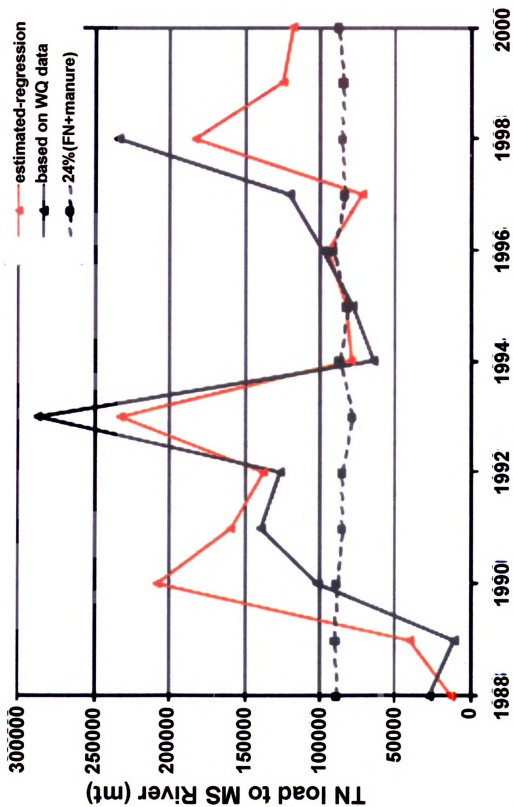
Figure 4.19 Comparison of calibrated TN model with actual data and GREET model for TN flows to the Mississippi River (from NREL/TP-510-37500)
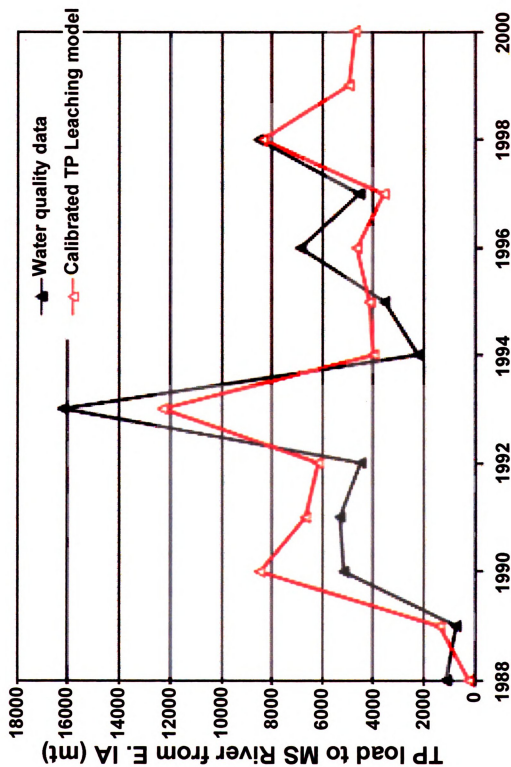
Figure 4.20 Comparison of calibrated TP model with actual data for TP flows to the Mississippi River (from NREL/TP-510-37500)

As mentioned before, this NREL study presents soybean production data for 13 years (1988-2000) so as to account of weather variations, where such variations can significantly impact the fertilizer nutrient outflows from the soil. Therefore, in the current LCA study, 13 year-average data were used for modeling soybean agriculture and transport in TEAM™ software. As specified in the NREL study, soybean cultivation is part of corn-soybean rotation (90% of the selected region has C-S rotation based on the actual data), with conventional till and no corn stover collection. These assumptions are based on the actual farming practices in Eastern Iowa watershed region. Data regarding energy and emissions from the farming operations were obtained from Sheehan et al. (1998)[35]. Farming input data reported by Sheehan et al. are from USDA's 1990 Farm Costs and Returns Survey (FCRS), and relevant to farming in Iowa. It is assumed that soybean plants uptake CO_2 from atmosphere while growing (by photosynthesis); CO_2 is then sequestered as biological carbon in soybeans. However, Sheehan et al., have not considered CO_2 sequestered in soybean plant roots. In the current LCI study, sequestered carbon in soybeans was accounted as CO_2 – biomass (see Table 4.18 below). For farming operations, energy consumption is by use of diesel, gasoline, and motor oil for planting, cultivation, and harvesting of soybeans. Diesel and gasoline consumption is assumed to be for diesel and gasoline tractors respectively. Emission factors for these tractors, as specified by Sheehan et al., are mentioned below in Table 4.17. Also herbicide use for soybeans is reported by Sheehan et al. and in the current study it was assumed that all the herbicide use is in the form of Trifluralin.

LCI of Trifluralin production was modeled based on the data from Sheehan et al. and details of the model are mentioned before in Section 4.3.4.

The 13 year-average data for soybean agriculture, which includes data from farming operations, and fertilizer-nutrient flows is mentioned below in Table 4.18. As recommended by Sheehan et al., soybean yield data reported in the NREL study was adjusted to account for the soybean seed use in growing soybeans. Soybeans seeds require more energy compared to soybeans because of additional storage, packaging and transport requirements. Therefore, soybean yield was adjusted by subtracting 1.5 times the soybean seed use from total soybean yield, so as to account for additional energy requirements of soybean seeds[SA30].

Table 4.17 Emission factors for fuel combustion in Farming Tractors (obtained from Sheehan et al. (1998), LCI of Biodiesel, NREL)

Fuel type	Emission factors (g/MJ)							
	Hydrocarbons (HC)	CO	NO_x	PM10	SO_2	CH_4	N_2O	CO_2
Diesel	0.085	0.32	0.89	0.041	0.12	0.0042	0.0019	75.5
Gasoline	0.2	1.14	0.63	0.0074	0.0046	0.032	0.0019	67.7

Table 4.18 (a) Soybean agriculture average data (1988-2000)-Inputs[viii]

Soybean agriculture, C-S rotation, conventional till, no corn stover collection

Inputs	Units	Average (1988-2000)
Land use	ha (hectares)	1,319,608
FN (fertilizer nitrogen)	mt-N	104,645
FP (fertilizer phosphorus)	mt-P	14,598
FK (fertilizer potassium)	mt-K	47,078
Trifluralin	mt	7,070
Soybean seed use	mt	78,526
Gasoline	mt	26,057
Diesel	mt	53,972
Motor Oil	mt	2,253

Table 4.18 (b) Soybean agriculture average data (1988-2000)-Outputs[ix]

Soybean agriculture, C-S rotation, conventional till, no corn stover collection

Outputs	Units	Average (1988-2000)
Soybean yield	mt	3,857,989
Adjusted-Soybean yield	mt	3,740,200
(a) CO_2 – biomass	mt-CO_2	-6,855,712
(a) NH_3-N	mt-N	26,398
(a) NO_x as NO_2	mt-N	1,946
(a) N_2O as N	mt-N	1,395

[viii] mt = Metric Tons
[ix] mt = Metric Tons, prefix (a) signifies air emissions and (w): water emissions

126

Soybean agriculture, C-S rotation, conventional till, no corn stover collection

Outputs	Units	Average (1988-2000)
(a) HC (unspecified)	mt	1,689
(w) TN – SW	mt-N	43,929
(w) NO₃⁻ - GW	mt-N	3
(w) TP – SW	mt-P	1,168

The next step after harvesting soybeans is to transport them to the soybean crushing facility. Sheehan et al. have assumed a distance of 75 miles for transporting harvested soybeans to the crushing facility. Additionally, it was assumed that 16 ton-diesel trucks were used for this transportation step.

Based on the information provided above in Tables 4.17 and 4.18, Soybean cultivation, harvesting, and transport steps were modeled in TEAM™ software and are described below in Figure 4.21. For this model, motor oil production data was substituted with lubricant inventory data, because motor oil LCI data was unavailable. Fertilizer application for soybean agriculture included ammonia (NH_3), superphosphate (triple as P_2O_5), and potash (KCl as K_2O).
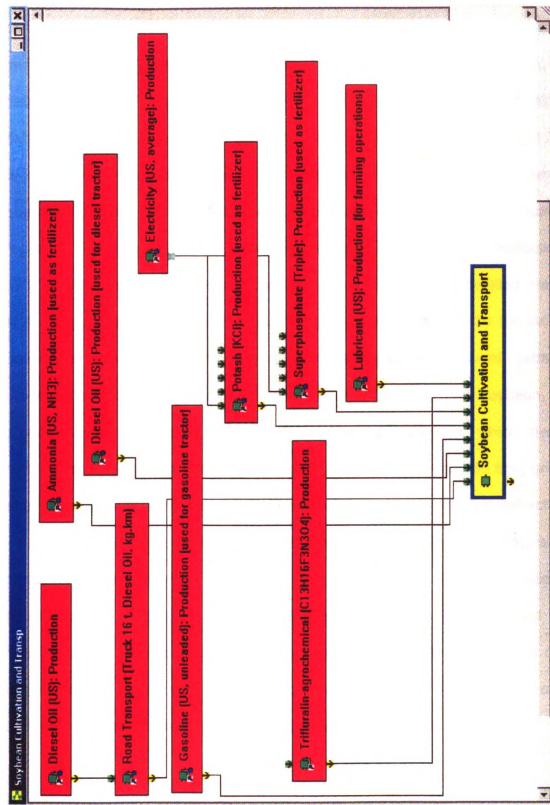
Figure 4.21 Model for Soybean Cultivation, Harvesting, and Transport

4.3.5.2 Soybean Crushing

In the current LCA study, it was assumed that soybean oil is used as a carbon source for fermentative production of PHB. Soybean oil is obtained by milling/crushing of soybeans, as described before in Figure 4.15 and oil milling data reported by Akiyama et al.[12], was replaced with more recent and detailed data reported by Sheehan et al.[35], in a 1998 NREL study regarding LCI of Biodiesel. Oil milling data reported by Sheehan et al., is based on a detailed engineering study of a single soybean oil production facility in the southeastern region of the United States[47]. However, this data corresponds to production in 1981 and to improve its accuracy, authors have developed a detailed material and energy balance for soybean crushing, which was critiqued by the industry specialists (National Oil Processors Association-NOPA). Solvent extraction process has been used by Sheehan et al., to obtain oil from soybean. This process involves following steps: 1) Preparation of soybeans, which involves removal of hulls, grinding and flaking of soybeans 2) Oil is extracted from grinded and flaked beans using hexane as a solvent in a counter-current extractor 3) Recovery of oil from hexane is done using multiple effect evaporators with maximum solvent recovery and reuse, while the extracted beans are processed by drying and grinding to produce saleable soy meal 4) The recovered oil is finally washed with hot water, so as to separate gums from the oil and crude degummed oil is shipped as final product. A simplified flow diagram of the soybean crushing process is described below in Figure 4.22.
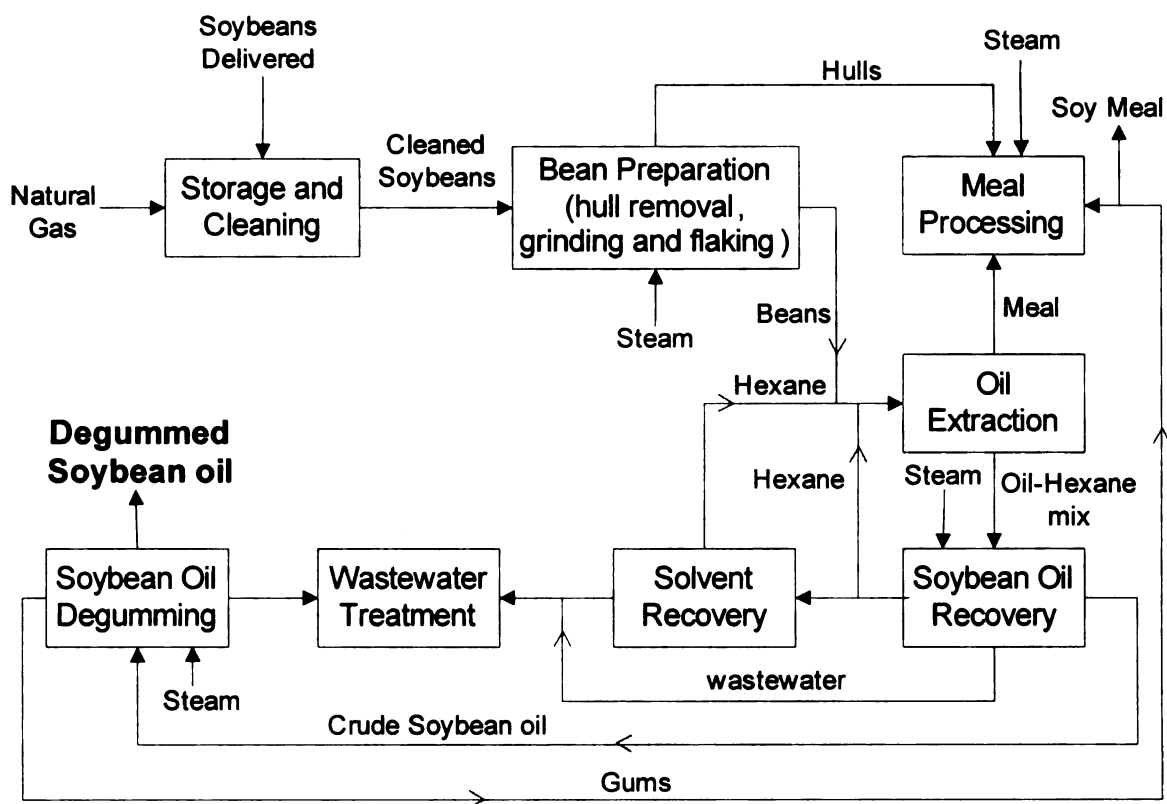
Figure 4.22 Overview of Soybean Crushing Process

The material and energy balance developed by Sheehan et al., assumes the soybean flowrate of 94,697 kg/hr, which goes through initial cleaning to remove dirt, trash, and moisture and final flow of 88,047 kg/hr soybeans to the extraction process. Since soybean oil and soy-meal are the only products from this process, allocation of inputs, emissions and energy flows is done on a mass basis of the products and output flows from the extraction process are shown below in Table 4.19. However, amount of soybeans used to obtain 1 kg of oil was calculated based on the soybeans delivered to the crushing facility not the soybeans obtained after initial cleaning. Allocated raw material, energy inputs, and significant emissions for soybean crushing are mentioned below in Table 4.20. Hexane is used as a solvent for oil extraction and is recycled by oil

130

recovery, solvent recovery and meal processing steps; where hexane air emissions are due to vent losses from meal processing and solvent recovery steps. Natural gas is used as fuel in the air-drying systems for removing moisture from soybeans in the storage step. Emissions from burning of natural gas in the air-drying system were calculated based on a DEAM™ dataset for combustion of natural gas in an Industrial boiler. Steam is primarily required for bean preparation and meal processing. Water emissions from the crushing process were not considered in the current LCA study, since the majority of the water outflow is due to steam condensates, with small contribution from soybean oil (~1 wt% of the total outflow), and therefore categorizing such flow as water emissions in TEAM software was not possible.

Table 4.19 Co-products from the Soybean Crushing facility (from Sheehan et al., 1998)

Products	Hourly flow (kg/hr)	Mass (%), for allocation purposes
Soybean Oil	16,072	18.25%
Soybean Meal	71,975	81.75%
Total	88,047	100%

Based on the input and emission data in Table 4.20, Soybean crushing process was modeled in TEAM™ software and is described below in Figure 4.23. DEAM™ datasets for electricity, natural gas, steam production and combustion of natural gas in industrial boiler were included in the model for soybean crushing process. LCI data for hexane production is not available in DEAM™ database or from other sources, therefore not included in this model.

131
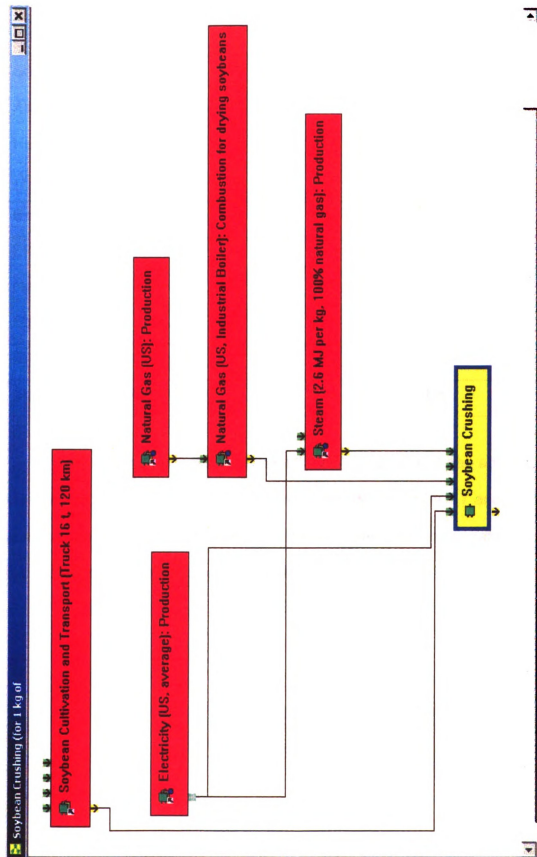
Figure 4.23 Model for Soybean Crushing Process

Table 4.20 Allocated inputs and emissions to Soybean Crushing process

Inputs	Amount/kg of soybean oil produced
Soybeans delivered (kg)	5.89
Allocated Soybeans (kg)	1.076
Hexane (kg)	0.002
Water (kg)	0.004
Energy Inputs	
Electricity (MJ-electricity)	0.27
Natural Gas (MJ)	1.20
Steam (kg)	0.305
Emissions	
(a) Hexane (grams)	1.85

Assumptions for majority of the datasets used for Soybean agriculture and crushing process model have already been included in Table 4.7 and 4.13 of this chapter, and Table 4.21 provides details for the remaining datasets, which include gasoline, ammonia, and lubricant production.

Table 4.21 DEAM datasets used for modeling of Soybean Agriculture and Crushing Process

DEAM™ datasets	Data characterization	Sources
Gasoline (US, unleaded) Production	Includes:- domestic and foreign crude oil production. US refinery operations only.	EIA (1994), EPA (1993, 90, 87, 85), DOE (1988, 83)
Lubricant (US) Production	Includes:- domestic and foreign crude oil production. US refinery operations only.	Ibid.
Ammonia (US, NH3) Production	Production of synthetic anhydrous ammonia. Natural Gas used as feedstock (60%) and fuel (40%), Natural gas reforming process, no CO_2 recovery.	Energy requirements data based on Fertilizer Institute data for 1994-weighted average for US plants. Air emissions: EPA AP-42 process emissions and emissions from a Natural Gas Industrial Boiler. Water emissions: DEAM database, for NH_3 production.

4.3.5.3 Polyhydroxybutyrate (PHB) LCI model

As discussed in the beginning of section 4.3.5.1, soybean agriculture and oil milling data reported by Akiyama et al., was replaced with more recent and detailed data and modeled in TEAM™ software, as described in previous sections 4.3.5.1 and 4.3.5.2. Additionally, energy and CO_2 values for electricity, ammonia, and steam usage were subtracted from the total energy and CO_2 numbers reported by Akiyama et al. (for PHB fermentation), because DEAM™ datasets for these resources were included in the LCI model for PHB production. LCI data reported by Akiyama et al., for production of these resources is relevant to production in Japan, therefore replacement with datasets from DEAM™ makes the current PHB LCI more accurate and relevant to production in US.

The final product from the PHB fermentation is in the form of granules and it was assumed that PHB granules are transported 100 km in 40-ton diesel truck to composites processing plant. Based on the raw material inputs (Table 4.16) for PHB production and soybean oil milling model developed, PHB production process was modeled in TEAM™ software and is described below in Figure 4.24. Assumptions for DEAM™ datasets included in this model have already been described before in Table 4.7, 4.13, and 4.21 of this chapter. Table 4.22 below shows LCI data for the production of 1 kg of PHB, obtained from the modeling of PHB production process in TEAM™ software (Figure 4.24).
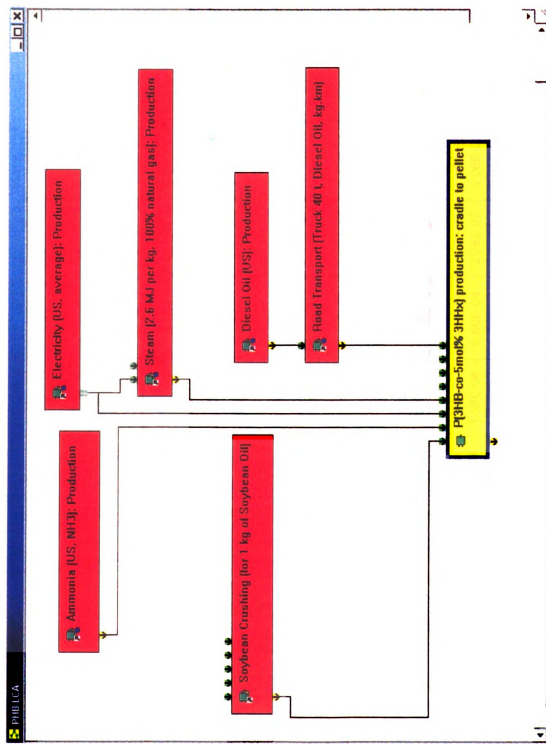
Figure 4.24 Model for PHB production process

Table 4.22 LCI of P(3HB-co-5mol% 3HHx) (cradle to pellet): Production of 1 kg of PHB

Flow	Units	PHB Production (total)	Ammonia Production	Electricity Production	Steam Production	Diesel Oil Production	Road Transport (Diesel Truck 40 t)	Soybean Crushing (for 1 kg of Soybean Oil)	P(3HB-co-5mol% 3HHx) production
Inputs:									
(r) Coal (in ground)	kg	0.806	0.002	0.753	0.001	8.70E-05	0	0.049	0
(r) Iron (Fe, ore)	kg	1.51E-03	0	0	1.30E-03	0	0	2.07E-04	0
(r) Limestone (CaCO3, in ground)	kg	0.064	1.40E-04	0.059	5.21E-04	6.90E-06	0	0.004	0
(r) Natural Gas (in ground)	kg	0.445	0.023	0.005	0.272	2.81E-04	0	0.145	0
(r) Oil (in ground)	kg	0.066	1.16E-04	0.005	7.76E-04	0.003	0	0.057	0
(r) Phosphate Rock (in ground)	kg	0.186	0	0	0	0	0	0.186	0
(r) Potassium Chloride (KCl, as K2O, in ground)	kg	0.043	0	0	0	0	0	0.043	0
(r) Uranium (U, ore)	kg	1.31E-06	2.98E-08	1.09E-06	2.52E-08	1.46E-09	0	1.62E-07	0
Hexane (C6H14)	kg	2.82E-03	0	0	0	0	0	2.82E-03	0
NaOCl	kg	0.491	0	0	0	0	0	0	0.491
SDS	kg	0.222	0	0	0	0	0	0	0.222
Water Used (total)	liter	10.201	0.027	0.081	0.404	0.061	0	1.735	7.895
Outputs:									
(a) Ammonia (NH3)	g	12.101	0.052	5.46E-04	1.17E-05	1.33E-05	0	12.048	0
(a) Arsenic (As)	g	7.06E-04	1.56E-06	6.60E-04	3.25E-07	9.06E-08	0	4.39E-05	0
(a) Benzene (C6H6)	g	0.049	0.008	0.002	0.004	8.81E-05	2.40E-06	0.034	0
(a) Beryllium (Be)	g	8.11E-05	1.81E-07	7.58E-05	1.79E-09	9.08E-09	0	5.09E-06	0
(a) Carbon Dioxide (CO2, biomass)	g	-2554.590	8.92E-06	0.019	0	4.32E-07	0	-2554.610	0
(a) Carbon Dioxide (CO2, fossil)	g	4584.19	64.42	1883.17	661.81	0.93	7.56	596.31	1370

137

Flow	Units	PHB Production (total)	Ammonia Production	Electricity Production	Steam Production	Diesel Oil Production	Road Transport (Diesel Truck 40 t)	Soybean Crushing (for 1 kg of Soybean Oil)	P(3HB-co-5mol% 3HHx) production
(a) Carbon Monoxide (CO)	g	2.459	0.235	0.387	0.214	0.003	0.019	1.602	0
(a) Dioxins (unspecified)	g	6.50E-09	1.43E-11	6.09E-09	4.88E-12	7.03E-13	0	3.98E-10	0
(a) Ethylene (C2H4)	g	0.154	0	0	0.133	0	0	0.021	0
(a) Halon 1301 (CF3Br)	g	5.31E-07	1.11E-13	3.52E-12	2.95E-07	2.94E-12	0	2.36E-07	0
(a) Hydrogen Fluoride (HF)	g	0.061	1.32E-04	0.056	3.92E-05	6.51E-06	0	0.004	0
(a) Mercury (Hg)	g	4.65E-05	1.01E-07	4.10E-05	2.14E-06	5.62E-09	0	3.23E-06	0
(a) Methane (CH4)	g	6.117	0.340	3.371	0.688	0.005	2.88E-04	1.713	0
(a) Methyl Bromide (CH3Br)	g	6.42E-05	1.41E-07	6.01E-05	0	6.94E-09	0	3.93E-06	0
(a) Methyl Chloride (CH3Cl)	g	2.13E-04	4.68E-07	1.99E-04	0	2.30E-08	0	1.30E-05	0
(a) Nickel (Ni)	g	9.85E-04	2.55E-06	8.77E-04	1.11E-05	8.19E-07	0	9.36E-05	0
(a) Nitrogen Oxides (NOx as NO2)	g	11.465	0.110	6.012	0.336	0.004	0.098	4.905	0
(a) Selenium (Se)	g	5.27E-04	1.15E-06	4.89E-04	3.86E-06	6.07E-08	0	3.27E-05	0
(a) Sulphur Dioxide (SO2)	g	0.107	0	0	0	0	0	0.107	0
(a) Sulphur Oxides (SOx as SO2)	g	8.203	0.018	6.704	0.158	0.005	0.006	1.312	0
(a) Trichloroethane (1,1,1-CH3CCl3)	g	8.03E-06	1.76E-08	7.52E-06	0	8.68E-10	0	4.91E-07	0
(a) Vanadium (V)	g	1.02E-04	2.76E-07	2.74E-06	9.57E-06	1.80E-06	0	8.75E-05	0
(s) Zinc (Zn)	g	9.82E-05	0	0	8.47E-05	0	0	1.35E-05	0
(w) Acids (H+)	g	2.017	1.43E-03	1.29E-08	0	5.73E-10	0	2.016	0
(w) Barium (Ba++)	g	7.07E-04	6.13E-11	1.94E-09	4.12E-04	1.62E-09	0	2.94E-04	0
(w) Nitrate (NO3-)	g	5.13E-03	1.07E-06	3.92E-05	4.98E-05	3.57E-07	0	5.04E-03	0
(w) Nitrogenous Matter (unspecified, as N)	g	16.369	3.45E-12	1.09E-10	8.90E-05	9.14E-11	0	16.369	0
(w) Phenol (C6H5OH)	g	6.62E-04	7.92E-07	2.50E-05	6.38E-05	2.09E-05	0	5.51E-04	0

Flow	Units	PHB Production (total)	Ammonia Production	Electricity Production	Steam Production	Diesel Oil Production	Road Transport (Diesel Truck 40 t)	Soybean Crushing (for 1 kg of Soybean Oil)	P(3HB-co-5mol% 3HHx) production
(w) Phosphorus (P)	g	0.435	0	0	1.57E-06	0	0	0	0
(w) Suspended Matter (unspecified)	g	0.499	1.87E-04	0.006	0.281	0.005	0	0.208	0
(w) Water: Chemically Polluted	liter	0.141	2.51E-04	0.007	0	0.006	0	0.128	0
P(3HB-co-5mol% 3HHx)	kg	1	0	0	0	0	0	0	1
Waste (hazardous)	kg	9.86E-05	1.34E-07	4.23E-06	0	3.54E-06	0	9.07E-05	0
Waste (total)	kg	0.580	0.009	0.337	0	4.66E-04	0	0.233	0
Reminders:									
Soybean Oil	kg	1.296	0	0	0	0	0	0	1.296
Soybeans	kg	1.394	0	0	0	0	0	1.394	0
Diesel Oil	kg	0.036	0	0	0	0	0.002	0.034	0
E Feedstock Energy	MJ	5.60	0.59	2.00	-0.01	0.11	-0.10	3.02	0
E Fuel Energy	MJ	56.17	0.65	26.25	11.21	0.02	0.10	8.11	9.83
E Non Renewable Energy	MJ	56.27	1.24	23.05	11.20	0.12	0	10.82	9.83
E Renewable Energy	MJ	5.50	0.00	5.18	0.00	0.00	0	0.31	0
E Total Primary Energy	MJ	61.78	1.25	28.25	11.20	0.12	0	11.13	9.83
Electricity	MJ elec	9.435	0	0	0.163	0	0	0.371	8.901
Natural Gas	kg	0.030	0	0	0	0	0	0.030	0
Natural Gas (used as fuel)	MJ	1.554	0	0	0	0	0	1.554	0
Steam	kg	3.419	0	0	0	0	0	0.395	3.024
Transport: Road (diesel oil, kg.km)	kg.km	268.22	0	0	0	0	0	168.22	100

4.3.6 Composites Processing data

System boundaries for the current study were selected to include composites processing steps, as discussed before in section 4.2 (goal and scope definition) of this chapter, and LCA results were normalized to the production of 1000 composite tensile coupons (functional unit). Energy requirements for extrusion and injection molding of composites were calculated based on the actual processing data for these composites at CMSC (Composite Materials Structures Center). The detailed calculations are described in Appendix 4.3.6 and summarized in Table 4.23 below.

Table 4.23 Composites processing energy requirement (MJ-Electricity) per 1000-tensile coupons

Material	Amount of composites processed (kg)	$E_{Extrusion}$ (MJ)	E_{IM} (MJ)
PHB-(30wt%)Kenaf	10.805	17.25	19.72
PP-(30wt%)Glass	9.805	13.55	15.93

Energy requirement for processing composites is only in the form of electricity consumption for extrusion and injection molding steps. Higher electricity consumption for PHB-Kenaf as compared to PP-Glass composites was expected because of greater amount of PHB and kenaf fibers used for producing tensile coupons and higher specific heat of PHB, kenaf fibers compared to PP, glass fibers respectively; though this increase is partially offset by higher injection molding temperature for PP-Glass composites.

4.3.7 Composites LCI models

Inventory analysis for production of PP-(30wt%)Glass and PHB-(30wt%)Kenaf composites was conducted by combining the component models described in previous subsections (Sections 4.3.2 – 4.3.5) and calculating energy requirements for processing these composites (see Section 4.3.6). Similar to component models, composite models were set-up in TEAM™ software and are described below in Figures 4.25 and 4.26.

For PP-Glass composites model, PP production data was obtained from DEAM™ database, referring to a 1997 study published by Association of plastic manufacturers in Europe (APME)[26]. Similar to other component LCI models, transportation step for PP-pellets was included in the current LCI model, assuming a 100 km transport in a 40-ton diesel truck to the composites processing plant. Electricity consumption data for extrusion and injection molding of PP-Glass composites was included from the calculations mentioned in Table 4.23 above. LCI data for production of 1000 tensile coupons of PP-(30wt%)Glass composites was obtained from the LCI model (Figure 4.25) and shown below in Table 4.24.

In case of PHB-Kenaf composites model, PHB and Kenaf LCI data was combined with electricity consumption for extrusion and injection molding data obtained from Table 4.23 and Table 4.25 below, shows the LCI data for production of 1000 tensile coupons of PHB-(30wt%)Kenaf composites.
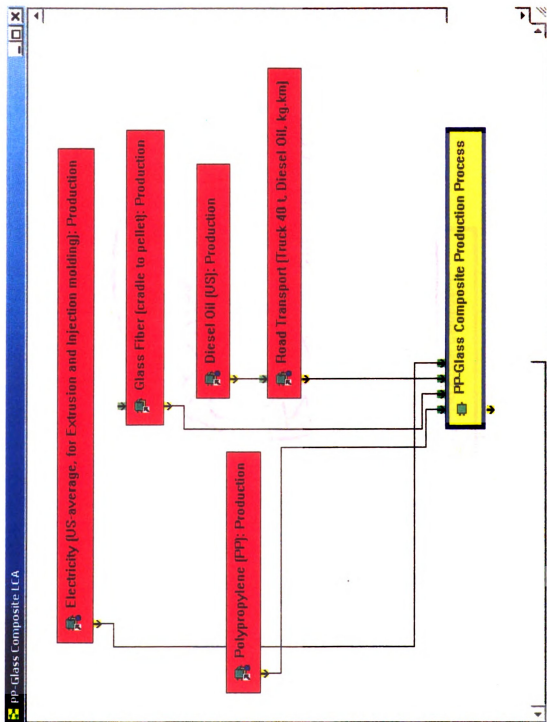
Figure 4.25 Model for Production of PP-(30wt%)Glass composites
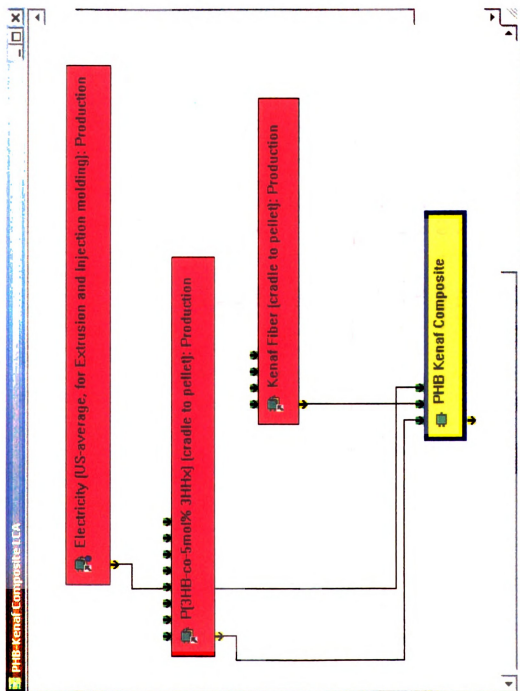
Figure 4.26 Model for Production of PHB-(30wt%)Kenaf composites

Table 4.25 LCI of PHB Kenaf Composite (cradle to pellet): Production of 1000 tensile coupons

Flow	Units	PHB-Kenaf Composite LCI (total)	P(3HB-co-5mol% 3HHx) Production	Kenaf Fiber Production	Electricity Production (for Extrusion and Injection molding)	PHB Kenaf Composite Production Process
Inputs:						
(r) Coal (in ground)	kg	9.193	6.096	0.024	3.073	0
(r) Iron (Fe, ore)	kg	0.011	0.011	3.53E-05	0	0
(r) Limestone (CaCO3, in ground)	kg	0.729	0.485	0.002	0.243	0
(r) Natural Gas (in ground)	kg	3.417	3.365	0.030	0.022	0
(r) Oil (in ground)	kg	0.548	0.496	0.032	0.020	0
(r) Phosphate Rock (in ground)	kg	1.455	1.405	0.050	0	0
(r) Potassium Chloride (KCl, as K2O, in ground)	kg	0.340	0.326	0.013	0	0
(r) Uranium (U, ore)	kg	1.44E-05	9.89E-06	1.01E-07	4.44E-06	0
Hexane (C6H14)	kg	0.021	0.021	0	0	0
NaOCl	kg	3.716	3.716	0	0	0
SDS	kg	1.682	1.682	0	0	0
Water Used (total)	liter	78.482	77.161	0.992	0.329	0
Outputs:						
(a) Ammonia (NH3)	g	92.919	91.532	1.385	0.002	0
(a) Arsenic (As)	g	8.05E-03	5.34E-03	2.04E-05	2.69E-03	0
(a) Benzene (C6H6)	g	0.383	0.371	0.001	0.010	0
(a) Beryllium (Be)	g	9.25E-04	6.14E-04	2.32E-06	3.09E-04	0
(a) Carbon Dioxide (CO2, biomass)	g	-19323.1	-19323.1	0.001	0.079	0
(a) Carbon Dioxide (CO2, fossil)	g	42575.5	34675.2	219.628	7680.72	0
(a) Carbon Monoxide (CO)	g	20.498	18.598	0.321	1.579	0
(a) Dioxins (unspecified)	g	7.42E-08	4.92E-08	1.86E-10	2.48E-08	0
(a) Ethylene (C2H4)	g	1.166	1.163	0.004	0	0
(a) Halon 1301 (CF3Br)	g	4.08E-06	4.02E-06	6.35E-08	1.44E-11	0
(a) Hydrogen Fluoride (HF)	g	0.690	0.458	0.002	0.230	0
(a) Mercury (Hg)	g	5.20E-04	3.52E-04	1.32E-06	1.67E-04	0

147

Flow	Units	PHB-Kenaf Composite LCI (total)	P(3HB-co-5mol% 3HHx) Production	Kenaf Fiber Production	Electricity Production (for Extrusion and Injection molding)	PHB Kenaf Composite Production Process
(a) Methane (CH4)	g	60.566	46.270	0.548	13.749	0
(a) Methyl Bromide (CH3Br)	g	7.33E-04	4.86E-04	1.84E-06	2.45E-04	0
(a) Methyl Chloride (CH3Cl)	g	2.43E-03	1.61E-03	6.08E-06	8.13E-04	0
(a) Nickel (Ni)	g	0.011	0.007	4.04E-05	0.004	0
(a) Nitrogen Oxides (NOx as NO2)	g	112.802	86.725	1.556	24.521	0
(a) Selenium (Se)	g	5.99E-03	3.98E-03	1.51E-05	1.99E-03	0
(a) Sulphur Dioxide (SO2)	g	0.840	0.809	0.031	0	0
(a) Sulphur Oxides (SOx as SO2)	g	89.918	62.047	0.528	27.343	0
(a) Trichloroethane (1,1,1-CH3CCl3)	g	9.16E-05	6.07E-05	2.30E-07	3.07E-05	0
(a) Vanadium (V)	g	8.17E-04	7.71E-04	3.49E-05	1.12E-05	0
(s) Zinc (Zn)	g	7.45E-04	7.43E-04	2.28E-06	0	0
(w) Acids (H+)	g	15.802	15.256	0.546	5.25E-08	0
(w) Barium (Ba++)	g	5.42E-03	5.35E-03	7.83E-05	7.92E-09	0
(w) Nitrate (NO3-)	g	0.039	0.039	2.66E-05	1.60E-04	0
(w) Nitrogenous Matter (unspecified, as N)	g	123.819	123.819	2.35E-05	4.45E-10	0
(w) Phenol (C6H5OH)	g	5.37E-03	5.01E-03	2.64E-04	1.02E-04	0
(w) Phosphorus (P)	g	3.293	3.293	1.54E-07	0	0
(w) Suspended Matter (unspecified)	g	3.879	3.777	0.078	0.024	0
(w) Water: Chemically Polluted	liter	1.168	1.068	0.070	0.029	0
PHB-Kenaf Composite	kg	10.806	0	0	0	10.806
Waste (hazardous)	kg	8.06E-04	7.46E-04	4.24E-05	1.73E-05	0
Waste (total)	kg	5.827	4.386	0.067	1.374	0
Reminders:						
Soybean Oil	kg	9.802	9.802	0	0	0
Soybeans	kg	10.542	10.542	0	0	0
Diesel Oil	kg	0.300	0.272	0.028	0	0
E Feedstock Energy	MJ	50.98	42.39	0.45	8.15	0

Flow	Units	PP-Glass Composite LCI (total)	Polypropylene Production	Glass Fiber Production	Electricity Production (for Extrusion and Injection molding)	PP-Glass Composite Production Process
Diesel Oil	kg	0.024	0.016	0.007	0	0
E Feedstock Energy	MJ	320.86	307.01	7.35	6.50	0
E Fuel Energy	MJ	434.73	207.79	141.57	85.37	0
E Non Renewable Energy	MJ	716.73	509.23	132.52	74.98	0
E Renewable Energy	MJ	38.80	5.56	16.38	16.86	0
E Total Primary Energy	MJ	755.59	514.79	148.93	91.87	0
Electricity	MJ elec	58.042	0	28.562	0	29.48
Glass Fiber	kg	2.942	0	0	0	2.942
Polypropylene (PP)	kg	6.864	0	0	0	6.864
Transport: Rail (kg.km)	kg.km	294.151	0	294.151	0	0
Transport: Road (diesel oil, kg.km)	kg.km	980.503	0	294.151	0	686.352

Flow	Units	PHB-Kenaf Composite LCI (total)	P(3HB-co-5mol% 3HHx) Production	Kenaf Fiber Production	Electricity Production (for Extrusion and Injection molding)	PHB Kenaf Composite Production Process
E Fuel Energy	MJ	535.07	424.89	3.12	107.06	0
E Non Renewable Energy	MJ	523.06	425.62	3.42	94.02	0
E Renewable Energy	MJ	62.86	41.57	0.15	21.14	0
E Total Primary Energy	MJ	586.06	467.28	3.57	115.21	0
Electricity	MJ elec	108.622	71.365	0.288	0	36.968
Natural Gas	kg	0.227	0.227	0	0	0
Natural Gas (used as fuel)	MJ	11.753	11.753	0	0	0
P(3HB-co-5mol% 3HHx)	kg	7.564	0	0	0	7.564
Processed-Kenaf BAST fiber	kg	3.242	0	0	0	3.242
Steam	kg	25.861	25.861	0	0	0
Transport: Road (diesel oil, kg.km)	kg.km	2515.1	2028.84	486.263	0	0

4.4 Life Cycle Impact Assessment (LCIA)

For a better understanding and comparison of the LCI results for PHB-Kenaf and PP-Glass composites, impact assessment methods were used to categorize inventory flows based on their environmental impacts, for e.g. CO_2, CH_4, N_2O air emissions are categorized under Greenhouse effect/Global warming impact method, since they all contribute to global warming in varying degrees. Impact assessment methods published by Center of Environmental Science (CML)[19] at Leiden University, were used in the current study, and are listed before in Table 4.2. These methods are briefly reviewed in Section 4.4.1 below.

4.4.1 Impact Assessment Methods

4.4.1.1 Acidification

Acidification refers to the process of increase in hydrogen ion concentration, [H^+], in terrestrial and aquatic ecosystems. This increase is because of deposition (due to oxidation and hydrolysis) of air emissions, such as NH_3, NO_2, SO_2; and can cause reduced fish production in water bodies, effect forests, man-made resources (buildings, automobiles), and human health.

Characterization method developed by CML is based on the RAINS (Regional Acidification Information and Simulation) model and computes average European characterization factor for acidification. Total acidification potential is calculated by converting individual emissions into g SO_2 equivalents, as defined below:

$$\text{Acidification} = \sum_i AP_i \times m_i \, ,$$

where total acidification is expressed as g SO_2 equivalents, AP_i is the acidification potential for air emissions of substance i, and m_i is the amount of substance i emitted in grams.

CML acidification method and characterization factors are location independent, for research study in Europe; but the current study focuses on comparative LCA for US production. Still, this acidification method is used, because it is based on an internationally accepted RAINS model and best method available at the time of this analysis.

4.4.1.2 Human Toxicity, Freshwater-Aquatic and Terrestrial EcoToxicity

These impact categories refer to the impacts of toxic substances on human health, aquatic and terrestrial ecosystems. The characterization factors for these impact categories have been developed using USES-LCA (Huijbregts 1999[48]), which models exposure route, intake and fate of toxic substances introduced in one of the environmental compartments (Global spatial scale has three compartments: air, (sea)water, and soil; Regional and continental spatial scale has six compartments: air, freshwater, seawater, natural soil, agricultural soil, industrial soil).

Human toxicity potential for a single substance i emitted in compartment *ecomp* is calculated by adding the contribution to each environmental compartment via different exposure routes (for Human toxicity calculations, six exposure routes are considered: air, fish, drinking water, crops, cattle meat, and

milk) and dividing it by a similar sum for a reference substance, 1,4-dichlorobenzene. This calculation is described below:

$$HTP_{i,ecomp} = \frac{\sum_r \sum_s PDI_{i,ecomp,r,s} \times E_{i,r} \times N_s}{\sum_r \sum_s PDI_{1,4\text{-}dichlorobenzene,air,r,s} \times E_{1,4\text{-}dichlorobenzene,r} \times N_s}$$

where :

$HTP_{i,ecomp}$ = Human toxicity potential of substance i emitted to emission compartment ecomp (dimensionless);

N_s = population density at scale s;

$PDI_{i,ecomp,r,s}$ = Predicted daily intake via exposure route r at scale s for substance i emitted to emission compartment ecomp (day^{-1}) and is a combination of $F_{i,ecomp,fcomp}$, $T_{i,fcomp,r}$ and I_r;

$E_{i,r}$ = effect factor, representing the human toxic impact of substance i, and is calculated as reciprocal of the ADI (Acceptable Daily Intake) of the substance via exposure route r (day);

$F_{i,ecomp,fcomp}$ = fate factor, representing intermedia transport of substance i from emission compartment ecomp to final compartment fcomp and degradation within compartment ecomp;

$T_{i,fcomp,r}$ = transfer factor, fraction of substance i transferred from fcomp to exposure route r;

I_r = intake factor, representing human intake via exposure route r.

Based on the selected time span, total human toxicity is calculated as follows:

$$\text{human toxicity}_t = \sum_i \sum_{ecomp} m_{i,ecomp} \times HTP_{i,ecomp,t}$$

where :

human toxicity$_t$ = total human toxicity for time span t (kg);

HTP$_{i,ecomp,t}$ = Human toxicity potential of substance i emitted to emission compartment $ecomp$ for time horizon t;

m$_{i,ecomp}$ = emission of substance i to compartment $ecomp$ (kg).

Freshwater-Aquatic and Terrestrial EcoToxicity impacts are calculated similar to Human Toxicity, with difference being the use of PNEC (Predicted No Effect Concentration) instead of ADI (Acceptable Daily Intake) as a reference level for risk evaluation. PNEC is determined based on an extrapolation of selected toxic effects for few species to entire ecosystem, so as to obtain acceptable risk levels. Freshwater-Aquatic and Terrestrial EcoToxicity potentials and total toxicity results are calculated as follows:

$$FAETP_{i,ecomp} = \frac{PEC_{i,ecomp,freshwater} \times E_{i,freshwater}}{PEC_{1,4\text{-}DCB,freshwater,freshwater} \times E_{1,4\text{-}DCB,freshwater}}$$

$$TETP_{i,ecomp} = \frac{PEC_{i,ecomp,soil} \times E_{i,soil}}{PEC_{1,4\text{-}DCB,soil,soil} \times E_{1,4\text{-}DCB,soil}}$$

where :

FAETP$_{i,ecomp}$ = Freshwater-Aquatic EcoToxicity potential of substance i emitted to emission compartment $ecomp$;

TETP$_{i,ecomp}$ = Terrestrial EcoToxicity potential of substance i emitted to emission compartment $ecomp$;

PEC = Predicted concentration of substance i in freshwater or soil, due to the emission in compartment $ecomp$, similarly PEC$_{1,4\text{-}DCB}$ predicts concentration for 1,4-dichlorobenzene in either freshwater or soil;

E = effect factor representing the toxic impact of substance i or reference material 1,4-dichlorobenzene in either freshwater or soil, calculated as reciprocal of the PNEC (Predicted No Effect Concentration).

$$\text{Freshwater-Aquatic EcoToxicity}_t = \sum_i \sum_{ecomp} m_{i,ecomp} \times FAETP_{i,ecomp,t}$$

$$\text{Terrestrial EcoToxicity}_t = \sum_i \sum_{ecomp} m_{i,ecomp} \times TETP_{i,ecomp,t}$$

where:

Freshwater – Aquatic and Terrestrial EcoToxicity are total ecotoxicity results in respective compartments for time span t (kg).

The CML study has selected infinite time span and global spatial scale for its baseline Human Toxicity and EcoToxicity methods, and these methods were selected for the current study because of their global scale selection, which increases the relevance of impact assessment analysis for US production.

USES-LCA method presents a comprehensive modeling of fate of toxic substances released in the environment, but has some uncertainties, which were considered while interpreting the current LCA results and are mentioned below:

a) Weak modeling of fate of metals. Intermedia transport of metals is highly dependent on environmental conditions and USES-LCA model does not include any spatial difference for fate, exposure/intake, or effect parameters

b) Fate of geochemically reactive metals such as beryllium (Be) does not include removal mechanism of hydrolysis (at salt water pH) and inclusion into minerals such as ferro-mangenese nodules

c) USES model does not consider any variation in the safe level concentration of some of the essential metals (e.g. Co, Cu, Cr, Mn, Se, Zn, these are heavy metals), based on the original environmental concentrations of the these metals

Therefore, Huijbregts[48] (1999) recommends careful interpretation of the results, in case of a significant contribution from heavy metals. This method models the fate of 180 substances, which represents a small percentage of known and unknown toxic substances and therefore it is possible that some of the toxic substances in the current LCI are not included in the total toxicity results.

4.4.1.3 Depletion of abiotic resources

Abiotic resources are defined as non-living natural resources, which include for e.g. iron ore, crude oil, natural gas, wind energy. Generally, abiotic resources are classified into three categories: deposits, funds, and flows. Deposits are resources, which are non-renewable during human lifetime, examples are: fossil fuels, minerals, sediments, clays. Funds are resources, which can be regenerated within human lifetime, examples are: groundwater, soil. Flows are resources, which are continuously regenerated, examples are: wind, river water, solar energy. Further distinction of abiotic resources is done by classifying resources based on whether they can be depleted or competitively used and thus deposits are classified in the first category, while flows are grouped in the latter and funds may belong to either of these categories.

CML impact method for this category uses the method developed by Guinee & Heijungs[49], 1995, which calculates abiotic depletion potential based on ultimate reserves and rates of extraction and the formula for this potential and total abiotic depletion is shown below:

$$ADP_i = \frac{DR_i}{(R_i)^2} \times \frac{(R_{ref})^2}{DR_{ref}}$$

$$\text{Abiotic Depletion} = \sum_i ADP_i \times m_i$$

where:

Abiotic Depletion = total result in terms of kg of antimony;

ADP_i = Abiotic Depletion Potential of resource i;

m_i = amount of resource i extracted (kg);

R_i & R_{ref} = ultimate reserves of resource i and reference resource, Antimony (kg);

DR_i & DR_{ref} = extraction rate of resource i and R_{ref}(kg/yr).

The method described above has few limitations: the depletion potentials have been calculated only for elements and similar potentials for minerals & ores are missing; this method only include resources which can be depleted, thus no competitively used resources (all flows and some funds) are considered. Other than these limitations, this method is time and location independent and thus it was used for the current LCA study for US production.

4.4.1.4 Depletion of the stratospheric ozone

Stratospheric ozone depletion refers to the thinning (disappearance in worst cases) of stratospheric ozone layer and is caused due to anthropogenic emissions. This thinning of ozone layer leads to greater amount of solar UV-B

radiations reaching earth's surface, which can have harmful impacts on human health, natural resources, natural and man-made environment. In the CML study, total ozone depletion impact and depletion potential for individual emissions are based on a 1988 study by Wuebbles[50] and the formula used to calculate these results is described below:

$$ODP_i = \frac{\delta[O_3]_i}{\delta[O_3]_{CFC\text{-}11}}$$

$$\text{Ozone depletion} = \sum_i ODP_i \times m_i$$

where :

$\delta[O_3]_i$ & $\delta[O_3]_{CFC\text{-}11}$ = change in stratospheric ozone concentration at steady state due to annual emissions of substance i and reference substance, CFC-11 respectively;

ODP_i = ozone depletion potential for substance i,

in kg CFC -11 eq./kg of substance i;

m_i = mass of substance i released (kg);

Ozone depletion = total results expressed as kg CFC-11 equivalents.

The concept of ozone depletion potential (ODP) is similar to that of global warming potential (GWP); however it differs in the way it calculates these potentials, ODP's are calculated at steady state, while GWP's are calculated for varying time spans (20, 100, 500 years).

The ODP's used in the CML-Ozone depletion impact are based on the best estimates of ODP's published by World Meteorological Organization (WMO)[51] in 1999 and 1992 and calculates ODP's for an infinite time span (approximated by steady state ODP). Additionally, CML-Ozone depletion impacts

are time and location independent, and therefore the current LCA study for US production uses this impact assessment method.

4.4.1.5 Climate change

Climate change refers to the impact of anthropogenic emissions on increased radiative forcing of the earth's atmosphere. Radiative forcing is the net difference between the amount of radiation coming into the atmosphere and radiation going out; and net positive radiative forcing causes increase in earth's surface temperature, leading to changes in earth's climate (also known as greenhouse effect, global warming). Some of the critical endpoint impacts of global warming include sea-level rise, increased droughts, forest damage, and increased occurrence of extreme weather events, thus effecting all areas of protection (human health, natural environment, man-made environment, and natural resources). Example of greenhouse gases are: CO_2, CH_4, and N_2O and global warming potential (GWP) of all the greenhouse gases is calculated by normalizing it to CO_2 emissions, because CO_2 is usually the major component of total global warming impact.

CML-Climate change method is based on a 1996 study by the Intergovernmental Panel on Climate Change (IPCC)[52], which has calculated GWP for greenhouse gases with varying time spans of 20, 100, and 500 years. The calculation for GWP and total climate change impact is shown below:

$$GWP_{T,i} = \frac{\int\limits_{0}^{T} a_i \cdot c_i(t)dt}{\int\limits_{0}^{T} a_{CO_2} \cdot c_{CO_2}(t)dt}$$

$$\text{Climate change} = \sum_i GWP_{T,i} \times m_i$$

where :

$GWP_{T,i}$ = Global warming potential of greenhouse gas i,

for a time span of T years;

Climate change = cumulative climate change impact,

expressed in kg CO_2 – equivalents;

a_i = radiative forcing per unit increase in concentration

of greenhouse gas i $(w \cdot m^{-2} \cdot kg^{-1})$;

$c_i(t)$ = concentration of greenhouse gas i at time t after the release $(kg \cdot m^{-3})$;

m_i = amount of greenhouse emissions (kg).

The CML baseline method calculates GWP's for a time span of 100 years and does not include net GWP's for ozone-depleting gases (which have a positive impact on global warming), because of the high uncertainties in these net GWP's. This CML-Climate change method is time and location independent; therefore, it was used in the current LCA study to compute climate change impact.

4.4.1.6 Eutrophication

Eutrophication refers to the impacts of excessive amount of nutrients (N & P being the most important) in terrestrial and aquatic ecosystems. Over-fertilization in aquatic ecosystems causes excessive biomass production (e.g.

159

algae), thus creating hypoxic (low oxygen concentration) conditions and effecting other aquatic species (fish, marine mammals, etc.). Additionally, high nutrient concentrations in surface water may lead to surface water being unfit for human consumption. Use of N & P fertilizers for crop cultivation is a major contributor to eutrophication. The CML-Eutrophication method is based on a 1992 study by Heijungs et al.[53], which computes eutrophication impact for N & P compounds normalized to PO_4^{3-} eutrophication. The formula used to calculate eutrophication potentials and total eutrophication impact is described below:

$$EP_i = \frac{v_i / M_i}{v_{ref} / M_{ref}}$$

$$Eutrophication = \sum_i EP_i \times m_i$$

where :

EP_i = Eutrophication potential of substance i;

Eutrophication = total eutrophication impact in kg PO_4^{3-} equivalents;

v_i & v_{ref} = eutrophication contributions of one mole of substance i & reference (PO_4^{3-}) respectively;

M_i & M_{ref} = mass of substance i & reference (PO_4^{3-}) respectively (kg·mol^{-1});

The method developed by Heijungs et al.[53], combines the eutrophication potential for air and water emissions and does not consider any changes in the overall result due to the sensitivity of the nutrient receiving environment and limiting nutrient in that environment. Therefore, eutrophication results obtained by this method are time and location independent.

However, their is significant variation in eutrophication results, if the influence of location on atmospheric and hydrologic transport and deposition is

considered. TRACI[17]-eutrophication potentials developed by Norris[54], considered these influences, while calculating average eutrophication potentials for United States. For water emissions, these potentials are similar to those calculated by Heijungs et al.[53]; while eutrophication potentials for air emissions have large variation, as shown below in Table 4.26.

Table 4.26 Comparison of CML and TRACI Eutrophication potentials

Substance	Heijungs et al. (1992), kg N equivalents/kg	Norris (2002), kg N equivalents/kg
Air emissions		
Ammonia (NH_3)	0.83	0.12
Nitric oxide (NO)	0.48	0.07
Nitrogen dioxide (NO_2)	0.31	0.04
Nitrogen oxides (NO_x as NO_2)	0.31	0.04
Phosphorus (P)	7.29	1.12
Water emissions		
Ammonium (NH_4^+)	0.79	0.78
Nitrogen (N)	1.00	0.99
Nitrate (NO_3^-)	0.24	0.24
Phosphate (PO_4^{3-})	2.38	2.38
Phosphorus (P)	7.29	7.29
Chemical oxygen demand (COD)	0.05	0.05

Since significant variation exists between CML and TRACI air-eutrophication potentials (Table 4.26), sensitivity analysis was done for CML eutrophication impacts by comparing them with impacts calculated using TRACI method (Section 4.5.2).

4.4.1.7 Photo-oxidant formation

This method covers the impact of formation of harmful chemical substances (photo-oxidants) in troposphere due to the action of sunlight on air emissions such as volatile organic compounds (VOCs) and carbon monoxide (CO) in presence of nitrogen oxides (NO_x). Some of the most important photo-oxidants are ozone (O_3) and peroxyacetylnitrate (PAN), and exposure to these compounds effect human health (e.g. asthma) and ecosystems (reduced plant growth).

The CML photo-oxidant formation method is based on a 1992 study by Heijungs et al.[53], which defines the total impact in terms of photochemical ozone creation potentials (POCPs). The POCPs for this method, uses the characterization factors published by Derwent et al.[55] (1998), Jenkin & Hayman[56] (1999), which combine the incremental ozone production due to incremental VOC emissions with basic emission scenario (referred as 'marginal' approach) and Derwent et al.[57] (1996) (specifically for inorganic substances, including NO and NO_2), which calculates POCPs based on the difference in ozone formation with and without the particular substance (referred as 'average' approach). All of these characterization factors use the data from a 5-day trajectory model of VOC

transportation above Europe, and assumes high background NO_x concentration.

The formula used for calculating POCPs and total impact is mentioned below:

$$POCP_i = \frac{a_i / b_i}{a_{C_2H_4} / b_{C_2H_4}}$$

$$Photo-oxidant\ formation = \sum_i POCP_i \times m_i$$

where :

$POCP_i$ = photochemical ozone creation potential of substance i,

in kg ethylene equivalents/kg substance i;

Photo-oxidant formation = total impact expressed in kg ethylene equivalents;

a_i & $a_{C_2H_4}$ = ozone concentration change, due to change in the emission of

substance i & reference substance C_2H_4;

b_i & $b_{C_2H_4}$ = integrated emission of substance i & reference substance C_2H_4;

m_i = mass of substance i released.

As described above, the CML method is based on a European VOC emission model, with high background NO_x concentrations and considered time and location independent for a LCA study in Europe. This method was used for the current study, because of the non-availability of a reliable impact assessment method for US production.

4.4.1.8 Normalization and normalization factors

Normalization is an optional component of impact assessment as defined by ISO 14042[15] and is used to calculate relative significance of impact assessment results, check for inconsistencies, and prepare for additional analysis, e.g.: grouping, weighting, life cycle interpretation. For the current study,

normalization was used to determine the relative significance of calculated impacts. CML normalization method[58] and factors were used, so as to be consistent with previous results. CML method calculates normalization factors based on the yearly emissions of the substance in the reference region and computing normalized impacts by dividing the total impact result with cumulative normalization factor. The formula used for this calculation is mentioned below:

$$A_{e,s} = \sum_{r} \sum_{i} \sum_{x} Q_{e,x,i,r} \times M_{x,i,r,s}$$

$$N_{e,s} = \frac{S_e}{A_{e,s}}$$

where :

$A_{e,s}$ = normalization factor for impact category e in reference situation s (kg equivalents yr^{-1});

$Q_{e,x,i,r}$ = chracterization factor related to impact category e for substance x emitted to compartment i in region r (kg equivalents kg^{-1});

$M_{x,i,r,s}$ = annual emission of substance x to compartment i in region r for reference situation s (kg yr^{-1});

S_e = total impact for category e (kg equivalents);

$N_{e,s}$ = normalized impact for category e in reference situtation s.

This CML study reports normalization factors for four different reference situations: The Netherlands in 1997/1998, Western Europe in 1995, World in 1990 and 1995 and reported normalized factors for all the impact categories considered in the current study. This study recommends using global normalization factors for regionally undefined LCA studies; therefore in the current study global factors were used, even though the study was conducted for

US production of composites, using global factors is the best option rather than using Netherlands or Western Europe factors, which can introduce a West-European bias to normalized impacts. Thus, normalization factors for the World in 1995 were used, since these are the most recent factors reported by the CML study for global impacts. These factors are shown below in Table 4.27.

Table 4.27 Normalization impact factors for the World in 1995

Impact Category	Units	Reference situation: World, 1995
Depletion of abiotic resources	kg antimony (Sb) equivalent yr^{-1}	1.6×10^{11}
Climate change (100 years)	g CO_2 equivalent yr^{-1}	4.1×10^{16}
Depletion of the stratospheric ozone	g CFC-11 equivalent yr^{-1}	5.2×10^{11}
Human Toxicity	g 1,4-dichlorobenzene (DCB) equivalent yr^{-1}	5.7×10^{16}
Freshwater-Aquatic EcoToxicity	g 1,4-dichlorobenzene (DCB) equivalent yr^{-1}	2.0×10^{15}
Terrestrial EcoToxicity	g 1,4-dichlorobenzene (DCB) equivalent yr^{-1}	2.7×10^{14}
Photo-oxidant formation	g ethylene equivalent yr^{-1}	9.6×10^{13}
Acidification	g SO_2 equivalent yr^{-1}	3.2×10^{14}
Eutrophication	g PO_4^{3-} equivalent yr^{-1}	1.3×10^{14}

Theoretically, the CML study has computed normalization factors using region specific emission data and characterization factors. However, there are

impact categories, for which the emission data is extrapolated and/or characterization factor for a different reference situation are used. Such extrapolations may contribute toward the uncertainty in normalized impact factors and the potential areas of concern have been well documented in this study. For example:

- majority of toxic emissions to air, freshwater, and industrial soil for Western Europe and World reference situations have been extrapolated from emission data for Netherlands using GDP extrapolation

- emissions of N and P to water and soil for Western Europe and the World have been extrapolated from the data for the Netherlands, based on human and animal population numbers

4.4.2 Impact Assessment Results

The impact assessment results were computed as a sum of product of individual emission mass flows with their respective characterization factors for a particular impact. As mentioned before in section 4.2.2.5, impact assessment methods developed by Center of Environmental Science (CML)[19] at Leiden University were used to determine the impacts for current LCA study. For the current study, contribution analysis of the impact assessment results was done to determine the flows, which made significant contribution to selected impact categories and only these significant flows are presented in the LCI and impact assessment results, thus keeping the final results brief, but not missing any important flows. This contribution analysis was previously presented in section

4.3.1, Table 4.3. Impact assessment results for PP-Glass and PHB-Kenaf composites are presented below in Table 4.28 and 4.29 respectively. The results include data about contribution from major production steps and contribution (%) of individual emissions to the total impact.

Table 4.29 Impact Assessment results for PHB Kenaf Composite (cradle to pellet)

Flow	Units	Characteriza tion Factor	PHB-Kenaf Composite LCI (total)	P(3HB-co-5mol% 3HHx) Production	Kenaf Fiber Production	Electricity Production (for Extrusion and Injection molding)
Method : CML2000-Air Acidification	g SO₂ eq.	*	**313.98**	**265.24 (85%)**	**3.67 (1%)**	**45.08 (14%)**
(a) Ammonia (NH3)	g	1.60E+00	47.35%	55.21%	60.47%	0.01%
(a) Nitrogen Oxides (NOx as NO2)	g	5.00E-01	17.96%	16.35%	21.23%	27.20%
(a) Sulphur Dioxide (SO2)	g	1.20E+00	0.32%	0.37%	1.02%	0.00%
(a) Sulphur Oxides (SOx as SO2)	g	1.20E+00	34.37%	28.07%	17.28%	72.79%
Method : CML2000-Aquatic Toxicity	g 1,4- DCB eq.	*	**36.13**	**25.52 (71%)**	**0.27 (1%)**	**10.34 (29%)**
(a) Arsenic (As)	g	5.00E+01	1.11%	1.05%	0.38%	1.30%
(a) Beryllium (Be)	g	1.70E+04	43.53%	40.87%	14.66%	50.83%
(a) Hydrogen Fluoride (HF)	g	4.60E+00	8.79%	8.26%	3.11%	10.23%
(a) Nickel (Ni)	g	6.30E+02	19.31%	18.40%	9.48%	21.80%
(a) Selenium (Se)	g	5.50E+02	9.12%	8.58%	3.09%	10.60%
(a) Vanadium (V)	g	1.70E+03	3.84%	5.14%	22.07%	0.18%
(w) Barium (Ba++)	g	2.30E+02	3.45%	4.82%	6.70%	0.00%
(w) Phenol (C6H5OH)	g	2.40E+02	3.57%	4.71%	23.56%	0.24%
Method : CML2000-Depletion of abiotic resources	kg antimony eq.	*	**0.20**	**0.16 (78%)**	**0.002 (1%)**	**0.04 (21%)**
(r) Coal (in ground)	kg	1.34E-02	62.13%	52.79%	20.86%	98.06%
(r) Natural Gas (in ground)	kg	1.87E-02	32.23%	40.67%	36.90%	0.97%
(r) Oil (in ground)	kg	2.01E-02	5.55%	6.44%	41.95%	0.96%

Flow	Units	Characteriza tion Factor	PP-Glass Composite LCI (total)	Polypropylene Production	Glass Fiber Production	Electricity Production (for Extrusion and Injection molding)
(r) Oil (in ground)	kg	2.01E-02	54.13%	74.69%	1.40%	0.96%
Method : CML2000-Depletion of the stratospheric ozone	g CFC-11 eq.	*	1.74E-04	2.17E-08 (0.01%)	8.64E-05 (50%)	8.80E-05 (50%)
(a) Halon 1301 (CF3Br)	g	1.20E+01	0.00%	1.12%	0.00%	0.00%
(a) Methyl Bromide (CH3Br)	g	3.70E-01	82.22%	81.30%	82.22%	82.22%
(a) Methyl Chloride (CH3Cl)	g	2.00E-02	14.72%	14.56%	14.72%	14.72%
(a) Trichloroethane (1,1,1-CH3CCl3)	g	1.10E-01	3.06%	3.02%	3.06%	3.06%
Method : CML2000-Eutrophication	g PO_4^{3-} eq.	*	19.30	9.07 (47%)	7.59 (39%)	2.54 (13%)
(a) Ammonia (NH3)	g	3.50E-01	0.10%	0.00%	0.24%	0.02%
(a) Nitrogen Oxides (NOx as NO2)	g	1.30E-01	99.08%	99.33%	99.71%	99.93%
(w) Nitrate (NO3-)	g	1.00E-01	0.07%	0.15%	0	0
(w) Nitrogenous Matter (unspecified, as N)	g	4.20E-01	0.15%	0.32%	0	0
Method : CML2000-Climate change (100 years)	g CO2 eq.	*	27132.15	12217.1 (45%)	8731.29 (32%)	6125.54 (23%)
(a) Carbon Dioxide (CO2, biomass)	g	1.00E+00	0.00%	0	0.00%	0.00%
(a) Carbon Dioxide (CO2, fossil)	g	1.00E+00	99.99%	100.00%	99.98%	99.99%
(a) Methane (CH4)	g	2.10E+01	0.01%	0	0.01%	0.01%
Method : CML2000-Human Toxicity	g 1,4-DCB eq.	*	4182.19	105.48 (3%)	2455.70 (59%)	1621.01 (39%)
(a) Arsenic (As)	g	3.50E+05	35.63%	0.21%	30.08%	46.35%
(a) Benzene (C6H6)	g	1.90E+03	19.55%	1.12%	32.62%	0.94%
(a) Beryllium (Be)	g	2.30E+05	2.71%	0.01%	2.30%	3.50%
(a) Dioxins (unspecified)	g	1.90E+09	1.78%	0.01%	1.50%	2.32%

Flow	Units	Characterization Factor	PP-Glass Composite LCI (total)	Polypropylene Production	Glass Fiber Production	Electricity Production (for Extrusion and Injection molding)
(a) Hydrogen Fluoride (HF)	g	2.90E+03	25.68%	18.99%	21.25%	32.81%
(a) Nickel (Ni)	g	3.50E+04	4.78%	0.19%	4.07%	6.16%
(a) Nitrogen Oxides (NOx as NO2)	g	1.20E+00	4.22%	78.88%	2.84%	1.45%
(a) Selenium (Se)	g	4.80E+04	3.62%	0.02%	3.05%	4.71%
Method : CML2000-Photo-oxidant formation	g ethylene eq.	*	0.77	0.13 (17%)	0.54 (69%)	0.10 (13%)
(a) Benzene (C6H6)	g	2.20E-01	12.23%	0.10%	17.28%	1.70%
(a) Carbon Monoxide (CO)	g	2.70E-02	50.10%	99.68%	41.00%	32.98%
(a) Methane (CH4)	g	6.00E-03	29.59%	0.17%	30.36%	63.82%
Method : CML2000-Terrestrial Toxicity	g 1,4- DCB eq.	*	16.34	0.04 (0.25%)	8.19 (50%)	8.11 (50%)
(a) Arsenic (As)	g	1.60E+03	41.70%	2.42%	41.25%	42.35%
(a) Beryllium (Be)	g	1.80E+03	5.43%	0.27%	5.41%	5.47%
(a) Mercury (Hg)	g	2.80E+04	46.16%	2.63%	46.49%	46.04%
(a) Nickel (Ni)	g	1.20E+02	4.20%	1.64%	4.19%	4.22%
(a) Selenium (Se)	g	5.30E+01	1.02%	0.05%	1.01%	1.04%
(a) Vanadium (V)	g	6.70E+02	0.38%	20.13%	0.59%	0.07%

170

Flow	Units	Characterization Factor	PHB-Kenaf Composite LCI (total)	P(3HB-co-5mol% 3HHx) Production	Kenaf Fiber Production	Electricity Production (for Extrusion and Injection molding)
(a) Nickel (Ni)	g	3.50E+04	5.66%	5.45%	6.80%	6.16%
(a) Nitrogen Oxides (NOx as NO2)	g	1.20E+00	1.98%	2.17%	8.97%	1.45%
(a) Selenium (Se)	g	4.80E+04	4.20%	3.99%	3.48%	4.71%
Method : CML2000-Photo-oxidant formation	g ethylene eq.	*	2.35	2.20 (94%)	0.02 (1%)	0.13 (5%)
(a) Benzene (C6H6)	g	2.20E-01	3.59%	3.71%	1.60%	1.70%
(a) Carbon Monoxide (CO)	g	2.70E-02	23.58%	22.82%	48.50%	32.98%
(a) Ethylene (C2H4)	g	1.00E+00	49.69%	52.84%	20.04%	0.00%
(a) Methane (CH4)	g	6.00E-03	15.48%	12.62%	18.41%	63.82%
(a) Sulphur Dioxide (SO2)	g	4.80E-02	1.72%	1.77%	8.38%	0.00%
Method : CML2000-Terrestrial Toxicity	g 1,4- DCB eq.	*	32.76	22.46 (69%)	0.13 (0.4%)	10.17 (31%)
(a) Arsenic (As)	g	1.60E+03	39.32%	38.04%	24.74%	42.35%
(a) Beryllium (Be)	g	1.80E+03	5.08%	4.92%	3.16%	5.47%
(a) Mercury (Hg)	g	2.80E+04	44.45%	43.83%	28.05%	46.04%
(a) Nickel (Ni)	g	1.20E+02	4.06%	3.98%	3.67%	4.22%
(a) Selenium (Se)	g	5.30E+01	0.97%	0.94%	0.61%	1.04%
(a) Vanadium (V)	g	6.70E+02	1.67%	2.30%	17.70%	0.07%
(s) Zinc (Zn)	g	1.40E+03	3.18%	4.63%	2.42%	0.00%

4.4.2.1 Acidification

Acidification impacts were calculated in SO_2 equivalents and PHB-Kenaf composites have 17% higher impacts compared to PP-Glass composites for the same functional unit of production of 1000 tensile coupons and the higher impacts are due to nutrient runoff from soybean cultivation and higher electricity consumption for PHB-Kenaf composites. Comparison of these composites and stepwise contribution towards acidification impact is shown below in Figure 4.27.
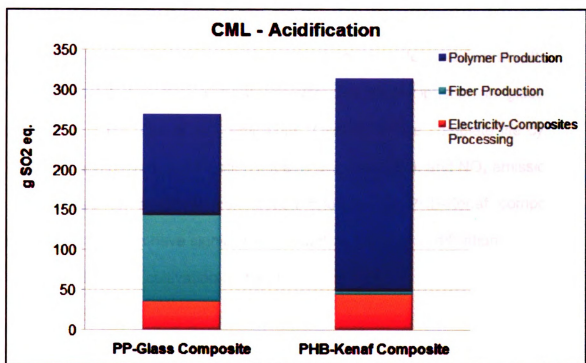
Figure 4.27 Acidification impact for PP-Glass and PHB-Kenaf Composites

The processes, which contribute the most towards this impact were determined using contribution analysis. For PP-Glass composites, these processes are:

- PP production = 47%

- Electricity production (for all sub-steps) = 26%

- Glass fiber production process = 23%

- Natural Gas production & combustion (glass fiber production) = 4%

In glass fiber production process (Table 4.6), major contribution is due to SO_x and NO_x emissions from melting and refining step, with small contribution due to NO_x emissions from post forming and finishing step. Additionally, there is a small contribution from natural gas use and its combustion in glass fiber production in the form of NO_x emissions. Overall, for the complete life cycle of PP-Glass composites, acidification impacts are due to SO_x and NO_x emissions.

Based on a similar contribution analysis for PHB-Kenaf composites, following processes have significant contribution towards acidification:

- Soybean cultivation (nutrient runoff) = 50%

- Electricity production = 42%

- Superphosphate production = 2%

- Steam production = 1%

In case of soybean cultivation, NH_3 and NO_x emissions (Table 4.18) cause acidification. As in the case of PP-Glass composites, electricity production (composites processing and for PHB production) has significant contribution to the total acidification impact because of NO_x and SO_x emissions.

4.4.2.2 Freshwater-Aquatic EcoToxicity

Freshwater aquatic ecotoxicity (FAET) impact in the current study was computed in 1, 4-dichlorobenzene (DCB) equivalents. Impacts for PHB-Kenaf composites were 115% higher compared to PP-Glass composites, primarily because of electricity consumption for PHB-Kenaf composites, which was roughly twice the electricity used for PP-Glass composites. Cumulative impacts for PP-Glass and PHB-Kenaf composites, highlighting stepwise contribution are shown below in Figure 4.28.
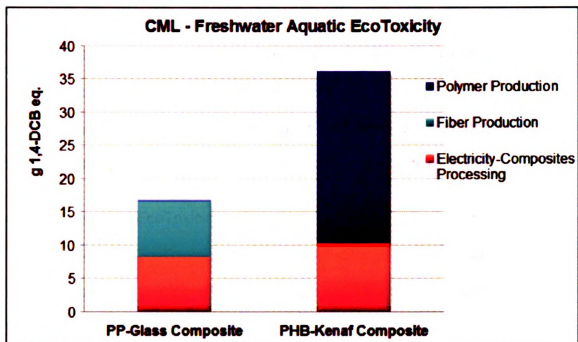
Figure 4.28 Freshwater Aquatic EcoToxicity impact for PP-Glass and PHB-Kenaf Composites

For PP-Glass composites, the air emissions of Be, Ni, Se, HF were most significant and following processes contribute towards the majority of FAET impact:

- Electricity production (composites processing and glass fiber production) = 96.5%

- Natural Gas production & combustion (glass fiber production) = 1.5%

In case of PHB-Kenaf composites, air emissions of Be, Ni, Se, HF are significant, along with small contributions due to Vanadium air emissions and water emissions of barium and phenol. The following processes are main contributors towards the FAET impact for PHB-Kenaf composites:

- Electricity production (composites processing, PHB production process, soybean crushing and cultivation) = 85%

- Steam production (used in PHB production process and soybean crushing to obtain soybean oil) = 6%

- Miscellaneous steps associated with soybean and kenaf cultivation (tractor use, transport by truck, fertilizer production) = 10%

4.4.2.3 Terrestrial EcoToxicity

Terrestrial EcoToxicity results measured in 1, 4-dichlorobenzene (DCB) equivalents were similar to the results obtained for Freshwater-Aquatic EcoToxicity, in terms of comparative impacts for both systems and processes with major contribution to the total impacts. For both the systems, air emissions of mercury, arsenic, beryllium, and nickel caused majority of terrestrial ecotoxicity. These results are compared below in Figure 4.29, and PHB-Kenaf composites have twice the impacts for PP-Glass composites. The higher impacts for PHB-Kenaf composites were due to high electricity consumption, which is roughly twice as high as the electricity consumption for PP-Glass composites.

For PHB-Kenaf composites, following processes made significant contribution to the total terrestrial ecotoxicity impacts:

- Electricity production (consumed in PHB production process, composites processing, soybean crushing and cultivation) = 92%

- Steam production (for PHB fermentation and soybean crushing) = 5%

- Miscellaneous steps associated with soybean and kenaf cultivation (fertilizer production, tractor and truck transport steps) = 3%
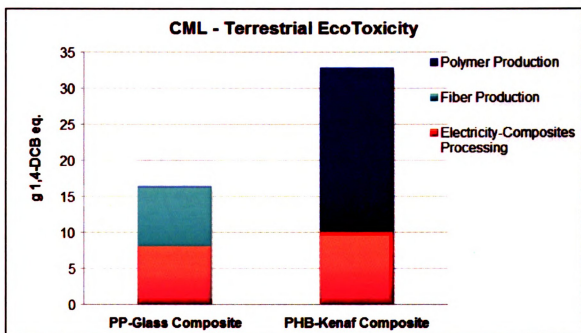
Figure 4.29 Terrestrial EcoToxicity impact for PHB-Kenaf & PP-Glass composites

In case of PP-Glass composites, terrestrial toxicity impacts were largely due to emissions from Electricity production, and details about processes with significant contribution to the total impact are mentioned below:

- Electricity production (for composites processing, glass fiber production) = 98%

- Natural gas production and combustion (glass fiber production) = 1%

4.4.2.4 Human Toxicity

Similar to ecotoxicity impacts, electricity consumption contributed towards the majority of human toxicity for both the systems. Overall, human toxicity impacts for PHB-Kenaf composites were 64% higher compared to PP-Glass composites, with air emissions of arsenic, hydrogen fluoride, and benzene being the main contributor towards this impact. The total impacts for both the systems are compared below in Figure 4.30.
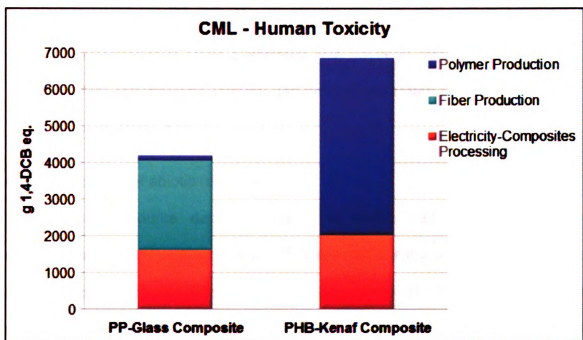
Figure 4.30 Human Toxicity impacts for PP-Glass and PHB-Kenaf composites

For PP-Glass composites, following processes had significant contribution towards total impacts:

- Electricity production (for composites processing, glass fiber production process) = 77%

- Natural gas production (for glass fiber production) = 19%

- PP production process = 3%

- Glass fiber production process and raw material production = 2%

Similarly, in case of PHB-Kenaf composites, processes with major contribution to the total human toxicity impacts are mentioned below:

- Electricity production (consumed for PHB fermentation process, composites processing, soybean crushing and cultivation) = 88%

- Ammonia production (used as fertilizer for soybean agriculture and as nutrient in PHB fermentation process) = 6%

- Miscellaneous steps associated with soybean agriculture & crushing, PHB fermentation (natural gas production, steam production, fertilizer production) = 6%

4.4.2.5 Depletion of abiotic resources

Abiotic resource depletion impact is determined in antimony (Sb) equivalents. For the current study, PP-Glass composites involve 55% greater depletion of abiotic resources, compared to PHB-Kenaf composites (stepwise comparison shown below in Figure 4.31) and for both the systems, it was due to consumption of fossil fuels: coal, natural gas, crude oil. The higher abiotic resource depletion for PP-Glass composites was primarily because of oil and natural gas consumed for PP production, where it is used as both fuel and feedstock (propylene production).
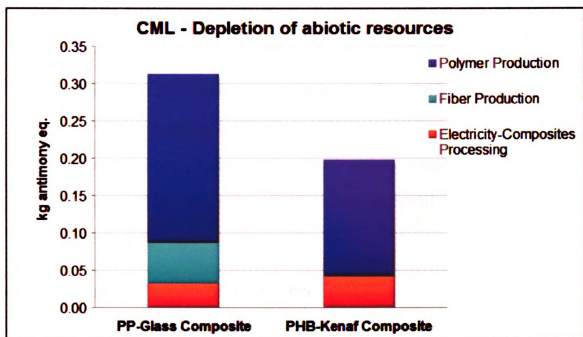
Figure 4.31 Depletion of abiotic resources for PP-Glass and PHB-Kenaf Composites

The processes, which consumed majority of abiotic resources for PP-Glass composites were:

- PP production (mainly Oil and Natural gas, used both as fuel and feedstock) = 72%

- Electricity production (used for composites processing and glass fiber production) = 21%

- Natural gas production (for glass fiber production) = 7%

In case of PHB-Kenaf composites, abiotic resources consumption was mainly because of electricity and steam production processes, with details mentioned below:

- Electricity production (used for composites processing, PHB production process, soybean crushing and cultivation processes) = 62%

181

- Steam production (used in PHB production and soybean crushing processes) = 22%

- Ammonia production (used as nutrient in PHB fermentation and fertilizer in soybean agriculture) = 5%

- Miscellaneous steps associated with soybean crushing and cultivation (natural gas production, tractor use, transport by truck, fertilizer production) = 10%

4.4.2.6 Depletion of the stratospheric ozone

Stratospheric ozone depletion impact (in CFC-11 equivalents) for PHB-Kenaf composites was 118% higher as compared to PP-Glass composites, mainly because of their high electricity consumption, which is roughly twice compared to PP-Glass composites. Air emissions of Halon 1301, methyl bromide, methyl chloride, and trichloroethane contributed towards this impact for both systems. A stepwise comparison of the total impact is presented below in Figure 4.32.

For PP-Glass composites, almost all of the impacts were due to electricity production process, with equal amounts of electricity consumed for glass fiber production and composites processing.

Similarly, in case of PHB-Kenaf composites, majority of the impacts were related to electricity production, with minor contributions from other processes. The details of these contributions are mentioned below:

- Electricity production (used for composites processing, PHB production process, soybean crushing and cultivation processes) = 86%

- Steam production (used in PHB production and soybean crushing processes) = 8%

- Miscellaneous steps associated with soybean cultivation (fertilizer production, tractor use, transport by truck) = 5%
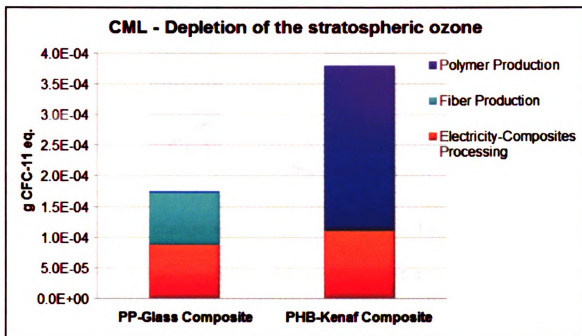
Figure 4.32 Depletion of the stratospheric ozone impact for PP-Glass and PHB-Kenaf composites

4.4.2.7 Climate change

Climate change or global warming impact of greenhouse gases is computed in CO_2 equivalents and in the current study, PHB-Kenaf composites had 14% lower impacts compared to PP-Glass composites. Lower impacts for PHB-Kenaf composites were mainly due to CO_2 sequestration by soybean crops, thus reducing the net CO_2 emissions of PHB-Kenaf composites. Stepwise contribution and comparison of PP-Glass and PHB-Kenaf composites to Climate change impact is presented below in Figure 4.33.

Figure 4.33 Climate change impact for PP-Glass and PHB-Kenaf composites

For PP-Glass composites, following processes contributed towards majority of climate change impact:

- PP production process = 45%

- Electricity production (used for glass fiber production and composites processing) = 45%

- Natural gas production and combustion (used for glass fiber production) = 10%

If CO_2 sequestration by soybean crops was not considered as a negative contribution, the total global warming impact for PHB-Kenaf composites would be 57% higher compared to PP-Glass composites, mainly because of CO_2 emissions related to PHB production process. The details of the contribution by individual processes are mentioned below:

- Electricity production (primarily used for PHB production process and composites processing) = 94%

- Soybean cultivation (CO_2 sequestration by soybean crop, emissions from raw material production and transport steps) = -72%

- PHB production process (CO_2 emissions from fermentation step and production of raw materials used in PHB fermentation process) = 68%

- Soybean crushing (emissions from electricity, natural gas, and steam production) = 8%

4.4.2.8 Eutrophication

Eutrophication impact in the current study was computed in phosphate equivalents (PO_4^{3-}) and production of PHB-Kenaf composites had approximately six times the nutrifying impact compared to PP-Glass composites, as presented below in Figure 4.34. Such a high impacts were due to nutrient runoff emissions (Table 4.18) associated with soybean cultivation, in form of air emissions of NH_3 and NO_x, water emissions of nitrogenous matter (TN as N) and phosphorus (TP as P). For PHB-Kenaf composites, following processes contributed towards majority of eutrophication impacts:

- Soybean cultivation (nutrient runoff) = 89%

- Electricity production (consumed for composites processing and PHB production process) = 8%

In case of PP-Glass composites, NO_x air emissions caused eutrophication impacts, with major contribution to this impact from following processes:

- PP production process = 47%

- Glass fiber production process (NO$_x$ emissions from melting & refining, post forming & finishing steps; from natural gas production and combustion) = 26%

- Electricity production (used for glass fiber production and composites processing) = 25%
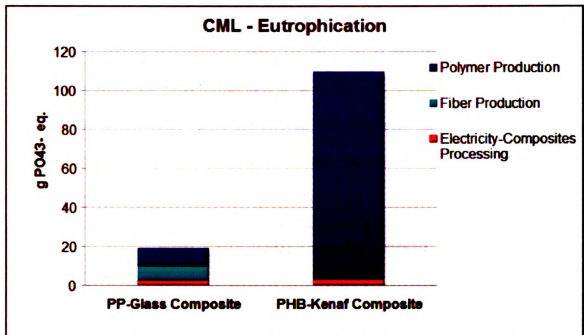
Figure 4.34 Eutrophication impact for PP-Glass and PHB-Kenaf composites

4.4.2.9 Photo-oxidant formation

Photo-oxidant impact (in ethylene equivalents) for PHB-Kenaf composites was approximately three times (205%) higher as compared to PP-Glass composites, primarily due to air emissions (of ethylene, CO, methane, and benzene) related to production of steam and electricity. Comparison of the total impacts, along with stepwise contribution for PHB-Kenaf and PP-Glass

composites is presented below in Figure 4.35. Following processes contributed towards majority of this impact for PHB-Kenaf composites:

- Steam production (consumed in PHB fermentation and soybean crushing) = 57%

- Electricity production (mainly for PHB production and composites processing) = 17%

- Ammonia production (used as fertilizer in soybean cultivation and as nutrient for PHB fermentation) = 10%

- Miscellaneous steps associated with soybean cultivation and crushing (fertilizer production, tractor use, transport by truck, natural gas production & combustion) = 16%

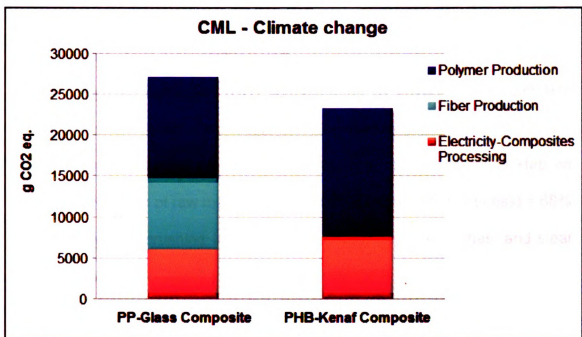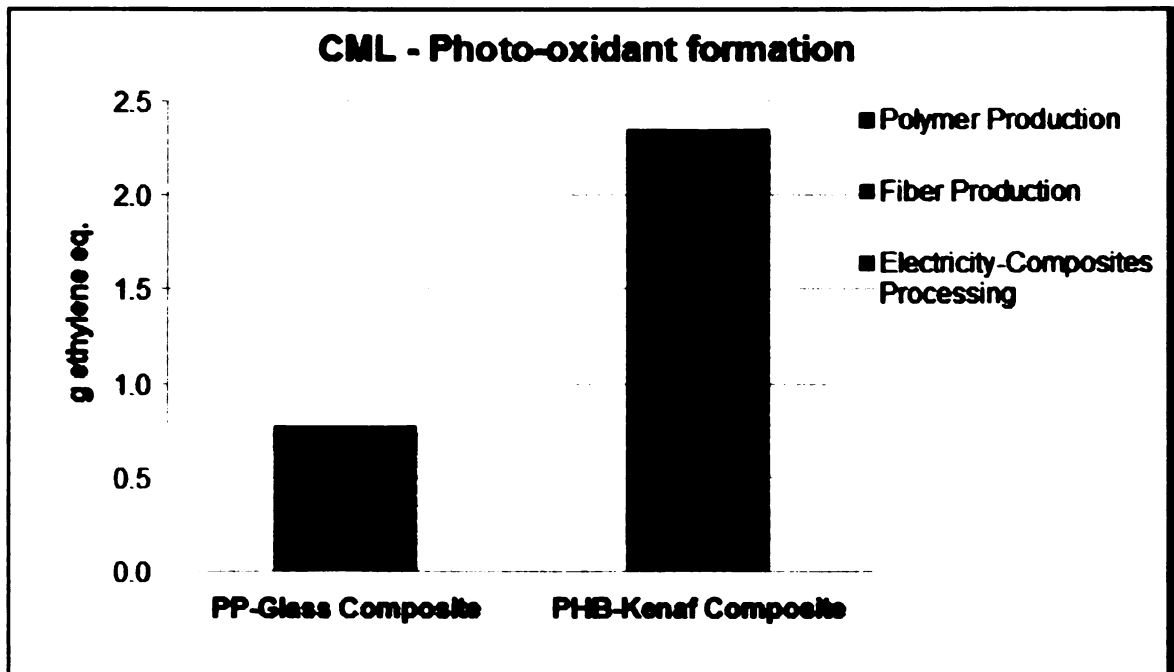Figure 4.35 Photo-oxidant formation for PP-Glass and PHB-Kenaf composites

Similarly, for PP-Glass composites, following processes contributed towards majority of photo-oxidant formation:

- Natural gas production & combustion (in glass fiber production) = 43%

- Electricity production (used for glass fiber production and composites processing) = 26%

- PP production process = 17%

- Glass fiber production process (emissions from melting & refining, post forming & finishing, and raw material production) = 13%

4.4.2.10 Normalization results and Discussion

Final impact assessment results in the current study were normalized, in order to determine their relative significance, and were computed using CML normalization factors defined for the World in 1995. This normalization method was briefly reviewed before in Section 4.4.1.8. The normalized impacts for PHB-Kenaf and PP-Glass composites are presented below in Table 4.30 and compared in Figure's 4.36 and 4.37.

Without normalizing the impacts, PHB-Kenaf composites had higher impacts in 7 out of 9 categories, compared to PP-Glass composites, with lower impacts for Climate change and Abiotic resource depletion categories. However, after normalizing the impacts, only following four impacts categories had significant contribution ($\sum$ impacts > 90%) to the cumulative normalized impacts: Abiotic resource depletion, Acidification, Eutrophication, and Global warming.

Depletion of abiotic resources was greater for PP-Glass composites mainly because of PP production process, in which 60% of the energy used was

as feedstock (crude oil and natural gas). Additionally, their was significant contribution from composites processing and glass production steps, in the form of coal consumption for electricity production and natural gas used for glass fiber production. In comparison, for PHB-Kenaf composites, PHB polymer and Kenaf fibers were produced using renewable resources and abiotic resource depletion was mainly due to electricity production and energy requirements for auxiliary processes, such as production of steam, ammonia, etc.

PP-Glass composites had a higher global warming impact, primarily due to CO_2 emissions from PP production process and electricity production; whereas for PHB-Kenaf composites, global warming impacts were lower compared to PP-Glass composites because of CO_2 sequestration by soybean crops, even though electricity consumption for PHB-Kenaf composites was approximately twice the consumption for PP-Glass composites. Another observation from global warming results was regarding the cradle-to-factory-gate scope of the current study. Because of this scope, CO_2 absorbed by soybean plants was considered as sequestered and similarly carbon from feedstock energy (60% of total energy for PP production) used for PP production was assumed to be sequestered in the final product. However, there is a difference between the sequestration for soybeans and PP. If the scope of the current study is changed to cradle-to-grave analysis i.e. including disposal phase for the composites, then soybean cultivation process will be considered carbon-neutral, because of the annual frequency of soybean crops. However, PP LCA will then contain CO_2 emissions from feedstock carbon (with incineration as a disposal option), because the

feedstock carbon is obtained from non-renewable resources and cannot be balanced with carbon, which has accumulated over thousands of years.

Acidification impacts were higher for PHB-Kenaf composites, because of NH_3 and NO_x emissions from soybean cultivation and high electricity consumption (thus more NO_x and SO_x emissions) compared to PP-Glass composites. The nutrient emissions for soybean cultivation were based on the second allocation approach specified in a 2005 NREL study[40] (Section 4.3.5.1), which allocates approximately equal nitrate leaching rates for corn and soybean crops, even though little or no N fertilizer is applied during soybean cultivation. The original allocation approach in the NREL study allocated nitrogen flows to the crop to which N fertilizer is applied. However, this allocation approach was deemed simplistic because of nitrogen fixing by soybean crops (fixed N available for future corn cultivation) and soil-absorption of excess N left from corn cultivation (absorbed N available for future soybean cultivation). Because of the large variation in N-allocation between these two methods, the NREL study suggested that the most accurate allocation would be between these two extremes and therefore variation in nutrient emissions and impacts (especially acidification and eutrophication) using first allocation method is discussed in the interpretation of the LCA results.

For eutrophication category, as expected, PHB-Kenaf composites had very high impact compared to PP-Glass composites, because of nutrient emissions (N and P flows) from soybean agriculture. However, as mentioned above in the discussion for acidification impact, nutrient emissions from soybean

cultivation can vary based on the allocation approach selected and the effect of such variation on final impacts is discussed in the interpretation of the LCA results. Additionally, there is significant difference in the air-eutrophication potentials for CML and TRACI methods (Section 4.4.1.6) and the variation in eutrophication results by using TRACI methods is discussed in the interpretation phase.

Summarizing the normalized results, more than 90% of the cumulative normalized impacts for both systems were attributed to abiotic resource depletion, acidification, eutrophication, and global warming impacts. Abiotic resource depletion had the highest contribution to the cumulative impact, with contribution of more than 50% and 30% for PP-Glass and PHB-Kenaf composites respectively.

Regarding classification of the normalized impacts, normalization makes it possible to have a quantitative comparison of the impacts, but not a qualitative comparison. Methods such as weighting or valuation are usually used to obtain a qualitative comparison and ISO 14042[15] standard recommends that in case of a comparative LCA study disclosed to the public, weighting should not be used to draw conclusions about superiority of one product over another. Additionally, Guine'e et al.[19] recommends avoiding weighting if possible, reiterating the condition set by ISO 14042 standard and in case weighting is performed; using a weighting method, which is widely accepted and covers all the impact categories. Since, such a method is still not available, the scope of the current study was limited to normalization.

Table 4.30 Normalized impacts for PHB-Kenaf and PP-Glass composites (Reference situation: World, 1995)

Method	Units[xi]	Normalization impact factors, World, 1995	PHB-Kenaf Composite	Factor[xii]	PP-Glass Composite	Factor[xi]
Abiotic Depletion	kg antimony eq. / yr	1.6E+11	1.3E-12	1.00	2.0E-12	1.00
Acidification	g SO$_2$ eq. / yr	3.2E+14	9.8E-13	0.77	8.4E-13	0.42
Eutrophication	g PO$_4^{3-}$ eq. / yr	1.3E+14	8.3E-13	0.65	1.5E-13	0.07
Aquatic Ecotoxicity	g 1,4-DCB eq. / yr	2.0E+15	1.8E-14	0.01	8.2E-15	4.E-03
Global Warming	g CO$_2$ eq. / yr	4.1E+16	5.6E-13	0.44	6.5E-13	0.33
Human Toxicity	g 1,4-DCB eq. / yr	5.7E+16	1.2E-13	0.09	7.3E-14	0.04
Ozone layer Depletion	g CFC-11 eq. / yr	5.2E+11	7.4E-16	6.E-04	3.4E-16	2.E-04
Photo-oxidant Formation	g ethylene eq. / yr	9.6E+13	2.4E-14	0.02	8.1E-15	4.E-03
Terrestrial Ecotoxicity	g 1,4-DCB eq. / yr	2.7E+14	1.2E-13	0.10	6.1E-14	0.03

[xi] Units for impact factors, normalized impacts are dimensionless
[xii] Factor = Normalized Impact / Largest Normalized Impact

192
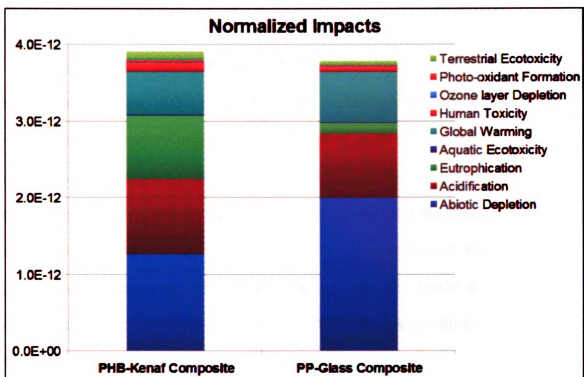
Figure 4.36 System-wide cumulative normalized impacts
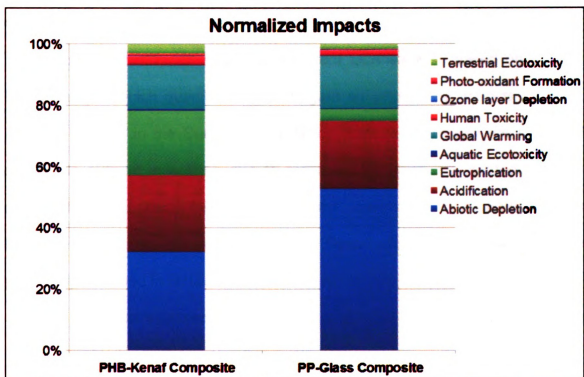
Figure 4.37 Normalized impacts: percentage contribution

4.5 Life Cycle Interpretation

For a better understanding of life cycle inventory (LCI) and impact assessment results, ISO 14043[21] standard recommends interpretation of these results using sensitivity analysis, contribution analysis, etc. In the current study, results were interpreted using contribution and sensitivity analysis. For LCI results, contribution from individual steps was presented along with total results and for impact assessment results contribution from individual steps as well as processes with major contribution were highlighted. Additionally, sensitivity of the results because of alternative allocation method for soybean farming and TRACI-Eutrophication method was determined, along with contribution analysis of energy consumption for both systems.

4.5.1 Sensitivity Analysis – Effect of nitrogen allocation to Soybean cultivation

Soybean cultivation data in the current LCA study is based on a 2005 NREL study[40], which quantifies cradle-to-gate emissions and impacts for corn, soybean farming in the State of Iowa. Since, corn and soybean are rotational crops, the nutrient emissions due to fertilizer application are related for both crops. The NREL study follows two different approaches to allocate nitrogen flows between corn and soybean crops. These allocation approaches were previously reviewed in Section 4.3.5.1 and are summarized below:

- C-S allocation: approximately equal nitrogen application and leaching rates for corn and soybean crops
- C-allocation: all nitrogen applied to corn crops is allocated to corn

For the current LCA study, C-S allocation approach was used to obtain LCI (life cycle inventory) of PHB-Kenaf composites. As discussed before in Section 4.4.2.10, NREL study indicates that actual nitrogen flows for corn and soybeans should lie between these two allocation approaches. Therefore, the effects of C-allocation on LCI and impacts for PHB-Kenaf composites were analyzed and compared with the base scenario (C-S allocation) and PP-Glass composites LCI. C-allocation approach, significantly reduces the amount of FN (fertilizer nitrogen) allocated to soybean crops and related nutrient outflows of NO_x, N_2O, TN-SW (total nitrogen to surface water bodies). The modified flows used for inventory analysis are mentioned below in Table 4.31, all other flows were same as those specified in Table 4.17 and 4.18 in Section 4.3.5.1.

Table 4.31 Modified-Soybean agriculture average data (1988-2000)[xiii], allocation of leaching based on application of N fertilizer (C allocation)

Soybean agriculture, C-S rotation, conventional till, no corn stover collection		
Inputs	**Units**	**Average (1988-2000)**
FN (fertilizer nitrogen)	mt-N	4,216
Outputs	**Units**	**Average (1988-2000)**
(a) NO_x as NO_2	mt-N	1,154
(a) N_2O as N	mt-N	607
(w) TN – SW	mt-N	1,782

Lower allocation of FN flows had most significant effect on the Eutrophication impacts, because of the major contribution (89%) of the nutrient

---

[xiii] mt = Metric Tons, prefix (a) signifies air emissions and (w): water emissions

flows from soybean cultivation to the total eutrophication impact. And, eutrophication impacts for PHB-Kenaf composites LCI using C-allocation approach were 47% lower compared to LCI results using C-S allocation approach. Overall, using C-allocation approach, PHB-Kenaf composites had lower impacts for all categories, with small but significant reductions for following impacts: Abiotic depletion (3%), Global Warming (4%), Acidification (2%), Human Toxicity (4%), Photo-oxidant formation (6%). For these impacts, except acidification, lower impacts were due to avoided impacts from lower nitrogen fertilizer consumption (FN) for C-allocation approach. While, in the case of acidification, both lower NO_x emissions and FN consumption from soybean cultivation caused a reduction in total impacts.

Regarding comparison of the normalized impacts, using C-S allocation approach, PHB-Kenaf composites had slightly higher impacts (3%) compared to PP-Glass composites, as shown before in Figure 4.36. However, because of the major reduction in eutrophication impacts using C-allocation approach, cumulative normalized impacts for PHB-Kenaf composites were 9% lower compared to PP-Glass composites. A comparison of the cumulative normalized impacts for PHB-Kenaf composites using both allocation approaches and PP-Glass composites is presented below in Figure 4.38.
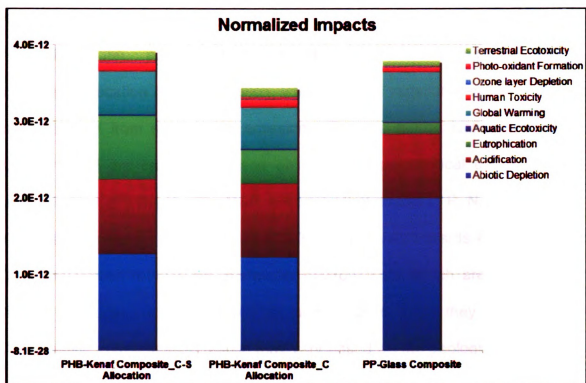
Figure 4.38 Effect of variable nutrient allocation (for soybean cultivation) on cumulative normalized impacts

As evident from the comparison above, based on the allocation method selected, cumulative normalized impacts for PHB-Kenaf composites, range between +3% to -9% of the cumulative impacts for PP-Glass composites. Additionally, the normalization of impacts clearly show that both systems have same impact categories (Abiotic resource depletion, Acidification, Eutrophication, and Global warming) making significant contribution to the cumulative normalized impacts.

Analysis of the energy consumption for both systems and effect of TRACI-eutrophication potentials on overall results is presented in the following sections.

4.5.2 Sensitivity Analysis – Effect of using TRACI Eutrophication impact factors

The CML eutrophication method computes the impacts without considering location related variation, where such a variation can influence the actual impact from site-specific emissions. For e.g. eutrophication impacts in CML method are calculated based on the average chemical composition of aquatic species[59]: $C_{106}H_{263}O_{110}N_{16}P$, assuming that a mole of P, N, and COD (as O_2) has contribution of 1, 1/16, and 1/138 respectively towards eutrophication. This assumption is valid for freshwater environments, which are generally P-limited, but does not hold for marine environments, since they are N-limited. Additionally, eutrophication results may vary based on the geological profile and amount of precipitation for a particular location. Therefore, to account for regional variability and understand its effect on overall results, eutrophication impacts using TRACI method were calculated, in addition to CML method.

Eutrophication potentials using TRACI are computed by multiplying the CML eutrophication potentials with U.S. state-level transport factors to obtain regional eutrophication factors, and based on these factors U.S. weighted average values are obtained. These values were previously compared with CML eutrophication potentials in Section 4.4.1.6, Table 4.26 and present a significantly lower potentials related to air emissions, while eutrophication potentials for water emissions are essentially the same. Therefore, TRACI-eutrophication impacts for PHB-Kenaf composites using C-S allocation and C-allocation were lower by 38% and 68% respectively. In case of PP-Glass composites, almost all of the impacts were due to NO_x air-emissions and therefore TRACI eutrophication impacts had

even higher percentage-reduction of 85% compared to CML eutrophication impacts.

Use of TRACI eutrophication factors had an interesting effect on cumulative normalized impacts. Since, eutrophication impacts had a higher contribution towards cumulative normalized impacts for PHB-Kenaf composites (Figure 4.38), reduction in eutrophication impacts using TRACI factors lead to greater reduction in cumulative impacts for PHB-Kenaf composites compared to PP-Glass composites, which is evident from the comparison of normalized impacts shown below in Figure 4.39. As a result, cumulative normalized impacts for PHB-Kenaf composites using C-S allocation and C-allocation were lower by 2% and 14% respectively, in comparison to PP-Glass composites.
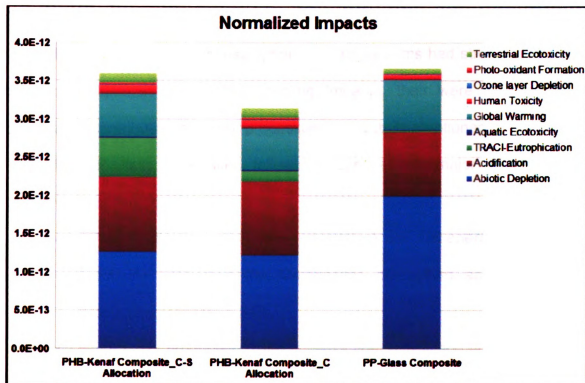
Figure 4.39 Effect of using TRACI impacts on cumulative normalized impacts

4.5.3 Analysis of Energy Consumption

Contribution analysis for both systems made it possible to highlight processes contributing towards the majority of energy consumption and this information can be useful for manufacturers by helping them focus on particular processes for energy reduction and environmental improvement initiatives. A stepwise comparison of energy consumption for PP-Glass and PHB-Kenaf composites (both C-S and C allocation approaches) is provided below in Figure 4.40. Total energy consumption for PHB-Kenaf composites was 22% (for C-S allocation) and 25% (for C allocation) lower compared to PP-Glass composites, primarily because of high energy consumption for PP production process, used both as feedstock and fuel energy and very low energy consumption for Kenaf fiber production compared to energy consumed for Glass fiber production.

Even though energy consumption for both systems had strong correlation to abiotic depletion and global warming impacts, their were differences in percentage contribution by major processes, with details mentioned below.

For PP-Glass composites, following processes had major contribution to total energy consumption:

- PP production process (used as feedstock and fuel energy) = 68%

- Electricity production (for Composites processing and Glass fiber production process) = 24%

- Natural gas production (used in Glass fiber production process) = 8%

In case of C-S allocation for PHB-Kenaf composites, major contribution to energy consumption was due to following processes:

- Electricity production (mainly due to electricity consumed during PHB production process and Composites processing, with minor contributions from soybean crushing and cultivation) = 58%

- Steam production (used mainly in PHB production process, with small contribution from consumption in soybean crushing process) = 16%

- PHB production process (energy consumed for processes such as cooling water supply and production of raw materials used in PHB production) = 13%

- Miscellaneous steps related to soybean crushing and cultivation = 8%

- Ammonia production (used as fertilizer in soybean cultivation and nutrient in PHB fermentation) = 5%
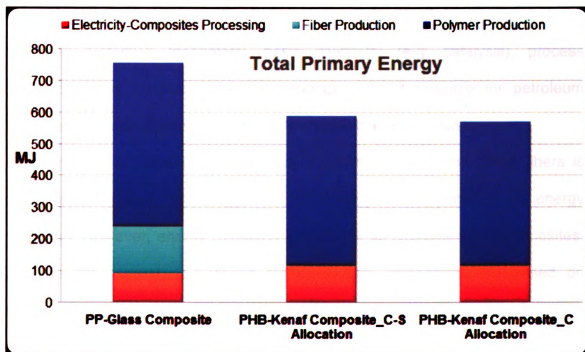
Figure 4.40 Total Energy Consumption for PP-Glass and PHB-Kenaf composites

Total energy consumption using C-allocation for PHB-Kenaf composites was lower compared to C-S allocation because of lower allocation of FN (fertilizer nitrogen) to soybean cultivation, thereby reducing the energy used for ammonia production.

Summarizing these results, major energy reductions for the life cycle of PHB-Kenaf composites are possible by increasing the efficiency of PHB production process, thus reducing the consumption of electricity, steam, and other raw materials as mentioned above. Since the technology for PHB production is still in nascent stage[14], increased commercial production will definitely improve its efficiency. Similar improvements have happened for current mature technologies, for e.g. petroleum and petrochemical industry started in early 20th century, when coal based industry was dominant; however, advances in crude extraction technology, basic chemistry (e.g. catalysis), process technology (e.g. fluidized catalytic cracking) made it possible for petroleum industry to provide building blocks for the current chemical industry.

In case of PP-Glass composites, production of PP and Glass fibers is based on a mature technology, thus presenting little opportunity for energy reduction. However, energy reduction is possible for processing of composites, because the current calculations for processing composites are based on production of composites in a laboratory environment (Section 4.3.6) and industrial production of composites will reduce the energy consumed for processing composites.

References:

[1] Sitarz, D., Sustainable America: America's Environment, Economy and Society in the 21st Century

[2] Netravali, A.N., Chabba, S. Composites get greener. Materials Today, April 2003.

[3] Mohanty, A. K., Misra, M., Hinrichsen, G., Biofibres, biodegradable polymers and biocomposites: An overview. Macromolecular Materials Engineering 276/277, 2000.

[4] www.apme.org, Plastics & Environment: Life cycle & Eco-profiles.

[5] ISO 14040: Environmental management – Life cycle assessment – Principles and framework. First edition, 1997.

[6] Internal communication – Composite Materials and Structures Center.

[7] ISO 14041: Environmental management – Life cycle assessment – Goal and scope definition and inventory analysis. First edition, 1998.

[8] Eco-profiles of the European Plastics Industry – Polypropylene (PP). A report by I. Boustead for PlasticsEurope, March 2005.

[9] http://www.eere.energy.gov/industry/glass/analysis.html, Energy and Environmental Profile of the U.S. Glass Industry. April 2002.

[10] http://www.metabolix.com/, Metabolix Brochure, accessed May 2006.

[11] http://www.biomer.de/, Production of PHB, accessed May 2006.

[12] Akiyama, M. et al., Environmental life cycle comparison of polyhydroxyalkanoates produced from renewable carbon resources by bacterial fermentation. Polymer Degradation and Stability, 80 (2003), 183-194.

[13] Kim S, Dale BE (2002): Allocation Procedure in Ethanol Production System from Corn Grain: I. System Expansion. Int J LCA 7 (4) 237–243.

[14] Kim S, Dale BE (2005): Life Cycle Assessment Study of Biopolymers (Polyhydroxyalkanoates) Derived from No-Tilled Corn. Int J LCA 10 (3) 200–210.

[15] ISO 14042: Environmental management – Life cycle assessment – Life cycle impact assessment. First edition, 2000.

[16] Bare, J.C., Gloria, T.P. Critical Analysis of the Mathematical Relationships and Comprehensiveness of Life Cycle Impact Assessment Approaches. Environmental Science & Technology / Vol. 40, No. 4, 2006.

[17] Bare, J. C., G. Norris, D. W. Pennington, and T. McKane. 2002. TRACI: The tool for the reduction and assessment of chemical and other environmental impacts. Journal of Industrial Ecology 6(3–4): 49–78.

[18] BEES® 3.0, Building for Environmental and Economic Sustainability, Technical Manual and User Guide. Barbara C. Lippiatt, Office of Applied Economics, NIST. October 2002.

[19] Guine´e, J. B. (Ed.) Handbook on Life Cycle Assessment. Operational Guide to the ISO Standards; Springer: New York, 2002.

[20] Jolliet O et al. (2004). The LCIA Midpoint-damage Framework of the UNEP/SETAC Life Cycle Initiative. Int J LCA 9 (6) 394 – 404 (2004)

[21] ISO 14043: Environmental management – Life cycle assessment – Life cycle interpretation. First edition, 2000.

[22] Personal communication, May 2006: Jane Bare, U.S. EPA - Office of Research and Development.

[23] H.L. Brown, B.B. Hamel, B.A. Hedman, Energy Analysis of 108 Industrial Processes, Fairmont Press, Liburn, GA 1996.

[24] Profile of the Stone, Clay, Glass and Concrete Products Industry, U.S. Environmental Protection Agency (EPA), Office of Compliance Sector Notebook Project, September 1995.

[25] Glass Industry Scoping Study, Electric Power Research Institute, EPRI EM 5912S, 1988.

[26] Eco-profiles of the European plastics industry. Report 10: POLYMER CONVERSION. I. Boustead, May 1997

[27] Budget for producing kenaf for year 1999, obtained from Mr. Eugene P. Columbus, Mississippi State University.

[28] Webber, Charles L. 1993. Yield components of five kenaf cultivars. Agronomy Journal, 85: 533-535.

[29] Baldwin, B., Kurtz, M., Hovermale, C., Neill, S.W., 1996, Kenaf: A guide for production in Mississippi. MAFES.

[30] Stover, J.R., Method for separating Kenaf into core and fiber. United States Patent Number: 5,970,582. October 1999.

[31] McKee, H.S., Growing and processing natural renewable BAST fibers for natural fiber composites. 2nd Annual Automotive Composites Conference, Society of Plastics Engineers, September 2002.

[32] Hansson, P-A. and Mattsson, B. Influence of derived operation specific tractor emission data on results from an LCI on wheat production. Int. J. of LCA 4, 202-206 (1999).

[33] http://www.epa.gov/ttn/chief/ap42/ch09/, section 9.2.2 Pesticide Application, Final Section-January 1995.

[34] http://www.dowagro.com/usag/prod/054.htm, safety data sheet for Trifluralin herbicide.

[35] Sheehan, J. et al., Life Cycle Inventory of Biodiesel and Petroleum Diesel for Use in an Urban Bus. NREL/SR-580-24089; May 1998.

[36] Personal communication with Mr. Brent Brasher, Kengro Corporation.

[37] Tillman U. Gerngross, Can biotechnology move us toward a sustainable society? Nature Biotechnology, Vol 17, June 1999.

[38] Tillman U. Gerngross and Steven C. Slater, How green are green plastics? Scientific American, August 2000.

[39] Kurdikar et al., Greenhouse gas profile of a biopolymer, Journal of Industrial Ecology, 4 (2000), 107-122.

[40] Powers, Susan E. Quantifying Cradle-to-Farm Gate Life Cycle Impacts Associated with Fertilizer used for Corn, Soybean, and Stover Production. NREL/TP-510-37500; May 2005.

[41] Sheehan, J. Aden, A., Riley, C., Paustien, K., Killian, K., Brenner, J., Lightle, D., Nelson, R., Walsh, M., Cushman, J., Is ethanol from corn stover sustainable? Adventures in cyber-farming. Draft Report prepared for the DOE National Renewable Energy Laboratory, 2002.

[42] Van Zeijts, H., Leneman, H., Wegener-Sleeswijk, A. Fitting fertilization in LCA: Allocation to crops and cropping plan. J Cleaner Production, 7: 69-74, 1999.

[43] Weed, D.A.J., Kanwar, R.S., Water quality - Nitrate and water present in and flowing from root-zone soil. J Environmental Quality, 25(4): 709-719, 1996.

[44] Bjorneberg, D.L., Kanwar, R.S., Melvin, S.W., Seasonal changes in flow and nitrate-N loss from subsurface drains. T ASAE, 39(3): 961-967, 1996.

[45] Bakhsh, A., Kanwar, R.S., Bailey, T.B., et al., Cropping system effects on NO3-N loss with subsurface drainage water. T ASAE, 45 (6): 1789-1797, 2002.

[46] Wang, M.Q., GREET 1.5 – Transportation Fuel-Cycle Model, Volume 2: Appendices of data and results. Argonne National Laboratory, Argonne, IL, ANL/ESD-39, 1999.

[47] Adams, C. H.; Luttges, W.E.; Mullen, M.; Rand, M.C.; Peters, J.F.; Schroer, B.J.; Ziemke, M.C. Study on Production, Marketing, and Utilization of Degummed Soybean Oil as a Diesel Fuel Extender. UAH Report No. 297. University of Alabama in Huntsville, 1981.

[48] Huijbregts, M. A. J. 1999. Priority assessment of toxic substances in the frame of LCA: Development and application of the multi-media fate, exposure, and effect model USES-LCA. IVAM environmental research, University of Amsterdam.

[49] Guinee, J. B. and R. Heijungs. 1995. A proposal for the definition of resource equivalency factors for use in product Life-Cycle Assessment. Environ. Toxicol. Chem. 14 (5): 917-925.

[50] Wuebbles, D.J., 1988. Relative effects on stratospheric ozone of halogenated methanes and ethanes of social and industrial interest. UNEP, Nairobi.

[51] WMO (World Meteorological Organisation), 1992 & 1999. Scientific assessment of ozone depletion: 1991 & 1998. Global Ozone Research and Monitoring Project – Report no. 25 & 44. Geneva.

[52] IPCC (Intergovernmental Panel on Climate Change). 1996. Climate change 1995: The science of climate change. Edited by Intergovernmental Panel on Climate Change: J. T. Houghton, L. G. Meira Filho, B. A. Callander, N. Harris, A. Kattenberg, and K. Maskell. Cambridge, UK: Cambridge University Press.

[53] Heijungs, R., J. Guinee, G. Huppes, R. Lankreijer, H. Udo de Haes, A. Wegener Sleeswijk, A. Ansems, P. Eggels, R. van Duin, and H. de Goede. 1992. Environmental life cycle assessment of products. Vol. 1, Guide and Vol. 2, Backgrounds. Leiden, The Netherlands: Centre of Environmental Science, Leiden University.

[54] Norris, G. 2002. Impact characterization in the tool for the reduction and assessment of chemical and other environmental impacts: Methods for acidification, eutrophication, and ozone formation. Journal of Industrial Ecology 6(3-4): 79–101.

[55] Derwent, R.G., M.E. Jenkin, S.M. Saunders & M.J. Pilling, 1998. Photochemical ozone creation potentials for organic compounds in Northwest Europe calculated with a master chemical mechanism. Atmospheric Environment, 32. p 2429-2441.

[56] Jenkin, M.E. & G.D. Hayman, 1999: Photochemical ozone creation potentials for oxygenated volatile organic compounds: sensitivity to variations in kinetic and mechanistic parameters. Atmospheric Environment 33: 1275-1293.

[57] Derwent, R.G., M.E. Jenkin & S.M. Saunders, 1996. Photochemical ozone creation potentials for a large number of reactive hydrocarbons under European conditions. Atmospheric Environment 30: 181-199.

[58] Huijbregts M.A.J., Breedveld L., Huppes G., De Koning A., Van Oers L. & Suh S. (2003). Normalisation figures for environmental life cycle assessment The Netherlands (1997/1998), Western Europe (1995) and the world (1990 and 1995), Journal of Cleaner Production, 11, 737-748. Updated Normalisation factors downloaded from CML website: http://www.leidenuniv.nl/interfac/cml/ssp/domains/lca.html.

[59] Stumm, W.; Morgan, J. J. Aquatic chemistry : an introduction emphasizing chemical equilibria in natural waters; Wiley: New York, 1981.

205

Chapter 5: Biodegradation study of Biobased Composites

5.1 Introduction

It is important to determine the rate of biodegradation of biocomposites and the effects of disposal end products to the environment. These results can be very useful in estimating the time to achieve significant levels of biodegradation and environmental impacts of the end products from composting; both of the results are valuable in Industry[1], where they are developing biobased products and will be required to provide these numbers to meet industry standards as well as federal regulations.

Based on the properties of the material developed there are various end-of-life disposal options available, such as: composting, incineration, sanitary landfills, and recycling. Recycling is a feasible option, if the recyclable products can be easily collected and sent to the recycling facility, where they are converted to same or new products. For biodegradable materials, disposal option leveraging upon the property of these materials to degrade makes sense. Composting and sanitary landfills are established biodegradation options. If the material developed is non-biodegradable and cannot be recycled, then disposal by incineration is a viable option, in which energy can be recovered by controlled combustion of the material.

Sanitary landfills are considered a poor disposal option because of the way they are designed there is little moisture and microbial activity present, thus preventing effective biodegradation. Incineration leads to complete disposal, however incineration facilities are energy intensive and leave toxic residuals.

Composting is an aerobic decomposition of organic matter by a mixed population of microorganisms under controlled conditions[2]. Compost material behaves as a porous material with moisture content of 50 to 60 percent and through which air can be circulated to supply O_2 and to remove evaporated H_2O. Composting is an environment friendly approach to convert biodegradable waste including biodegradable plastics into useful soil enhancement products[3] as discussed in more detail in section 2.c.

It is clear that composting has significant advantages over other disposal modes for biodegradable products. Therefore, it was selected as the way to determine the rates of biodegradation and environmental impacts of disposal end products.

ASTM and ISO standards relevant to demonstrating compostability of plastic materials have been discussed in section 2.c.II. ASTM D 6400 and D 6002 do not have equivalent ISO standards, and since ASTM standards provide greater detail about experimental set-up and related calculations, they formed the basis of this experimental study. ASTM D 5338 provides lot of details about setting up a controlled composting apparatus, and is reviewed in the following section on experimental set-up and procedure.

5.2 Experimental set-up and Procedure

ASTM standard D 5338 defines the percentage of biodegradability as obtained by determining the percentage of carbon in the test material that is converted to CO_2 during the duration of the test. The percentage biodegradation does not include the amount of carbon converted from the test substance to cell biomass, which in turn is not converted to CO_2 during the test. In the past there have been studies done, where the complete carbon balance for the composting vessel was accounted for by using an inert solid medium with all necessary nutrients for microbial growth and inoculated with aqueous compost eluate[4],[5],[6]. However, such a study is very time consuming and is beyond the scope of D 5338, which is intended to provide rapid and reproducible determination of biodegradability of the test substance.

The standard described above recommends two options for experimental set-up in order to capture CO_2 from controlled composting experiment. In the first option CO_2 can be captured using a carbon-dioxide scrubbing solution such as $Ba(OH)_2$ and regular determination of CO_2 is made by titrating the scrubbing solution with HCl.

The schematic in figure 5.1 describes the set-up required for testing only one sample by this option. The standard requires users to test samples in triplicates in a composting vessel volume of 2 to 5 Liters. Other requirements are:

I. Controlled temperature conditions of $58°C$ ($±2°C$), which can be maintained by using a water bath or other temperature controlling apparatus such as convection or radiation heaters.

II. A pressurized air system, which provides CO_2 free, water saturated air to each composting vessel at accurate flow rates. If direct determination of exhaust air is being done (further explained in second option) then normal air may be used.

III. Suitable device such as sensors, gas chromatograph to measure the O_2 and CO_2 concentrations in the exhaust air of composting vessels.

IV. Recommended carbon dioxide trapping apparatus for individual composting vessel should be combination of three 5 Liter bottles fitted with gas sparging and containing $Ba(OH)_2$ carbon-dioxide scrubbing solution. End of experiment titration with 0.05 N HCl provides the amount of CO_2 produced by the test substance.

Based on these requirements, conducting the controlled composting study by this option requires a large amount of laboratory space and a controlled temperature environment large enough to hold a minimum of 12 composting vessels required for testing the biodegradability of one sample.

The second option for conducting the experiment is by flow measurement of exhaust gas from composting vessels and using a gas detection apparatus such as a gas chromatograph or CO_2/O_2 sensors to measure the CO_2 and O_2 concentrations for each vessel. An example of such a set-up is provided in figure 5.2 (reproduced from ASTM D 5338 standard).

B = Blank

P = Positive Control

N = Negative Control

 = Test Specimen

 = Scrubbing solution $Ba(OH)_2$
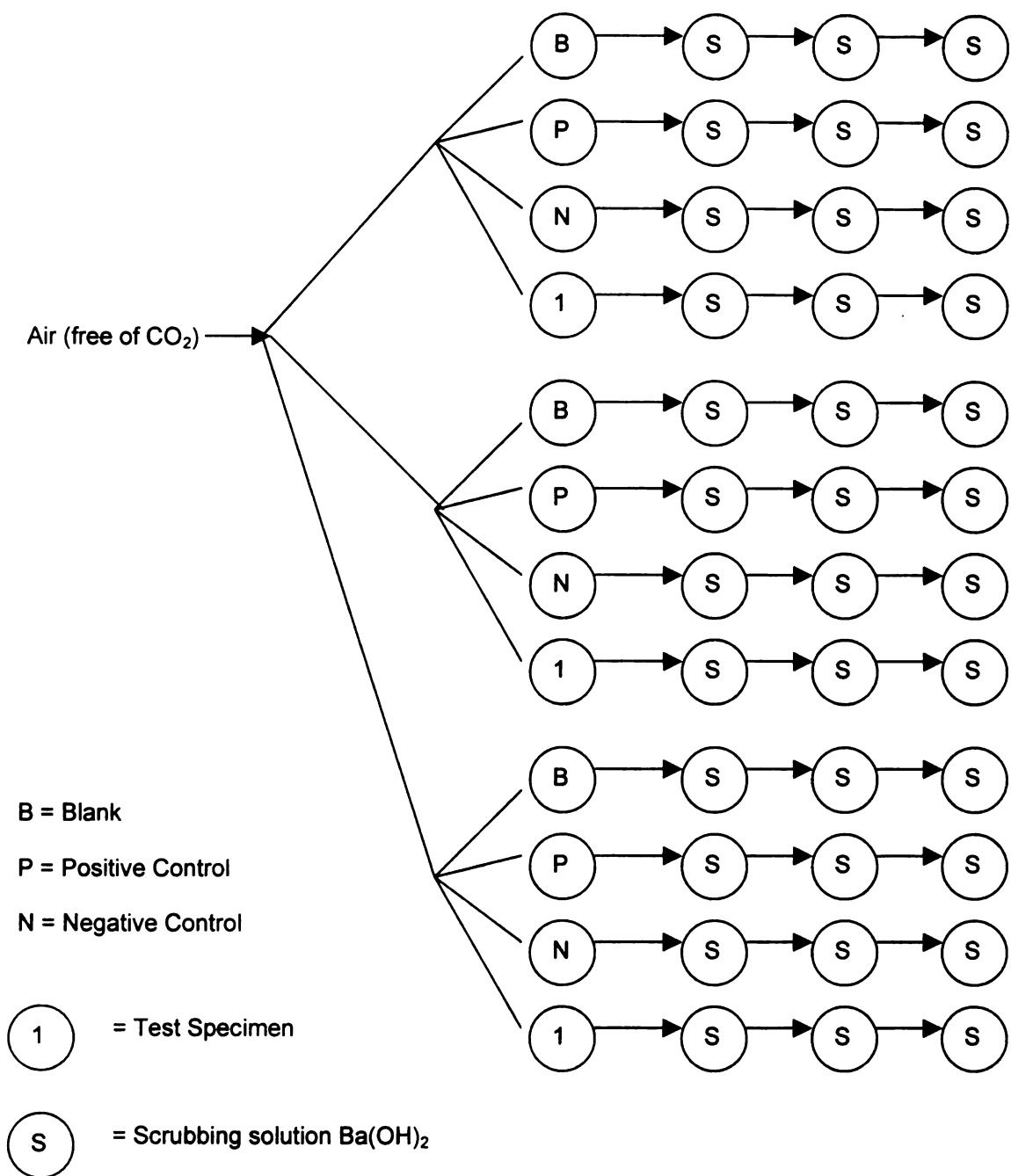
Figure 5.1 Experimental set-up using Carbon-dioxide trapping apparatus

CONTROLLED-COMPOSTING BIODEGRADABILITY
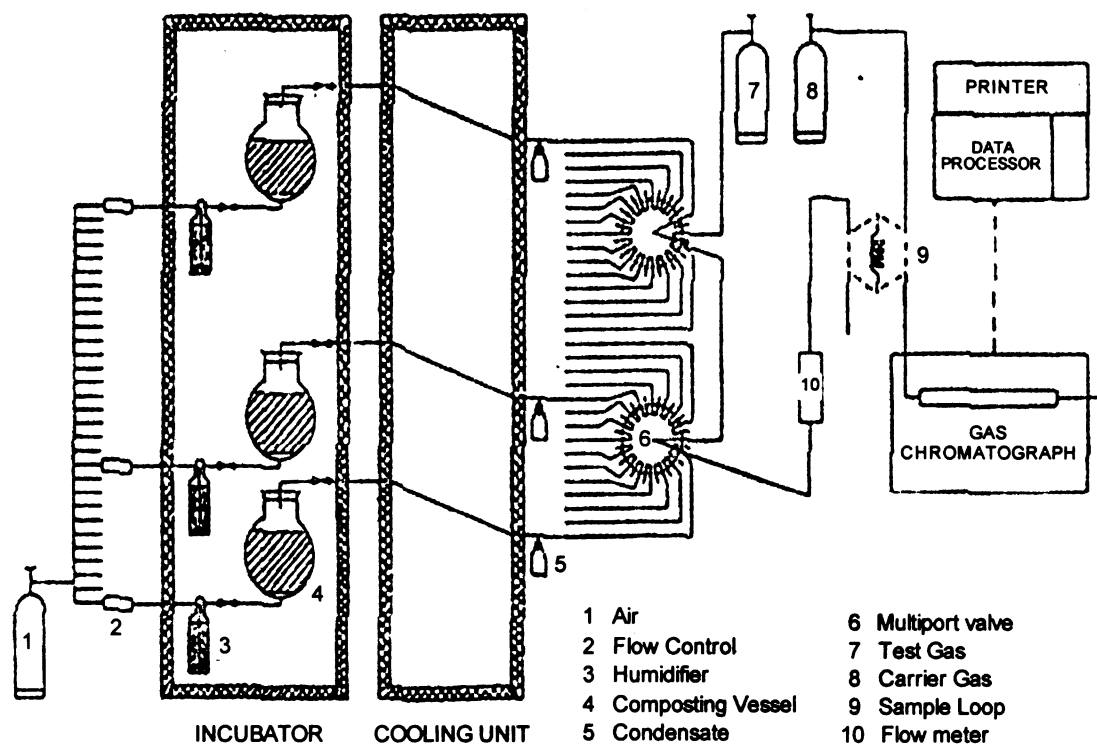
Figure 5.2 Experimental set-up using Gas Chromatograph (reproduced from ASTM D 5338 - 98)

In order to determine the rate of biodegradation by this second option, ASTM D 5338 recommends analyzing the CO_2 concentration on a frequent basis during the test period (frequency of 3 to 6 hours is provided as an example in this standard). Frequent CO_2 analysis ensures the reliability of the cumulative CO_2 production numbers obtained over the course of the test.

Experimental set-up for the current study was constructed similar to second option and is described in figure 5.3 (details in figure 5.3.1 through 6). Figure 5.3.1 describes the set-up used to obtain clean air at a reduced pressure. Laboratory air was available; however because of the high pressure in the range of 100-120 psi and excess moisture and oil

Pressure regulator   Air Filter   Desiccant-Air dryer

Figure 5.3.1 Pressure Regulator and Air treatment

Flow direction

Flow meter/ controllers

Thermometer

Temperature controller
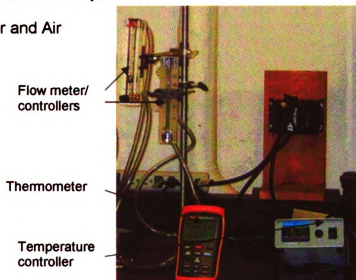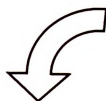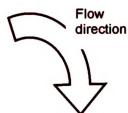
Figure 5.3.2 Flow controller and Temperature controller

Air Process Heater

Humidifying Flask

Needle valves

Flow distribution Manifold
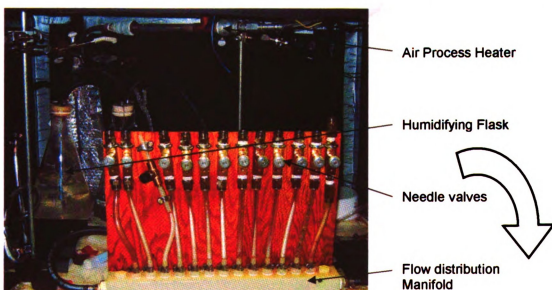
Figure 5.3.3 Heater set-up and Flow distribution
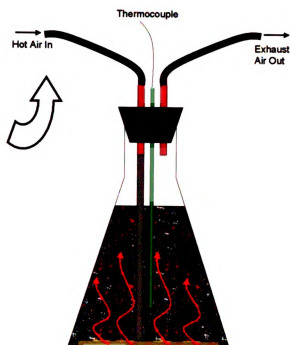
Figure 5.3.4 Composting vessel
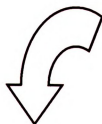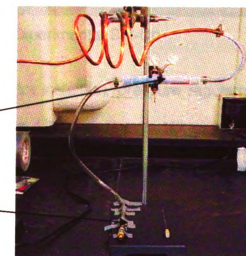
Figure 5.3.5 Exhaust air collection set-up
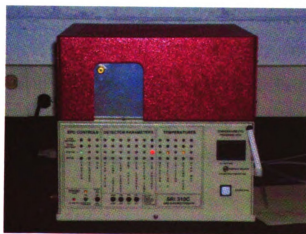
Figure 5.3.6 Gas Chromatograph with TCD detector

Figure 5.3 Overview of the Composting Study - Experimental Set-Up

present (because a refrigerated air dryer was not installed), pressure regulator (Precision aluminum stacked filter/regulator 0 to 10 psi pressure, ¼'' pipe, 22 SCFM Max, ControlAir Inc., NH U.S.A) coupled with air filter (Speedaire® Air Line Filter, ½ inches, Dayton Electric Mfg. Co., IL U.S.A) and desiccator (Excelon 74 Desiccant Compressed Air Dryer, ¼'' pipe, 20 SCFM Max, 100 psi, Norgren, CO U.S.A) were used to obtain clean-dry air at a reduced pressure ranging from 2-6 psi.

Air obtained from the set-up described in Figure 5.3.1 was bifurcated using a barbed T-connection and distributed through two flowmeters (Model VFB-55-BV, Range 20 – 200 SCFH Air (ft³/hr), Dwyer Instruments, Inc., IN U.S.A) to Glove box A and B as shown in Figure 5.3. Air-flow to the glove boxes was recorded in the range of 50 – 60 SCFH and acted as an indicator to identify any flow obstruction and also to ensure that minimum flow requirement for the Air

process heaters was met. The temperature inside the glove box was controlled using a dedicated benchtop temperature controller (Monogram Benchtop Controller, Model CSC32T using T type thermocouple, Omega Engineering, Inc., CT U.S.A). Assuming a cuboid-shape for the glove box, a thermocouple was suspended to get a reading from the approximate center of the glove box and connected to the benchtop temperature controller so that temperature inside the glove box was controlled based on the average temperature of the glove box. Set-up for flow and temperature control is illustrated in figure 5.3.2.

Clean dry air was required for the experiment, so as to avoid any contamination due to excess oil and water in the compressed air, and to meet the requirements for operating air process heater used for this study. Air Process heater (Model AHP 7561, In-Line Air and Gas Heater, 750 Watts, Omega Engineering, Inc., CT U.S.A) used for the study requires clean, dry incoming air, in order to avoid heater filament burn out. Wattage requirement for the glove box was calculated based on the specific heat of compost and test materials and estimated as 815 Watts for heating 15 composting vessels in a glove box to $58^{\circ}C$ in one hour, detailed calculation is provided in Appendix 5.2.1.

As specified in Appendix 5.2.1, exit air temperature from the air process heater can reach up to 250°C. Copper tubing with ¼" OD and 0.030" wall thickness was used to transfer air from heater to a modified 2 L Erlenmeyer flask, acting as a humidifying vessel for the experiment. The Erlenmeyer flask was modified with ¼" glass-to-metal union made at 700 mL gradation of the flask, as shown in figure 5.4. The flask was modified in order to avoid the gradual

degradation of the rubber stopper from exposure to the high temperatures (in excess of 150°C) of the copper tubing transferring heated air from the air process heater.
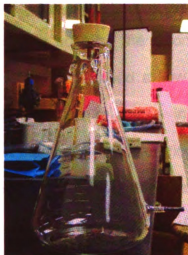
Figure 5.4 Modified 2 Liter Erlenmeyer flask

To ensure uniform temperature distribution and eliminate any cold-spots in the glove box, two circulating fans (3'' AC Fan, Radioshack) were mounted in the glovebox.

Since, ASTM standard D 5338 requires the incoming air to the composting vessels to be water saturated, two humidifying flasks were used in succession. A total of 13 composting vessels were tested in one glove box. Heated and water saturated air from the second humidifying flask was bifurcated and transferred to a 15 outlet, Nylon Manifold Block (3/4'' NPT Inlet x 3/8'' NPT Outlet, McMaster-Carr, OH, USA) using high temperature rubber tubing. Two outlets at the

extremes of the manifold were closed using plugs, since the experiment required only 13 outlet connections.

A manifold was used to create an ideal flow condition with equal flow rates to individual composting vessels. Previous controlled composting studies provided a good starting point to optimize the incoming flow rate to individual composting vessels. Gattin et al.[5] have used a flow rate of 500 mL/min in the study to calculate the mineralization of starch in compost media. While, Jayasekara et al.[7] in their study to evaluate biodegradability for cellulose, newspaper and starch-based polymers used a flow rate of 166 mL/min for each 3 Liter composting vessel. In the current study, based on the preliminary experiments with compost and positive control (compost + cellulose), flow rates in the range of 100 mL/min, lead to CO_2 detection in the range of 0-6% using a gas chromatograph with a TCD detector. However, direct flow of air from the manifold outlets was too high to obtain low flows of ~100 mL/min; therefore needle valves (F200B flow control, 11 LPM Max Flow, Parker Hannifin Corporation, OH, USA) were used to reduce the flow rate of air into composting vessels. A nylon manifold block along with needle valves was mounted on a wooden board, with push-connect fittings used on both ends of needle valves to connect to manifold as well as composting vessels. Heater set-up and flow distribution have been described in figure 5.3.3.

Sufficient care was taken to properly imbed the incoming air tubing into composting mix, in order to create an aerobic environment for composting and have uniform heat transfer. Regular temperature readings of the composting

vessels were taken using the imbedded T-type thermocouple in composting vessels; so as to ensure that temperature of around 58°C were maintained in the composting vessels as per ASTM D 5338 standard. An example of the composting vessel is shown in figure 5.3.4.

Moisture removal and cooling to room temperature of the air is necessary in order to get an accurate reading using Gas Chromatograph. Exhaust air from the composting vessel was cooled to room temperature and dried, before collecting the sample for Gas Chromatograph analysis. Collection set-up used for the experiment is described in figure 5.3.5. Coiled-Copper tubing (¼" OD and 0.030" wall thickness) was used to cool the exhaust air from composting vessels, before drying it using a Drierite drying tube (Fisher Scientific, USA).

Sample collection consisted of collecting sample from 125 mL Erlenmeyer flask; however because of the possibility of contamination due to inflow of air during sample drawing, final set-up was modified to collect sample directly from flexible tubing using removable Swagelok® fitting, fitted with 5" long luer hub-22 gauge sideport needle. Sideport needle was passed through silicon-septa in order to create a gas tight environment for the gas collection apparatus. Modified set-up is shown in figure 5.5.

Gas samples were collected using 1 mL SGE GT (Gas-Tight) Syringe with Retro-fit SLLV-syringe valve (both syringe and valve purchased from Alltech Associates, Inc., IL, USA). SLLV-syringe valve is used to ensure a gas-tight environment, and to release excess pressure and equilibrate to atmospheric pressure in case of a pressurized sample. Since the composition of gas sample

measured by gas chromatograph is in relative terms of percentage of particular component (say CO_2) in the total sample, pressurized gas sample can significantly increase the percentage reading and thus produce error in the actual gas composition reading. Assuming an exhaust gas flow rate of 60 mL/min, flushing time of two minutes and sampling time of four minutes was found to be sufficient after connecting the exhaust from composting vessel to the collection apparatus.
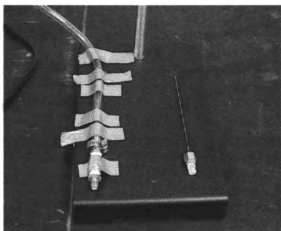
Figure 5.5 Modified exhaust gas collection set-up

Samples from the collection apparatus were manually injected (using 1 mL SGE GT syringe fitted with Luer Precision Side-Port Needle 0.028" OD x 0.016" ID x 2" Long) into an on-column injector on SRI-Gas Chromatograph (Model 310C, SRI Instruments, CA, USA) with TCD (Thermal Conductivity Detector) detector, as shown in figure 5.3.6. A packed column (packing: PORAPAK Q 80/100, 6' x 1/8" SS column, purchased from Alltech Associates, Inc., IL, USA) with ability to separate Air/O_2 from CO_2 was used to determine the CO_2 concentration of the injected sample. The gas chromatograph was connected to

a computer and data was collected using chromatography integration software, PeakSimple 2.83 (SRI Instruments, CA, USA).

For sample analysis and developing standard calibration curve, following GC conditions were used:

Career Gas: Helium, 99.995% purity, <0.5 ppm THC (Total Hydrocarbons)

Carrier Gas Pressure: 11 psi

Oven Temperature: 40°C

Standard Calibration Gases: Pure Carbon Dioxide 99.8%; Multicomponent gas mixture, 3% CO_2, 17% O_2 in N_2 (both MicroMAT 14 L, purchased from Alltech Associates, Inc., IL, USA); Scotty Gas Mix 1% CO_2, 20% O_2 in N_2 (14 L, Sigma-Aldrich, PA, USA)

A brief review of the concepts of Gas Chromatography and reasoning behind using TCD detector for the current study were presented earlier.

Based on the preliminary degradation experiments, CO_2 calibration curve for the concentration range of 20% - 0.2% CO_2 was developed. Additionally for greater precision in measuring low concentration readings, another calibration curve with a range of 3% - 0.2% CO_2 was also developed. Calibration data (table 5.1) was collected using 1 mL SGE GT syringe; the same kind of syringe was also used for sample collection and injection. Calibration curves along with linear equations and correlation coefficients are shown in figures 5.6 and 5.7.

Table 5.1 CO$_2$ calibration data

Standard Calibration Gas type	Sample size (mL)	CO$_2$ Concentration (%)	Retention time (minutes)	Area
99.8 % CO$_2$	0.20	19.96	1.083	185.82
99.8 % CO$_2$	0.14	13.97	1.116	117.56
99.8 % CO$_2$	0.10	9.98	1.116	64.99
3% CO$_2$, 17% O$_2$ *	1.00	2.95	1.166	33.55
3% CO$_2$, 17% O$_2$ *	0.50	1.48	1.166	17.29
3% CO$_2$, 17% O$_2$ *	0.30	0.89	1.183	9.87
1% CO$_2$, 20% O$_2$ **	1.00	1.02	1.183	11.57
1% CO$_2$, 20% O$_2$ **	0.50	0.51	1.183	5.62
1% CO$_2$, 20% O$_2$ **	0.20	0.20	1.183	2.09

*actual standard CO$_2$ concentration = 2.952 %
**actual standard CO$_2$ concentration = 1.02 %

221

Calibration curve for CO_2 GC Analysis
(20% - 0.2% CO_2)

$$y = 8.6522x + 0.7436$$
$$R^2 = 0.9786$$
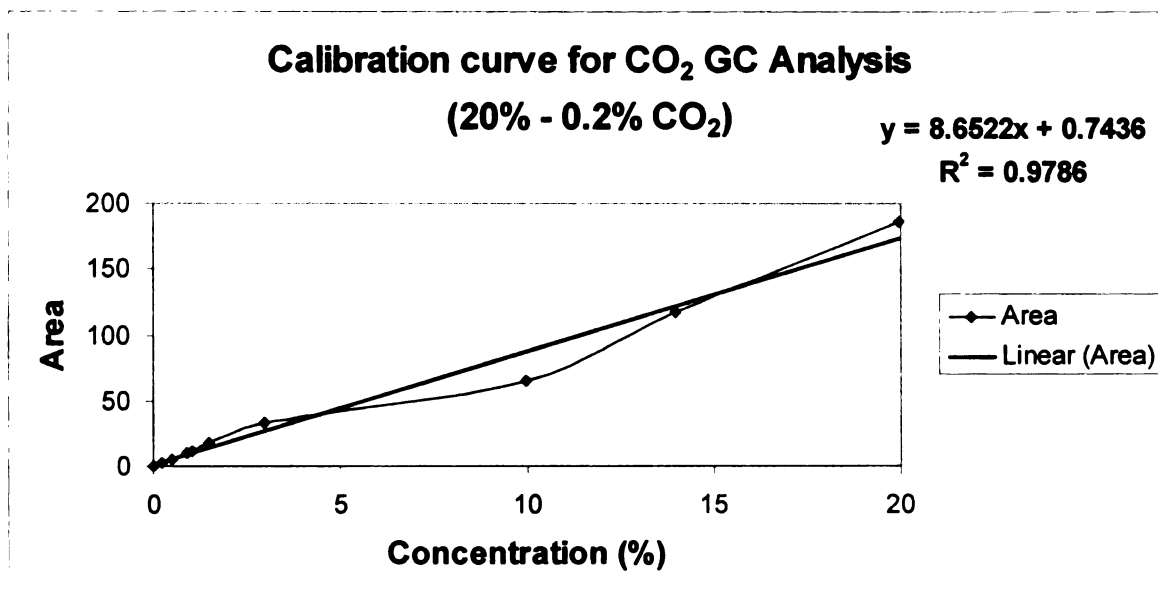
Figure 5.6 CO_2 calibration curve (20% - 0.2%)

Calibration curve for CO_2 GC Analysis
(3% - 0.2% CO_2)

$$y = 11.453x - 0.105$$
$$R^2 = 0.9996$$
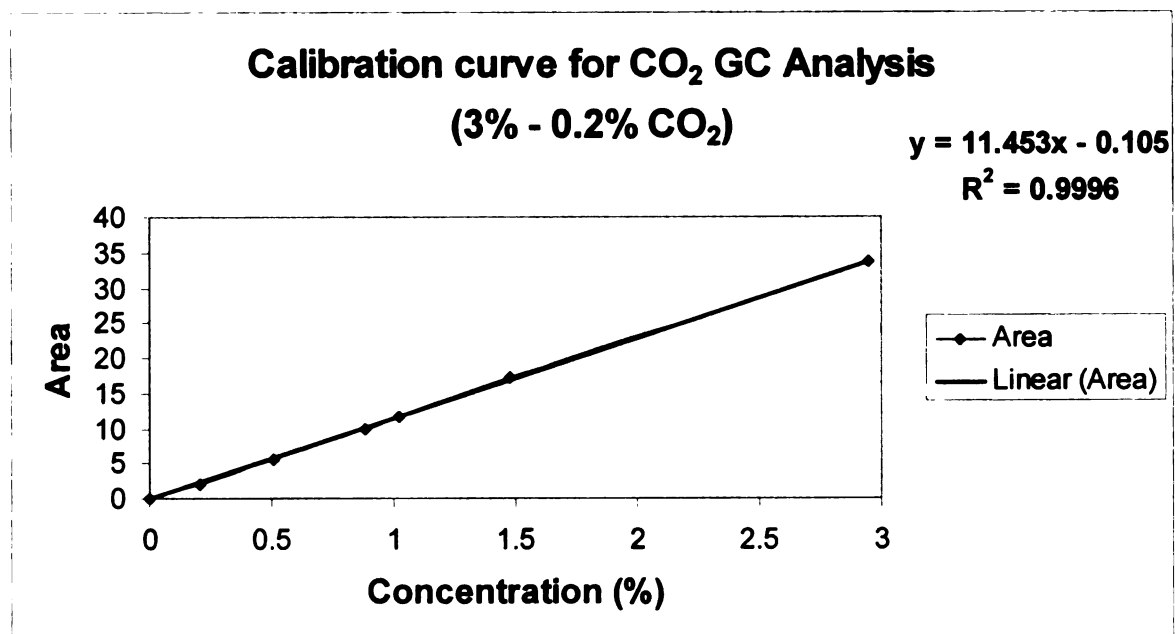
Figure 5.7 CO_2 calibration curve (3% - 0.2%)

5.4 Compost Characterization

Compost used for the biodegradation study was characterized, in order to determine its suitability for the study as required by ASTM D 5338 standard. The standard recommends that compost used should be two to four months old, obtained from municipal solid waste or plants or yard waste or a mixture of either of them. Additionally the compost should have ash content of less than 70%, pH between 7 and 8.2, and total dry solids between 50 and 55%. The compost inoculum should be free from inert substances such as glass, stones, metals, etc., and should be screened in order to remove such material from the compost received.

In this study, plant and yard waste based compost was used and had following characteristics:

Total dry solids = 60.08%

Volatile solids = 61.74%

pH = 7.9

% Nitrogen = 1.8, C/N = 16:1

Percent Nitrogen of the compost was determined at Soil and Plant Nutrient Laboratory (Dept. of Crop and Soil Sciences, Michigan State University) using TMECC 04.02-D[8] using N-Analyzer and following Dumas Method.

In addition to compost characteristics above, the maturity of the compost was determined using the *Solvita® procedure*[9] and the *Maturity Index* of the compost sample. The maturity index measurement was carried out by detecting carbon dioxide and ammonia levels in the compost, in order to assess the

maturity, which is defined in the Solvita® procedure as "resistance to further decomposition and absence of phytotoxic compounds".

For the Solvita® test, compost was screened to remove inert materials and obtain uniform size compost and the moisture content was adjusted to create ideal composting conditions. This compost was loaded into standard solvita jar (without compression) to the indicated line. Maturity index is a two-dimensional index, which depends on CO_2 and ammonia measurement. Therefore, two separate standard solvita jars were used to measure compost-CO_2 and ammonia emissions using chemically sensitive gel paddles. These paddles have different initial color (CO_2 paddle is purple, Ammonia paddle is yellow) and based on the CO_2 and ammonia emissions (over the test period of four hours in the closed jar) change color. These changes are compared to the standard scales, in order to determine the CO_2 and ammonia indices, which in turn provide an overall Compost maturity index as described in Figure 5.8. Interpretation of the compost maturity index is provided in Table 5.2.

Compost in the current study was similarly tested for 4 hours for CO_2 and ammonia emissions and at the end of the test; paddles were removed from the jar and compared to the standard color chart. These comparisons are provided in Figures 5.9 and 5.10. With carbon dioxide test result of 7 and ammonia test result of 5, compost maturity index was 7, which corresponds to well matured, aged compost with few limitations for usage, as described in Table 5.2.

COMPOST MATURITY CARBON - DIOXIDE TEST (paddle "C")
· please see instructions for use ·

COMPOST MATURITY AMMONIA TEST (paddle "A")
· please see instructions for use ·

Table 1. Compost Maturity Index Table[a]

use the Ammonium and CO_2 paddle color numbers and read across and down to where the columns meet

Solvita Ammonia Test Result is:		SOLVITA Carbon Dioxide Test Result is:							
		1	2	3	4	5	6	7	8
5	Very Low NH₃	1	2	3	4	5	6	7	8
4	Low NH₃	1	2	3	4	5	6	7	8
3	Medium NH₃	1	1	2	3	4	5	6	7
2	High NH₃	1	1	1	2	3	4	5	6
1	Very High NH₃	1	1	1	1	1	2	3	4

a. Example: If the NH₃ result is 2, and the CO_2 result is 6, then the Maturity Index is: 4

Figure 5.8 Carbon Dioxide, Ammonia standard scales and Compost Maturity Index table (reproduced from Official Solvita Guideline and www.solvita.com)

Table 5.2 Interpretation of Compost Maturity Index (adapted from Official Solvita®
Guideline)

Composting Maturity Index	Corresponding Composting Process:	
8	Inactive, highly matured compost	Finished Compost
7	Well matured, aged compost	
6	Curing; aeration requirement reduced for the compost	Curing
5	Compost moving past the active phase of decomposition and ready for curing	Active Compost
4	Compost in medium or moderately active stage of decomposition	
3	Active Compost	Very Active Compost
2	Very active; putrescible fresh compost; high respiration rate	Raw Compost
1	Fresh, raw compost	

START **END**

COMPARISON

Figure 5.9 Solvita Carbon Dioxide Test Result

START **END**
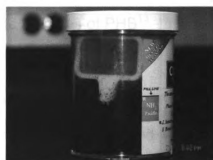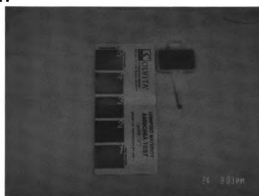
COMPARISON

Figure 5.10 Solvita Ammonia Test Result

5.5 Samples tested: processing and characterization

A list of the materials, whose biodegradability was tested, is provided below in Table 5.3.

Table 5.3 Materials tested for Biodegradability

Test Substance	Type of material	No. of samples
Compost	Aged, mature compost	3
Cellulose-positive control	Microcrystalline Cellulose[10], 13 μm particle size	3
PP – (30wt%) Glass-negative control	Injection molded composite samples of PP[11] (Polypropylene) and ¼ " Textile Glass fibers[12]	3
PHB – (30wt%) Kenaf	Injection molded composite samples of PHB[13] and ¼ " Kenaf[14] fibers	3
PHB – (5wt%)PHB-g-MA + (30wt%) Kenaf	Injection molded composite samples of PHB and ¼ " Kenaf fibers with maleated PHB added as a compatibilizer	3
PHB	Injection molded samples of PHB (Polyhydroxybutyrate) polymer	1
PLA	Injection molded samples of PLA[15] (Poly-lactic acid) polymer	1
CA – (30wt%) TEC	Injection molded samples of CA[16] (Cellulose Acetate) plasticized with TEC[17] (Triethyl Citrate)	1

Microcrystalline cellulose powder[10] with a particle size of 13 μm was selected as a positive control, since under standard composting conditions it is biodegradable and additionally it satisfies the ASTM D 5338 criteria of selecting analytical-grade cellulose with a particle size of less than 20 μm.

All the composites and polymer samples except PLA were initially extruded using twin-screw extruder ZSK 30 (Werner Pfleiderer), pelletized and then injection molded into dogbone shape, standard tensile coupons using 85 ton-Cincinnati Milacron injection molder. PLA polymer was available as pellets; therefore tensile coupons were directly obtained by injection molding.

As recommended by ASTM D 5338; dry solids, volatile solids, carbon and nitrogen content data was determined for all the samples and provided in Table 5.4 below.

Dry solids and volatile solids content of the samples were determined using APHA (American Public Health Association) standard 2540 G-Total, fixed, and volatile solids in solid and semisolid samples[18]. For calculating dry solids content, samples were dried in a convection oven at 103 to 105°C, until weight change was less than 4% or 50 mg, whichever was less. For the volatile solids test, the dried residue samples from dry solids test were heated in a Muffle Furnace (Thermolyne – Type 30400, Automatic Furnace) to 550°C, until weight change was less than 4% or 50 mg, whichever was less. Carbon and Nitrogen content of the samples was determined using Carlo Erba NA15 Series 2, CNS Analyzer (Plant, Soil, and Carbon-Nitrogen Analysis Laboratory, Dept. of Crop and Soil Sciences, Michigan State University).

For a good composting process, the C/N ratio of the mixture of compost and test substance should be between 10 and 40, as recommended by ASTM D 5338. The C:N ratio for the compost-sample mix (see Table 5.4 below) was in the recommended range between 10 and 40.

Table 5.4 Sample Characterization

Test Substance	Dry Solids content (%)	Volatile Solids content (%)	Carbon Content (%)	Nitrogen Content (%)	Compost+ Sample C:N
Cellulose-positive control	96.10	95.34	42.07	0.00	20:1
PP – (30wt%) Glass-negative control	99.94	74.47	78.26	0.00	23:1
PHB – (30wt%) Kenaf	98.83	98.35	52.67	0.00	21:1
PHB – (5wt%)PHB-g-MA + (30wt%) Kenaf	98.90	97.99	51.97	0.00	21:1
PHB	*	99.92	54.10	0.00	21:1
PLA	*	100.00	46.70	0.00	20:1
CA – (30wt%) TEC	*	97.18	46.60	0.00	20:1

---

* Not determined, but assumed to be 100% because of neat polymer being used

5.6 Controlled composting experiment: start-up, operating procedure, and results

5.6.1 Start-up

Main objective of this experiment was to simulate the actual composting conditions in a laboratory environment and study the degradation behavior of the polymers and their composites listed in Table 5.3. And, optimal composting conditions exist with moisture content/dry solids of 50% and temperature of 58°C (±2°C). As discussed before in experimental set-up, temperature was maintained around 58°C using a combination of temperature controller, air-process heater and circulation fans in the glove box. Based on the dry solids content of compost and test samples, moisture content was adjusted using distilled water to 50% by weight.

All the test materials (polymers and composites, except positive control and compost) were in the shape of standard dogbone-tensile coupons. Therefore, their size was reduced to less than 2 by 2 cm, so as to increase the available surface area for degradation and better mixing of samples with compost. Cellulose positive control was available in powder form with a particle size of 13 μm. Mixing of test material with compost and addition of moisture leads to significant reduction in the porosity of the mixture; therefore an inert mineral-material called Perlite[19] was used to increase the porosity of the mixture. Perlite was obtained from The Scotts® Company (OH, USA) and 400 mL or less (based on the density of the mixture) was well mixed with the compost-test material mixture.

After sufficient mixing has been obtained, the mixture was loaded into 2-Liter Erlenmeyer flasks. Proper precautions were taken to avoid filling up the test material upto the top of the flask, which can lead to insufficient headspace for gas collection and periodic manual mixing of the test sample. As a rule of thumb, samples were filled upto three quarters of the volume of 2-L Erlenmeyer flask.

These loaded Erlenmeyer flasks were closed with size 10, 3-hole Twistit rubber stoppers (VWR International, IL, USA), and sealed with silicone sealant to ensure gas-tight environment. One of the three holes was used to embed the incoming hot-air line into the compost, another for embedding the T-type thermocouple in the compost for regular temperature readings, and third hole for exhaust gas collection from the headspace above the sample in the flask.

Before connecting the loaded and sealed samples to the flow manifold, these samples were weighed to record the initial weight at the beginning of the experiment. This reading in combination with final weight reading at the end of the experiment was useful in determining the weight loss and amount of sample converted to carbon dioxide.

5.6.2 Operating Procedure

Since composting is an aerobic degradation process, proper aeration in the composting vessels was maintained. ASTM D 5338 standard recommends that oxygen levels should not drop below 6% in the exhaust air. In the current experiment maximum CO_2 level of 13.4% was recorded, therefore based on the

original composition of air[i], oxygen levels greater than 6% were present in the composting vessels at all times during the degradation study.

As described in section 5.2, temperature in the glove box was controlled using temperature controller, which controlled the operation of air process heater and additionally circulation fans were used to have uniform heating in the glove box. Daily temperature readings were recorded from individual composting vessels using Fluke digital thermometer. These readings provided a good indication of the status of the composting process. For example, if the temperature reading was above 58 ± 2°C, it indicated either hyperactive composting conditions or low flowrates. In case of temperatures below the above-mentioned range it was due to retarded composting conditions or extremely high flowrates. Based on the CO_2 concentration readings using gas chromatograph and temperature readings, optimal composting conditions were maintained by either adjusting the incoming air flowrate or changing the set point for temperature controller.

Two glove boxes (A&B) were used for this study (see figure 5.3) and samples loaded were named based on their position in the glove box and suffixed with glove box name (A or B). Rate of biodegradation of the samples was determined using gas chromatography analysis of the effluent gas from composting vessels on regular basis. In section 5.2 (experimental set-up and procedure), I have discussed two different ASTM recommended methods to

---

[i] Dry air composition at sea level is: nitrogen 78.08%, oxygen 20.95%, argon 0.93%, carbon dioxide 0.03%, neon 0.0018%, helium 0.0005%, krypton 0.0001%, and xenon 0.00001%. Reference: "Earth's atmosphere" A *Dictionary of Chemistry*. Oxford University Press, 2000. *Oxford Reference Online*.

measure biodegradability: titration, gas chromatography. Gas chromatograph method was selected because it requires less bench space as compared to titration method. Average gas sampling from samples in glove box A was 1.1 days, and for glove box B was 1.3 days.

Proper aeration and moisture content was maintained in the composting vessels, for optimal composting conditions during the experiment. The complete aeration system for the glove box was checked for leaks regularly. If any composting vessel had excessively dry conditions, additional water was added to increase the moisture content. In addition to these specific adjustments, every two weeks, the whole system was shut down in order to fix any leaks, add moisture and manual shaking of all the composting vessels.

ASTM D 5338 standard recommends 45 day controlled composting study, which can be extended in case significant biodegradation is still being observed. In the current research, biodegradation study was conducted for 60 days, because of time constraints and fulfilling the project objective of determining the rate of biodegradation of biocomposites.

5.6.3 Results

Concentration of CO_2 (%) in the exhaust gas from composting vessels was measured by a gas chromatograph and converted to mass basis using ideal gas law equation and flow rate measurement of the exhaust gas. An example calculation is provided in Appendix 5.6.3.

As described in Appendix 5.6.3, %age CO_2 detected in the exhaust of composting vessels was converted to grams of CO_2 per reading and grams of

carbon per reading. Biodegradation progress for all the samples is described in time plots by displaying cumulative carbon dioxide evolution over time. The percent biodegradation for all the samples was calculated using the formula mentioned in ASTM D 5338 standard:

$$\% \text{ biodegradation} = \frac{\text{mean } C_g(\text{sample}) - \text{mean } C_g(\text{blank})}{C_i} \times 100$$

where:

C_g = amount of carbon produced in biodegradation, grams

C_i = total amount of carbon in the test sample, grams

Additionally, standard error, S_e and confidence interval (CI) of the biodegradation readings were calculated to determine the variability of the results obtained.

Standard error (S_e) is defined as:

$$S_e = \sqrt{\left(\left(\frac{s^2_{sample}}{n1}\right) + \left(\frac{s^2_{blank}}{n2}\right)\right)} \times \frac{100}{C_i}$$

where n1, n2 are number of test sample and compost control samples respectively; s is standard deviation for carbon production during biodegradation, and C_i is the total amount of carbon in the test sample.

Confidence interval (CI) is defined as:

$$x\% \text{ CI} = \%\text{biodegradation} \pm (t \times S_e)$$

where t is the t-distribution value for x% CI with (n1+n2-2) degrees of freedom.

5.6.3.1 Results-Compost Control

A cumulative CO_2 evolution curve for compost control samples is shown in Figure 5.11 below.

Cumulative CO2_Compost Control
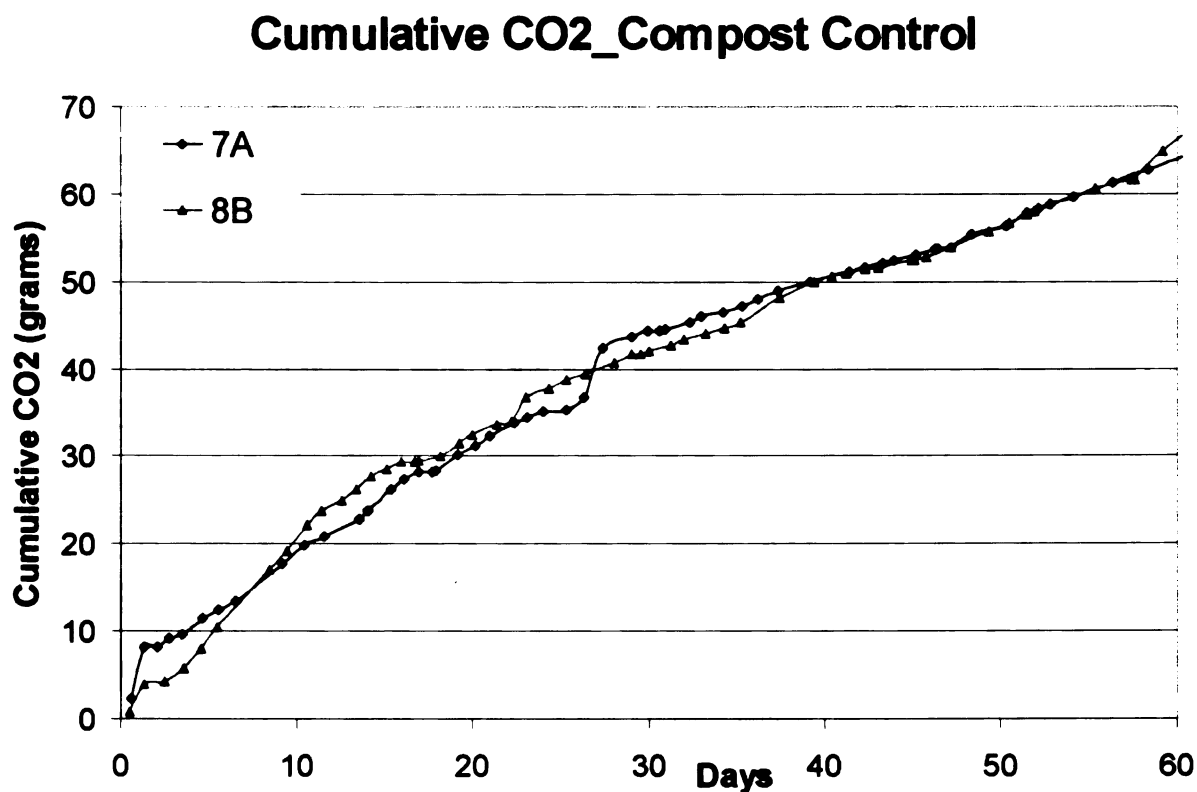
Figure 5.11 CO_2 evolution time plot for Compost Control

Composting study was started with compost control samples in triplicates; however one of the samples was rejected because of non-ideal conditions during the study and thus difficulty in obtaining reliable readings. CO_2 evolution curve for the other two samples indicate a similar rate, which by the end of the experiment at 60 days achieves similar amount of CO_2 being produced, even though the samples are in separate glove boxes (glove box A&B). This result indicates a

good quality control for this study. Cumulative amount of carbon produced during the study for these samples is provided in table 5.5 below.

Table 5.5 Cumulative amount of carbon produced-Compost Control

Sample ID	Cumulative carbon produced (grams)
7A	17.53
8B	17.72
Mean ± Standard Deviation	17.63 ± 0.13

5.6.3.2 Results-Cellulose positive control

Cumulative CO_2 production time plot for the cellulose positive control-compost mix and compost control sample-7A is presented below in Figure 5.12. Compost control sample was included in the time plot, in order to provide a CO_2 evolution comparison between cellulose and compost control samples. One of the three cellulose positive control samples was rejected because of non-ideal conditions. For other two positive control samples CO_2 production during the composting study was very similar; therefore similar to compost control results, it indicates good quality control for the experiment. Cumulative carbon production and percentage-biodegradation numbers for cellulose-positive control samples are reported in Table 5.6, below.

Cumulative CO2_Cellulose-positive control
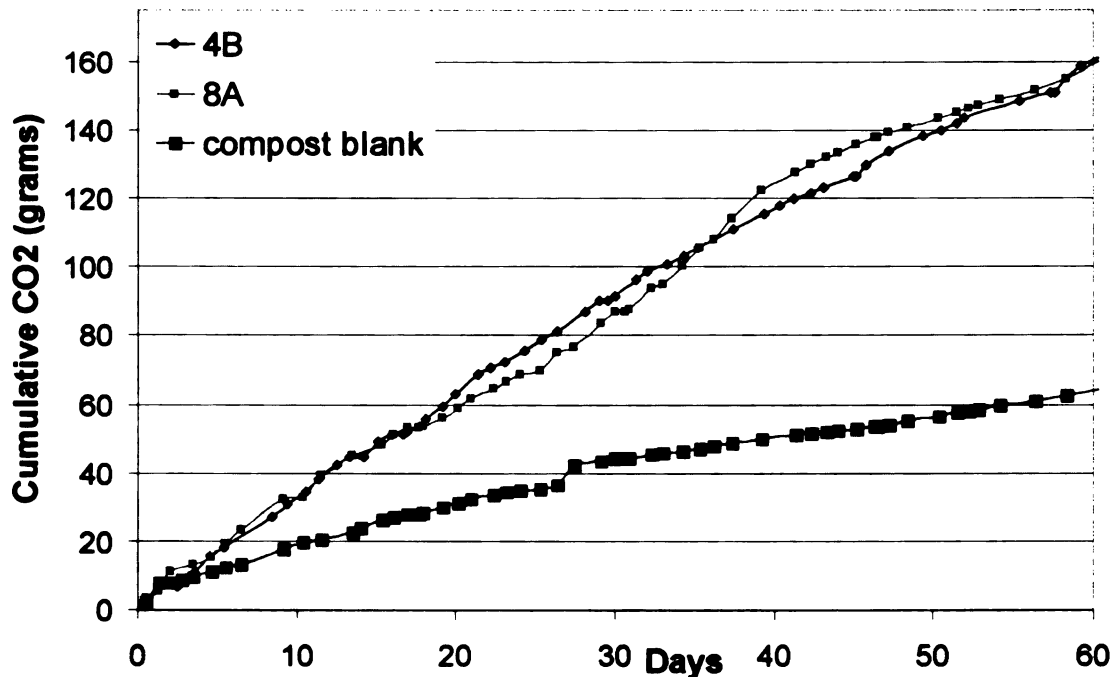
Figure 5.12 CO_2 evolution time plot for Cellulose positive control

In addition to percent-biodegradation, standard error and 95% confidence interval was calculated of the percent-biodegradation results for cellulose-positive control. Standard error and 95% confidence interval values were calculated using following inputs:

$n1$ = number of cellulose positive control samples = 2

$n2$ = number of compost control samples = 2

t = t-distribution value for 95% confidence interval with 2 degrees of freedom = 4.303

Thus, standard error (S_e) and 95% confidence interval of percent-biodegradation of cellulose samples was 0.37% and 61.42% ± 1.59% respectively.

Table 5.6 Cumulative amount of carbon produced-Cellulose positive control

Sample ID	Cumulative carbon produced (grams)/ Percentage (%)
4B	43.34 g
8A	43.59 g
Mean ± Standard Deviation	43.46 ± 0.18
Percent-biodegradation	61.42%

5.6.3.3 Results-Polypropylene-Glass negative control

Biodegradation results for PP-Glass composites (Polypropylene- (30wt%) Glass fiber) and compost control (for comparison) are presented below in Figure 5.13. Referring to the CO_2 evolution curve, only sample 1B has CO_2 evolution comparable to compost control sample for this study. Other two replicates of PP-Glass negative control had lower cumulative CO_2 produced as compared to compost control sample, even though negative control and compost control samples contained equal amounts of compost subjected to similar composting conditions. This result indicates PP-Glass composites are non-biodegradable and can act as a hindrance to the existing composting environment. Cumulative amount of carbon produced during the study and percent-biodegradation of PP-Glass composites is presented below in Table 5.7.

Cumulative CO2_PP-Glass-negative control
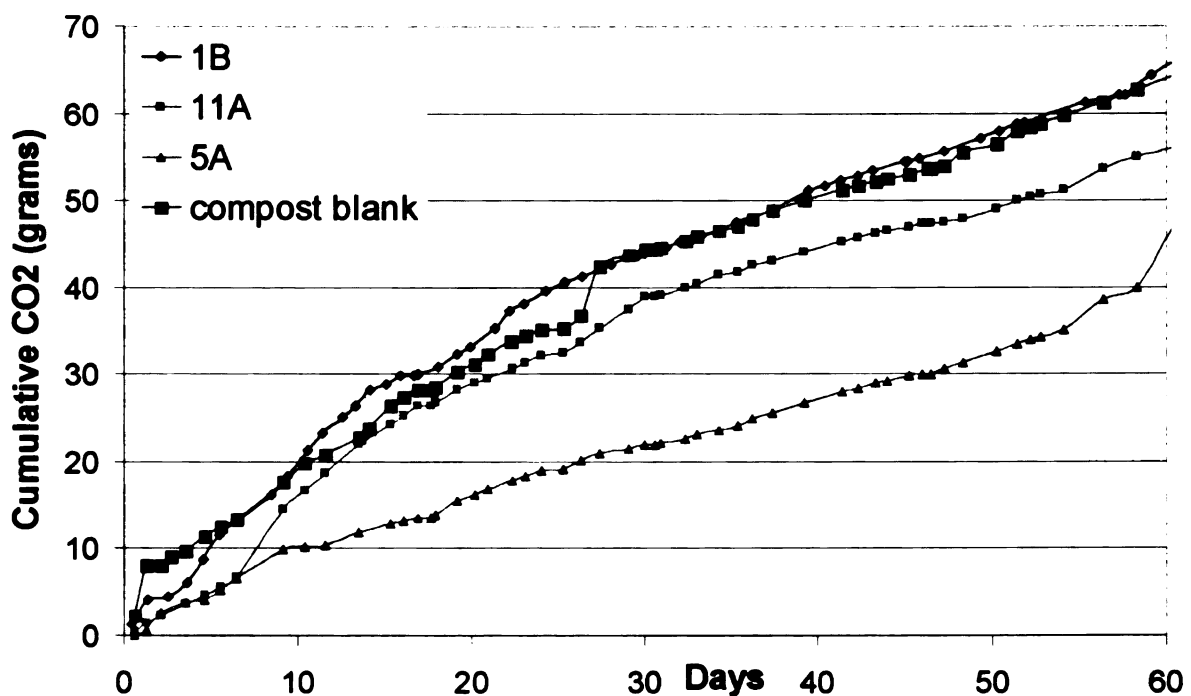
Figure 5.13 CO_2 evolution time plot for PP-Glass composites negative control

Table 5.7 Cumulative amount of carbon produced-PP-Glass negative control

Sample ID	Cumulative carbon produced (grams)/ Percentage (%)
1B	17.54
11A	15.26
5A	12.75
Mean ± Standard Deviation	15.18 ± 2.40
Percent-biodegradation	0%

5.6.3.4 Results-PHB-Kenaf Composites

PHB- (30wt%) Kenaf composites were tested in triplicates and CO_2 evolution results for these samples and compost control are presented below in Figure 5.14. As per the time plot below, their was variation in the cumulative evolution of carbon dioxide from PHB-Kenaf composite samples. This variation can be attributed to the processing technique for these composites; extrusion and injection molding which produce a random mix of fibers with matrix. And, since kenaf fibers with significant amount of lignin content are less biodegradable as compare to PHB (Polyhydroxybutyrate) biopolymer, such random mixing of kenaf fibers with PHB caused the variation in biodegradation results for PHB-Kenaf composite replicates.

Cumulative CO2_PHB-Kenaf Composite
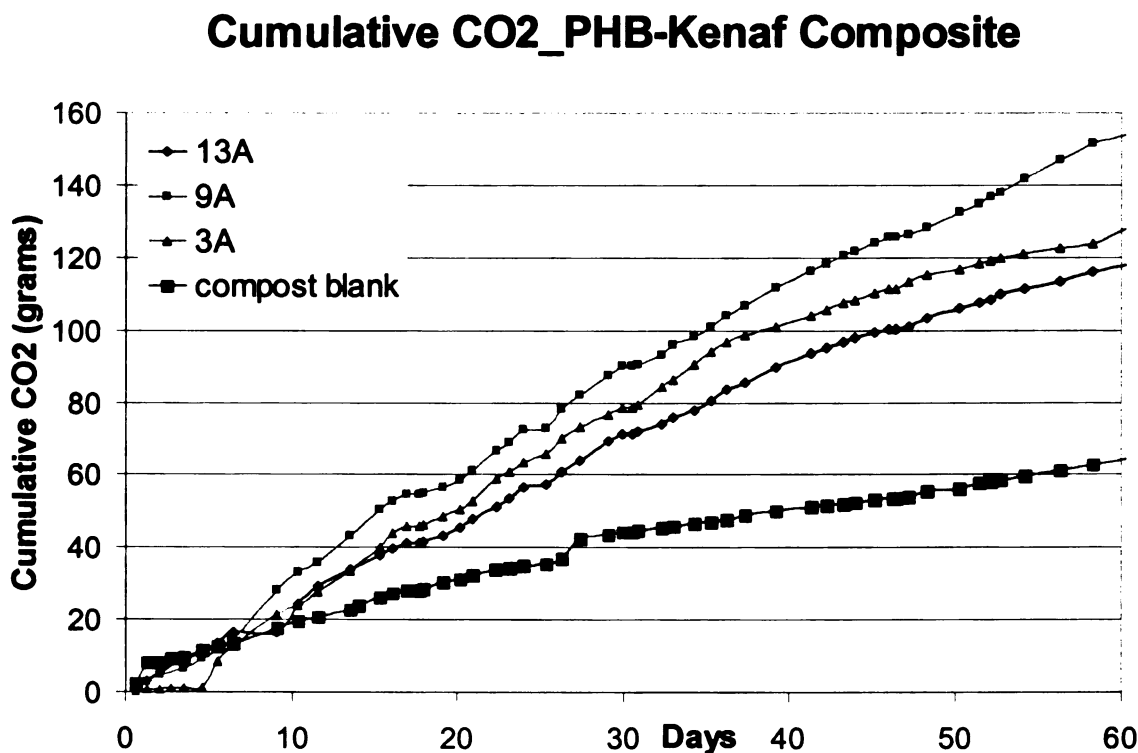
Figure 5.14 CO_2 evolution time plot for PHB-Kenaf composites

Cumulative carbon produced during the study for PHB-Kenaf composites and percent-biodegradation of these composites is reported below in Table 5.8.

Table 5.8 Cumulative amount of carbon produced-PHB-Kenaf composites

Sample ID	Cumulative carbon produced (grams)/ Percentage (%)
13A	32.21
9A	41.97
3A	34.90
Mean ± Standard Deviation	36.36 ± 5.04
Percent-biodegradation	35.58%

Since, their was variation in the cumulative evolution of CO_2 from three PHB-Kenaf composite samples, 90% confidence interval instead of 95% was calculated in addition to standard error calculation using following inputs:

n1 = number of PHB-Kenaf composite samples = 3

n2 = number of compost control samples = 2

t = t-distribution value for 90% confidence interval with 3 degrees of freedom = 2.353

The standard error (S_e) and 90% confidence interval of percent-biodegradation of PHB-Kenaf composite samples was calculated as 5.53% and 35.58% ± 13.02% respectively.

5.6.3.5 Results-PHB-g MA-PHB-Kenaf Composites

In addition to PHB- (30 wt%) Kenaf composites tested for biodegradation, PHB- (30 wt%)Kenaf composites with 5 wt% MA-PHB as compatibilizer were also tested for biodegradability. The main objective behind testing compatibilized PHB-Kenaf composites was to determine any variation in the biodegradation rate of these composites as compared to PHB-Kenaf composites. These composites were also tested in triplicates and the cumulative CO_2 evolution results for these samples are presented below in Figure 5.15.

Cumulative CO2_PHB-g MA-PHB-Kenaf Composite
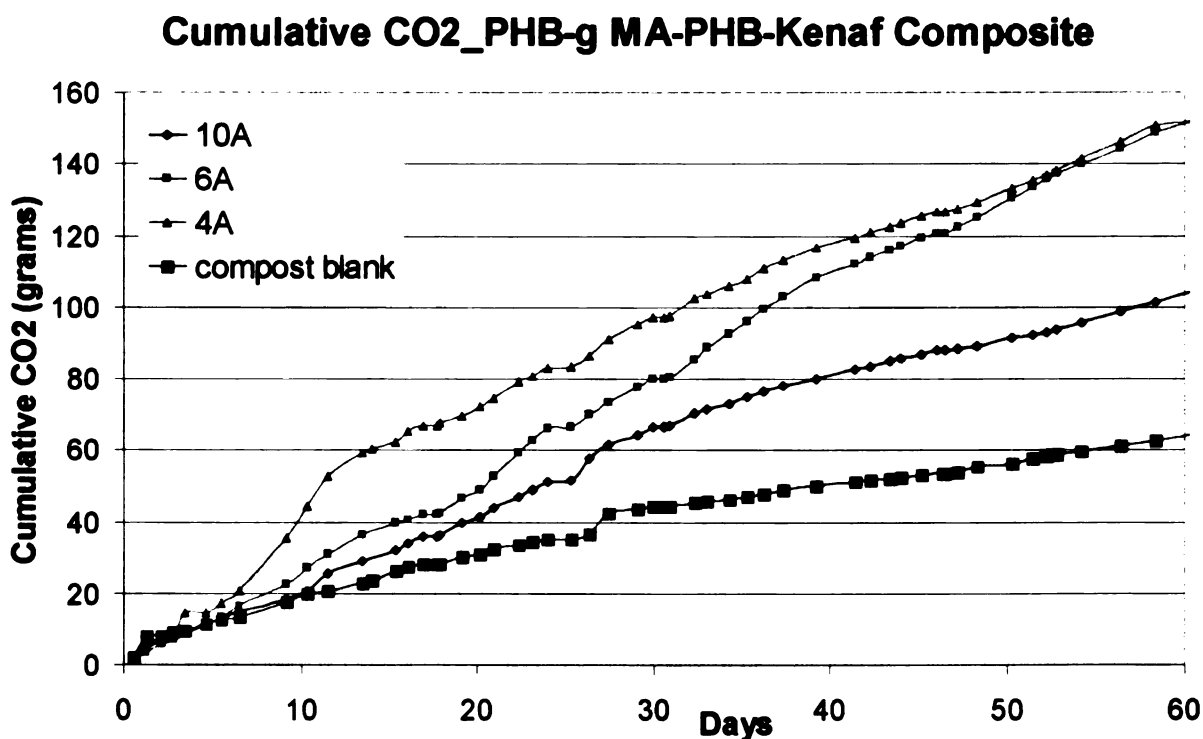
Figure 5.15 CO_2 evolution time plot for PHB-g MA-PHB-Kenaf composites

CO_2 evolution time plot above, indicates variation in the cumulative amount of CO_2 produced for three PHB-g MA-PHB-Kenaf samples, and such variation can be attributed to the processing technique, which was same as the

244

processing technique for PHB-Kenaf composites. However, this variation was more than the variation in similar readings for PHB-Kenaf composites. Cumulative amount of carbon produced and percent-biodegradation of these samples is reported below in Table 5.9.

Table 5.9 Cumulative amount of carbon produced-PHB-g MA-PHB-Kenaf composites

Sample ID	Cumulative carbon produced (grams)/ Percentage (%)
10A	28.37
6A	41.32
4A	41.40
Mean ± Standard Deviation	37.03 ± 7.50
Percent-biodegradation	37.35%

Standard error (S_e) and 90% confidence interval of percent-biodegradation of PHB-g MA-PHB-Kenaf samples was calculated as 8.33% and 37.35% ± 19.61% respectively, using following inputs:

n1 = number of PHB-g MA-PHB-Kenaf composite samples = 3

n2 = number of compost control samples = 2

t = t-distribution value for 90% confidence interval with 3 degrees of freedom = 2.353

5.6.3.5 Results-Neat Polymer samples

Biodegradation profile of three biopolymers: PHB (Polyhydroxybutyrate), PLA (Poly-lactic acid), and CA- (30wt%) TEC (Cellulose acetate plasticized with Triethyl citrate) was obtained in this study. These polymers were selected for this study because they are obtained from renewable raw materials and are some of the currently studied biobased polymers. Additionally, it was useful to determine the biodegradability of PHB polymer samples, in order to compare the results with that of PHB-Kenaf composites. Such comparison was helpful in determining the difference in biodegradability between PHB and Kenaf fibers.

These neat polymers were tested as single samples because of limited available space in two glove boxes used for this study. Cumulative CO_2 time plots for these samples are presented below, in Figure 5.16.

Based on the CO_2 evolution curves below, rate of biodegradation for neat polymer samples (in descending order) was as follows: PHB > PLA > CA - (30wt%)TEC. Cumulative carbon produced and percent-biodegradation for these samples is reported below in Table 5.10.

Table 5.10 Cumulative amount of carbon produced-Neat Polymer samples

Polymer	Sample ID	Cumulative carbon produced (grams)	Percent-biodegradation (%)
PHB	12A	45.00	51.15
PLA	7B	38.59	45.34
CA- (30wt%)TEC	10B	29.06	24.81

Cumulative CO2_Neat Polymer samples
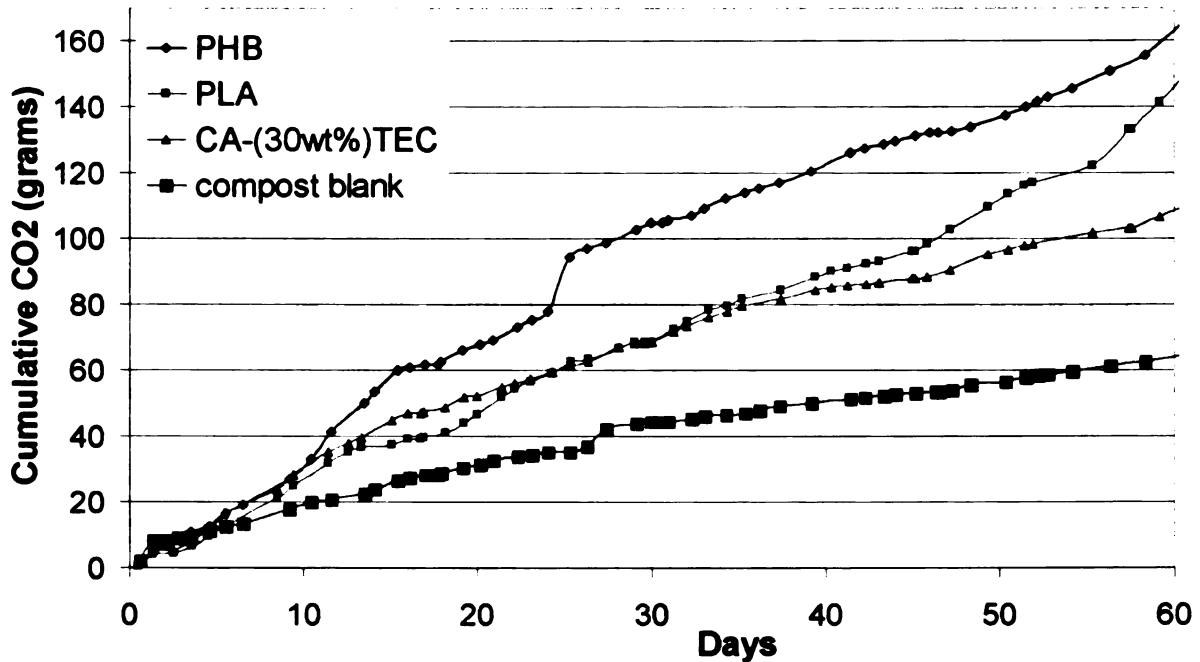
Figure 5.16 CO_2 evolution time plot for Neat Polymer samples

At the end of the biodegradation study as recommended by ASTM D 5338 standard, pH of the compost-sample mix was determined. In addition dry solids content, weight loss and visual observations of the compost-sample mix were recorded. Finally, plant growth tests with cress seed and lettuce were conducted in order to determine any adverse impacts of compost-sample mix on germination of plants, once the final material at the end of the study is mixed with soil.

5.7 End of study observations

To conclude the biodegradation study, a group of observations were recorded including pH, dry solids content, weight loss, thickness, and pictures of samples. pH of every compost-sample mix was recorded in order to confirm the aerobic nature of the experiment. If a pH value of less than 7 is recorded, ASTM D 5338 standard recommends measuring the volatile fatty acids content for the compost-sample mix. And, in case volatile fatty acids content of more than 2 g per kilogram of dry solids of compost-sample mix are recorded, that sample must be regarded as invalid and rejected.

Composting vessels were weighed at the end of the study and dry solids content of the compost-sample mix was determined. Thus weight loss of the samples was calculated using final weight and dry solids content data. Weight-loss data obtained was correlated to the cumulative CO_2 evolution, percent-biodegradation data for the samples tested.

For a qualitative analysis of the extent of biodegradation, images of the degraded samples were taken. Additionally, thickness of the samples (if possible) was also recorded for a quantitative comparison between samples at the beginning and end of the study.

Plant growth test for the final compost-sample mix was carried out as recommended by ASTM D 6400 standard and based on OECD Guideline 208.

5.7.1 pH determination

Compost-sample mix pH was measured using the method developed by Warncke[20] (for additional information, please refer to Test methods for the

examination of composting and compost[21]). 500 mL plastic containers were ¾ filled with compost-sample mix and distilled water was slowly added until the sample was saturated. This saturated sample was allowed to equilibrate for 20 minutes and pH reading with standard laboratory pH meter was recorded. Since the pH for the compost-sample mix was expected between 7 and 10, the pH meter was calibrated with pH 7 and 10 standard solutions. pH readings recorded are presented below in Table 5.11.

As noted in table 5.11, none of the samples had pH less than 7, which indicates that none of the composting vessels went anaerobic. Therefore, no volatile fatty acid measurements were recorded at the end of the biodegradation study.

5.7.2 Dry solids and weight loss data

Total weight of the composting vessels was recorded at the beginning and end of the composting study. Additionally, dry solids content of the samples at the end of the study was used to calculate weight loss of samples during the biodegradation study. Dry solids content and weight loss data is presented below in Table 5.12. Correlations between weight loss and percent-biodegradation data of test-samples are presented in the discussion section of this chapter.

Table 5.11 End of study pH readings

Sample ID	Sample Description	pH Reading
7A	Compost control	7.649
8B	Compost control	7.587
8A	Cellulose positive control	7.859
4B	Cellulose positive control	7.795
5A	PP-Glass negative control	7.725
11A	PP-Glass negative control	7.747
1B	PP-Glass negative control	7.692
3A	PHB-Kenaf	7.652
9A	PHB-Kenaf	7.774
13A	PHB-Kenaf	7.637
4A	PHB-g MA-PHB-Kenaf	7.768
6A	PHB-g MA-PHB-Kenaf	7.830
10A	PHB-g MA-PHB-Kenaf	7.756
12A	PHB	7.914
7B	PLA	7.394
10B	CA- (30wt%)TEC	7.545

Table 5.12 Dry solids content and weight loss of samples at the end of biodegradation study

Sample ID	Sample Description	Dry solids content (%)	Weight loss (g)
7A	Compost control	63.88	ND*
8B	Compost control	95.41	20.60
8A	Cellulose positive control	61.25	80.93
4B	Cellulose positive control	87.50	72.79
5A	PP-Glass negative control	67.65	12.74
11A	PP-Glass negative control	81.62	5.91
1B	PP-Glass negative control	90.18	8.32
3A	PHB-Kenaf	86.31	67.13
9A	PHB-Kenaf	62.02	43.97
13A	PHB-Kenaf	64.51	63.07
4A	PHB-g MA-PHB-Kenaf	63.35	49.22
6A	PHB-g MA-PHB-Kenaf	67.87	71.49
10A	PHB-g MA-PHB-Kenaf	61.01	63.41
12A	PHB	55.45	51.84
7B	PLA	96.89	82.78
10B	CA- (30wt%)TEC	97.33	41.72

* Not determined because of error in final weight reading

5.7.3 Sample images and thickness

Thickness of the dogbone shape tensile coupons of composites and neat-polymers was measured at the beginning and end of the biodegradation study. Since no biodegradation was observed for PP-Glass composite test samples, their was no change in the thickness of these samples. For other samples, end of study average thickness and percent-reduction data is presented below in Table 5.13.

Table 5.13 End of study sample thickness

Sample Description	Original sample thickness (mm)	Average end of study sample thickness (mm) ± standard deviation	Average percent reduction in thickness (%)
PHB-Kenaf	3.18	2.72 ± 0.06	14.39
PHB-g MA-PHB-Kenaf	3.22	2.51 ± 0.35	21.94
PHB	3.18	2.83 ± 0.17	11.11
PLA	3.25	2.72 ± 0.11	16.23
CA- (30wt%)TEC	3.21	3.09	3.59

Images of compost-sample (PP-Glass negative control, dogbone shape test samples) mix were taken at the end of the study, in order to qualitatively analyze the extent of biodegradation. These images are presented below along-with additional observations and explanation.

PP-Glass negative control

PP-Glass composite samples were used as a negative control for the biodegradation study and as expected composite samples did not show any signs of deterioration. Images of samples 5A and 11A are presented below in Figures 5.17 and 5.18.

Figure 5.17 Sample 5A PP-Glass negative control-End of study image
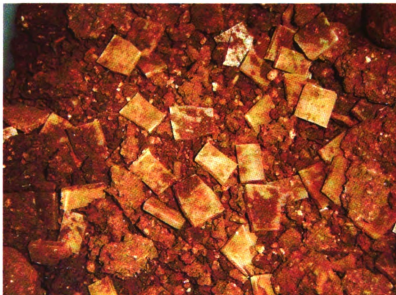
Figure 5.18 Sample 11A PP-Glass negative control-End of study image

PHB-Kenaf composites

PHB-Kenaf composites showed significant degradation, which was evident from significant microbial growth and deterioration of composite samples. Though composite samples had weakened, degradation was still surface limited indicating that the significant degradation could be carried out for more than two months. Degradation images of sample 3A, 9A, and 13A are presented below in Figures 5.19, 5.20, and 5.21 respectively.

Figure 5.19 Sample 3A PHB-Kenaf composites-End of study image

Figure 5.20 Sample 9A PHB-Kenaf composites-End of study image
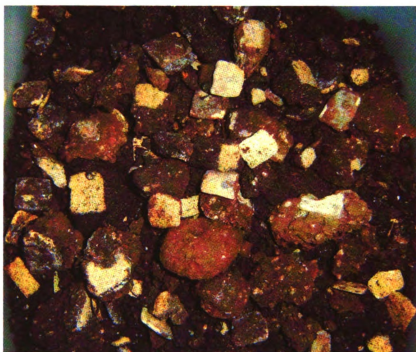
Figure 5.21 Sample 13A PHB-Kenaf composites-End of study image

PHB-g MA-PHB-Kenaf composites

PHB-g MA-PHB-Kenaf composites had similar levels of degradation as compared to PHB-Kenaf composites at the end of biodegradation study. End of study images for samples 4A, 6A, and 10A are presented below in Figures 5.22, 5.23 and 5.24 respectively. Deterioration and microbial growth on the samples was evident as can be seen in the images below.
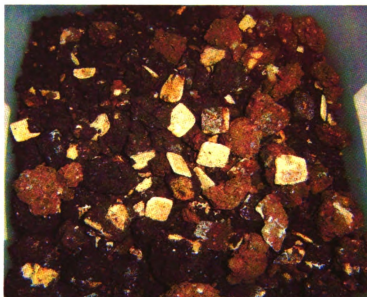
Figure 5.22 Sample 4A PHB-g MA-PHB-Kenaf composites-End of study image

Figure 5.23 Sample 6A PHB-g MA-PHB-Kenaf composites-End of study image

Figure 5.24 Sample 10A PHB-g MA-PHB-Kenaf composites-End of study image

Neat polymer samples

Neat polymer samples exhibited varying levels of degradation by the end of biodegradation study and such differences were apparent from the images taken at the end of study. PHB samples had significant microbial growth and were disintegrating into smaller segments; however degradation process could be carried out for more than two months. For PLA samples even though microbial growth was not evident, samples had become brittle and were disintegrating into smaller segments. Surface degradation was present for CA-(30wt%) TEC samples; however there was no disintegration and no significant reduction in strength of these samples. End of study images for PHB, PLA, and CA- (30wt%) TEC are presented below in Figures 5.25, 5.26, and 5.27.
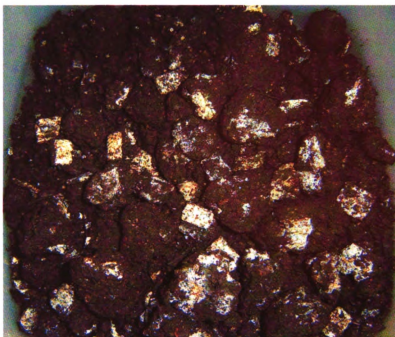
Figure 5.25 Sample 12A PHB-End of study image
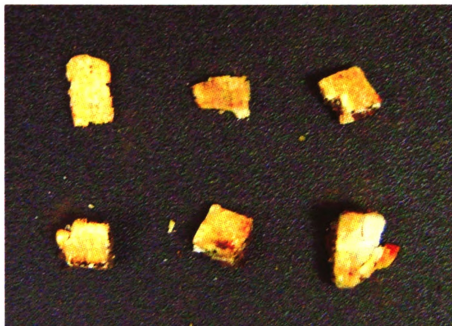
Figure 5.26 Sample 7B PLA-End of study image

Figure 5.27 Sample 10B CA- (30wt%)TEC-End of study image

5.7.4 Plant growth test

OECD Guideline 208 "Terrestrial Plants, Growth Test"[22] was followed to determine the toxic effects of materials tested in this study on early stages of growth of various terrestrial plants. OECD guideline recommends testing samples in varying concentrations mixed with soil, with minimum of four replicates per sample, and minimum of five seeds per replicate. A minimum of three plant species should be tested with at least one from each of the three categories defined by OECD Guidelines represented in terms of percent emergence of plants and of growth in plant-weight.

In the current study, compost-sample mixes were directly tested, without mixing with soil. The samples were tested with four replicates, with each replicate comprising of 25 cells in a 200-cell tray and a total of 25 seeds per replicate. Each cell contained approximately 7 g of compost-sample mix. These samples were watered daily and at the end of study total number of cells in which seeds germinated was recorded, in order to calculate percent germination.

Initially plant growth test was started with cress seeds; however because of concerns over cress-seed quality, additional tests with lettuce seeds were conducted. It should be noted that cress and lettuce seeds belong to category 3 of plant species defined by OECD guidelines and no seeds were selected from other two categories because of insufficient amount of available compost-sample mix. Additionally plant growth tests could not be conducted for PLA and CA-(30wt%) TEC samples, because of insufficient amount of sample available at the end of biodegradation study.

Percent germination for cress seed samples was recorded after 3 ½ weeks, while for lettuce seed samples it was recorded after 2 ½ weeks. Percent germination results for cress seed and lettuce seed are presented below in Tables 5.14 and 5.15 respectively.

As per the germination results below, PHB-Kenaf, PHB-g MA-PHB-Kenaf, and PHB samples had higher percent germination as compared to PP-Glass negative control samples and slightly higher or comparable germination compared to Compost control samples; thus indicating the suitability of PHB polymer and its natural fiber reinforced composites to support plant growth at the

end of biodegradation study. Cellulose positive control samples had the lowest percent germination among the samples tested. This unexpected result could be attributed to the small particle size of cellulose (13 μm), which acted as a binding agent causing the compost-cellulose mix to clump when water was added, therefore hindering the plant germination.

Table 5.14 Cress seed-percent germination results

Sample description	Cress seed (25 seeds per sample replicate)				
	Replicate 1	Replicate 2	Replicate 3	Replicate 4	Average percent germination ± standard deviation
Control*	92	88	96	88	91 ± 4
Compost control	84	72	80	68	76 ± 7
Cellulose positive control	68	72	68	64	68 ± 3
PP-Glass negative control	68	76	84	68	74 ± 8
PHB-Kenaf	84	76	80	84	81 ± 4
PHB-g MA-PHB-Kenaf	76	76	80	76	77 ± 2
PHB	72	80	84	68	76 ± 7

---

* Scotts® potting mix was used as a control for this test

Table 5.15 Lettuce seed-percent germination results

Sample description	Lettuce seed (25 seeds per sample replicate)				
	Replicate 1	Replicate 2	Replicate 3	Replicate 4	Average percent germination ± standard deviation
Control*	96	100	100	92	97 ± 4
Compost control	96	92	96	88	93 ± 4
Cellulose positive control	84	88	84	76	83 ± 5
PP-Glass negative control	88	84	84	88	86 ± 2
PHB-Kenaf	92	96	96	96	95 ± 2
PHB-g MA-PHB-Kenaf	88	100	96	92	94 ± 5
PHB	84	96	100	92	93 ± 7

* Scotts® potting mix was used as a control for this test

5.8 Discussion

The motivation behind this study was to understand the behavior of biobased composites and polymers under composting environment. These results are useful since they can be used to establish the superior end of life profile of biobased composites over conventional composites and CO_2-neutral nature of biobased composites.

The cumulative carbon numbers for compost control and cellulose positive control replicates had very less standard deviation; thus indicating good quality control, which was evident from a smaller 95% confidence interval for percent biodegradation of cellulose samples. ASTM D 5338 standard (based on which this study was conducted) recommends a minimum of 70% degradation of cellulose positive control samples after 45 days. However, in the current study 61% average degradation was achieved for cellulose samples in 60 days. This reduction in degradation numbers can be attributed to two factors. First, the compost used in this study was a well-matured compost (see section 5.4) with minimal CO_2 emissions and thus this compost might have retarded the normal rate of biodegradation as recommended by ASTM D 5338 standard. Second, cellulose[10] used for the study had a particle size of 13 μm and such small particle size acted as a binding agent and lead to agglomeration of compost-cellulose mix, thus reducing the porosity of compost-cellulose mix and hindering the degradation of cellulose positive control samples.

To improve the porosity of compost-sample mix, Perlite[19] was added; however, the results obtained were mixed as indicated by low percent-

biodegradation of positive control samples. For future studies, other porosity-enhancing inert materials such as wood chips, gravel could be used.

PP-Glass composite samples (100 grams PP-Glass composites + 600 grams compost control, dry solids only) were tested as negative control in this study and average cumulative CO_2 production for these samples was lower than CO_2 production for compost control samples (600 grams of compost control, dry solids only). This result indicates that if non-degradable component (such as PP-Glass) is mixed with compost control, it can reduce the original CO_2 production from compost and therefore hindering the biodegradation process.

PHB-Kenaf and PHB-g MA-PHB-Kenaf composite samples were still actively degrading at the end of study and exhibited variation among replicates for degradation results. Such variation can be attributed to the processing (extrusion and injecting molding) of these composites, which induces a random mixing of kenaf fibers (less degradable) with PHB biopolymer (readily degradable).

Percent-biodegradation of selected neat biopolymer was calculated, with rate of biodegradation (in descending order) as follows: PHB > PLA > CA- (30 wt%) TEC. PHB samples had a percent-biodegradation of 51% and using this number, percent-biodegradation of kenaf fibers in PHB-Kenaf composites was calculated[i]. This calculation indicates that kenaf fiber portion of composites is essentially non-degradable, which is due to high lignin content of kenaf fibers[23].

---

[i] 100 grams of PHB-Kenaf composites have 70 grams of PHB. 70 grams of PHB have 37.87 grams of carbon (54.10% carbon content). Using 51.15% biodegradation rate for PHB, 19.37 grams of carbon is produced. Average carbon produced for PHB-Kenaf composites is 36.36 grams and with average carbon production of 17.63 grams from compost, 18.73 grams is the

The extent of biodegradation of the samples was determined based on two parameters: percent biodegradation and weight loss. Correlation between these two parameters is presented in Table 5.16. Ideally, percent biodegradation of a sample should have a positive correlation with weight loss; but in the current study this is not the case. Additionally, cumulative carbon produced and weight loss recorded have different values, when ideally it should be the same number.

These deviations can be attributed to two factors: 1) biodegradation mechanism of test-samples 2) gas sampling procedure and frequency.

During biodegradation, complex polymeric samples are broken down into oligomers, and generally the end products are CO_2 and H_2O. For example degradation of PHB (as described by Albertsson and Karlsson[24], shown below in figure 5.28) takes place through TCA (tricarboxylic acid cycle) cycle, producing CO_2 and H_2O[25]. Since the gas chromatograph readings of the test-samples only measure CO_2, water produced during biodegradation partially accounts for the difference between cumulative carbon produced and weight loss of test-samples.

Gas sampling of the test-samples was done approximately once a day and point reading of CO_2 percentage in combination with exhaust gas flow rate was converted to cumulative CO_2 produced/day, as explained in Appendix 5.6.3. This calculation assumes that the rate of CO_2 production remained constant during that time-period. Therefore, this assumption might also account for the difference between cumulative carbon produced and weight loss of test-samples.

---

contribution from PHB-Kenaf composites. As we can see theoretically calculated contribution from PHB approximately matches the experimental carbon contribution from PHB-Kenaf composites!

Despite these deviations in the biodegradation study, the final results do not conflict with the objectives of the study, which were to determine the rate of biodegradation and environmental impacts of degradation end-products. This study should be considered preliminary, and is currently being repeated under similar controlled composting conditions at Composite Materials and Structures Center (CMSC) at Michigan State University.
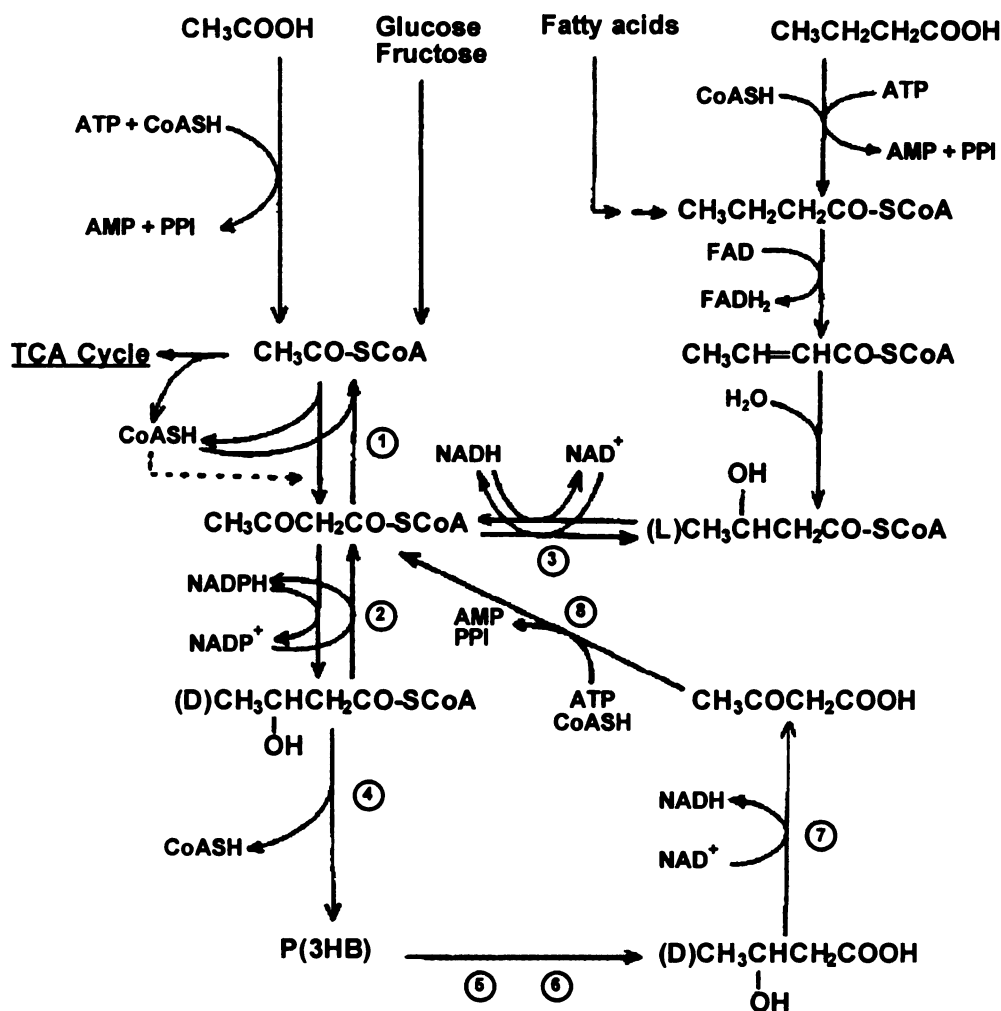
Figure 5.28 Cyclic metabolic pathway of the biosynthesis and degradation of P(3HB), reproduced from Albertsson, Karlsson (1995), see ref. 24

In the current study, dogbone samples of composites and polymers were reduced to an approximate size of 2 cm x 2 cm x 3.2 mm and the rate of biodegradation could have been improved by further reducing the sample size, thus increasing the surface area of samples exposed to microbial degradation. Such improvements in the rate of biodegradation have been previously recorded by Buchanan et al.[26], where polymer films (0.051 to 0.203 mm thick) have been tested under controlled composting environment. For example: PHB films had 75.8% weight loss in 14 days, and 70/30 CA/TEC films had 100% weight loss in 12 days, while 70/30 CA/TEC injection molded bars (3.1 mm thick) lost 10.1% of their weight under controlled composting cycle of 30 days.

Addition of surfactants to reduce hydrophobicity and increase surface area has been used to increase the rate of biodegradation of powdered polyethylene in biotic samples[27]. However, in another study by Walter et al.[28], addition of surfactants to poly(trimethylene succinate) film samples reduces the rate of biodegradation. Such a behavior is due to the fixed surface area of solid film samples, and adding surfactants only reduces the hydrophobicity of film samples and hydrophobic character of samples is known to aid enzymatic degradation[29]. Therefore, addition of surfactants may increase rate of biodegradation, only if the test samples are in powder form.

Table 5.16 Correlation between cumulative carbon produced/percent biodegradation and weight loss at the end of the study

Sample ID	Sample Description	Cumulative carbon produced (g)	Percent-biodegradation	Weight loss (g)
7A	Compost control	17.53	NA[ii]	ND*
8B	Compost control	17.72	NA[ii]	20.60
8A	Cellulose positive control	43.59	61.71	80.93
4B	Cellulose positive control	43.34	61.12	72.79
5A	PP-Glass negative control	12.75	0.00	12.74
11A	PP-Glass negative control	15.26	0.00	5.91
1B	PP-Glass negative control	17.54	0.00	8.32
3A	PHB-Kenaf	34.90	32.81	67.13
9A	PHB-Kenaf	41.97	46.24	43.97
13A	PHB-Kenaf	32.21	27.70	63.07
4A	PHB-g MA-PHB-Kenaf	41.40	45.76	49.22
6A	PHB-g MA-PHB-Kenaf	41.32	45.60	71.49
10A	PHB-g MA-PHB-Kenaf	28.37	20.69	63.41
12A	PHB	45.00	51.15	51.84
7B	PLA	38.59	45.34	82.78
10B	CA- (30wt%)TEC	29.06	24.81	41.72

[ii] Not Applicable
* Not determined because of error in final weight reading

268

References:

[1] A. Keller et al., Degradation kinetics of biodegradable fiber composites. Journal of Polymers and the Environment, Vol. 8, No. 2, 2000.

[2] Rynk, Robert, editor. On-Farm Composting Handbook. Ithaca, New York: Northeast Regional Agricultural Engineering Service. 1992.

[3] R. Narayan, Drivers for biodegradable/compostable plastics & role of composting in waste management & sustainable agriculture. Bioprocessing of Solid Waste & Sludge, Vol. 1, 2001.

[4] A. Starnecker, M. Menner, Assessment of biodegradability of plastics under simulated composting conditions in a laboratory test system. International Biodeterioration & Biodegradation (1996) 85-92

[5] Gattin, R. et al., Comparison of mineralization of starch in liquid, inert solid and compost media according to ASTM and CEN norms for the composting of packaging materials. Biotechnology letters 22: 1471-1475, 2000.

[6] Copinet, A. et al., Photodegradation and biodegradation study of a starch and poly(lactic acid) coextruded material. Journal of Polymers and the Environment, 11(4), 2003.

[7] R Jayasekara et al. (2001), Journal of Chemical Technology and Biotechnology

[8] Test methods for the examination of composting and compost (TMECC), Section 04.02-D, Total Nitrogen by Oxidation. May 11, 2002.

[9] Official Solvita® Guideline-Compost Maturity Index, Version 4.0, Woods End Research Laboratory, Inc. Mt Vernon ME. URL: http://www.solvita.com/aaa/solvita.html

[10] Lattice® Microcrystalline Cellulose, Type: NT-013, FMC BioPolymer, Philadelphia, PA, USA.

[11] Pro-fax 6523, Polypropylene homopolymer, Basell North America Inc., Elkton, MD, USA.

[12] Chopped Strand 756F, ¼" length, Johns Manville, Waterville, OH, USA.

[13] Biomer® P226, Poly((R)3-hydroxybutyric acid) pellets, Biomer, Krailling, Germany.

[14] Kenaf fiber (un-chopped), Flaxcraft, NJ, USA.

[15] Biomer® L9000, Poly-L-lactate pellets, Biomer, Krailling, Germany.

[16] Powdered Cellulose Acetate (CA), plasticizer and additive free, degree of substitution of cellulose acetate was approximately 2.5. Eastman Chemical Company, Kingsport, TN, USA.

[17] Triethyl Citrate (TEC), Morflex Inc., Greensboro, NC, USA.

[18] Standard Methods for the examination of water and wastewater, 19th Edition, 1995, American Public Health Association, Washington, DC.

[19] Perlite is a natural volcanic glass; it can be classified as amorphous mineral containing fused sodium-potassium-aluminum silicate. Definition obtained from www.cdc.gov. Additional information available at www.perlite.org

[20] Warncke, D. 1998. Greenhouse root media. pp. 61-64. In Recommended chemical soil test procedures for the North Central Region. North Central Regional Research Publication No. 221 (Revised) Missouri Agricultural Experiment Station SB 1001.

[21] Test methods for the examination of composting and compost (TMECC), Section 04.11 Electrometric pH determinations for compost. March 21, 2002.

[22] OECD Guideline for testing of chemicals, adopted April 1984. Available from Organization for Economic Development (OECD), Director of Information, 2 rue Andre' Pascal, 75775 Paris Cedex 16, France.

[23] Mohanty, A.K. et al., Biofibres, biodegradable polymers and biocomposites: An overview. Macromolecular Materials and Engineering, 276/277, 1-24 (2000)

[24] A.-C. Albertsson and S. Karlsson, Degradable polymers for the future. Acta Polymer., 46, 114-123 (1995)

[25] H.-M. Muller and D. Seebach, Poly(hydroxyalkanoates) : A Fifth Class of Physiologically Important Organic Biopolymers? Angew. Chem. Int. Ed. Engl. 1993, 32, 477-502

[26] Buchanan, C.M. et al., Biodegradation of Cellulose Esters: Composting of cellulose ester-diluent mixtures. Journal of Macromolecular Science – Pure and Applied Chemistry, A32(4), 683-697 (1995)

[27] Karlsson, S., Ljungquist, O. and Albertsson, A.-C. Biodegradation of polyethylene and the influence of surfactants. Polym. Degr. Stab.1988, 21, 237-250

[28] Walter, T. et al., Enzymatic degradation of a model polyester by lipase from Rhizopus delemar. Enzyme and Microbial Technology 17:216-224, 1995

[29] Blow, D. Lipases reach the surface. Nature 1991, 351, 444-445

Chapter 6: Conclusions and Future Work

6.1 LCA study conclusions

A cradle to pellet LCA study for production of 1000 tensile coupons of PHB-(30wt%)Kenaf and PP-(30wt%)Glass composites was conducted in the present research work. Thus, effectively making a volumetric comparison for both the composites. Resource consumption and emissions for both the systems were computed as part of the LCI (Life Cycle Inventory) analysis and for a better understanding of this data, CML impact assessment methods were used to classify inventory flows based on their environmental impacts.

In 7 out of 9 impact categories evaluated, PHB-Kenaf composites had higher impacts compared to PP-Glass composites, with lower impacts for global warming and abiotic resource depletion categories. Normalizing the impact assessment results based on the factors defined for the World in 1995, four impact categories of Abiotic resource depletion, Acidification, Eutrophication, and Global warming accounted for more than 90% of the cumulative normalized impacts. Normalization made it possible to have a quantitative comparison of various impacts, whereas a qualitative comparison of the impacts can be done using weighting or valuation methods. However, because of the unavailability of widely acceptable valuation/weighting methods, only quantitative comparison of the impacts was done for the current study.

Nutrient outflows (N&P) from soybean cultivation are important contributors towards eutrophication and acidification impacts. Since corn and soybean are rotational crops, nutrient outflows from them are related. In the

default allocation approach (C-S allocation), approximately equal N-application and leaching rates were considered for corn and soybean crops; while in the alternative C-allocation approach, all N-application and emissions were allocated solely to corn cultivation. As determined in the sensitivity analysis, using C-allocation approach, all impacts were lower compared to C-S allocation approach, with significant reduction of 47% for eutrophication impacts. Therefore, cumulative normalized for PHB-Kenaf composites range between +3% (C-S allocation) to -9% (C-allocation) of the cumulative normalized impacts for PP-Glass composites.

In addition to analyzing the sensitivity of LCA results due to different allocation methods, effect of different eutrophication impact assessment method on final results was also analyzed. Contrary to global impacts such as climate change, eutrophication is considered to be a regional and/or local impact. The CML eutrophication method computes the impacts without considering location related variation, where such a variation can influence the actual impacts due to site-specific emissions. An alternative method developed by EPA, TRACI considers such variation by multiplying CML eutrophication potentials with US state-level nutrient transport factors, and computing US weighted-average eutrophication potentials, and in comparison to CML eutrophication potentials were significantly lower for air emissions, but remained the same for water emissions of nutrients. Thus, TRACI eutrophication impacts for PHB-Kenaf composites using C-S and C-allocation methods were lower by 38% and 68% respectively compared to impacts calculated using CML eutrophication method.

This reduction had significant effect on cumulative normalized impacts of PHB-Kenaf composites, which ranged from -2% (C-S allocation) to -14% (C allocation) of those computed for PP-Glass composites.

Comparing energy consumption, PHB-Kenaf composites used 22% (for C-S allocation) and 25% (for C-allocation) lower energy compared to PP-Glass composites, mainly due to low energy consumption for kenaf fiber production (97.6% reduction compared to glass fiber production) and high energy consumption for PP production process.

Summarizing LCA results, majority of environmental impacts and energy consumption for PHB-Kenaf composites were due to PHB production, specifically from electricity and steam production, and nutrient emissions from soybean cultivation. Unlike PP production, technology for PHB production is in its infancy and increased research emphasis and commercial production will definitely improve its efficiency, thus reducing material and energy requirements.

6.2 Biodegradation study conclusions

The motivation behind biodegradation study was to determine the rate of biodegradation of biobased composites and polymers under controlled composting environment, and study the environmental impacts of degradation end-products. These results are useful since they can be used to establish the superior end of life profile of biobased composites over conventional composites and CO2-neutral nature of biobased composites.

PP-Glass composites were tested as negative control (100 grams PP-Glass composites + 600 grams compost control, dry solids only) in this study,

and cumulative CO_2 production for these samples was lower as compared to compost control samples (600 grams of compost control, dry solids only), indicating a hindering effect of negative control sample on the biodegradation process. At the end of the study in 60 days, PHB-Kenaf composites had degraded by 36% and still actively degrading, where the degradation might have reached appreciable levels (70% or above) in six months, if the experiment was continued. Among the neat polymer samples, PHB had the highest percent-biodegradation of 51%, followed by 45% for PLA and 25% for CA-(30wt%)TEC.

Environmental impacts of degradation end-products were determined by recording percent germination of cress and lettuce seed in compost-sample mixes (using OECD Guideline 208). Based on the germination results, PHB-Kenaf, PHB-g MA-PHB-Kenaf, and PHB samples had higher germination compared to PP-Glass samples and comparable or slightly higher germination than compost control samples; thus indicating the suitability of PHB polymer and its natural fiber reinforced composites to support plant growth at the end of biodegradation study.

Finally, in order to improve the rate of biodegradation, using an active compost and further reduction of the sample size (in the current study, it was approximately 2 cm x 2 cm x 3.2 mm) is recommended.

6.3 Future work and Recommendations

LCA and biodegradation evaluation for the current study were conducted for composites with equal fiber weight fraction (30wt%) and comparable tensile modulus. And, composites with higher natural fiber weight fraction were not

processed because of the limitations due to automatic fiber addition during extrusion processing of composites. Future studies should develop biocomposites with higher fiber content and evaluate the impacts of varying fiber weight fraction on mechanical properties of biocomposites. The past studies by Sanadi et al.[1], Nishino et al.[2], and Wambua et al.[3], clearly shows a direct relationship between increase in natural fiber weight fraction and mechanical properties of the resulting natural fiber composites. As an example, Figure 6.1 (Wambua et al.[3]) shows an increase in tensile modulus of PP-Kenaf composites with increasing kenaf fiber weight fraction.
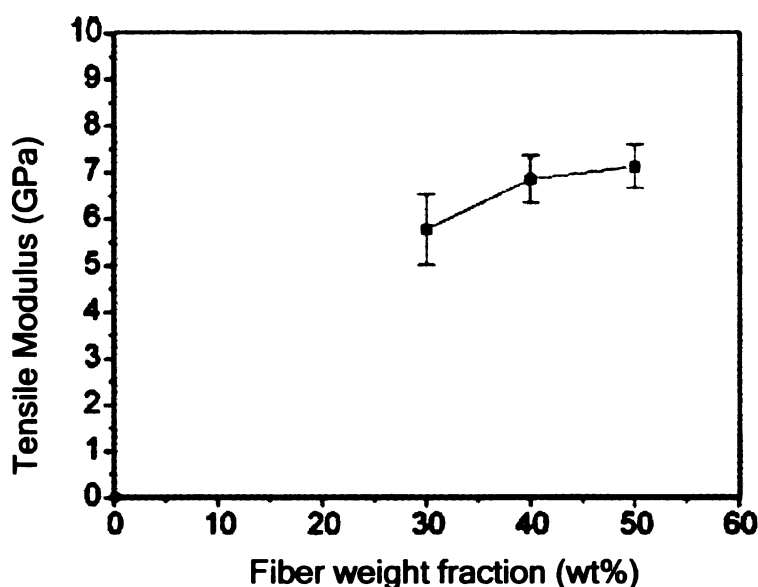
Figure 6.1 Effect of fiber weight fraction on tensile modulus of PP-Kenaf fiber composites (Wambua et al.[3])

Additionally, future studies should also evaluate the effect of increased fiber loading on sustainability of these composites. Since, the production of kenaf fibers has significantly lower energy consumption and environmental impacts compared to glass fibers, higher fiber reinforcement will lead to a significantly

weight (on volume basis) compared to PP-(30wt%)Glass composites. However, as shown below in Figure 6.2 (based on a theoretical calculation), with fiber loading of 45 wt% or more, PHB-Kenaf composites have weight advantage over PP-Glass composites. This weight advantage can have a significant effect on the LCA results, if the use-phase of composites is included in the study. For the current study use-phase was excluded because of unavailability of production data for composites used as automotive structural components. Therefore, for future LCA studies of biobased composites, partnership with automotive companies should be considered, so as to obtain accurate product information and study multiple scenarios with varying fiber composition.
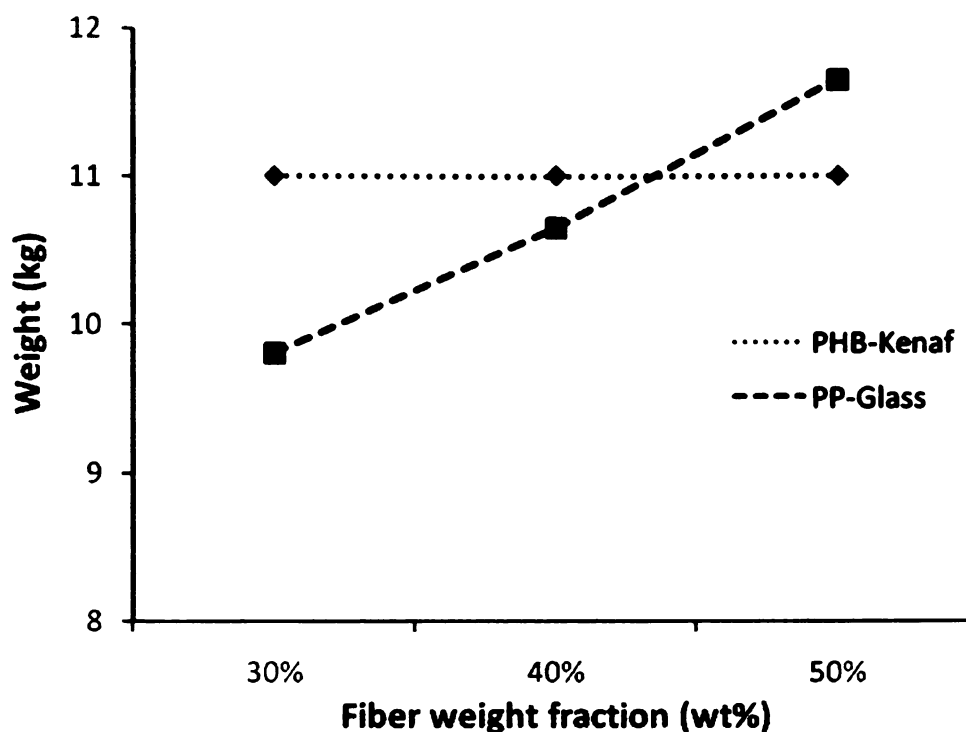
Figure 6. 2 Weight difference (volume basis) for PHB-Kenaf and PP-Glass composites

276

Even though disposal phase was not included in the current study, it was indirectly evaluated by testing the biodegradability of composites under controlled composting environment. The composting study clearly shows a superior end of life profile for PHB-Kenaf composites. The future LCA studies of composites should consider multiple disposal scenarios such as landfilling, incineration, and recycling in addition to composting. However, the biodegradable nature of PHB-Kenaf composites makes composting the preferred disposal option; while incineration and recycling are suitable for non-degradable PP-Glass composites.

Finally, future LCA studies should focus on obtaining more consistent and updated data. The inventory analysis for the current LCA study used data from a wide variety of sources such as DEAM™ database, APME, and journal publications and even though modifications were done to make it relevant to US production, using a single database for inventory analysis is the best option. The recent availability of US life cycle inventory data from NREL[4] is an encouraging development in this direction.

References:

[1] Sanadi AR, Caulfield DF, Jacobson RE, Rowell RM. 1995. Renewable Agricultural Fibers as Reinforcing Fillers in Plastics - Mechanical-Properties of Kenaf Fiber-Polypropylene Composites. Industrial & Engineering Chemistry Research 34(5):1889-1896.

[2] Nishino T, Hirao K, Kotera M, Nakamae K, Inagaki H. 2003. Kenaf reinforced biodegradable composite. Composites Science and Technology 63(9):1281-1286.

[3] Wambua P, Ivens J, Verpoest I. 2003. Natural fibres: can they replace glass in fibre reinforced plastics? Composites Science and Technology 63(9):1259-1264.

[4] NREL. 2006. U.S. Life-Cycle Inventory (LCI) Database, http://www.nrel.gov/lci/.

Appendix 4.3.4: Estimated resource use and costs for field operations, per acre Kenaf, 1999[1].

OPERATION/ OPERATING INPUT	SIZE/ UNIT	TRACTOR SIZE	PERF RATE	TIMES OVER	MTH	TRACTOR COST DIRECT	TRACTOR COST FIXED	EQUIP COST DIRECT	EQUIP COST FIXED	ALLOC LABOR HOURS	ALLOC LABOR COST	OPERATING INPUT AMOUNT	OPERATING INPUT PRICE	OPERATING INPUT COST	TOTAL COST
						----------dollars----------					dollars		------dollars------		
Disk Harrow 24'	24'	160 hp	0.078	2.00	Apr	1.77	2.69	1.16	2.30	0.156	1.29				9.23
Row Cond (Harrow)27'	27'	160 hp	0.053	1.00	Apr	0.60	0.91	0.37	0.79	0.053	0.44				3.12
Apply Chem 4.00	acre			1.00	May							1.0000	4.00	4.00	4.00
Herbicides	acre											1.0000	15.00	15.00	15.00
Apply Fert 4.00	acre			1.00	May							1.0000	4.00	4.00	4.00
Fertilizer	acre											1.0000	25.00	25.00	25.00
Plant 8R40	8R-40	160 hp	0.070	1.00	May	0.79	1.21	0.65	1.60	0.140	1.06				5.33
Seed	acre											1.0000	20.00	20.00	20.00
Cultivate (Early)	8R-40	160 hp	0.095	1.00	May	1.07	1.64	0.38	0.82	0.095	0.78				4.72
Cultivate (Late)	8R-40	160 hp	0.064	1.00	Jun	0.72	1.10	0.26	0.55	0.064	0.53				3.18
Irrigation	acre			1.00	Jul							1.0000	20.00	20.00	20.00
App Fert by Air 8.00	acre			1.00	Aug							1.0000	6.00	6.00	6.00
Fertilizer	acre											1.0000	15.00	15.00	15.00
App by Air 8.00	appl			1.00	Aug							1.0000	8.00	8.00	8.00
Herbicides	acre											1.0000	20.00	20.00	20.00
Silage Harvester 2R	2-R	100 hp	0.600	1.00	Mar	4.26	6.56	8.29	12.13	0.600	4.98				36.25
Boll Buggy	4 bale	160 hp	0.220	1.00	Mar	2.49	3.80	0.95	3.01	0.220	1.82				12.10
Module Builder 32'	32'	160 hp	0.220	1.00	Mar	2.49	3.80	1.09	3.45	0.440	3.34				14.20
TOTALS						14.23	21.75	13.19	24.69	1.768	14.28			137.00	225.16
INTEREST ON OPERATING CAPITAL															10.14
UNALLOCATED LABOR															0.00
TOTAL SPECIFIED COST															235.31

Note: Cost of production estimates are based on last year's input prices.

[1] Budget for producing Kenaf for year 1999, obtained from Mr. Eugene P. Columbus, Mississippi State University.

279

Appendix 4.3.6: Energy requirement for Extrusion and Injection molding

Extruder energy requirement

Electricity consumption for extruder drive and heater is the only form of energy requirement for extrusion, and was categorized either as fixed energy requirement (FER) or variable energy requirement (VER). FER accounts for the extrusion steps, which remains same irrespective of the amount of composites being processed, while VER accounts for the variation in the weight of the same. The ZSK-30 twin-screw extruder was used for processing composites in the current research and the formula for calculating extruder heater and drive energy requirements are mentioned below.

Actual drive power requirement was calculated using this formula:

$$kW = \frac{(RPM \times Torque \times 180)}{9550 \times 94\%},$$

where RPM = Screw speed = 100 rpm (for the current study)

Torque = 40% (in 40-60% range, lower value selected)

Drive efficiency[1] = 94% (1-2% motor and 4-6% gearbox losses)

Thus, drive energy requirement, E_D = kW x t, where t is the time in seconds to extrude composites.

Heater energy requirements[2] were calculated based on the thermodynamic properties of the materials being extruded as follows:

$$Q = \frac{m \times ((C_p \times \Delta T) + \Delta H_{fusion})}{75\%},$$

where m = mass of composites extruded in kilograms

C_p = specific heat of the material in KJ/kg.K

ΔT = Temperature rise during extrusion in Kelvins

ΔH_{fusion} = heat of fusion in KJ/kg

Heater efficiency[3] = 75% (accounting for losses to surroundings and energy removed by cooling water)

Thermodynamic properties of the extruded materials are mentioned below in Table Appendix 4.3.6.1.

Table Appendix 4.3.6.1 Thermodynamic properties of the extruded materials

Material	C_p, KJ/kg.K	ΔH_{fusion}, KJ/kg
LDPE	2.30	218.60
PHB	3.18	101.50
Kenaf fiber[i]	1.34	NA
PP	2.09	102.00
Glass fiber[ii]	0.66	NA

[i] Specific heat of Kenaf fibers assumed to be same as Cellulose
[ii] Specific heat of Glass fibers assumed to be same as Glass wool

Following assumptions were made for extruder energy calculations:

- Initial purge time of 5 minutes with the material being processed, so as to avoid contamination with the previous material processed

- Final purge time of 5 minutes with the purge material (LDPE used as purge material)

- Energy consumption for warm-up of the extruder not considered

- Extrusion feed rate of 57.10 grams/min

Based on these assumptions, fixed energy and variable energy requirements were calculated as follows:

$$FER = (E_D + Q)_{\text{Initial Purge}} + (E_D + Q)_{\text{Final Purge}}$$

$$VER = (E_D + Q)_{\text{Material}}$$

$$E_{\text{Extrusion}} = FER + VER$$

Energy requirements for PHB-(30wt%)Kenaf and PP-(30wt%)Glass composites are mentioned below in Table Appendix 4.3.6.2.

Table Appendix 4.3.6.2 Extrusion energy requirement (MJ-Electricity)

Material	Amount of composites extruded (kg)	ΔT (K)	FER (MJ)	VER (MJ)	$E_{\text{Extrusion}}$ (MJ)
PHB-(30wt%)Kenaf	10.805	160	1.05	16.20	17.25
PP-(30wt%)Glass	9.805	155	0.99	12.57	13.55

Injection molding energy requirement

Energy requirement for injection molding is from two processes: shot preparation and forming. As per Rosato et al.[4], energy requirement for shot preparation is generally an order of magnitude greater than required for forming. The details for calculating these requirements are mentioned below.

Shot preparation step involves phase change of polymer from solid to melt phase and is achieved by using barrel heaters. Energy requirement for this step is calculated as follows:

$$E_S = m \times ((C_p \times \Delta T) + \Delta H_{fusion}),$$

where m = amount of composites injection molded in kilograms

ΔT = Temperature rise during injection molding in Kelvins,

And, thermodynamic properties specified in Table 1 were used to calculate energy requirement for shot preparation step.

Forming step requires drive mechanism, so as to mold the melt into final product shape. Forming energy requirement is calculated as follows:

$$E_F = \frac{N \times (P \times Q) \times \text{fill time}}{116379},$$

where Q is volumetric injection rate in cm^3/sec, and calculated as:

$Q = $ fill speed $\times$ Screw cross-sectional area,

Screw diameter = 3.20 cm,

P = injection pressure in psi = 1000 psi,

N = Number of tensile coupons molded = 1000

$$\text{Fill time} = \frac{\text{Shot size}}{\text{Fill speed}}$$

Thus, total energy requirement for injection molding is defined as follows:

$$E_{IM} = \frac{(E_S + E_F)}{25\%},$$

where Process efficiency = 25% (Rosato et al.[4], have specified injection molding efficiency in the range of 10-25%, higher value was selected for the current study). The total energy values calculated for composites are mentioned below in Table Appendix 4.3.6.3.

Table Appendix 4.3.6.3 Injection molding energy requirement (MJ-Electricity)

Material	Amount of composites molded (kg)	ΔT (K)	Shot size (cm)	Fill speed (cm/sec)	E_S (MJ)	E_F (MJ)	E_{IM} (MJ)
PHB-(30wt%)Kenaf	10.805	140.56	0.95	0.25	4.76	0.17	19.72
PP-(30wt%)Glass	9.805	190.56	1.0	0.5	3.81	0.18	15.93

References:

[1] Data obtained from Coperion Corporation (ZSK-30 manufacturer).

[2] Extrusion: the definitive processing guide and handbook / by Harold F. Giles, Jr., John R. Wagner, Jr., Eldridge M. Mount, III.

[3] Process efficiency for extruders range from 35% to 75%, higher value selected. Ref: Injection molding handbook / Dominick V. Rosato, Donald V. Rosato, Marlene G. Rosato. 3rd ed.

[4] Injection molding handbook / Dominick V. Rosato, Donald V. Rosato, Marlene G. Rosato. 3rd ed.

Appendix 5.2.1: Wattage requirement for controlled composting environment

Wattage requirement in the glove box can be classified into two categories, first to raise the temperature of the incoming air and secondly for raising the temperature of the material in the composting vessels.

<u>Air wattage requirement</u>

As per Omega Engineering catalogue for air process heater, power requirement can be calculated as:

Watts = SCFM × ΔT / 3

SCFM = Standard cubic feet per minute

ΔT = Temperature rise in degrees F from the inlet to the outlet

Exit air from AHP series heaters can reach temperatures upto 540°C (1000°F). In our experiment, exit air temperatures of around 250°C were recorded. Therefore, air wattage requirement was calculated based on the temperature rise from room temperature of 21°C to 250°C. As mentioned in section 5.2, air-flow to each glove box was recorded in the range of 50 – 60 SCFH, thus air-flow of 1 SCFM was assumed for this calculation.

ΔT = 482°F – 69.8°F = 412.2°F

Wattage$_{air}$ = 1 SCFM x 412.2°F / 3 = 137 Watts

<u>Composting vessels wattage requirement</u>

Each composting vessel in the glove box consisted of 600 grams of dry solids of compost with or without 100 grams of dry solids of test substance and the dry solids of the overall sample adjusted to approximately 50%, as per ASTM standard D 5338. Each glove box had capacity to hold 15, 2 Liter Erlenmeyer

Flasks, which were used as composting vessels. For simplifying the calculations each composting vessels was assumed to contain 600 grams of compost plus 100 grams of extruded-injection molded Poly(3-hydroxybutyric acid) (PHB) dogbone samples.

Therefore, wattage requirement for the composting vessels was calculated by determining the energy required to raise the temperature of a mix of compost, test substance (assumed all the samples as PHB) and water to 58°C.

To determine the energy required (Q), specific heat capacity (C_p) of the materials should be known and calculated as:

$$Q = m \times C_p \times \Delta T;$$

where:

Q = energy in Joules

m = weight of substance in grams

C_p = specific heat capacity of the substance in J/g/K

ΔT = temperature rise in °C / °K

Mears et al.[1] have calculated specific heat capacity for the compost, obtained from a mix of swine wastes and straw. For a 35-day mature dry compost (with zero% moisture), specific heat is reported as 0.1551 cal/g/°C. But in the current study this value was not used because Mears et al. reported that swine waste used for the study contained significant amount of inorganic materials such as bones, glass etc., thus modifying the actual specific heat numbers. In addition the dry compost specific heat value is extrapolated from calculations made at higher moisture content, therefore increasing the error of such a value.

In the current study yard-waste based compost was used and screened to remove any large inert items (glass, stone, wood, etc.). As mentioned by Narayan[2], compost provides organic matter in eroded soils, acting well as a substitute for organic carbon in soils. Therefore, specific heat of soil organic matter reported as 0.46 cal/g/°C by Farouki[3] was used to estimate the energy requirement for compost.

Poley et al.[4] have calculated specific heat capacity of PHB films measured by temperature rise method under continuous white-light illumination and reported as 3.98 ± 0.20 (J/cm^3/K). Using the density[5] value of 1.25 g/cm^3, specific heat capacity was converted to mass units as 3.184 ± 0.16 (J/g/K).

Wattage requirement for composting vessels was estimated based on heating the vessels in an hour.

$$\text{Wattage}_{composting} = n \times [\, (W_{compost} \times C_{p\text{-}compost}) + (W_{PHB} \times C_{p\text{-}PHB}) + (W_{water} \times C_{p\text{-}water}) \,] \times \Delta T\, /\, t;$$

n = number of composting vessels = 15

$W_{compost}$ = weight of compost per vessel = 600 grams

W_{PHB} = weight of PHB per vessel = 100 grams

W_{water} = weight of water per vessel = 700 grams

$C_{p\text{-}compost}$ = specific heat of compost = 0.46 cal/g/°C = 1.925 J/g/K

$C_{p\text{-}PHB}$ = specific heat of PHB = 3.184 J/g/K

$C_{p\text{-}water}$ = specific heat of water[6] = 4.1774 J/g/K

ΔT = temperature rise in °C / °K = 37

t = heating time for the vessels = 1 hour = 3600 sec

Thus wattage requirement for composting vessels was calculated as:

$$\text{Wattage}_{composting} = 678 \text{ watts;}$$

And total wattage requirement for each glove box was calculated as:

$$\text{Wattage}_{total} = \text{Wattage}_{air} + \text{Wattage}_{composting} = 815 \text{ watts.}$$

References:

[1] Mears D.R. et al., Thermal and physical properties of compost. Energy, agriculture, and waste management: proceedings of the 1975 Cornell Agricultural Waste Management Conference.

[2] R. Narayan, Drivers for biodegradable/compostable plastics & role of composting in waste management & sustainable agriculture. Bioprocessing of Solid Waste & Sludge, Vol. 1, 2001.

[3] Omar T. Farouki, Thermal Properties of Soils. Series on Rock and Soil Mechanics, Vol. 11 (1986).

[4] Poley, L.H. et al., Photothermal Methods and Atomic Force Microscopy Images Applied to the Study of Poly(3-Hydroxybutyrate) and Poly(3-Hydroxybutyrate-co-3-Hydroxyvalerate) Dense Membranes. Journal of Applied Polymer Science, Vol. 97 (2005).

[5] Material Safety Data Sheet PHB, Biomer, www.biomer.de

[6] Perry's Chemical Engineers' Handbook (7th Edition), 1997

Appendix 5.6.3: Sample Calculation for carbon dioxide evolution on mass basis

Sample calculation for converting concentration reading for Compost Blank sample is provided below. This calculation is for the first reading after starting the experiment.

Sample: Compost Blank-7A

Date of reading: 12/16/2004

Gas Chromatograph Reading:

Retention time (minutes): 1.166

Area: 22.4780

% age CO_2: 1.972

Note: As discussed in section 5.2 (Experimental Set-up and Procedure) of my thesis, two different CO_2 calibration curves were developed: one for a CO_2 concentration range of 20% - 0.2% and another of 3% - 0.2% range. In the reading above, calibration curve with 3% - 0.2% range was used for greater accuracy in determining CO_2 concentration.

Flow rate of the exhaust gas: 80 mL/min = 1.33 mL/sec

V_{CO_2} = sample volume of CO_2 = (% age CO_2) x (Flow rate of the exhaust

gas) = $0.0263 \dfrac{mL}{sec}$

Using ideal gas law equation and room temperature & pressure conditions, mass of CO_2 was calculated as follows:

$$m_{CO_2} = \frac{P \times V_{CO_2} \times M_{CO_2}}{R \times T}, \text{ where}$$

P = 1 atmosphere

T = 298 Kelvin

R = gas constant = 82.057 (mL.atm/moles.K)

M_{CO_2} = molecular weight of CO_2 = 44

Therefore mass of CO_2 (m_{CO_2}) was calculated as: $4.731 \times E - 05 \frac{g}{sec}$

Start up date and time: 12/15/2004, 5:00 pm

Flowrate adjustment date and time: 12/16/2004, 6:30 am

Net days (N_D): 0.56

Thus grams of $\frac{CO_2}{reading}$ = $4.731 \times E\text{-}05 \frac{g}{sec} \times 3600 \frac{sec}{hr} \times 24 \frac{hr}{day} \times 0.56$ day

$$= 2.299 \frac{g}{reading}$$

Converting grams of $\frac{CO_2}{reading}$ to carbon, C_g = $2.299 \frac{g}{reading} \times \frac{12}{44}$

$$C_g = 0.627 \frac{g \text{ of } C}{reading}$$

Dry weight of the compost blank sample = 599.95 g

Therefore, $\frac{g \text{ of } CO_2 / reading}{g \text{ of sample}}$ = 0.0038.